Dokuz Eylül University
Faculty of Engineering
Department of Textile Engineering

ITTC 8th international technical textiles congress

13-14 October 2022

PROCEEDINGS BOOK

13-14 October 2022

LIVE Online Congress

ITTC 8th international technical textiles congress


SUN
TEKSTİL
Dünyaya modayı,
modaya geleceği sunar.
1987 yılında kurulan, Türkiye konfeksiyon üretim ve ihracat sektörünün liderlerinden Sun Tekstil'de 1.800+ kişilik bir aileyiz. Global pazarda önde gelen hazır giyim markalarının çözüm ortağı olmanın yanında ülkemizin en büyük 500 şirketi arasında bulunmanın gururunu yaşıyor, 2018 yılından beri her sene Ege bölgesi hazırgiyim ve konfeksiyon ihracat şampiyonu olarak sektöre liderlik ediyoruz.
www.suntekstil.com.tr

TECHTEX IS OUR BUSINESS!

We, as the Aegean Apparel Exporters' Association and the Aegean Textiles&Raw Materials Exporters' Association are proud of investing in technical textiles and protective clothing.

With its over 1.500 members, the textile and apparel industries of the Aegean Region achieve 1,9 billion US$ export volume annually.

We'd like to share our expertise and hi-tech production quality with you.

eib
AEGEAN EXPORTERS ASSOCIATIONS

www.eib.org.tr
tekstil@eib.org.tr

KIPAS TEXTILES

WE ARE PASSIONATE

about producing highly functional technical yarns and fabrics.

Kipas Textiles incorporates an advanced
Research and Development facility and is recognized
as the leading vertically integrated technical fabric producer in Europe.

KIPAS TEC™

www.kipastec.com

Dokuz Eylül University
Faculty of Engineering
Department of Textile Engineering

8th INTERNATIONAL TECHNICAL TEXTILES CONGRESS

13-14 October 2022
Izmir / Türkiye

Editors
Prof. Dr. Tuba ALPYILDIZ
Prof. Dr. Merih SARIIŞIK
Res. Assist. Dr. Gizem Ceylan TÜRKOĞLU
Res. Assist. Dr. Gülşah Ekin KARTAL
Res. Assist. Dr. Mehmet KORKMAZ

8th International Technical Textiles Congress

13-14 October 2022, İzmir, Türkiye

ISBN 978-975-441-562-9

Cover Design

Dr. Rahşan AKGÜL

Dr. Ali Serkan SOYDAN

PREFACE

Technical textiles have attracted more and more attention in recent years. These high-performance materials are widely used in civil engineering, electrical engineering and electronics, agriculture, medical and automotive industries in addition to protective and military clothing.

Developed countries have focused their strategy on technical textiles to carry forward their competitive advantage and to control technical textiles market and consequently have held the global technical textiles market.

8th International Technical Textiles Congress is held online on 13-14 October 2022. The congress targets to gather all the players of the industry; the experts and the researchers with the manufacturers, the consumers and the investors from Turkey and abroad. 8th International Technical Textiles Congress provides the possibility to share the industrial experiences and scientific investigations, which have very important contributions to the development of the sector.

We would like to thank to all sponsor companies, to all authors and participants for their supports. We hope that this international event will also generate an occasion to create new opportunities.

We are happy to welcome you.

Organizing Committee

ORGANIZING COMMITTEE

- Prof. Dr. Tuba ALPYILDIZ
- Prof. Dr. Merih SARIIŞIK
- Res. Assist. Dr. Gizem Ceylan TÜRKOĞLU
- Res. Assist. Dr. Gülşah Ekin KARTAL
- Res. Assist. Dr. Mehmet KORKMAZ

SCIENTIFIC COMMITTEE

- *Prof. Dr. Rıza Atav (Tekirdağ Namık Kemal University, Türkiye)*
- *Prof. Dr. Ömer Berk Berkalp (İstanbul Technical University, Türkiye)*
- *Prof. Dr. Kadir Bilişik (Erciyes University, Türkiye)*
- *Prof. Dr. François Boussu (ENSAIT, France)*
- *Prof. Dr. Antonela Curteza (Gheorghe Asachi Technical University of Iaşi, Romania)*
- *Prof. Dr. Ümit Halis Erdoğan (Dokuz Eylül University, Türkiye)*
- *Prof. Dr. Raul Fangueiro (Minho University, Portugal)*
- *Assist. Prof. Dr. Aminoddin Haji (Yazd University, Iran)*
- *Prof. Dr. Yasemin Korkmaz (Kahramanmaraş Sütçü İmam University, Türkiye)*
- *Assoc. Prof. Dr. Kalev Kuklane (Netherlands Institute for Public Safety (NIPV), Netherlands)*
- *Prof. Dr. E. Perrin Akçakoca Kumbasar (Ege University, Türkiye)*
- *Prof. Dr. Dilek Kut (Uludağ University, Türkiye)*
- *Prof. Dr. Yordan Kyosev (Technical University of Dresden, Germany)*
- *Prof. Dr. Tuğrul Oğulata (Çukurova University, Türkiye)*
- *Dr. Alina Popescu (The National Research-Development Institute for Textile and Leather, Romania)*
- *Prof. Dr. Maja Radetic (University of Belgrade, Serbia)*
- *Prof. Dr. Seshadri Ramkumar (Texas Tech University, USA)*
- *Dr. Gilda Santos (CITEVE, Portugal)*
- *Prof. Dr. George Stylios (Heriot Watt University, UK)*
- *Prof. Dr. Mehmet Topalbekiroğlu (Gaziantep University, Türkiye)*
- *Prof. Dr. Yıldıray Turhan (Pamukkale University, Türkiye)*
- *Prof. Dr. İsmail Usta (Marmara University, Türkiye)*
- *Assoc. Prof. Dr. Seval Uyanık, (Gaziantep University, Türkiye)*
- *Prof. Dr. İbrahim Üçgül (Süleyman Demirel University, Türkiye)*
- *Prof. Dr. Vladan Koncar (University of Lille, ENSAIT, France)*

CONTRIBUTORS OF THE CONGRESS

- *BOSSA Ticaret ve Sanayi İşletmeleri T.A.Ş.*
- *BWF Endustri Filtreleri ve Teknik Kece Ltd. Sti.*
- *Ege Hazir Giyim ve Konfeksiyon İhracatçıları Birliği*
- *Ege Tekstil ve Hammaddeleri İhracatçıları Birliği*
- *KİPAŞ Mensucat Işletmeleri A.Ş.*
- *Sun Tekstil Sanayi ve Ticaret A.Ş*

**Confirmed companies until 30 September 2022.*

Names of the companies are listed alphabetically.

CONTENTS

PROCEEDINGS

13 October 2022 Thursday

Keynote Speaker

Session I: Medical Textiles

Session II: Nano Technical Textiles

Invited Speaker

Session III: Composite Materials

Invited Speaker

Session IV: Functional Fibres

14 October 2022 Friday

Invited Speaker

Session I: Functional Textiles

Session II: Sustainability and Ecological Aspects for Technical Textiles

Invited Speaker

Session III: Smart and Interactive Textiles

Session IV: Smart and Interactive Textiles & Protective Clothes

POSTER PRESENTATIONS

13 OCTOBER 2022

ORAL PRESENTATIONS

ANTIVIRAL FINISHING OF PET TEXTILE BASED ON Ag-TiO_2 DOPED CuO NANOPARTICLES BY SOL-GEL METHOD

Esra TOPEL ZEREN[1], Nurhan ONAR ÇAMLIBEL[2], Elif CİRELİ[3], Aysun AKŞİT[1]

[1] Dokuz Eylul University, Department of Textile Engineering, İzmir, Türkiye
[2] Pamukkale University, Department of Textile Engineering, Denizli, Türkiye
[3] Jacobs University, Medicinal Chemistry and Chemical Biology, Department of Life Sciences and Chemistry, Bremen, Germany

Corresponding author: aysun.cireli@deu.edu.tr

Abstract: *Recently, due to the coronavirus pandemic, there has been an increase in the use of medical masks in the world. Medical masks are generally made of nonwoven fabrics and do not have the efficiency or properties to kill or stop the growth of living organism (viruses, bacteria, microorganisms). However, their nonwoven structure is based on filtering the organism and blocking the pass-through to other sides. For this reason, the antibacterial and antiviral fabrics became attractive materials for manufacturing masks. Fabrics woven with copper-doped synthetic fibers have begun to be used in masks for their antibacterial or antiviral properties. In this study, the antiviral efficacy of PET woven fabric was obtained by doping silver and titanium using sol-gel method, and copper oxide using exhaustion methods. SEM and XPS were used for the characterization of the fabric and antiviral activity was determined according to the* BS ISO 18184: 2019 *" Textiles - Determination of Antiviral Activity of Textile Products" standard. The fabrics treated with silver, copper and titanium showed antiviral activity against Vaccinia virus, similarly the fabric treated only with titanium and silver performed the same in antiviral tests.*

Keywords: *Copper oxide, sol-gel, antiviral, PET fabric, medical mask*

1. INTRODUCTION

Most of the masks commonly used today are manufactured by combination of multiple nonwoven surfaces. These non-woven surfaces consist of spunbond water-repellent, melt-blown, and skin-compatible spunbond surfaces. These types of masks, which are widely used by the public, especially during the Covid-19 pandemic, keeps pathogens such as viruses and bacteria away from the person by filtration method (Zhou et al. 2020). According to the study of Iwata et al., (2015) these masks are 85% effective in filtrating pathogens, and this effect is provided by the thickness of the material used, fiber diameter, fiber electrical charge, and pore size. The efficiency of these masks also depends on the person wearing the mask and in order to obtain full protection the masks should be used the way described in the instructions. For example, touching the mask during use may cause pathogens such as viruses and bacteria to settle on the surface of the mask and reach the person by overcoming the protective barrier, increasing the risk of transmission (Zhou et al. 2020, Iwata et al. 2015, Oberg & Brosseau, 2008, Rubina & Hyo, 2017, Winski et al. 2019). Since the pathogens placed on the mask surface do not encounter any toxic material, the contaminated material is only suitable for single use which is cost-intensive and lead to environmental pollution.

For the production of antiviral and antimicrobial textiles there are various methods and thousands of nanomaterials available. Methods such as doped fiber spinning and fiber modification, surface coating, electrospinning, plasma, and magnetic sputtering are used for obtaining antibacterial textiles. Natural substances such as chitosan and triclosan and synthetic organic compounds (N-halamin and so on) are

used in wet chemical antimicrobial finishing processes in textile materials. Also, metal (Ag, Ti, Zn etc.) and metal oxide (CuO, MgO, ZnO, TiO etc.) nanoparticles are widely used to improve the protection of textiles against both gram positive and gram negative microorganisms (Qiu et al. 2020).

In this study, Ag and TiO_2 were used for their antibacterial and CuO was used for its antiviral activity (Akşit et al. 2017, Sedighi & Montazer, 2016; Zhou et al. 2020). Sol-gel and exhaustion methods were used as effective methods to obtain antiviral and antibacterial textiles.

2. MATERIALS AND METHODS

2.1. Materials

Polyester fabric (PET, knitted, 330g/m^2) was used in this study. All chemicals were reagent grade. Titanium isopropoxide (TIP, Sigma-Aldrich, USA) and silver nitrate ($AgNO_3$, Merck, Germany) were used as precursors, isopropanol (IP, Merck, Germany) was used as solvent, hexadecyltrimethyl ammonium bromide (HDTA, Sigma-Aldrich, USA) as surfactant and stabilizer to avoid nanoparticle agglomeration and precipitation, hydrazine (Sigma-Aldrich, USA) as reducing agent and glacial acetic acid (GAA, Merck, Germany) for preparation solutions containing nanoparticles. Copper sulphate $CuSO_4$ (Merck, Germany) was used as an antiviral agent.

2.2. Sol-gel Process and Fabric Coating

To obtain antiviral mask fabrics, two different recipes were used for the application of Ag-Ti and Cu compounds to polyester (PET) fabric. In the first recipe, Ag and Ti solution was prepared by sol-gel technique and transferred to the fabric as dip-coating. In the second recipe, $CuSO_4$ was transferred to Ag-Ti coated fabric by exhaustion method and Cu_2O and CuO were formed (Sedighi & Montazer 2016; El-Nahhal et al. 2012). The process is illustrated in Figure 1.

$$CuSO_4 + 2\,NaOH \rightarrow Cu(OH)_2 + Na_2SO_4 \quad (1)$$

$$Cu(OH)_2 + 2\,OH^- \rightarrow [Cu(OH)_4]^{2-} \rightarrow CuO + H_2O + 2OH^- \quad (2)$$

$$Cu_2O + 4NH_4OH \rightarrow 2\,[Cu(NH_3)_2] + + 2OH^- \quad (3)$$

$$CuO + 4NH_4OH \rightarrow Cu[(NH_3)_4]_2 + + 2OH^- \quad (4)$$

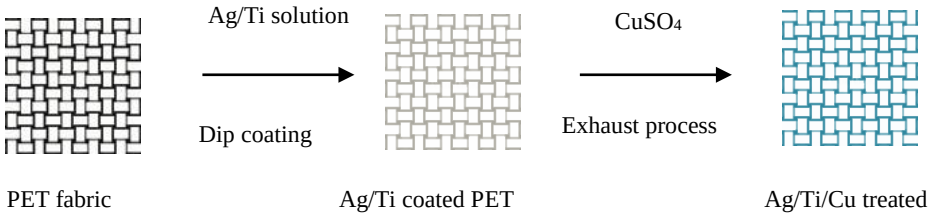

Figure 1. Schematic diagram of the application process of Ag/Ti/Cu on PET fabrics.

Process 1 - Application of Ag-Ti sol: Hexadecyltrimethyl ammonium bromide (HDTA) as a surfactant, $AgNO_3$ as an initiator, and Hydrazine (35% wt solution in water) as a reducing agent were each dissolved in distilled water separately and then mixed to obtain first solution. The second solution was prepared dissolving TIP in IP and then, aqueous glacial acetic acid (GAA) solution was added dropwise to the nanosols for acidic hydrolysis and pH value of the solution was adjusted to 4-4.5. These solutions were mixed together (Aksit et al. 2017). The flow chart of the process is shown in Figure 2.

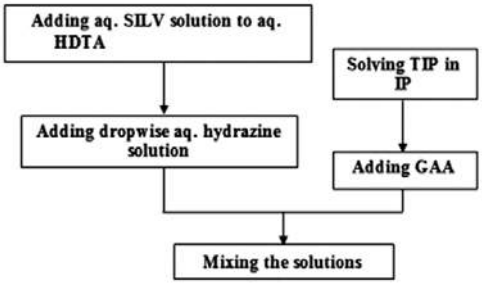

Figure 2. The flow chart of the sol-gel process to prepare Ag-doped TiO_2 nanoparticles

The fabric samples were dipped in the nanosol solution for 30-45 seconds at 25 °C and then the fabrics were squeezed with a padding machine for 80% pickup. The padded fabrics were dried at 100 °C for 10 minutes and the fabric was cured at 150 °C for 5 minutes.

Process 2 - Application of Cu: $CuSO_4$ was transferred by exhaustion method to the Ag-Ti coated fabric. The application graph is given in Figure 3.

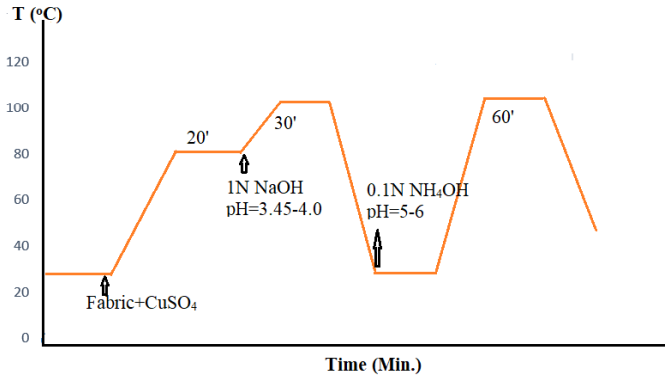

Figure 3. Process scheme of N-doped $CuSO_4$

2.3. Characterization of the Fabric Surface

The elemental composition of the fabric surface was determined by energy-dispersive x-ray spectroscopy (EDS) using an EDX detector of the scanning electron microscope (SEM). The binding of the fabric surface was evaluated by XPS Spectroscopy.

2.4. Assessment of Antiviral Properties

The antiviral effectiveness of Ag/Cu/Ti/PET fabric was tested against selected representatives of enveloped (Vaccinia virus) and non-enveloped (Adenovirus) viruses according to BS ISO 18184: 2019 in the Czech Republic. Control samples of 100% cotton and test samples of test material with the weight of 0,30 g ± 0,05 g were prepared. These were then sterilized in an autoclave (121 °C ± 2 °C). 150 µl of virus suspension was then applied to the samples. Three control samples were used immediately after inoculation at zero time. Three control and three test samples were tested after a 2-hour contact time, when 15 ml of extraction medium was added to each sample.

3. RESULTS AND DISCUSSION

Figure 4 shows the XPS spectrum for Ag, CuO and Ti on the coated fabric surface. Ag3d and Cu2p peaks were detected on Ag/Ti/Cu treated PET fabric, showing the presence of Ag and Cu nanoparticles on the fabric surface (Figure 4a). For Cu on the treated PET fabric (Figure 4b), the Cu2p

have two major peak at 932.6eV ($Cu2p_{3/2}$) and at 952.5 eV ($Cu2p_{1/2}$), which confirms the presence of Cu on the surface of fabrics (Figure 4b) (Liang et al. 2017; Wang et al., 2020). These results are compatible with EDS results.

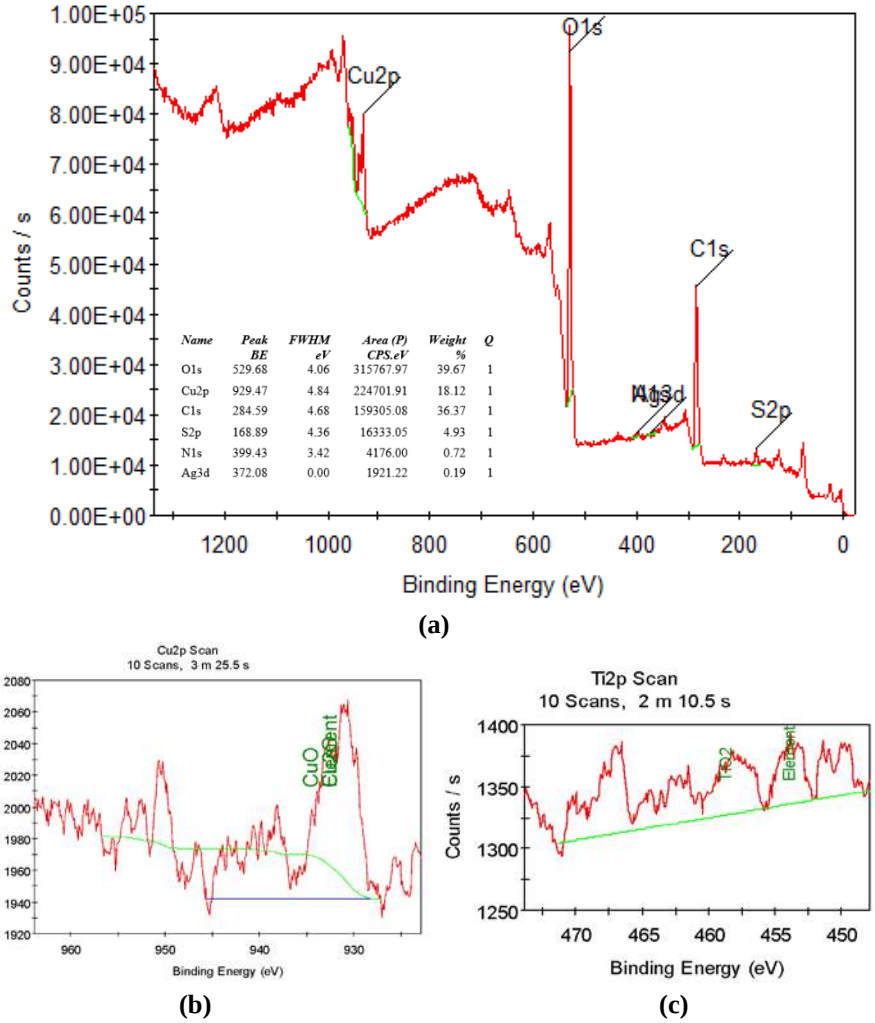

Figure 4. XPS spectra of Ag/Cu/Ti treated PET fabric

In Figure 5, the elemental composition of coated PET fabric was given. It was determined that Ag, Ti, and Cu elements were present on the fabric surface. After the deposition of Ag and Cu on fabric, silver (Ag) and cupper (Cu) elements were detected (Figure 5), confirming the presence of Ag NPs on the surface of fibers.

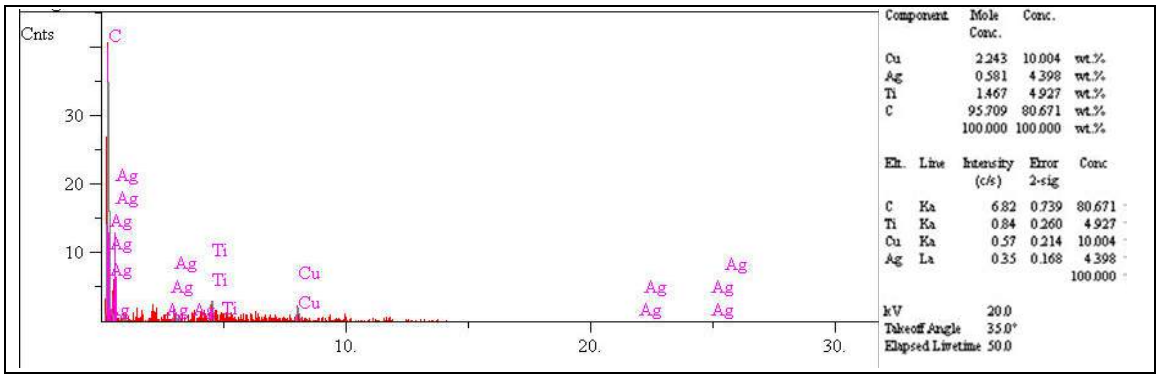

Figure 5. Energy dispersive X-ray spectroscopy (EDS) spectra of Ag/Ti/Cu treated PET fabric

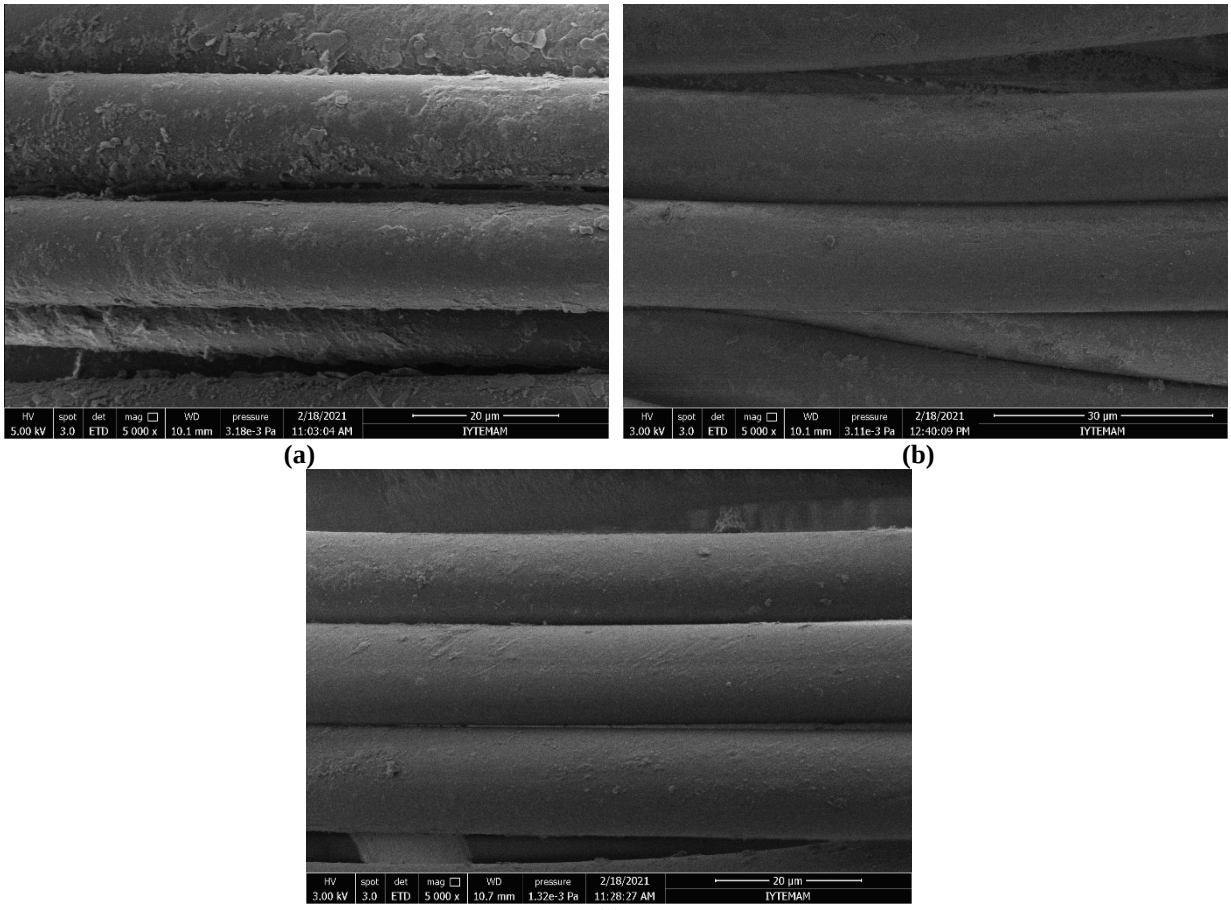

Figure 6. SEM images of coated PET fabric; (a) Ag/Cu/Ti treated PET fabric, (b) after first washing process, (c) after second washing process

In Figure 6 the morphology of the coated PET fabric is shown, and the Ag/Ti/Cu nanoparticles were uniformly deposited on the surface of fibers.

Antivirus effectiveness values against enveloped and non-enveloped viruses according to BS ISO 18184: 2019 are given in Table 1.

Table 1. Antivirus effectiveness values of PET fabric

Sample	***Human adenovirus 5, Adenoid 75 strain***	***Vaccinia virus, Modified Vaccinia virus Ankara strain***	**Evaluation**
	Antivirus effectiveness value (Mv)		
PET fabric	1,250 ± 0,542	2,250 ± 0,314	Sample with good antiviral effectiveness against Vaccinia virus

The coated textile sample was evaluated for the antiviral effectiveness against selected representatives of enveloped (Vaccinia virus) and non-enveloped (Adenovirus) viruses. If the antiviral effectives value is in the range of 2 <A <3, the effectiveness is evaluated as good. If the value is A> 3, the effectiveness is evaluated as excellent. PET test sample showed good antiviral effectiveness against the representative of Vaccinia enveloped virus. But the sample tested did not show antiviral effectiveness against the representative of non-enveloped Adenovirus virus.

4. CONCLUSION

In this study, Ag and Ti was prepared by sol-gel method without depending on commercial products. And also, Cu was applied on Ag/Ti treated fabric by exhaustion method. By using Sol-gel method less chemicals and water are used. It has been observed that conventional wet procedure for deposition of copper onto PET fabric is more effective. The PET fabric used in this study, was tested according EN 149 protocol and the fabric characterized as non-skin irritant, breathable and showed high filtration properties.After Ag/Cu/Ti dopping on the surface the treated PET fabric showed antiviral activity against Vaccinia virus.

ACKNOWLEDGMENT

Thanks for their support and cooperation to GreenChem Tekstil Kimyasalları A.Ş., Fourkim Tekstil Kimyasalları A.Ş., Aloha Tekstil, and Ostrava Health Institute for antiviral tests.

REFERENCES

Aksit, A., Onar Camlibel, N., Topel Zeren, E., Kutlu, B. (2017). Development of antibacterial fabrics by treatment with Ag-doped TiO_2 nanoparticles. The Journal of the Textile Institute, 1-11.doi:10.1080/00405000.2017.1311766.

BS ISO 18184: 2019 Textile - evaluation of antiviral effectiveness of textile materials (absorbent materials).

El-Nahhal, I.M., Zourab, M.S., Kodeh, F.S., Selmane, M., Genois, I., (2012). Nanostructured copper oxide-cotton fibers: synthesis, characterization, and applications. International Nano Letters, 2,14.

Iwata M, Tanizaki H, Fujii H, Endo Y, Fujisawa A, Tanioka M, Miyachi Y, Kabashima K. (2015). Contact urticaria due to a face mask coated with disinfectant liquid spray. *Acta Derm Venereol*. 95:628.

Liang, Y., Chen, Z. Yao, W., Wang, P., Yu, S., and Wang, X., (2017). Decorating of Ag and CuO on Cu Nanoparticles for Enhanced High Catalytic Activity to the Degradation of Organic Pollutants. *Langmuir*, 33, 7606−7614.

Oberg T, Brosseau L. (2008). Surgical mask filter and fit performance. *Am J Infect Control.* 36:276.

Rubino I, Hyo C. (2017). Respiratory protection against pandemic and epidemic diseases. *Trends Biotechnol.*35:907.

Sedighi, A., Montazer, M., (2016). Tunable shaped N-doped CuO nanoparticles on cotton fabric through processing conditions: synthesis, antibacterial behavior and mechanical properties. *Cellulose*, 23(3), 2229–2243. doi:10.1007/s10570-016-0892-3.

Qiu, Q., Chen, S., Li, Y., Yang, Y., Zhang, H., Quan, Z., Qin, X., Wang, R., Yu, J., (2020). Functional nanofibers embedded into textiles for durable antibacterial properties. Chemical Engineering Journal, 384, 123241.

Wang, K., Ma, Q., Zhang, Y., Wang, S., and Han, G., (2020). Ag NPs-Assisted Synthesis of Stable Cu NPs on PET Fabrics for Antibacterial and Electromagnetic Shielding Performance. *Polymers*, 12, 783.

Winski T, Mueller W, Graveling R. (2019). If the mask fits: facial dimensions and mask performance. *Int J Ind Ergonom*. 72:308.

Zhou, J., Hu, Z., Zabihi, F. et al. (2020). Progress and Perspective of Antiviral Protective Material. *Adv. Fiber Mater*. 2, 123–139 https://doi.org/10.1007/s42765-020-00047-7

DEVELOPMENT OF ANTIMICROBIAL FIBERS FOR MEDICAL APPLICATIONS

Figen SELLİ[1], Ayşe Gül TOKTAŞ[2], Aydın DOĞAN[3], Mustafa Erdem ÜREYEN[1]

[1] Eskişehir Technical University, Advanced Technologies Application and Research Center
[2] Nanotech, Eskişehir
[3] Eskişehir Technical University, Department of Material Science and Engineering

Corresponding author: figenselli@eskisehir.edu.tr

Abstract: *In this study, polyvinyl alcohol (PVA) fibres were melt-spun to evaluate their potential as medical textiles. In fibre spinning, silver doped calcium phosphate-based inorganic powder (Ag1) was used as the antimicrobial additive. The powder was synthesized using a wet chemical manufacturing method. The polymer and antimicrobial additive were melt-mixed with microcompunder and monofilaments were collected at a constant speed. Results indicate that fine PVA monofilaments (<135 μm) having 0.5% and 1% antimicrobial additive were successfully produced. The inorganic additive did not cause a drastic change in thermal stability. Monofilaments containing 1 % antibacterial additive exhibited over 98.0 % reduction in both S. aureus and E. coli.*

Keywords: *polyvinyl alcohol, antimicrobial additive, silver, medical fibres*

1. INTRODUCTION

Textiles can be used as materials in many different medical products, ranging from medical masks to wound dressings and scaffolds to surgical threads. The added functionality to fibres, such as antimicrobial response, promotes new applications for the current textile industry (Morris &Murray, 2020). In medical textile production, antimicrobial agents are applied by various methods during the finishing of fabrics or during spinning in-fibre incorporation. Incorporation into fibres has superior advantages like the sustained quality of drape, softness, strength of the textile material, and increase in washing durability of additives (Hufenus et al. 2020, Jeong et al. 2005).

In recent years, the usage of biocompatible polymers having different biodegradability rates and mechanisms such as polyvinyl alcohol (PVA) has gained importance in medical textile applications for instance tissue engineering and drug delivery systems (Teodorescu et al. 2019). The synthetic water-soluble PVA is thermoplastic in nature; therefore, numerous studies have applied melt-extrusion for PVA and its blends (Tran et al. 2013, Zhou et al. 2021).

In the present study, a biocompatible nano-sized antimicrobial additive containing silver content was used. The efficiency of silver against a wide range of microorganisms is a known fact. Moreover, the silver-doped antimicrobial additive used in the present study has antimicrobial activity in different applications (Kose et al. 2016, Toktaş, 2019). Therefore, the goal of this study is the development of melt-spun PVA fibres loaded with an antimicrobial additive to evaluate their potential as medical textiles. The study also aims to characterize these fibres.

2. MATERIALS AND METHODS

2.1 Antimicrobial Additive Synthesis

Silver doped calcium phosphate-based antimicrobial powder (Ag1) was synthesized using wet chemical method. Ortho-phosphoric acid (99%), silver nitrate ($AgNO_3$, 99.0%), and calcium hydroxide ($Ca(OH)_2$, 96.0%) were all laboratory-grade reagents and purchased from Sigma-Aldrich. Calcium hydroxide was mixed in pure water. Dissolved silver nitrate in pure water was mixed with calcium hydroxide. Then, ortho-phosphoric acid diluted with pure water was added to the solution to

control the pH of the solution to form a hydroxyapatite-based structure. The precipitate formed was filtered and dried.

The crystal structure of the powder was monitored by X-ray diffractometer (XRD, Rikagu Rint 2200) using the CuKα radiation and 2θ scan rate of 2° min^{-1}. The particle size distribution of the synthesized powder was measured using Malvern NanoZS 2000 device.

2.2 PVA Fiber Production

The water-soluble, non-toxic thermoplastic PVA polymer (T_m=165 ºC) was purchased from Kuraray, Germany. PVA monofilaments were melt-spun at 170 ºC and 100 rpm screw speed with microcompounder (Xplore, MC15). Three monofilaments were melt-spun: neat fibre PVA_L0, PVA_L05_Ag1 fibre having % 0.5 w/w antimicrobial additive, and PVA_L1_Ag1 fibre having %1 w/w antimicrobial additive. Thermal analysis of the as-spun fibres was conducted by thermogravimetric analysis (TGA). Measurement was carried out from 25 to 700℃ at a heating rate of 10℃ /min using a simultaneous thermal analyser (SDT-Q600, TA Instruments).

The antibacterial efficiency was quantitatively evaluated by the ASTM 2149 Standard Dynamic Contact Conditions. The samples were tested against Gram-negative bacteria (Escherichia coli) and Gram-positive bacteria (Staphylococcus aureus). The antibacterial activity was expressed in % reduction of the microorganisms after contact with the PVA monofilaments at the time ‘0’compared to the number of bacterial cells surviving after contact with the sample after 24 hours. The surface morphology of PVA fibres was investigated by stereo microscope (Carl Zeiss, Discovery V20, Germany). Stereo microscope was also used to analyse the diameter of PVA monofilaments by averaging over 10 measurements.

3. RESULTS AND DISCUSSION

3.1 Structural properties of antibacterial additive

The wet chemical method was used to synthesise antimicrobial additive. The particle size distribution test results revealed that the silver ion incorporated antimicrobial additive has an average diameter of 255,3 nm (Figure 1).

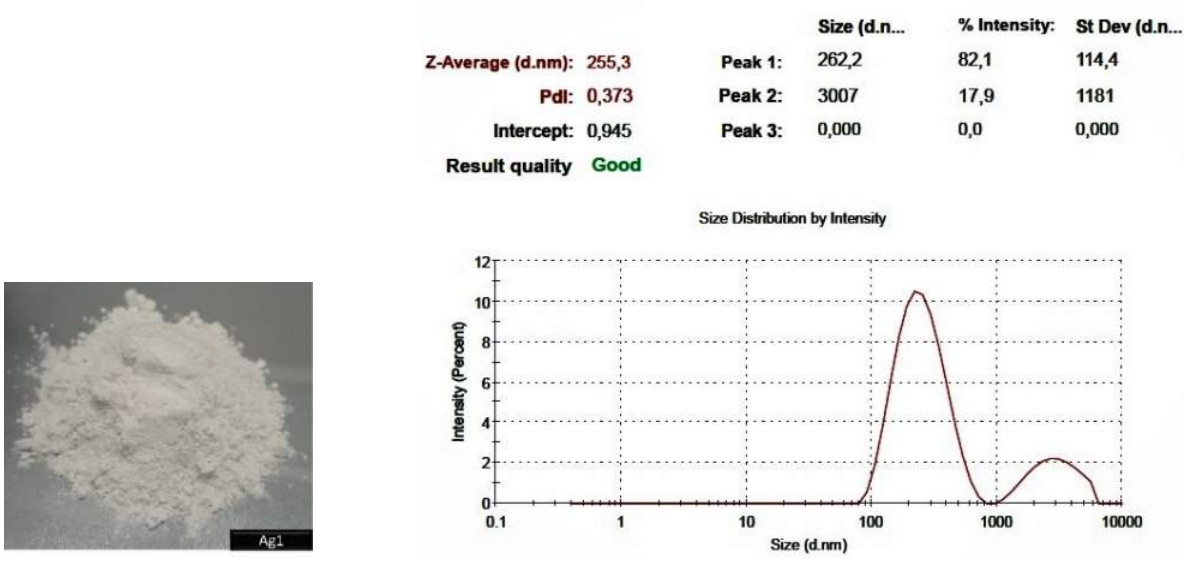

Figure 1. Antimicrobial additive Ag1 and particle size distribution

The XRD analysis of the synthesized powder is displayed in Figure 2. XRD results show that, the crystal structure of synthesized powder is completely hydroxyapatite (*HA). Prior to fibre spinning,

the nano-sized antimicrobial powder was mechanically mixed with PVA polymer without any further surface modification.

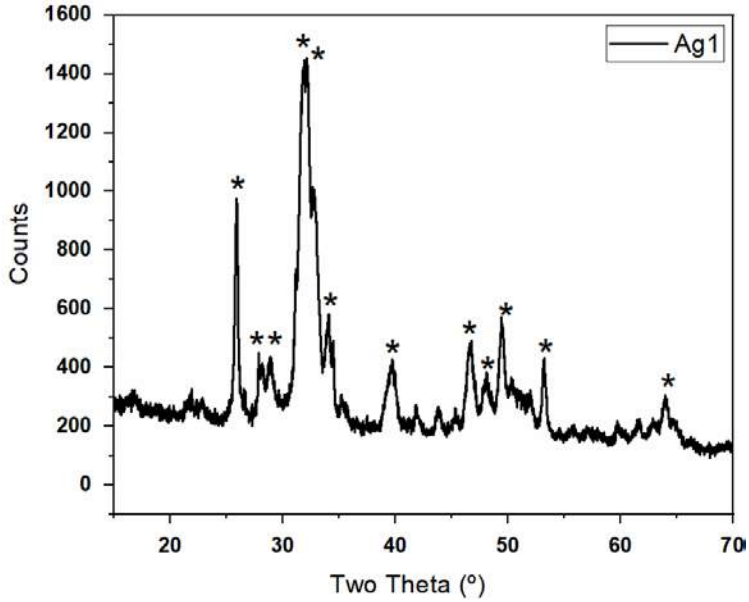

Figure 2. XRD spectra of antimicrobial additive Ag1

3.2 Fibre extrusion and winding of PVA monofilaments

PVA fibres were produced using a twin-screw microcompounder. Following the melt-mixing, polymer melt was extruded through the 1 mm die and monofilaments were winded at a constant rate of 85 m/min (Figure 3a).

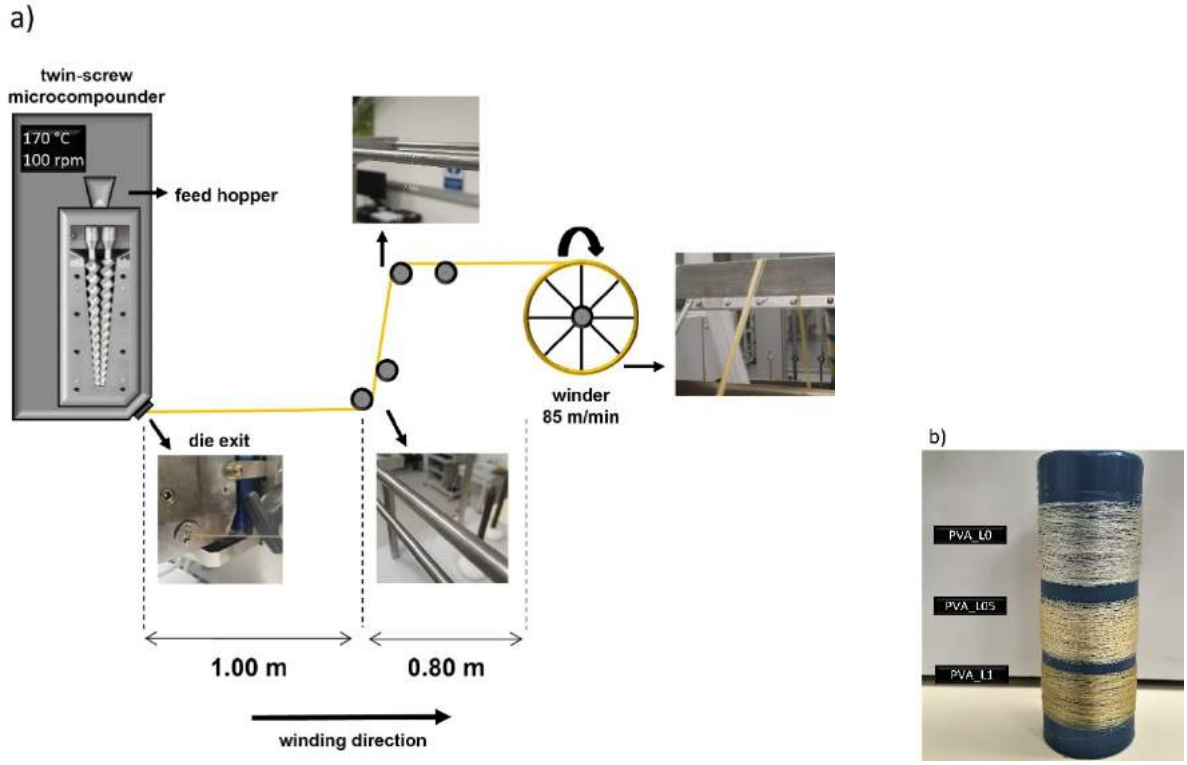

Figure 3. PVA monofilament production a) schematic assembly of monofilament winding b) monofilaments winded onto a bobbin

First, neat fibres were winded at different screw speeds of 15 rpm, 10 rpm and 5 rpm with the aim of finer fibre production. Reduced screw speed enabled to control the throughput rate and flow instabilities resulting in smooth and finer fibre extrusion. Accordingly, composite fibres were also winded at 5 rpm screw speed. Monofilaments are manually winded onto a bobbin for further characterization (Figure 3b). Fine fibres (diameter<135 µm) were successfully spun (Figure 4). The diameters of the individual fibres have been determined from micrographs as 93.6 µm, 107.0 µm and 131.2 µm, for PVA_L0, PVA_L05_Ag1 and PVA_L1_Ag1, respectively.

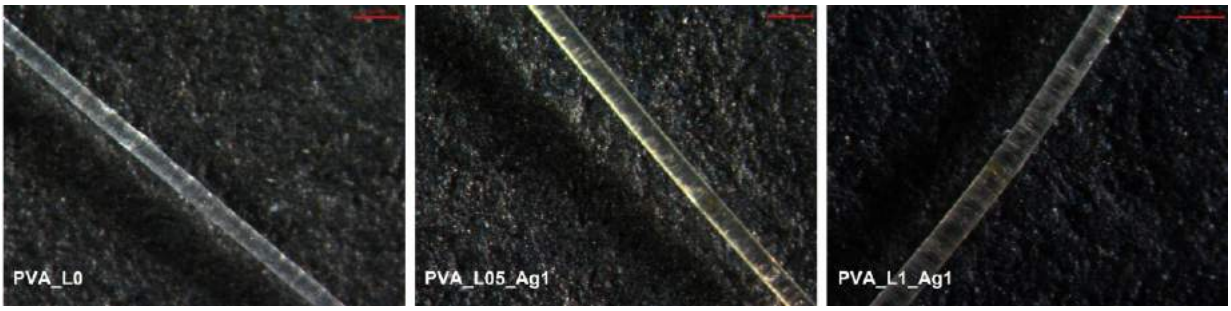

Figure 4. Neat and composite PVA fibres with antimicrobial additive (magnification 50X, scale bar 0.2 mm)

3.3 Thermal properties of PVA monofilaments

Thermal degradation of PVA fibres was studied by determining the weight loss of a sample using TGA. Figure 5 shows the temperature dependence of the PVA weight loss. The TGA curve of fibres displays three degradation steps with an inflection point at 325.2 ºC, 365.3 ºC and 438.2 ºC for the neat fibre PVA_L0. The onset degradation temperature is 285.6 ºC, 287.2 ºC and 284.6 ºC for the fibres PVA_L0, PVA_L05_Ag1 and PVA_L1_Ag1, respectively. Results suggested that the inorganic additive did not cause a drastic change on thermal stability.

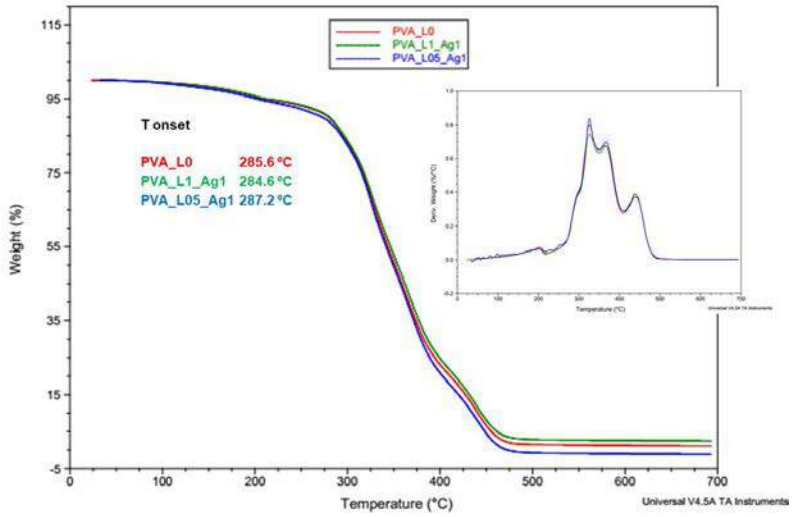

Figure 5. Thermal stability of PVA fibres (heating rate of 10 ºC/min)

3.4 Antimicrobial properties of PVA monofilaments

Antimicrobial activity was assessed quantitatively using two microorganisms, *Staphylococcus aureus* (*S. aureus*) and *Escherichia coli* (*E. coli*). The antibacterial activities of monofilaments are shown in Table 1 as the percentage reduction of *S. aureus* and *E. coli*. Monofilaments containing 0.5 % Ag1

exhibited a 98.72 % reduction in *S. aureus*. However, the same monofilaments exhibited only a 48.24 % reduction in *E. coli*. Thus, we increased the Ag1 concentration to 1 % and examined the antimicrobial activity of the monofilaments. The number of *S. aureus* and *E. coli was reduced by over 98.0 %* when Ag1 concentration of 1 % was used (Table 1).

Table 1. The antibacterial activity results against *E. coli* and *S. aureus* according to test method ASTM 2149

PVA monofilament	**additive concentration (% w/w)**	**the antibacterial activity after 24 h**	
		reduction rate of bacteria (%)	
		E.coli	S. aureus
PVA_L05	0.5	48.24	98.72
PVA_L1	1.0	98.94	99.97

4. CONCLUSION

In this work, it is aimed to melt-spun PVA fibres containing an antimicrobial additive. It was shown that the PVA polymer was well processable in the presence of nano-sized silver-doped calcium phosphate-based antimicrobial additive, and thermal stability of antimicrobial fibres remained unchanged. Fine antimicrobial PVA fibres (diameter<135 µm) were successfully melt-spun. The antimicrobial efficiency test revealed that, the number of *S. aureus* and *E. coli* was reduced by over 98.0 % when Ag1 concentration of 1 % was used. In the later stages of the study, antimicrobial efficiency of PVA composite fibres having various additive ratios will be examined.

ACKNOWLEDGEMENT

This research was financially supported by The Scientific and Technological Research Council of Turkey (TÜBİTAK 2218 to Figen Selli, project number 118C519).

REFERENCES

Hufenus R, Yan Y, Dauner M, Kikutani T (2020): Melt-Spun Fibers for Textile Applications. *Materials* (Basel) 13

Jeong SH, Yeo SY, Yi SC (2005): The effect of filler particle size on the antibacterial properties of compounded polymer/silver fibers. *Journal of Materials Science* 40, 5407-5411

Kose N, Caylak R, Peksen C, Kiremitci A, Burukoglu D, Koparal S, Dogan A (2016): Silver ion doped ceramic nano-powder coated nails prevent infection in open fractures: In vivo study. *Injury* 47, 320-4

Morris H, Murray R (2020): Medical textiles. *Textile Progress* 52, 1-127

Teodorescu M, Bercea M, Morariu S (2019): Biomaterials of PVA and PVP in medical and pharmaceutical applications: Perspectives and challenges. *Biotechnology Advances* 37, 109-131

Toktaş AG 2019: Metal İmplantların Aerosol Kaplama ve Elektrosprey Kaplama Yöntemi Kullanılarak Gümüş Katkılı Hidroksiapatit Seramik ile Kaplanması ve Antibakteriyel Özellik Kazandırılması, Eskişehir Teknik Üniversitesi, Eskişehir

Tran NHA, Brünig H, Hinüber C, Heinrich G (2013): Melt Spinning of Biodegradable Nanofibrillary Structures from Poly lactic acid. *Macromolecular Materials and Engineering* 299, 219-227

Zhou T, Wang M, Chen N (2021): Study on Preparation of Triangular Melt-Spinning Poly (Vinyl Alcohol) Fibers and Its Fabric Strengthening and Toughening Epoxy. *Polymers* (Basel) 13

INVESTIGATION OF ANTIBACTERIAL AND COMFORT PERFORMANCES OF COTTON-SILVER KNITTED FABRIC

Hatice AÇIKGÖZ TUFAN[1], Elçin EMEKDAR[1], Umut Kıvanç ŞAHİN[1], Senem KURŞUN BAHADIR[2], Cansu BATÇIK GENÇ[3], Türkan Kübra BAYKAN[3], Ersen ÇATAK[3], Çağla Deniz ŞENTÜRK[3], Esra ERİCİ[3]

[1] İTÜ, Textile Technologies and Design Faculty, Textile Engineering Department, Istanbul, Türkiye
[2] İTÜ, Mechanical Engineering Faculty, Mechanical Engineering Department, Istanbul, Türkiye
[3] SANKO Textile, 3. Organize Sanayi Bölgesi 83209 No.lu Cd. No:4 Şehitkamil /Gaziantep, Türkiye

Corresponding author: acikgozh@itu.edu.tr

Abstract: *In this study, adding high amount of antibacterial activity level was aimed via knitting 10 % silver fiber containing cotton fabrics, for underwear products, in order to maintain comfort related features of the fabric that could decrease with traditional antimicrobial finishing chemicals and techniques. Antibacterial activity, wicking, drying rate, water absorbency, water vapor and air permeability tests were performed and compared with 100 % cotton fabric. It was proved that holding comfort related properties was possible while obtaining remarkable antibacterial properties even after 30 washing cycles.*

Keywords: *Cotton-silver blend yarn, antibacterial performance, comfort performance, cotton knitted fabric, underwear*

1. INTRODUCTION

Underwear products are expected to provide not only comfort but also antibacterial properties due to the interaction between the fabric and the human skin. The perception of comfort depends on the area of use; saving from the heat is essential for firefighter cloth, on the other hand keeping warm and being breathable are asked from an underwear due to the interaction with the human skin (Fangueiro et al. 2010). In order to provide a comfortable underwear, choosing the raw material is the key factor and cotton meets the expectations with strong, soft, durable, absorbent features (Hosseini Ravandi and Valizadeh 2011). Bending, breathability and elasticity are some of the required properties for underwear products, that can be provided by knitting structure (Oğlakcioğlu and Marmarali 2007). The structure of knitted fabrics is porous which makes them breathable, accelerates the removal of water vapor from human body for thermal comfort (Ibrahim et al. 2010). Addition to porous formation, knitted fabrics cover the body and takes the shape of it, that enables the ease of movement (Kizildag, Ucar, and Gorgun 2016). Apart from these advantages, knitted fabrics provide lightweight, simple care, low cost, fast production.

Customer needs are changing day by day, and it is expected from a garment to have multifunctional properties. Despite being physiologically comfortable, underwear products are awaited providing antibacterial properties. Cotton garments in direct contact with the human skin are ideal places for bacterial growth by being warm and humid (John Unango and M Ramasamy 2019). It is needed to avoid people from bacteria in order to protect the health, and that can be achieved with some antibacterial finishes. The antimicrobial agents are divided into controlled release or leaching and bound antimicrobials (Simoncic and Tomsic 2010). The first type, the most of the antimicrobial agents, is not chemically bounded to the textile fibers and the gradual decrease of the active substance is inevitable because of the leaching action (Paul 2015). However, the bound antimicrobials are chemically bonded to the textile material, and covalent bonding can be achieved if there are adequate reactive groups in the agent and the fibers (Paul 2015). Bonding makes them more resistant comparing controlled release ones against repeated laundering (Paul 2015). Yet, washing durability of the

chemical on the fiber surface cannot last the antimicrobial function forever. Main drawbacks of antimicrobial agents are listed as associated side effects, water consumption-pollution, action on non-target microorganisms, non-durable against repeated laundering and discomfort on the textile surface. The additive fixation chemicals for crosslinking of antimicrobial agents are mostly releasing formaldehyde which is carcinogenic and leading fabrics to lose their strength (Perumalraj 2013; Islam, Ghosh, and Akter 2020; Xie et al. 2007; El-Shafei, Elshemy, and Abou-Okeil 2015). Recently, environmental issues are taken into consideration while choosing the appropriate antimicrobial finish and the current studies were noticeably focused on the development and the application of environmentally friendly chemicals such as chitosan (Yıldız Varan 2018; Şahan and Demir 2016; Demir et al. 2008; Varan 2016), aloe vera (İnanç and Doğan 2020), some plant extracts (S. Mahesh, A. H. M. Reddy, and G. V. Kumar 2011). Although the natural products are non-toxic on environment and human health, they have some disadvantages including antibacterial efficiency, durability of finish, coloring the fabric (Simoncic and Tomsic 2010; Paul 2015; Rîmbu et al. 2015).

It is essential to investigate the effect of antibacterial finishes on the garment comfort, because most of finishes are applied onto textile products that are in contact with the skin. In last decades, metal and metallic compounds are getting trendy to achieve antibacterial efficiency(Simoncic and Tomsic 2010; Paul 2015; Deng, Wang, and Wang 2016; Nadiger and Shukla 2017; Majumdar, Butola, and Thakur 2015; Üreyen et al. 2010). Deng et al have studied with a composite agent of chitosan and silver as a finishing agent on cotton knitted fabric for intimate apparel, and antibacterial finishing applied fabrics evaluated for comfort (permeability, hydrophily and tactility) and antibacterial (Escherichia coli and Staphylococcus aureus) properties after 20 times laundering (Deng, Wang, and Wang 2016). They have found that increasing in the antibacterial efficiency requires the cumulation of agents on the fabric surface and results in higher bending rigidity. Nadiger and Shukla aimed to have a durable antibacterial activity on silk fabrics with aloe vera and silver nanoparticles, treatment of antibacterial materials is processed with 1,2,3,4-butane tetra carboxylic acid (BTCA) as crosslinking agent providing durable finish (Nadiger and Shukla 2017). Various amounts of BTCA, aloe vera and silver nano particles are fixed on fabrics, and it is found that increase in the BTCA concentration increases the add-on values of antimicrobial materials on the silk fabrics. Chemical treatments make the silk fabric more ductile and less strong to stresses, especially at high BTCA concentrations.

Chemically treated anti-bacterial cotton fabrics sacrifice some comfort properties due to the add-on values of anti-bacterial finish on the fabric surface. That situation causes fabric surface being stiff, brittle, less breathable and less porous; in other words, less comfortable. Yet, anti-bacterial products often contact with the skin and it is required to provide comfort for these products. Inserting an anti-bacterial agent into the fabric structure without chemical treatment provides not only anti-bacterial characteristics but also comfort features. In this study, 10 % silver fiber containing cotton yarn was used in order to produce a weft knitted fabric for developing an anti-bacterial underwear product, comfort and anti-bacterial properties were investigated.

2. MATERIALS AND METHODS

2.1. Fabric Production

The 1*1 rib fabric was knitted using 90 % cotton 10 % silver containing (Ne 40) yarn. Knitting process was performed on 36 gauges and 18” diameter Vanguard circular knitting machine. The fabric and optical microscope picture were shown in the Figure 1.a and 1.b, respectively.

Figure 1. a. 1*1 rib cotton-silver fabric **b.** Optical microscope picture

2.2. Test Methods

The fabric was tested for different comfort properties and antibacterial efficiency. All samples were conditioned in an atmosphere of 20 ± 2 °C and 65% ± 4% relative humidity for 24 hours prior to testing according to ISO 139.

Vertical wicking test was performed according to AATCC Test Method 197-2013. Rectangular shaped samples were cut into 25 mm width and 200 mm length. The sample was marked at 5 mm from bottom for dipping in the distilled water. Once the sample was immersed in the water, the test was started. The rise of the water was measured at 2 min and 10 min for short and long time period vertical wicking rates. Depending on the rise of the water on the sample, wicking rates were calculated with the given formula.

$$W_{Vs} = \frac{d_s}{t_s}$$

$$W_{Vl} = \frac{d_l}{t_l}$$

W_{Vs} (mm/s) = Short period wicking rate
d_s (mm) = Wicking distance in 2 min
t_s (s) = Wicking time (120 s)
W_{Vl} (mm/s) = Long period wicking rate
d_l (mm) = Wicking distance in 10 min
t_l (s) = Wicking time (600 s)

Horizontal wicking of samples was tested according to AATCC Test Method 198-2013. The samples were cut into 200 mm * 200 mm and marked for 100 mm diameter for testing. The testing sample was placed onto a 2 liters beaker without any tension and crease with an elastic rubber, then a 10 mL burette filled with distilled water was fixed onto the middle of the sample with a 10 mm distance. 1 mL distilled water was dropped onto the test sample for 10 seconds, the test was prolonged for 5 min. After the termination of test, the length and the width of the wicking on the fabric was measured, then the horizontal wicking rate was calculated for each sample with below equation.

$$W_h = \frac{\pi * \left(\frac{1}{4}\right) * d_1 * d_2}{t}$$

W_h (mm^2/s) = Horizontal wicking rate
d_1 (mm) = Wicking distance in the length direction
d_2 (mm) = Wicking distance in the width direction
t (s) = Wicking time

For determining the water vapor permeability of test samples Rotating Platform Method was used (BS 7209:1990). In this method, metal test dishes were filled with water at a predetermined level, test samples were placed and fixed with roller tape onto test dishes. After putting test samples onto rotating platform, test was started and continued for 5 hours. The weight measurements before and after the test were noted, then water vapor permeability of the fabric was calculated according to given formula.

$$WVP = \frac{(W_1 - W_2) * 24}{A * 5}$$

WVP ($g/m^2/day$) = Water vapor permeability
W_1 (g) = Weight of test dish with fabric sample before testing
W_2 (g) = Weight of test dish with fabric sample after testing
A (m^2) = Area of the test sample

Drying rate of the samples were measured depending on the literature (Cimilli Duru and Candan 2016). Prior to testing dry samples' weights were measured. The test was started with wetting samples in distilled water for 30 min, continued with squeezing extra water on the samples and laying the samples' each side on the blotting paper for 2 min. The weight of the samples was measured at 30 min, 1 hour, 2 hours, 3 hours, until the weight was 105 % of the dry weight. Drying rate of the fabric was expressed as average weight loss over the initial water content per unit area per unit hour.

$$DR = \frac{(W_1 - W_2)}{A * t}$$

DR ($g/m^2/h$) = Drying rate
W_1 (g) = Weight of the samples after wetting (0 min)
W_2 (g) = Weight of the samples when dried (when reached 105 % of dry weight)
A (m^2) = Area of the sample
T (h) = Total drying duration

Water absorbency of the samples were tested according to AATCC Test Method 79-2000. One drop of distilled water was dropped onto test fabric and the duration that the water absorbed by sample was recorded. For being water absorbent, the fabric should absorb the drop in 60 seconds.

Air permeability tests were performed as stated in ISO 9237-1995. Samples were placed on the circular specimen holder without any tension or wrinkles. Air flow through the fabric was recorded approximately 1 min. An average of 10 reading was reported.

Antibacterial efficiency of fabric was tested according to ISO 20743-2013 with Staphylococcus aureus and Klebsiella pneumoniae microorganisms. Among the inoculation methods specified in ISO 20743, absorption method was selected as it involves direct inoculation of bacterial suspension on the specimen to be tested, thus being more convenient for determination of performance expectation from a textile fabric to be used in intimate apparel manufacturing. After 5, 10, 20 and 30 washing cycles (4N according to ISO 6330-2012), antibacterial efficiency test was performed subsequently versus 100% cotton fabric of the same structure without FBA or any other finish. The evaluation of the test was based on calculation and comparison of the antibacterial activity value. The antibacterial activity value (A) is the difference between the growth value on the control specimen and that on the testing specimen. The growth value corresponds to the logarithm of arithmetic average of the number of bacteria obtained from three specimens after 24 hours incubation at 37°C ± 2 °C.

3. RESULTS AND DISCUSSION

3.1. Comfort Performance of Fabric

Wicking performances of fabrics had an important role when the comfort properties of fabrics were taken into consideration. Wicking rates of fabrics were directly related with the moisture management of the product. Vertical and horizontal wicking rates of samples show the water absorption and diffusion capability by the capillary effect of the fabric in the vertical and horizontal direction.

Vertical wicking test was used to evaluate the ability of vertically aligned fabric specimens to transport the water along the fabric and the results were shown in Table 1. Five samples were conducted to the test and their average wicking rate result was reported. Average short and long period vertical wicking rates were 0,18 ± 0,02 mm/s and 0,13 ± 0,01 mm/s, respectively. However, the vertical wicking rate results of rib samples were relatively low comparing the results in the loose fabric structures, the short and long period vertical wicking rates were adequate for moisture management comfort in the product. Capillary effect in the rib fabric was lower because of denser structure and more contact areas between yarns (Kumar and Das 2014).

Horizontal wicking test was used to evaluate the ability of horizontally aligned fabric specimens to transport the water through the fabric. Five samples were tested and their average wicking rate results were reported. Average horizontal wicking rate was 6,11 ± 0,26 mm^2/s. Similar to vertical wicking rate results, horizontal wicking rates of samples were achieved as a result of capillary movement of water through the fabric and connected with the yarn and fabric structure. It is a known fact that density of the fabric had an essential effect on the horizontal wicking rate of the fabric and looser structures may lead to spread water through the fabric rapidly (Tang, Kan, and Fan 2017).

Water vapor permeability test was performed for demonstration of the removal of the perspiration from the human body to surface of the garment. Fabric structure, raw material, chemical applications on the garment were some of the main factors effecting the water vapor permeability of the fabrics (Abbasi, Marmaralı, and Ertekin 2020). Five samples were measured and their average was reported. Average water vapor permeability of the cotton-silver fabric was 1053,40 ± 52,10 $g/m^2/day$. The results showed that inserting silver fibers into the cotton yarn provided high water vapor permeability comparing 100 % cotton fabrics (Şahin and Cimilli Duru 2017).

Drying rate was one of the most important comfort properties required for intimate apparel products. The 105% of the dry weight was achieved approximately 5 hours later from the beginning of the test. Five fabric pieces were tested and their average was reported as 62,36 ± 5,18 $g/m^2/h$. It was found that

addition of the silver fibers in the cotton yarn improved drying rate of the fabric considering 100% cotton ones (Cimilli Duru and Şahin 2020).

Dropping test was repeated five times and average water absorbency time was calculated as 20,6 ± 2,07s.

Air permeability of a fabric was connected with the structural properties of the fabric (yarn count, fiber fineness, density, etc.) (Selli and Turhan 2017). 10 different areas on the fabric were measured by the device and their average was given as 2507,76 ± 126,29 mm/s. Comparison of the 100 % cotton fabric with the 90 % cotton 10 % silver fabric in terms of air permeability showed that improvements were achieved by using silver in the structure (Selli and Turhan 2017).

3.2. Antibacterial Properties of Fabric

Antibacterial activity was achieved by presence of an antimicrobial agent which was silver fiber in this study. Antibacterial efficiency of knitted fabric containing 90 % cotton and 10 % silver against S. aureus and K. pneumonie was presented in Table 7. Antibacterial activity value presents significant activity when between two and three, and strong activity when over three. As shown in Table 1, antibacterial activity values against both bacteria were very strong even after 30 washing cycles with limited decrease comparing to initial antibacterial activity levels.

Table 1. Antibacterial activity level of sample before and after repeated washing

	S. aureus	***K. pneumonie***
Initial	5, 23	5,32
Washed (5 times)	5,16	5,25
Washed (10 times)	5,14	5,22
Washed (20 times)	4,69	4,97
Washed (30 times)	4,60	4,93

4. CONCLUSION

Imparting a functional property to a common fabric via conventional techniques usually puts the manufacturer on the horns of a dilemma where one is occasionally split between adding high amount of functionality and keeping the natural available desired features mostly coming out of proper selection of raw material. For underwear products, it is required to achieve an adequate level of bacterial protection while offering comfort demanded by the user, which is hard to fulfill in warm and humid conditions. This study aimed to impart high antibacterial efficiency to knitted fabrics without use of harsh chemicals which cause decrease in comfort naturally offered by cotton fiber. For this purpose, 90 % cotton and 10 % silver containing knitted fabric was produced and tested for antibacterial and comfort related properties, and test results were compared with those of 100 % cotton fabric. Wicking, drying rate, water absorbency, water vapor and air permeability results showed comparable performance to that of 100 % cotton fabric while achieving superior antibacterial properties even after 30 washing cycles. This technique could be a solution for comfortable and durable antibacterial fabrics aiming to serve for niche products.

ACKNOWLEDGMENT

The authors gratefully acknowledge the funding by SANKO Textile Facilities Research & Development Center “Development of Antiviral and Antibacterial Mask and Protective Equipment Fabrics”, under grants of “AP20” project.

REFERENCES

Abbasi, Sadaf Aftab, Arzu Marmaralı, and Gözde Ertekin. 2020. "Thermal Comfort Properties of Weft Knitted Quilted Fabrics." *International Journal of Clothing Science and Technology*, no. 14. https://doi.org/10.1108/IJCST-07-2019-0111.

Cimilli Duru, Sena, and Cevza Candan. 2016. "Wicking and Drying Behaviors of Knitted Fabrics Produced with Different Poliamide Yarns." *Tekstil ve Konfeksiyon* 26 (3): 280–86.

Cimilli Duru, Sena, and Umut Kıvanç Şahin. 2020. "Effects of Yarn Type, Process History, Softener Type and Concentration on Wicking and Drying Properties of Cotton Plain Knitted Fabrics." *Journal of the Textile Institute* 111 (8): 1166–75. https://doi.org/10.1080/00405000.2019.1689773.

Demir, Aslı, Ege Ü Tekstil, Mühendisliği Bölümü, Tülin Öktem, and Necdet Seventekin. 2008. "Investigation of the Usage of Chitosan As an Antimicrobial Agent in Textile Industry." *Tekstil ve Konfeksiyon* 2: 94–102.

Deng, Yong Mei, Si Fan Wang, and Shang Jun Wang. 2016. "Study on Antibacterial and Comfort Performances of Cotton Fabric Finished by Chitosan-Silver for Intimate Apparel." *Fibers and Polymers* 17 (9): 1384–90. https://doi.org/10.1007/s12221-016-6277-2.

El-Shafei, A., M. Elshemy, and A. Abou-Okeil. 2015. "Eco-Friendly Finishing Agent for Cotton Fabrics to Improve Flame Retardant and Antibacterial Properties." *Carbohydrate Polymers* 118: 83–90. https://doi.org/10.1016/j.carbpol.2014.11.007.

Fangueiro, R., A. Filgueiras, F. Soutinho, and Xie Meidi. 2010. "Wicking Behavior and Drying Capability of Functional Knitted Fabrics." *Textile Research Journal* 80 (15): 1522–30. https://doi.org/10.1177/0040517510361796.

Hosseini Ravandi, S.A., and M. Valizadeh. 2011. *Properties of Fibers and Fabrics That Contribute to Human Comfort*. *Improving Comfort in Clothing*. Elsevier Masson SAS. https://doi.org/10.1533/9780857090645.1.61.

Ibrahim, N. A., T. F. Khalifa, M. B. El-Hossamy, and T. M. Tawfik. 2010. "Effect of Knit Structure and Finishing Treatments on Functional and Comfort Properties of Cotton Knitted Fabrics." *Journal of Industrial Textiles*. https://doi.org/10.1177/1528083709357975.

İnanç, Levent, and Nazime Mercan Doğan. 2020. "Investigation of Antibacterial Activity of Footwear Leather Obtained from Different Tanning." *Tekstil ve Konfeksiyon* 30 (3): 184–89. https://doi.org/10.32710/tekstilvekonfeksiyon.622826.

Islam, Shaima, Joyjit Ghosh, and Nahida Akter. 2020. "Comparative Study on Crease Recovery Finishing of Silk Fabric with Citric Acid and Dimethylol Dihydroxy Ethylene Urea (DMDHEU) as Finishing Agent," no. April: 0–7. https://doi.org/10.5923/j.textile.20200901.01.

John Unango, Franco, and Karthikeyan M Ramasamy. 2019. "A Review on the Investigation of Biologically Active Natural Compounds on Cotton Fabrics as an Antibacterial Textile Finishing." *International Research Journal of Science and Technology* 1: 49–55. https://doi.org/10.46378/irjst.2019.010107.

Kizildag, Nuray, Nuray Ucar, and Belgin Gorgun. 2016. "Analysis of Some Comfort and Structural Properties of Cotton/Spandex Plain and 1×1 Rib Knitted Fabrics." *Journal of the Textile Institute* 107 (5): 606–13. https://doi.org/10.1080/00405000.2015.1054143.

Kumar, B., and A. Das. 2014. "Vertical Wicking Behavior of Knitted Fabrics." *Fibers and Polymers* 15 (3): 625–31. https://doi.org/10.1007/s12221-014-0625-x.

Majumdar, Abhijit, Bhupendra Singh Butola, and Sandip Thakur. 2015. "Development and Performance Optimization of Knitted Antibacterial Materials Using Polyester-Silver Nanocomposite Fibres." *Materials Science and Engineering C* 54: 26–31. https://doi.org/10.1016/j.msec.2015.04.026.

Nadiger, Vinay G., and Sanjeev R. Shukla. 2017. "Antibacterial Properties of Silk Fabric Treated with Aloe Vera and Silver Nanoparticles." *Journal of the Textile Institute* 108 (3): 385–96. https://doi.org/10.1080/00405000.2016.1167391.

Oğlakcioğlu, N., and A. Marmarali. 2007. "Thermal Comfort Properties of Some Knitted Structures." *Fibres & Textiles in Eastern Europe* Nr 5-6 (64 (5): 94–96.

Paul, R. 2015. "Antimicrobial Finishes for Textiles." In *Functional Finishes for Textiles: Improving*

Comfort, Performance and Protection, edited by Roshan Paul, 1–14. https://doi.org/10.1533/9780857098450.1.

Perumalraj, R. 2013. "Single-Stage Antimicrobial and Crease Proof Finishing of Cotton Materials." *Journal of Industrial Textiles* 42 (4): 376–91. https://doi.org/10.1177/1528083712441778.

Rîmbu, Cristina, Angela Cerempei, Rodica Muresan, Eleonora Guguianu, Mariana Ursache, Oana Borhan, and Augustin Muresan. 2015. "Eco-Friendly Antibacterial Finish for Natural Knitted Fabrics." *Tekstil ve Konfeksiyon* 25 (4): 359–64.

S. Mahesh, A. H. M. Reddy, and G. V. Kumar. 2011. "Studies on Antimicrobial Textile Finish Using Certain Plant Natural Products." *International Conference on Advances in Biotechnology and Pharmaceutical Sciences* 560059 (9980819835): 253–58.

Şahan, Görkem, and Asli Demir. 2016. "A Green Application of Nano Sized Chitosan in Textile Finishing." *Tekstil ve Konfeksiyon* 26 (4): 414–20.

Şahin, Umut Kivanç, and Sena Cimilli Duru. 2017. "Effects of Softener Applications on Air and Water Vapor Permeability of Cotton Knitted Fabrics Produced with Different Yarns." *Tekstil ve Konfeksiyon* 27 (3): 275–82.

Selli, Figen, and Yildiray Turhan. 2017. "Investigation of Air Permeability and Moisture Management Properties of the Commercial Single Jersey and Rib Knitted Fabrics." *Tekstil ve Konfeksiyon*.

Simoncic, Barbara, and Brigita Tomsic. 2010. "Structures of Novel Antimicrobial Agents for Textiles - A Review." *Textile Research Journal* 80 (16): 1721–37. https://doi.org/10.1177/0040517510363193.

Tang, Ka Po Maggie, Chi wai Kan, and Jin tu Fan. 2017. "Comparison of Test Methods for Measuring Water Absorption and Transport Test Methods of Fabrics." *Measurement: Journal of the International Measurement Confederation* 97: 126–37. https://doi.org/10.1016/j.measurement.2016.10.054.

Üreyen, Mustafa E., Özer Gök, Mustafa Ates, Göktug Günkaya, and Iefik Süzer. 2010. "Evaluation of Silver Content and Antibacterial Activities of Silver Loaded Fiber/Cotton Blended Textile Fabrics." *Tekstil ve Konfeksiyon* 20 (2): 137–44.

Varan, Nilufer Yildiz. 2016. "Binding Chitosan Cross-Linked with Dimethylol Dihydroxyethylene Urea onto Nylon 66 Fibres for Burn Scar Management." *Asian Journal of Chemistry* 28 (9): 2004–8. https://doi.org/10.14233/ajchem.2016.19869.

Xie, Yanjun, Andreas Krause, Holger Militz, Hrvoje Turkulin, Klaus Richter, and Carsten Mai. 2007. "Effect of Treatments with 1,3-Dimethylol-4,5-Dihydroxy-Ethyleneurea (DMDHEU) on the Tensile Properties of Wood." *Holzforschung* 61 (1): 43–50. https://doi.org/10.1515/HF.2007.008.

Yıldız Varan, Nilüfer. 2018. "The Effects of Chitosan Antimicrobial Treatments on the Physical and Mechanical Properties and Wear Performances of Highly Elastic Fabrics Used for Burn Scar Management." *Journal of the Textile Institute* 109 (1): 39–45. https://doi.org/10.1080/00405000.2017.1322477.

OBTAINING NANOFIBER TEXTILE SURFACE CONTAINING ANTIBACTERIAL MICROCAPSULES

Koray PEKTAŞ[1], Onur BALCI[1]

[1] Kahramanmaraş Sütçü İmam University, Department of Textile Engineering, Kahramanmaraş, Türkiye

Corresponding author: koraypektas@ksu.edu.tr

Abstract: *In this study, it was aimed to obtain nanofiber showing antibacterial activity and also containing ozonated oil microcapsules by using solution blowing spinning system. With this aim, firstly, olive oil and common st. john's wort oil was ozonized to obtain antibacterial activity of the oils. After that, ozonized oils were microencapsulated via simple coacervation method. To produce nanofiber containing ozonized oil microcapsules, Polyamide 6.6 polymer solution were prepared and then ozonated oil microcapsules were added the polymer solution. After mixing, nanofiber surfaces containing microcapsules were obtained by using solution blowing spinning system under certain conditions. In the scope of this study, from tip to toe, a set of test and analyses (the amount of the total unsaturated fatty acid, FT-IR, optic microscope, scanning electron microscope (SEM) and antibacterial activity test) were used to investigate the success of the ozonized oil, microcapsules, and the developed nanofiber surfaces. The data from these tests and analyses showed that ozonizing process of the vegetable oil, microencapsulation process and the nanofiber spinning were successful. Moreover, the nanofiber containing microcapsules showed antibacterial activity.*

Keywords: *ozonated oil, microencapsulation, solution blowing spinning, antibacterial activity, medical textiles.*

1. INTRODUCTION

Day by day, interest of the technical textile has been escalating. There is no doubt that one of the most popular technical textile areas is medical textile nowadays because of the pandemic effect. On examining of the medical textile surfaces, there are too many studies on wound dressing that conducted via electro spinning system. However, electro spinning system has a few disadvantages and some of them are conductivity required, electrical field required to fibre spin and also low fibre spinning speed. Apart from electro spinning system to produce synthetic fibre, there are many fibres spinning system such as solution spinning (wet and dry spinning), melt blowing but they cannot produce fibers with diameters in the same size range as electrospun fibers and they are limited to thermoplastic polymers (1,2). Because of the limitation of the electro spinning system, there is a need for alternative methods to fabricate non-woven webs of fibers with diameters in the same size scale as electrospinning.

With this aim, solution blowing spinning system originated. The solution blowing spinning system is to utilize from elements of both the electrospinning and melt blowing technologies to make micro- and nanofibers similar to electrospinning system (1). Solution blowing system has advantages in comparison with the electro spinning system because this system has high production rate, not required conductivity and not necessarily electric field for spinning (3). As for the studies on the solution blowing spinning system there are many studies on fiber spinning. However, there are hardly studies on wound care and wound dressing surfaces. Considering this situation, in the study, it was aimed to produce nanofiber showing antibacterial activity and healing. For this purpose, ozonated vegetable oils were used and their microcapsule forms mixed polyamide 6.6 polymer solution and then microcapsules loaded nanofiber were spun via solution blowing spinning system. All stage of the process, characterisation tests and analyses were employed and evaluated.

2. MATERIALS AND METHODS

2.1. Material

In the scope of this study, raw olive oil and common st. john's wort oil was used for obtaining ozonized vegetable oil. After ozonation process, ozonized vegetable oils were used in microencapsulation process as core material showing antibacterial activity. While Arabic gum was used in the microencapsulation process as a shell material. On the other hand, Polyamide 6.6 and formic acid were used for preparing fiber spinning solution.

2.2. Method

Raw olive oil and common st. john's wort oil was ozonated for two hours via ozone generator which generates 25g ozone in an hour. After ozonation process, the ozonized oil was microencapsulated via simple coacervation method. Flow chart of the microencapsulation process was given in Figure 1.

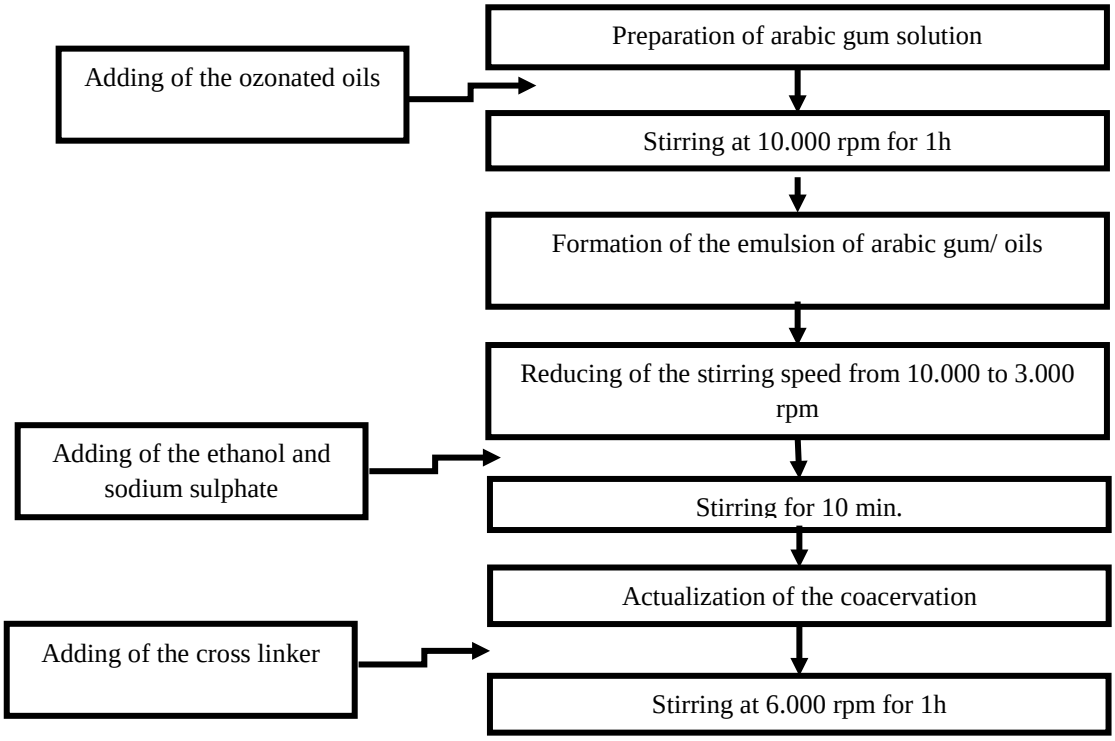

Figure 1. Flow chart of the simple coacervation

Then, fibre spinning solution was prepared by mixing polyamide 6.6 and formic acid for two hours with the help the magnetic stirrer at 60°C. Moreover, fiber spinning solution and microcapsule solution were mixed at room temperature and the nanofiber spinning were employed at the certain working condition given below.

- Solution feeding rate: 10ml/h.
- Air pressure: 2 bar
- Working distance: 37 cm
- Working time: 30 min.
- Distance between inner and outer nozzle: 2 mm

2.3. Tests and Analyses

In the scope of this study, the amount of the total unsaturated fatty acid, FT-IR, optic microscope, scanning electron microscope (SEM) and antibacterial activity test against to gram-negative bacteria (E. coli) according to ASTM E 2149-01 were employed for characterization of the ozonized oil, microcapsules and nanofiber containing microcapsules.

3. RESULTS AND DISCUSSION

After ozonizing process, unsaturated fatty acid amount in the ozonized oil were investigated (Table 1). The data showed that unsaturated fatty acid amount decreased sharply due the fading away of the C=C double bond which is found in unsaturated fatty acid such as oleic acid, linoleic acid, linolenic acid (4–7).

Table 1. Unsaturated fatty acid amount of the oil

Oil type	Oleic acid (%)	Linoleic acid (%)
Crude Olive oil	73,6	9,2
Ozonated olive oil	0,1	0,0
Crude common st. john's wort oil	75,2	7,8
Ozonated common st. john's wort oil	1,4	0,1

FT-IR spectrum of the crude and ozonated oil were given in Figure 2. FT-IR spectrum showed that C-O (ca 1100 cm-1) bound were formed after ozonation process and =C-H bound were broken. Namely, it was proved that the ozonation process were successful. Besides, the data supported the reduction of the total unsaturated fatty acid amount (4–7).

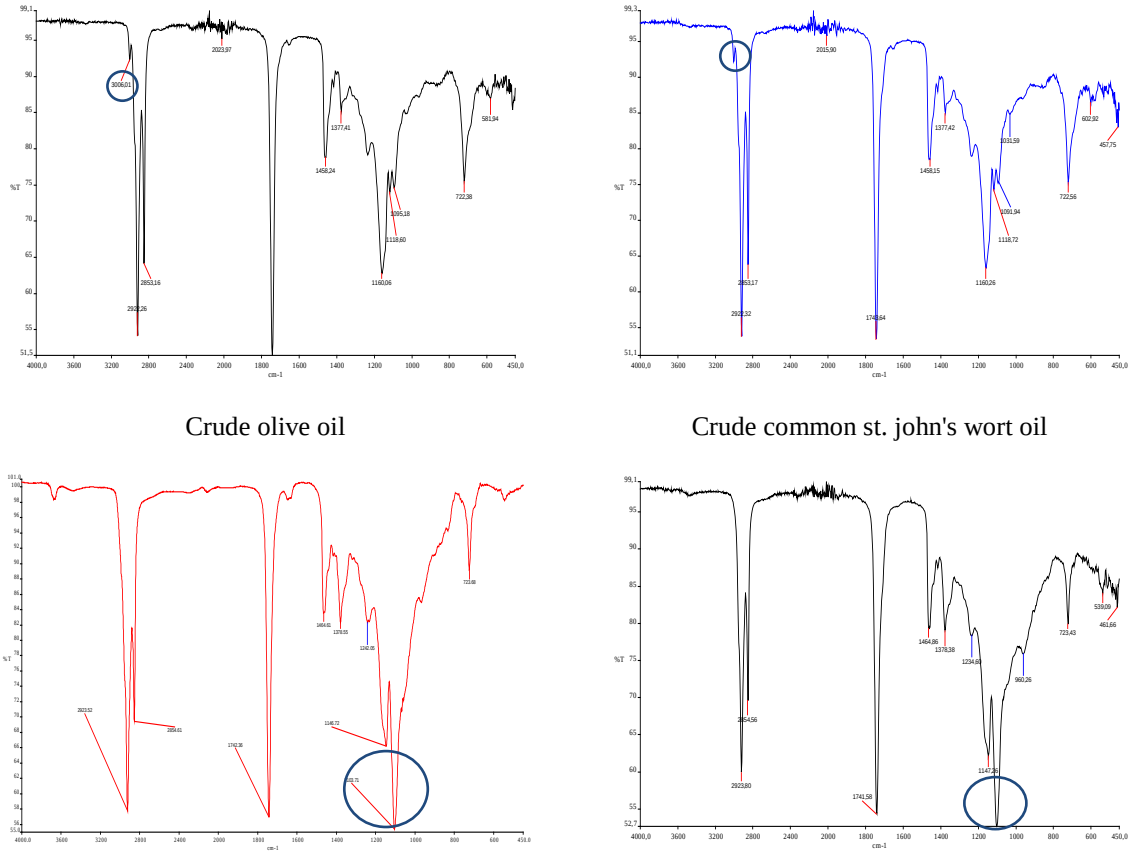

Crude olive oil

Crude common st. john's wort oil

Ozonated olive oil

Ozonated common st. john's wort oil

Figure 2. FT-IR spectrum of the crude and ozonated oils

Given in Figure 3, the optical microscope images showed that the ozonated oils were microencapsulated successfully and the microcapsules formation had spherical shapes.

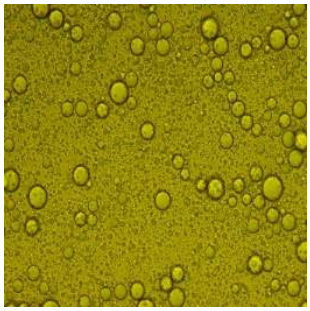
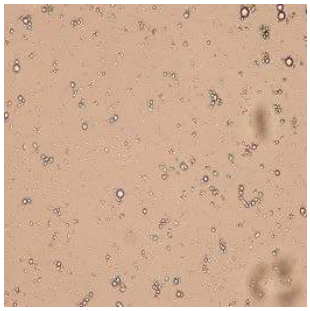

a b

Figure 3. Optical microscope images of the microcapsules a. ozonized olive oil b. ozonized common st. john's wort oil

After solution blowing spinning of the polyamide 6.6 and ozonized oil solution mixture, SEM photos were taken (Figure 4.) and they showed that nanofiber formation were obtained also microcapsules were loaded successfully in the structure.

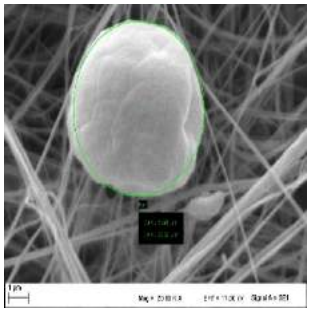
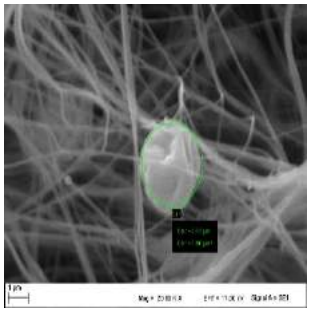

a b

Figure 4. SEM photos of the nanofiber surface containing microcapsules a. ozonated olive oil microcapsules containing nanofiber surface b. Ozonated common st. john's wort oil microcapsules containing nanofiber surface

In table 2, antibacterial activity test (ASTM E 2149-01) results were given according to the. These data showed that the nanofiber containing both ozonated olive oils microcapsules and ozonated common st. john's wort oil microcapsules had the antibacterial activity against to gram negative bacteria (*E.coli).*

Table 2. Antibacterial activity of the nanofiber containing ozonated oils microcapsules agains to *E.coli*

Sample code	**6 hours**	**24 hours**
	Bacteria reduction/proliferation (%)	
PA 6.6 Nanofiber surfaces	87,50	243,75
Ozonated olive oil microcapsules containing nanofiber surface	-100,00	-100,00
Ozonated common st. john's wort oil microcapsules containing nanofiber surface	-100,00	-100,00

4. CONCLUSION

In the scope of this study, ozonated vegetable oils were obtained successfully. After that microencapsulation of the ozonated oil via simple coacervation method were done. To produce nanofiber containing microcapsules showing antibacterial activity, polyamide 6.6 polymer solution and microcapsule solution were mixed together and spun via solution blowing spinning system. The data from SEM photos, it was seen that nanofiber surface containing microcapsules were successful done. According to ASTM E 2149-01, the nanofiber surfaces containing ozonated oils microcapsules showed antibacterial activity against gram negative (E.Coli) bacteria. For further studies, it is thought that healing activities of these surfaces investigate as in-vivo and in-vitro.

REFERENCES

Daristotle, J. L., Behrens, A. M., Sandler, A. D., & Kofinas, P. (2016). A Review of the Fundamental Principles and Applications of Solution Blow Spinning. *ACS Applied Materials and Interfaces*, 8(51), 34951–34963. https://doi.org/10.1021/acsami.6b12994

Medeiros, E. S., Glenn, G. M., Klamczynski, A. P., Orts, W. J., & Mattoso, L. H. C. (2009). Solution blow spinning: A new method to produce micro- and nanofibers from polymer solutions. *Journal of Applied Polymer Science*, 113(4), 2322–2330. https://doi.org/10.1002/app.30275

Zhang, L., Kopperstad, P., West, M., Hedin, N., & Fong, H. (2009). Generation of Polymer Ultrafine Fibers Through Solution (Air-) Blowing. *Journal of Applied Polymer Science*, 114, 3479–3486. https://doi.org/10.1002/app.30938

Beşen, B.S., Balcı, O., Güneşoğlu, C., Orhan, M., Somuncuoğlu, E., Çankaya, I. I. (2017). Obtaining medical textiles including microcapsules of the ozonated vegetable oils. *Fibers Polym.* 1;18(6):1079–90.

Beşen B.S., Balci, O., Orhan, M., Güneşoğlu, C., Çankaya, I. I. (2015). Ozonlanmış Yağlar ile İşlem Uygulanmış Dokusuz Yüzeylerin Antibakteriyel Etkinliklerinin İncelenmesi. *J Text Eng*, http://dx.doi.org/10.7216/1300759920152210003

Beşen, B.S., Güneşoğlu, C., Balci, O., (2016). Antibacterial Finishing of 100% Cotton Fabric with with β-Cyclodextrin-Ozonated Olive Oil Inclusion Complex. *AATCC J Res*, 3(6):12–8. http://www.ingentaconnect.com/content/10.14504/ajr.3.6.3

Soriano, N.U., Migo, V.P., Matsumura, M,. (2003) Ozonation of Sunflower Oil: Spectroscopic Monitoring of the Degree of Unsaturation. *JAOCS, J Am Oil Chem Soc*, 80(10):997–1001.

ELECTROSPINNING OF PVP/CARVACROL/LANOLIN COMPOSITE NANOFIBERS

Hülya KESİCİ GÜLER[1], Mustafa GEYSOĞLU[2], Funda CENGİZ ÇALLIOĞLU[1],

[1] Süleyman Demirel University, Engineering Faculty, Textile Engineering Department, Isparta, Turkiye
[2] Süleyman Demirel University, Graduate School of Natural and Applied Sciences, Bioengineering Department, Isparta, Turkiye

Corresponding author: kesicihulya@gmail.com

Abstract: *In this study, it was aimed to produce and characterize various concentrations of carvacrol and lanolin loaded PVP nanofibers via electrospinning. Various concentrations of carvacrol:lanolin were added to the PVP polymer solutions such as 2.5, 5, 7.5, 10, 12.5 and 15 wt %. Solution properties such as viscosity, conductivity, and surface tension were measured. In terms of characterization studies, SEM and FT-IR analysis were carried out. According to the results of the study, viscosity increased and conductivity decreased with carvacrol:lanolin concentration increasement. However, surface tension was not affected from carvacrol:lanolin concentration. Nanowebs quality improved with carvacrol:lanolin concentrations. Generally, nanofibers are quite fine, smooth, and uniform. FT-IR spectrums verified that PVP, carvacrol and lanolin exist in the structure of nanofibers chemically. Considering antibacterial properties of carvacrol and wound healing properties of lanolin, the composite nanofiber surfaces have a high potential for use in the biomedical field, especially as a wound dressing.*

Keywords: *Polyvinylpyrrolidone, carvacrol, lanolin, electrospinning, nanofiber.*

1. INTRODUCTION

Nanofibers have superior properties such as small fiber diameter (nm), small and open pores, high porosity, large specific surface area (m^2/g), and high loading capacity. With this high loading properties of nanofibers, different kinds of agents such as drugs, proteins, antibacterial agents, enzymes, and essential oils can be loaded nanofibers in terms of get much more functionally according to their end use application areas (Bhardwaj and Kundu, 2010; Haghi, 2011). In this study, carvacrol and lanolin were loaded to the biocompatible PVP nanofibers for their antibacterial and wound healing properties.

Carvacrol is the main constituent of thyme essential oils and is natural and inexpensive. Both of carvacrol and thyme essential oils have antibacterial, antifungal, odour, and pesticidal properties (Paster et al., 1995; Kordali et al., 2008). Lanolin, an organic ester derived from sheep fleece after shearing, produces an air-permeable temporary barrier and promotes moist wound healing when applied to damaged skin. Actually, lanolin is a kind of wax formed which is also known as wool yolk, wool wax, or wool grease. It softens and treats dry skin on the lips and nipples. Generally, new mothers, breastfeeding mothers, chemotherapy patients with dry, cracked, and damaged skin, and those with burn wounds use products containing lanolin. Lanolin is commercially available in many medical such as ophthalmic eye drops, burn and wound healing creams, and cosmetic products such as lotions, makeup, sunscreen and shaving creams or gels (Abou-Dakn et al., 2010; Uzun and Oymak, 2022).

PVP is a synthetic, water-soluble, non-toxic, biocompatible, and hydrophilic polymer which is used generally biomedical applications such as wound dressing, tissue engineering, and drug delivery

systems. PVP was chosen as the raw material for this study because of all of these features, which are important in biomedical and cosmetic applications (Wang et al., 2017).

Investigations on carvacrol and lanolin nanofibers have been published in the literature individually (Cengiz Çallıoğlu et al., 2020; Uzun and Oymak, 2020; Altan et al., 2018). However, no study has been conducted on PVP/Carvacrol/Lanolin nanofiber composites in combination. Therefore, the findings of this study are expected to be valuable in the literature.

2. MATERIALS AND METHODS

2.1. Materials

To produce nanofibers, PVP (360.000 g/mol) (Sigma–Aldrich (St. Louis, MO, USA)) was used as a polymer, carvacrol (Süleyman Demirel University, Natural Products Application and Research Center, with 96 % purity) and anhydrous lanolin (Galenic Chemicals, İzmir, Turkey) were used as an additive, deionized water was used as a solvent and Cremophor RH 40 (Ersa Chemistry, İzmir, Turkey) was used as a surfactant.

2.2 Preparation and Characterization of Polymer Solutions

Various concentration of carvacrol:lanolin added to the PVP polymer solutions (Table 1). According to our preliminary studies, optimum carvacrol:lanolin ratio was determined as 9:1. Then, solution properties such as viscosity, conductivity and surface tension were measured.

Table 1. Sample codes and composition of carvacrol:lanolin loaded PVP polymer solutions

Sample Codes	PVP Concentration (%)	Carvacrol:Lanolin Ratio	Carvacrol:Lanolin Concentration (%)
PVP0	12	9:1	0
PVP2.5	12	9:1	2.5
PVP5	12	9:1	5
PVP7.5	12	9:1	7.5
PVP10	12	9:1	10
PVP12.5	12	9:1	12.5
PVP15	12	9:1	15

2.3 Production and Characterization of Nanofibers

Nanofiber productions were carried out by electrospinning set up under the optimum process parameters (Table 2).

Table 2. Process parameters of electrospinning

Voltage (kV)	Distance between electrodes (cm)	Feed Rate (mL/h)	Humidity (%)	Temperature (°C)	Needle Diameter (mm)
17	24.0	0.2	30-35	22-24	0.8

After nanofibers production, characterization studies were achieved. In order to analyze of nanofibers morphology, SEM images were taken with different magnifications. ImageJ software was used to

measure the diameters of 100 fibers that were taken from different parts of the electrospun nanowebs. and in order to understand fiber diameter distribution, fiber diameter histograms curves were obtained via statistical analyze program. Then, average fiber diameter uniformity coefficient values were calculated below:

$$A_n = \frac{\sum n_i d_i}{\sum n_i} \text{(Number average)} \quad (1)$$

$$A_w = \frac{\sum n_i d_i^2}{\sum n_i d_i} \text{(Weight average)} \quad (2)$$

The closer the average fiber uniformity coefficient value is to 1, the more uniform fibers are (Cengiz and Jirsak, 2009). Lastly, FT-IR spectrums were carried out with Attenuated Total Reflection (ATR) technique between 4000 and 400 cm^{-1}.

3. RESULTS AND DISCUSSION

3.1 Solution Properties Results

The properties of polymer solutions, such as viscosity, electrical conductivity, and surface tension, all have an impact on the morphology of electrospun nanofibers. Therefore, within the scope of the study, the polymer solution properties were measured and the results are given in Figure 1.

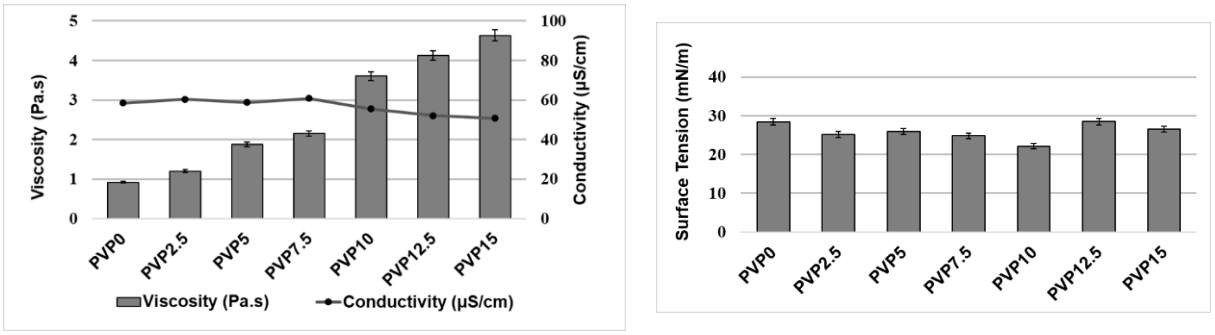

(a) (b)

Figure 1 Solution properties results a) viscosity and conductivity b) surface tension

According to the Figure 1; viscosity increase and conductivity decreases while carvacrol:lanolin concentration increases. However, surface tension was not effected from carvacrol:lanolin concentration.

3.2 Fiber Morphology Results

SEM images of various concentrations of carvacrol:lanolin nanofibers are given in Figure 2.

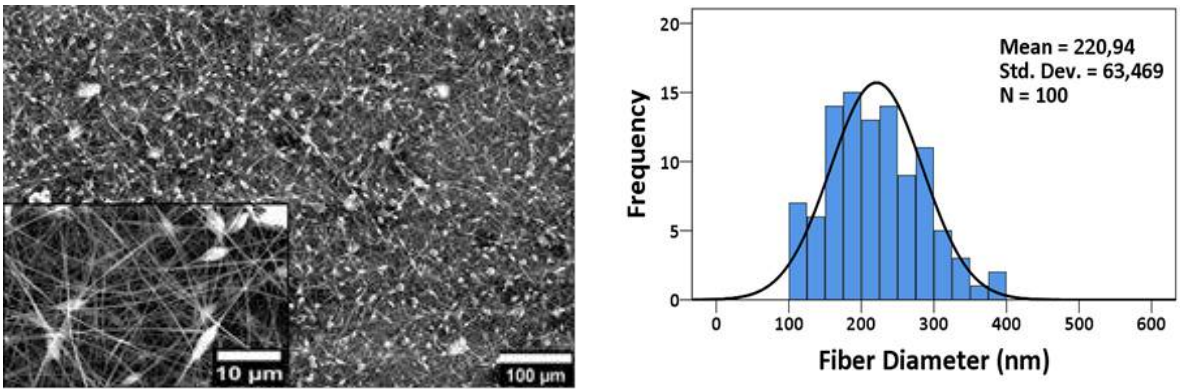

PVP0

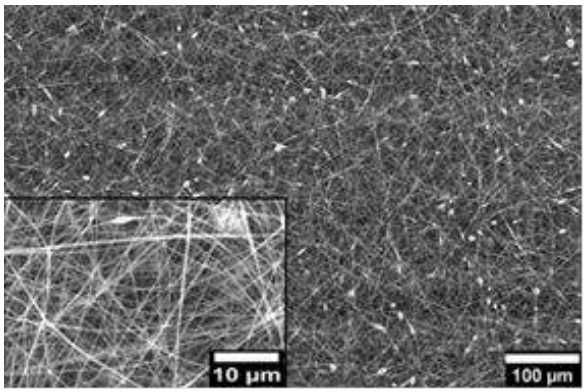

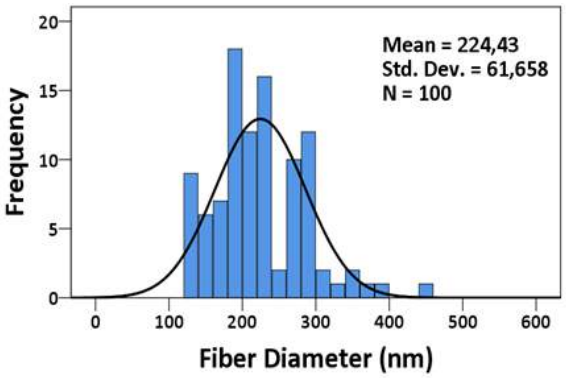

PVP2.5

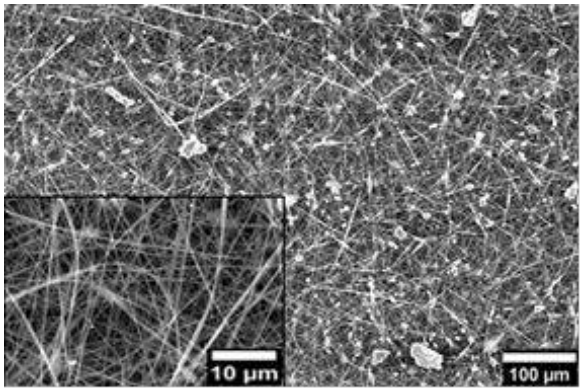

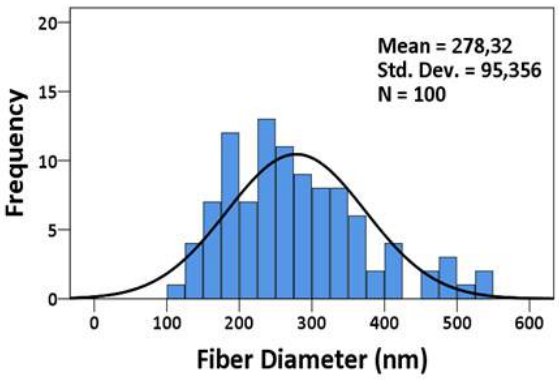

PVP5

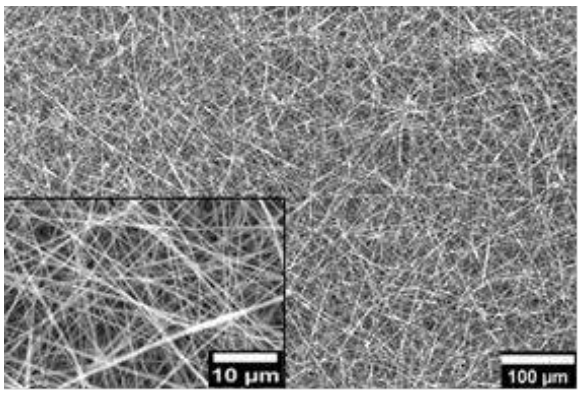

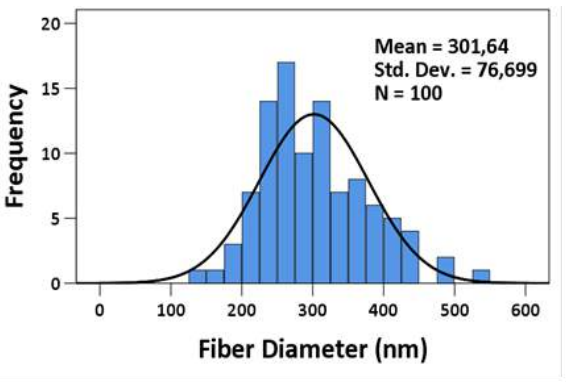

PVP7.5

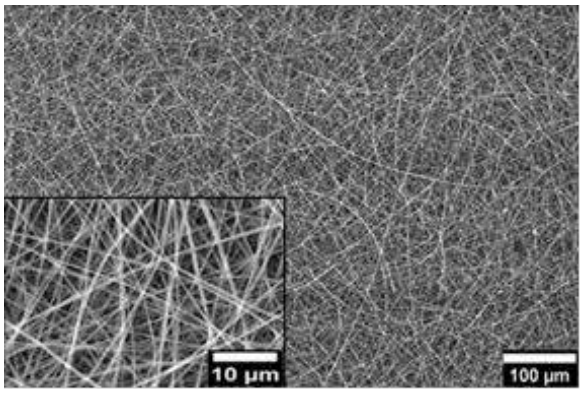

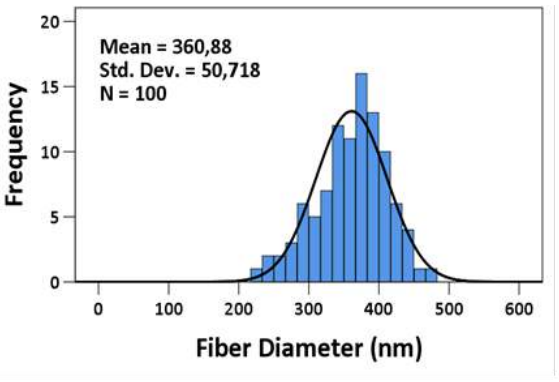

PVP10

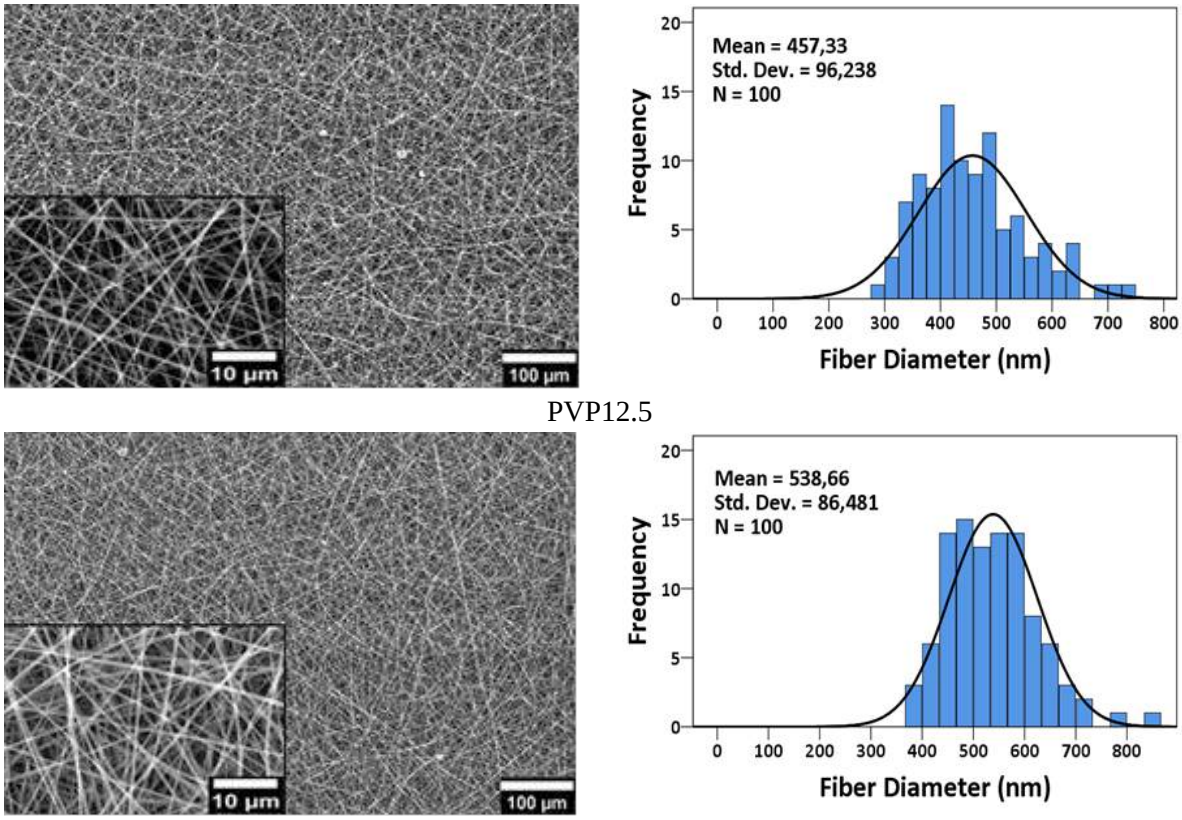

Figure 2. SEM images of PVP nanofibers with various concentrations of carvacrol:lanolin

It has been seen clearly that nanofiber morphology improved with carvacrol:lanolin concentrations. There are some bead defects in the nanoweb structure for concentrations of 0, 2.5, and 5 wt. % of carvacrol:lanolin. However, after these concentrations, nanoweb quality changed significantly. It is possible to say that nanofibers are quite fine, smooth and uniform for 7.5, 10, 12.5 and 15 wt % carvacrol:lanolin concentrations. Due to the fact that the interaction between macromolecules increased as solution viscosity increased, fiber spinning performance increased while beads decreased. Viscosity is known to influence the interaction between macromolecules (Cengiz Çallıoğlu and Kesici Güler, 2019). In electrospinning, it is well known that higher viscosity and lower conductivity result in less stretching of the jet, therefore producing thicker nanofibers (Bhardwaj and Kundu, 2010). When the histograms are analyzed, it can be said that all samples have a single peaked and unimodal distribution. Average fiber diameter and fiber diameter uniformity coefficient graph is given in Figure 3.

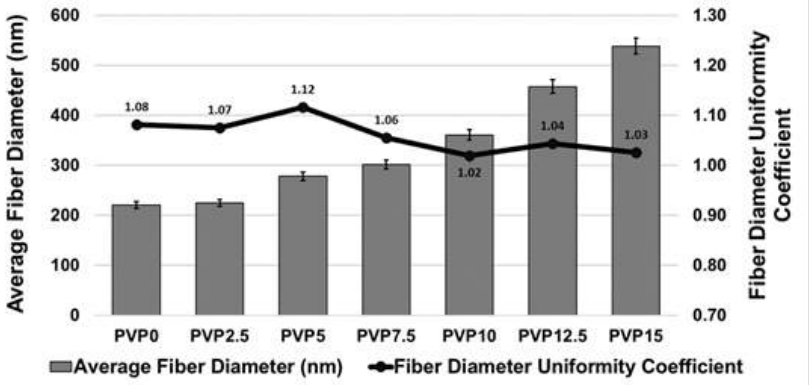

Figure 3. Average fiber diameter and fiber diameter uniformity coefficient of PVP nanofibers produced with various concentrations of carvacrol:lanolin

According to the Figure 3, it was determined that average fiber diameter increased and fiber diameter uniformity coefficient did not affected carvacrol:lanolin concentration. According to the viscosity results, it is expected that average fiber diameter increased from 220 (PVP0) to 538 (PVP15) nm with lanolin carvacrol concentrations. With 1.02, the most uniform nanofibers were obtained in the PVP10 sample. However, it is possible to say that the bead-free samples such as PVP7.5, PVP10, PVP12.5, and PVP15 are all uniform. As a nanofiber morphology results, it is possible to say that PVP10 were selected optimum sample in order to average fiber diameter, fiber diameter distribution, fiber uniformity and fiber morphology.

FT-IR spectrums of PVP, lanolin (LAN), carvacrol (CAR), and PVP10 nanofibers are given in Figure 4.

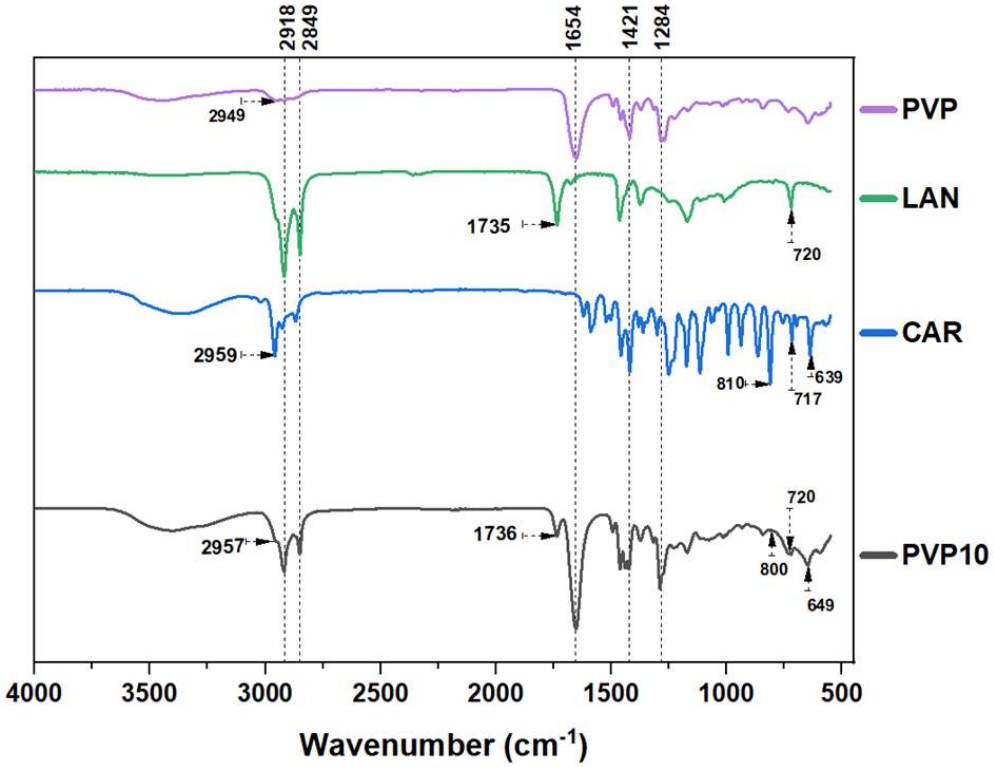

Figure 4. FT-IR spectra of PVP, LAN, CAR, and PVP10 nanofibers

FT-IR spectrums demonstrated that all characteristics peaks of PVP, lanolin and carvacrol arise in the spectra of the PVP10 nanofibers. This means, there was not undesirable reactions while preparing polymer solutions. In details, there is a sharp peak at 3434 cm^{-1} in the spectra of PVP. The O-H peak can attribute to the presence of water. The peak determined at 3403 cm^{-1} in the PVP10 spectra with an increase of intensity. Because, at this wavelength, carvacrol also has a wide peak. Since these two peaks overlapped in the PVP10 sample, the intensity of the peak increased. Another strong peak at 1654 cm^{-1} identified the existence of heteroatomic molecules and carbonyl groups in the pyrrolidone ring of PVP as a sign of C=O stretching. The peak arises at the same wavelength in the spectra of PVP10 (Kim et al., 2013; Yu et al., 2009; Torres-Giner et al., 2017). The most intense peak in the spectrum of carvacrol occurred at 811 cm^{-1} (C–H wagging vibrations). This peak also appears at 800 cm^{-1} in the spectra of PVP10. Additional peaks in the carvacrol spectrum at 639 cm^{-1} (C=C) and this peak also arise 649 cm^{-1} in the spectra of PVP10 (Daferera et al., 2002; Schulz et al., 2005). There are two characteristic absorption peaks at 2918 cm^{1} and 2849 cm^{-1} could be attributed to $–CH_2–$ and $–CH_3$. Another characteristic two peaks are at 1735 cm^{-1} and 720 cm^{-1} namely cis-CH=CH and

carbonyl compounds (Hassan and Collie, 2015; Lazzari and Chiantore, 1999). All of these characteristic peaks also appeared spectra of PVP10 nanofibers.

4. CONCLUSION

In this work, it is achieved to produce and characterize PVP based carvacrol and lanolin loaded composite nanofibers successfully. Pure PVP solution based nanofibers had a lot of bead defects but nanofibrous web quality was improved with addition of carvacrol:lanolin to the PVP polymer solutions with same PVP concentration. In this way, very smooth, fine, homogeneous, and uniform fibers were obtained without increasing the polymer concentration and without increasing the average fiber diameter too much. In addition, the chemical structure of the nanowebs was investigated by FT-IR analysis. No undesirable reaction occurred between the components during the preparation of the polymer solution including many components, and all the components in the polymer solution in the produced nanowebs were chemically determined. Considering the properties of carvacrol and lanolin in the content of biocompatible nanofiber surfaces, it is thought that there is a potential for use in the biomedical application areas especially as a wound dressing.

ACKNOWLEDGMENT

This research was supported by Süleyman Demirel University Scientific Research Project Funding Unit, Project No: Project No: FYL-2018-5824. The authors would like to thank Süleyman Demirel University Natural Products Application and Research Center for supplying carvacrol.

REFERENCES

Abou-Dakn, M., Fluhr, J. W., Gensch, M., & Woeckel, A. (2011). Positive effect of HPA lanolin versus expressed breastmilk on painful and damaged nipples during lactation. Skin pharmacology and physiology, 24(1), 27-35.

Altan, A., Aytac, Z., & Uyar, T. (2018). Carvacrol loaded electrospun fibrous films from zein and poly (lactic acid) for active food packaging. Food Hydrocolloids, 81, 48-59.

Bhardwaj, N., & Kundu, S. C. (2010). Electrospinning: a fascinating fiber fabrication technique. Biotechnology advances, 28(3), 325-347.

Çallıoğlu, F. C., Güler, H. K., & Çetin, E. S. (2019). Emulsion electrospinning of bicomponent poly (vinyl pyrrolidone)/gelatin nanofibers with thyme essential oil. Materials Research Express, 6(12), 125013.

Cengiz, F., & Jirsak, O. (2009). The effect of salt on the roller electrospinning of polyurethane nanofibers. Fibers and Polymers, 10(2), 177-184.

Daferera, D. J., Tarantilis, P. A., & Polissiou, M. G. (2002). Characterization of essential oils from Lamiaceae species by Fourier transform Raman spectroscopy. Journal of Agricultural and Food Chemistry, 50(20), 5503-5507.

Haghi, A. K. (2011). Advances in nanofibre research. Smithers Rapra.

Hassan, M. M., Barker, H., & Collie, S. (2015). Enhanced corrosion inhibition of mild steel by cross-linked lanolin-coatings. Progress in Organic Coatings, 78, 249-255.

Kim, G. M., Le, K. H. T., Giannitelli, S. M., Lee, Y. J., Rainer, A., & Trombetta, M. (2013). Electrospinning of PCL/PVP blends for tissue engineering scaffolds. Journal of Materials Science: Materials in Medicine, 24(6), 1425-1442.

Kordali, S., Cakir, A., Ozer, H., Cakmakci, R., Kesdek, M., & Mete, E. (2008). Antifungal, phytotoxic and insecticidal properties of essential oil isolated from Turkish Origanum acutidens and its three components, carvacrol, thymol and p-cymene. Bioresource Technology, 99(18), 8788-8795.

Lazzari, M., & Chiantore, O. (1999). Drying and oxidative degradation of linseed oil. Polymer degradation and stability, 65(2), 303-313.

Paster, N., Menasherov, M., Ravid, U., & Juven, B. (1995). Antifungal activity of oregano and thyme essential oils applied as fumigants against fungi attacking stored grain. Journal of food protection, 58(1), 81-85.

Schulz, H., Özkan, G., Baranska, M., Krüger, H., & Özcan, M. (2005). Characterisation of essential oil plants from Turkey by IR and Raman spectroscopy. Vibrational Spectroscopy, 39(2), 249-256.

Torres-Giner, S., Wilkanowicz, S., Melendez-Rodriguez, B., & Lagaron, J. M. (2017). Nanoencapsulation of Aloe vera in synthetic and naturally occurring polymers by electrohydrodynamic processing of interest in food technology and bioactive packaging. Journal of agricultural and food chemistry, 65(22), 4439-4448.

Uzun, M., & Oymak, H. (2022). Polylactic acid and lanolin based nanofibrous structures for wound management application. Indian Journal of Fibre & Textile Research, 47, 105-115.

Wang, L., Chang, M. W., Ahmad, Z., Zheng, H., & Li, J. S. (2017). Mass and controlled fabrication of aligned PVP fibers for matrix type antibiotic drug delivery systems. Chemical Engineering Journal, 307, 661-669.

Yu, D. G., Shen, X. X., Branford-White, C., White, K., Zhu, L. M., & Bligh, S. A. (2009). Oral fast-dissolving drug delivery membranes prepared from electrospun polyvinylpyrrolidone ultrafine fibers. Nanotechnology, 20(5), 055104.

ELECTROSPINNING OF PCL/OVALBUMIN NANOFIBERS

Mustafa GEYSOĞLU[1], Funda CENGİZ ÇALLIOĞLU[2]

[1] Suleyman Demirel University, Department of Textile Engineering, Izmir, Türkiye
[2] Suleyman Demirel University, Graduate School of Natural and Applied Sciences, Bioengineering Department, Isparta, Türkiye

Corresponding author: fundacengiz@sdu.edu.tr

Abstract: *In this study, electrospun Polycaprolactone/Ovalbumin (PCL/OVA) nanofibers were prepared successfully and then, these nanofibers were characterized both morphologically and chemically. The PCL concentration in the solutions was kept constant at 7 wt %. Various concentrations of ovalbumin were added to the PCL polymer solutions such as 0, 1, 5 and 9 wt % respectively. Before the electrospinning process, the solution properties were measured. The viscosity, conductivity and surface tension of the solutions increased with concentration increasement of ovalbumin. The electrospinning process was carried out under the optimum process parameters and ambient conditions. Smooth, uniform and homogeneous fibers were obtained by electrospinning. The SEM and FT-IR analyzes were performed in terms of characterization studies. When the SEM images were examined, particles of ovalbumin were seen on the web surface. According to the results of FT-IR analyzes, the presence of PCL and ovalbumin was chemically proven in the produced nano web.*

Keywords: *Polycaprolactone, ovalbumin, electrospinning, nanofiber.*

1. INTRODUCTION

Proteins are one of the primary constituents of living matter and also have a crucial value to nanofibers structure in terms of end uses. They are divided into two main classifications depending upon their source such as plant and animal proteins. To obtain electrospun nanofibers, plant proteins (such as zein, soy protein, gluten and amaranth protein) and animal proteins (such as casein, silk fibroin, tussah silk, elastin, gelatin, keratin, bovine serum albumin, fibrinogen, hemoglobin, collagen (Yardımcı and Tarhan, 2020; Babitha et al., 2017) and ovalbumin (Zahedi and Fallah-Darrehchi, 2015) are used widely.

Ovalbumin is the most important constituents of egg white proteins which has more than 40 varieties (Razi et al., 2018). Ovalbumin, which is a biodegradable, biocompatible, non-toxic and noncarcinogenic natural biopolymer (Zahedi and Fallah-Darrehchi, 2015), constitutes about 55% of the total proteins in egg white (Sheng et al., 2018). It has a wide range of uses in the medical field such as wound dressing, tissue regeneration, crosslinking agent. Also it is a suitable reagent to control drug release (Zahedi and Fallah-Darrehchi, 2015; Patel et al., 2021; Yadav and Kandasubramanian, 2013).

Polycaprolactone (PCL) is a synthetic biodegradable, semi-crystalline and hydrophobic polymer. The advantages of PCL are resistance of water, oil, solvent and chlorine, nontoxic, highly porous and inexpensive (Mohamed and Yusoh, 2016; Duling et al., 2008). Besides of these advantages, its good solubility, low melting point, and exceptional blend compatibility have supported extensive research into its potential application in the biomedical field (Temtem et al, 2008; Mohamed and Yusoh, 2016). PCL has a wide range of application area, especially in the biomedical field such as implants, tissue engineering, controlled drug release, wound dressing and is also used in the packaging (Mohamed and Yusoh, 2016, Duling et al., 2008).

In this study, electrospinning and characterization of PCL/ovalbumin nanofibers were achieved. According to the literature studies about electrospun nanofibers with ovalbumin are very limited. It is aimed to expand the use of ovalbumin nanofibers in the medical field by combining the superior properties of ovalbumin with biodegradable PCL polymer. Also it is thought that the results obtained from this study will be useful to the literature on biomedical textile materials.

2. MATERIALS AND METHODS

2.1. Materials

In this study the following materials were used: Polycaprolactone (average M_n 80,000) as a polymer, ovalbumin (62-88% (agarose gel electrophoresis)) as an active ingredient, chloroform and dimethylformamide (DMF) as the solvents. All materials were purchased from Sigma–Aldrich (St. Louis, MO, USA).

2.2 Preparation and Characterization of Polymer Solutions

The PCL polymer concentration was kept constant at 7 wt %. According to our previous studies, the ratio of chloroform:DMF was determined as 8:2. Firstly, PCL polymer was dissolved in chloroform and DMF. Then, different concentrations of ovalbumin such as 0, 1, 5, 9 wt % were added into the PCL solutions. The ovalbumin concentrations used are given in Table 1 along with the sample codes. All solutions were stirred at room temperature about 24 hours. After the solutions were prepared, the properties of solutions such as conductivity, viscosity and surface tension were measured. The conductivity of solutions was determined by Extech, ExStik II EC 500 conductivity meter device. The viscosity was measured by Lamy Rheology, B-One Touch Screen viscometer, with measurements achieved under 5 s^{-1} shear rates.

Table 1. The PCL/Ovalbumin solutions with sample codes

Sample Codes	PCL Polymer Concentration (%)	Ovalbumin Concentration (%)
OVA0	7	0
OVA1	7	1
OVA5	7	5
OVA9	7	9

2.3 Production and Characterization of Nanofibers

The nanofiber production was carried out via electrospinning under the optimized process parameters given in Table 2.

Table 2. Process parameters of the electrospinning

Voltage (kV)	Distance Between Electrodes (cm)	Feed Rate (mL/h)	Humidity (%)	Temperature (°C)
20	18	0.35	45	25

After the electrospinning process, the nanofiber morphology such as, web surface structure, fiber diameter, fiber diameter uniformity, was analyzed by scanning electron microscope (SEM). Average fiber diameters were calculated by image J analysing software. The SPSS statistics program was used

to obtain fiber diameter histograms. FT-IR was performed to determine the presence of PCL and ovalbumin in the nanofiber structure chemically.

3. RESULTS AND DISCUSSION

3.1. Solution Properties Results

When the solution properties were examined in Figure 1, it was observed that the conductivity and viscosity of solutions increased with the ovalbumin concentration increasement. However, surface tension decreased with ovalbumin addition, and then increased ovalbumin concentration increasement.

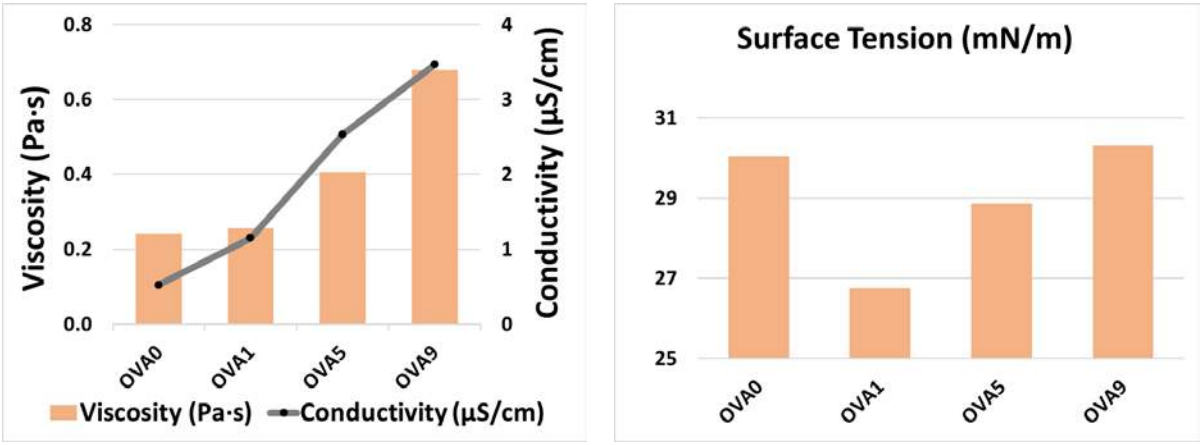

Figure 1. Results of solution properties such as, viscosity, conductivity and surface tension

The viscosity of the solution without ovalbumin (OVA0) was 0.24 Pa·s. With the addition of 1 wt % ovalbumin, there was no notable change in the viscosity value (OVA1=0.25 Pa·s). However, it is seen that there is an increasing trend in the viscosity value with the increasement of ovalbumin. The viscosity values of the OVA5 and OVA9 solutions were 0.41 Pa·s and 0.68 Pa·s respectively. These results are also compatible with the literature (Kesici Güler et al., 2019).

Conductivity values also show a similar trend to viscosity. The solution of ovalbumin-free has the lowest conductivity (0.52 µS/cm). The conductivity value increases with the increasement of ovalbumin concentration. OVA1, OVA5 and OVA9 solutions have conductivity values of 1.15, 2.53 and 3.47 µS/cm, respectively. When we compare the conductivity values with the literature, it is seen that the values are quite low (Cengiz Çallıoğlu, and Kesici Güler, 2020).

When the surface tension values are examined, it is seen that adding ovalbumin (1 wt %) reduces the surface tension value. However, with the increasement of ovalbumin concentration, the surface tension increases again. It was determined that the surface tension value of the solution with 9 wt % ovalbumin concentration (OVA9) was similar to the solution without ovalbumin (OVA0). The surface tension of OVA0 is 30 mN/m while OVA9 is 30.3 mN/m. OVA1 solution has 26.7 mN/m surface tension value and OVA5 has 28.9 mN/m.

3.2. Fiber Morphology Results

SEM images and histogram curves of nanofibers with various concentrations of ovalbumin are given in Figure 2. It was observed from Figure 2 that ovalbumin-free nanofibers (OVA0) have a smooth and uniform surface. But the average fiber diameter is higher than the others.

Ovalbumin addition resulted in a remarkable reduction of fiber diameters. The addition of ovalbumin reduced the fiber diameter approximately 100 nm. Besides, the average fiber diameter was not affected significantly by the variation of ovalbumin concentration. Average fiber diameter was measured as OVA1 343 nm, OVA5 337 nm, and OVA9 333 nm. Fine and smooth fibers were obtained at all concentrations of ovalbumin. But it is seen that some particles were formed on the web surface with the addition of ovalbumin.

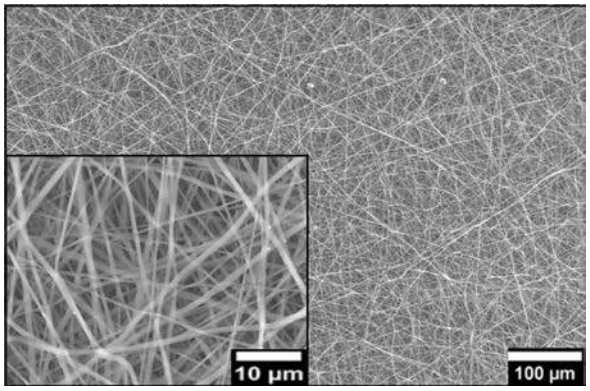

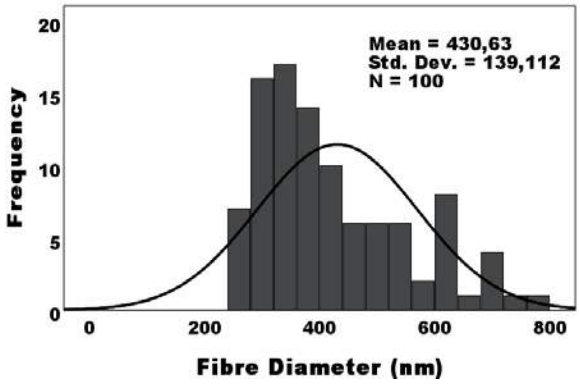

OVA0

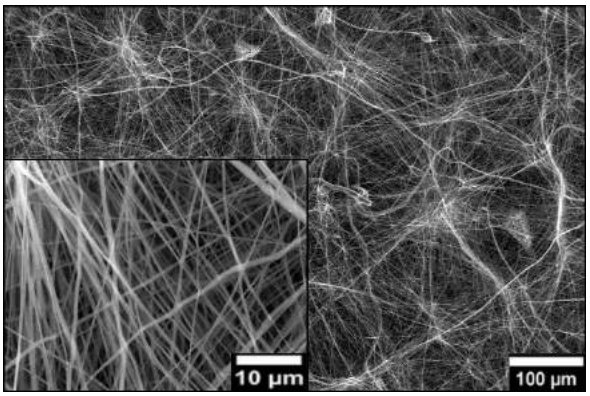

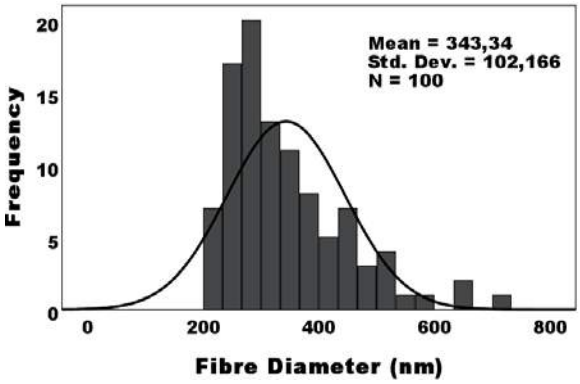

OVA1

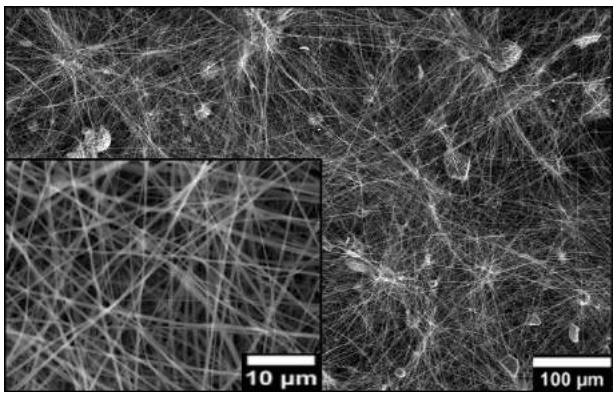

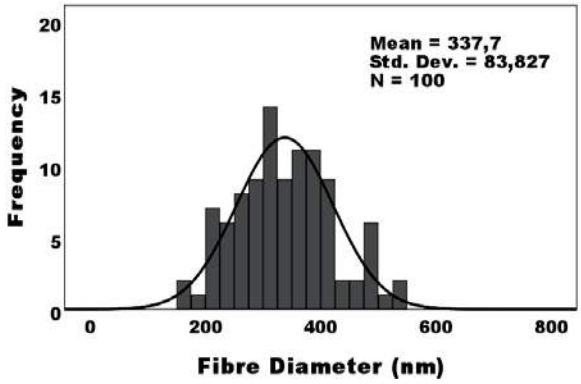

OVA5

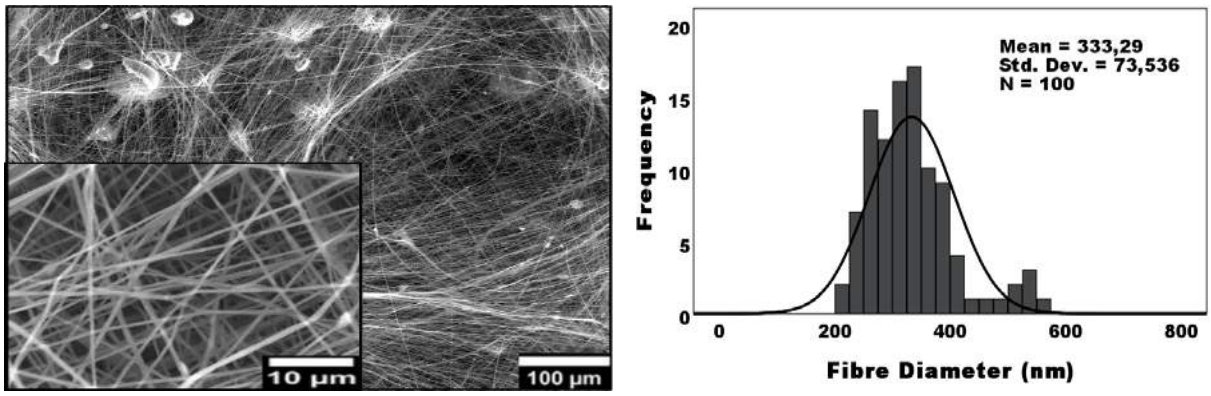

OVA9

Figure 2. SEM images and histograms of PCL nanofibers with various concentrations of ovalbumin

In Figure 3, effect of ovalbumin concentration on the average fiber diameter and fiber diameter uniformity coefficient was given.

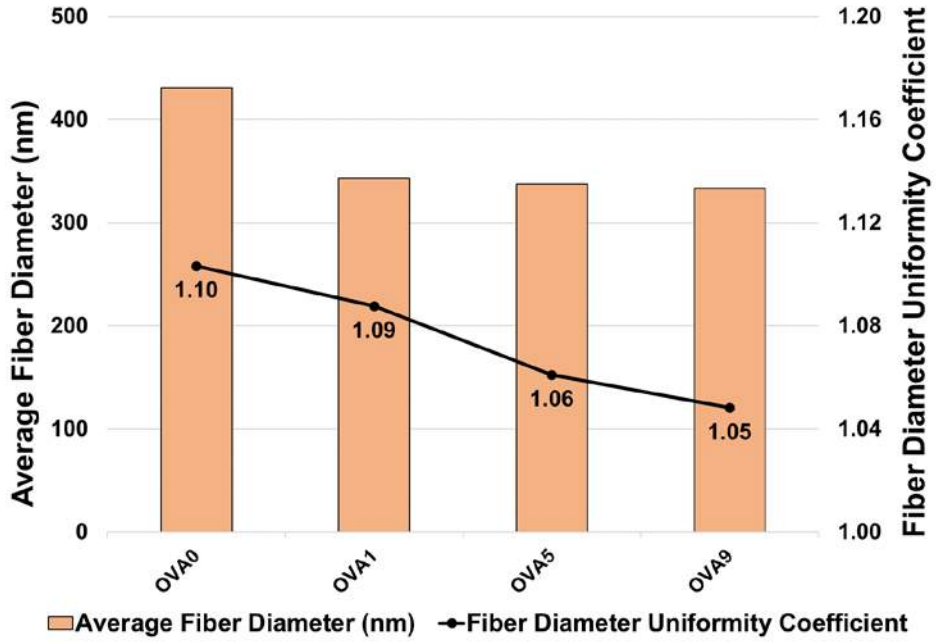

Figure 3. The effect of ovalbumin concentrations on the average fiber diameter and fiber diameter uniformity coefficient

When Figure 3 is examined, it is clearly seen that the addition of ovalbumin decreases the average fiber diameters. The smoothest fibers were obtained from the OVA9 sample with the 9 wt% ovalbumin concentration solution. The average fiber diameter obtained with this solution is 333 nm. The fiber diameter uniformity coefficient value is 1.1 for OVA0 sample without ovalbumin. On the other hand, the fiber diameter coefficient of OVA9 is 1.05. The fiber diameter uniformity coefficient value close to 1 means that it has a smooth fiber structure. This means that OVA9 has a more uniform fiber diameter than other fibers.

3.3. FT-IR Analyzes Results

FT-IR analysis was carried out to chemically reveal the presence of PCL and ovalbumin structures in the nanofibers. Figure 4 represents the FT-IR spectra of PCL polymer, ovalbumin and the nanofibers

obtained from them. The characteristic peaks were observed at the FT-IR spectra of PCL. PCL spectrum shows characteristic peaks at 2943 cm^{-1} and 2867 cm^{-1} that can be referred to the asymmetric and symmetric CH_2 stretching, respectively. Asymmetric CH_2 stretching peak was identified at 2944 cm^{-1} and symmetric CH_2 stretching was found at 2866 cm^{-1} in all PCL-based nanofibers. The sharp peak at 1722 cm^{-1} was the signal of C=O (carbonyl) stretching. This peak appeared prominently in nanofibers spectrums. The other remarkable peak at 1171 cm^{-1} corresponds to the symmetrical C-O-C stretch peak. And also, this peak was found in the nanofiber spectrum at 1166 cm^{-1} wavelength (Biscaia et al., 2015).

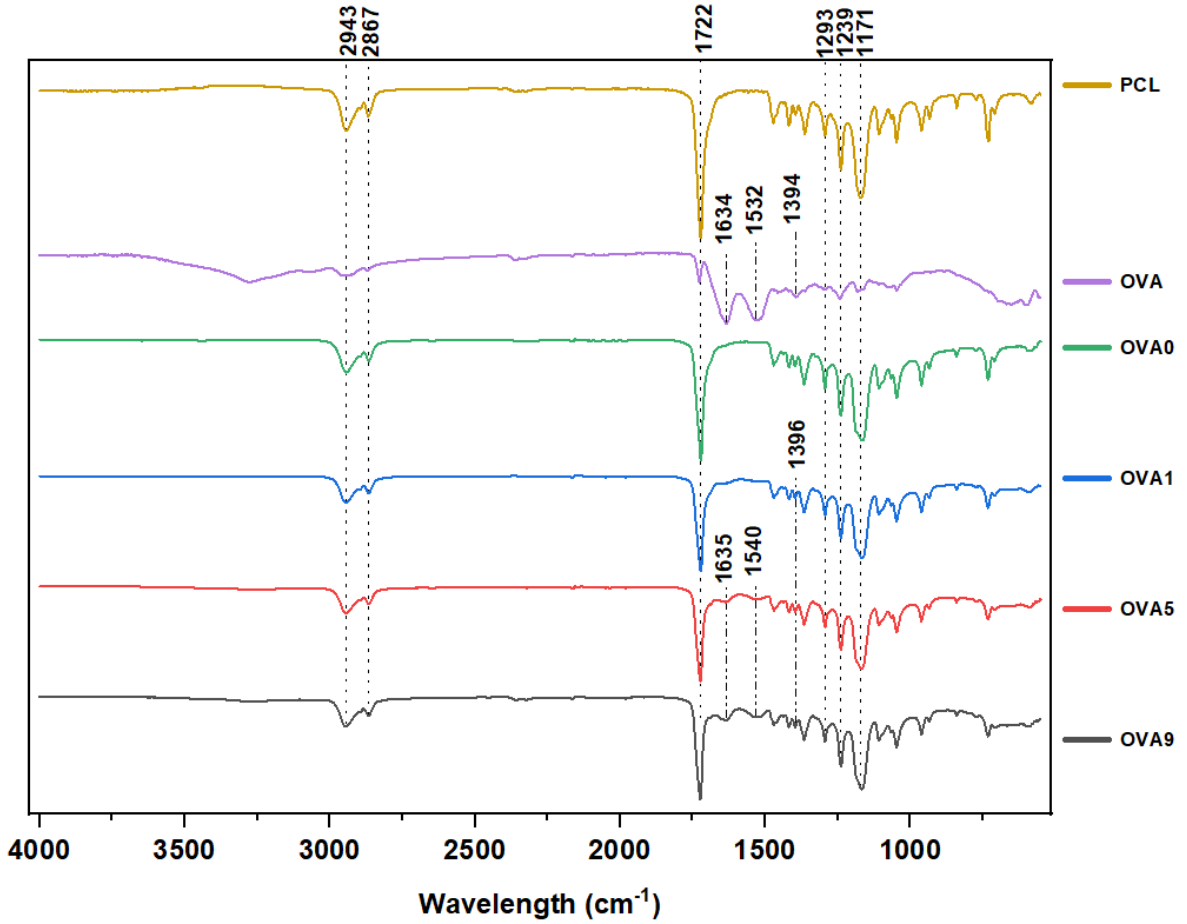

Figure 4. FT-IR spectra of PCL, ovalbumin and the nanofibers

In the spectrum of ovalbumin in Fıgure 4, the amide I band appeared at 1634 cm^{-1} (C=O stretch) and the amide II band at 1532 cm^{-1} (C-N stretch combined with the N-H bending mode), which shows the characteristic bands of the proteins (Bakkialakshmi and Barani, 2013). The OVA5 and OVA9 nanofibers spectrums showed these peaks at 1635 cm^{-1} and 1540 cm^{-1}, but not seen in the OVA1 nanofiber spectrum. The reason for this is considered to be the low concentration of ovalbumin. In addition, FT-IR spectra of ovalbumin showed at 1394 cm^{-1} for aliphatic C-H bending vibration. This peak was observed at 1396 cm^{-1} in all nanofibers containing ovalbumin (Jana et al., 2014).

FT-IR spectroscopy revealed the presence of PCL and ovalbumin structures of the nanofibers chemically.

4. CONCLUSION

In this study, it is successfully achieved to produce and characterize PCL/Ovalbumin nanofibers. When the solution properties were examined, it was observed that the viscosity, surface tension and conductivity were increased with ovalbumin concentration increasement. With the addition of ovalbumin, it was seen that particles were formed on the web surface, on the other hand average fiber diameter was reduced. It was clearly noticed that smooth, uniform and homogeneous fibers were obtained at all concentrations. By FT-IR analysis, the presence of PCL and ovalbumin proved in the chemical structure of the nanofibers. Considering the remarkable properties and applications of nanofibers that produced with biocompatible PCL polymer and ovalbumin protein, it is thought that they have the potential to be used in the medical field, especially in wound dressing.

ACKNOWLEDGMENT

The authors would like to express appreciation for the financial support of the Süleyman Demirel University Scientific Researches Project Unit (Project Number = FDK-2019-7164).

REFERENCES

Yardımcı, A. İ., & Tarhan, Ö. (2020). Electrospun protein nanofibers and their food applications. Mugla *Journal of Science and Technology*, 6(2), 52-62.

Babitha, S., Rachita, L., Karthikeyan, K., Shoba, E., Janani, I., Poornima, B., & Sai, K. P. (2017). Electrospun protein nanofibers in healthcare: A review. *International journal of pharmaceutics*, 523(1), 52-90.

Patel, P. R., Pandey, K., Killi, N., & Gundloori, R. V. N. (2021). Manipulating hydrophobicity of polyester nanofiber mats with egg albumin to enhance cell interactions. *Polymer Engineering & Science*, 61(10), 2496-2510.

Razi, S., Motamedzadegan, A., Shahidi, S., & Rashidinejad, A. (2018). Basil seed gum enhances the rheological and physical properties of egg albumin foams. *Food Nutrition J*: FDNJ-192. DOI, 10, 2575-7091.

Zahedi, P., & Fallah-Darrehchi, M. (2015). Electrospun egg albumin-PVA nanofibers containing tetracycline hydrochloride: Morphological, drug release, antibacterial, thermal and mechanical properties. Fibers and Polymers, 16(10), 2184-2192.

Sheng, L., Huang, M., Wang, J., Xu, Q., Hammad, H. H. M., & Ma, M. (2018). A study of storage impact on ovalbumin structure of chicken egg. Journal of Food Engineering, 219, 1-7.

Yadav, R., & Kandasubramanian, B. (2013). Egg albumin PVA hybrid membranes for antibacterial application. Materials Letters, 110, 130-133.

Mohamed, R. M., & Yusoh, K. (2016). A review on the recent research of polycaprolactone (PCL). Advanced materials research, 1134, 249-255.

Duling, R. R., Dupaix, R. B., Katsube, N., & Lannutti, J. (2008). Mechanical characterization of electrospun polycaprolactone (PCL): a potential scaffold for tissue engineering. Journal of biomechanical engineering, 130(1).

Temtem, M., Casimiro, T., Mano, J. F., & Aguiar-Ricardo, A. (2008). Preparation of membranes with polysulfone/polycaprolactone blends using a high pressure cell specially designed for a CO2-assisted phase inversion. The Journal of Supercritical Fluids, 43(3), 542-548.

Kesici Güler, H., Cengiz Çallıoğlu, F., & Sesli Çetin, E. (2019). Antibacterial PVP/cinnamon essential oil nanofibers by emulsion electrospinning. The journal of the Textile Institute, 110(2), 302-310.

Çallıoğlu, F. C., & Güler, H. K. (2020). Production of essential oil-based composite nanofibers by emulsion electrospinning. Pamukkale Üniversitesi Mühendislik Bilimleri Dergisi, 26(7), 1178-1185.

Biscaia, S. I., Viana, T. F., Almeida, H. A., & Bártolo, P. J. (2015). Production and characterisation of PCL/ES scaffolds for bone tissue engineering. *Materials Today: Proceedings*, *2*(1), 208-216.

Bakkialakshmi, S., & Barani, V. (2013). FTIR study on the interaction of quercetin and amantadine with egg albumin. International Journal of Pharmaceutical, Chemical & Biological Sciences, 3(3).

Jana, S., Manna, S., Nayak, A. K., Sen, K. K., & Basu, S. K. (2014). Carbopol gel containing chitosan-egg albumin nanoparticles for transdermal aceclofenac delivery. Colloids and surfaces B: Biointerfaces, 114, 36-44.

TEMPERATURE REGULATING POLYESTER SHORT STAPLE RING SPUN YARNS BY PCM NANOCAPSULE APPLICATION

Demet YILMAZ[1], Sennur Alay AKSOY[1]

[1] Suleyman Demirel University, Department of Textile Engineering, Isparta, Türkiye

Corresponding author: demetyilmaz@sdu.edu.tr

Abstract: *In this study, 1-teteradecanol phase change material (PCM) was nanoencapsulated into the poly(methyl methacrylate-co-methacrylic acid) wall by emulsion polymerization method and applied to the staple polyester yarn structure using the developed alternative capsule application process.*
The aim of the study was to develop an alternative application process that would allow nanocapsules to be included in the short staple yarn structure in the ring yarn production process and to use this process to produce polyester staple rin spun yarns containing nanocapsules. According to the results of the study, it was determined that nanocapsules with dimensions around 200-400 nm, uniform size distribution and spherical morphology were produced, they could store approximately 100 j/g heat and had sufficient thermal resistance. With the developed process, nanocapsules were successfully applied to the ring spun yarn structure. The yarns with temperature regulation function which exhibited temperature differences in the range of 2-5 °C compared with undoped reference ring spun yarns were produced.

Keywords: *Functional textiles, technical textile yarns, ring spinning, microcapsule, phase change materials (PCM), polyester yarn.*

1. INTRODUCTION

Phase change materials (PCMs) are among the smart materials. PCMs can store and release high latent heat energy as their physical state changes under the nearly isothermal condition and therefore show a temperature regulation effect by absorbing and emitting heat energy in a certain temperature range depending on the changes in ambient temperature. Thanks to the heat exchange properties of PCMs, it is possible to improve thermal comfort in clothes and to provide heating and cooling effects (Mattila, 2006; Mondal, 2008; Tao, 2008). Textile materials containing PCMs not only provide dynamic insulation properties (buffering effect against temperature change) in clothing fabrics, but also provide heating or cooling effects in different environmental conditions, in case of sudden temperature changes. Today, the use of PCMs in the textile industry is becoming increasingly important to improve the thermal comfort of clothing and to eliminate the effects such as sweating and sudden changes in body temperature as a heat regulator. Furthermore, the usage of PCMs has gained importance for the protection in extreme conditions and for the performance increase of professional athletes. The majority of PCMs, particularly paraffinic solid-liquid phase change PCMs, are used after microencapsulation. Encapsulation is a packaging technology that a tiny particle or droplet is enveloped by an organic or inorganic wall in order to develop micro or nano-sized capsules. Microencapsulation is an effective method in terms of reducing the interaction of the PCMs with the environment, preventing its separation from the textile structure by flowing when it enters the liquid phase, increasing the permanence in the textile structure, increasing the heat transmission surface and providing a constant volume (Sarıer and Önder, 2007; Önder et al., 2008). The application of PCMs to textile structures focuses on synthetic fiber production and fabric finishing. However, the methods used in the current microcapsule application have some important disadvantages. They can be summarized as reduced thermal conductivity, softness, flexibility, breathability or moisture transport

capability of textiles, and non-durable thermal properties in the final products. In this study, different present application methods, it is aimed to produce innovative yarns that can offer latent heat storage/dissipation and heat regulation (thermoregulation) properties by applying PCM nanocapsules to yarns obtained from staple fibers. In literature, Zhang et al. (2006) and Gao et al. (2009) stated that the incorporation of MPCM during fiber spinning process is a promising approach which can enhance the life time of the thermo-regulating effect of the woven or knitted fabrics made of such filament. From this point of view, in the study, FDM nanocapsules were applied to polyester fibers with an alternative method and ring spun yarns with Ne 30/1 yarn count (knitted twist) were produced. To the best of our knowledge, no article has, to date, focused on integration of the PCMs to the spun yarns from polyester staple fibres and this application is a new method for the thermo-regulating functional yarn production.

2. MATERIALS AND METHODS

2.1. Microcapsules Preparation and Characterization

Emulsion polymerization method was performed to synthesize nanocapsules. In nanocapsule production, wall polymer was synthesized with methyl methacrylate (MMA, Sigma-Aldrich) monomer and methacrylic acid (MAA, Sigma-Aldrich) comonomer. 1-tetradekanol (Alfa Aesar, %97+) was used as the core phase change material of the nanocapsules. PEG 1000 (Sigma Aldrich; Merck) was used as emulsifier and ethylene glycol dimethacrylate (EGDM, Sigma-Aldrich; Merck) was used as cross-linker. 2,2-Azobis(2-methyl-propionamidine) dihydrochloride (Acros Organics) was used as initiator in order to form free radicals and initiate addition polymerization via monomeric radicals. In the production of nanocapsules, the wall/core ratio was used as 1/1. In the first stage of production, 32.5 g of 1-tetradecanol was added in a 500 ml of deionized water heated to 50 °C and mixed at 1000 rpm for about 20 minutes. In order to emulsify 1-tetradecanol in the water phase, 10 g of PEG1000 was added to mixture and the emulsion was prepared by stirring at 1000 rpm for 30 minutes. A 29 g of MMA and a 3.5 g of MAA (approximately 12% by weight of comonomer) monomers, a 6.75 g of EGDM cross-linker and a 5 g of initiator were added to the emulsion. After the addition of each component, mixing was done for 5 minutes and finally the temperature was increased to 80 °C. The nanocapsule production process was completed after the reaction, which was carried out at 1000 rpm, at 80 °C for 3 hours. The produced nanocapsules were washed several times with hot water at 70 °C, then rinsed, filtered and stored in a refrigerator (+8 °C).

2.2. Method

In this study, an alternative method was used to impart the microcapsules into the staple polyester fiber bundle before the yarn formation. An alternative application method developed in previous study of the authors was used for production of the PCM nanocapsule doped composite ring yarns (Yılmaz et al., 2021). The method based on integrating the PCM nanocapsules into the open fibre bundle before yarn twisting during the ring spinning process and hence trapping the capsules in the twisted yarn structure. In the study, yarn production was realized by conventional ring spinning machine (Rieter G10 model) due to its widely usage in the spun yarn production and also proving superior yarn properties. In the method, a dispersion including PCM nanocapsules was prepared and then applied to the polyester fibres during the ring spun yarn production via a special feeding system. Nanocapsule dispersion contained surfactant (S), defoamer (D), water and also PMMA-co-MAA/1-tetradecanol nanocapsules. Mechanical homogenizer (IKA ULTRA-TURRAX® T 18 basic) and sonic mixer (BANDELIN SONOPULS HD 4200) devices were used to dispers nanocapsules in the water homogeneously. Nanocapsule concentration was determined by Alay Aksoy et al. as 6% based on their previous findings (Anayurt etc., 2017). It is worth noting that a nanocapsule concentration of 6%

is one of the lowest concentration values used for nanocapsule fabric applications. After the preparation of microcapsule dispersion, the mixtures were applied to staple fibres by the developed alternative method. With the application to the open fibre bundle, it is possible to integrate the capsules into the inner and outer parts of the yarn. In the study, Ne 30/1 polyester ring spun yarns were produced by using 2 different feeding rates of 62.5 mL/h and 80.0 mL/h. Yarn production parameters such as draft and spindle speed were kept constant during the yarn production.

2.3. Test and analysis

The thermal properties of the produced nanocapsules were investigated by DSC and TGA methods. Their morphology was characterized by SEM. The yarn samples without nanocapsules were named as a reference or undoped while the samples comprising nanocapsules were called as a doped or composite yarn. In the study, yarn images were taken with LEO 440 Computer Controlled Digital Scanning Electron Microscopy (SEM) in order to determine the morphological properties of the nanocapsule undoped and doped yarn structure. Thermal History (T-History) test method was used to determine the change in surface temperatures of yarn samples resulting from absorbed latent heat by the nanoencapsulated PCMs in their structure in variable temperature environments.

3. RESULTS AND DISCUSSION

3.1. Nanocapsule Properties

According to the SEM images (Figure 1), nanocapsules with homogeneous particle sizes and spherical morphology were obtained. When the size scale on the SEM images was examined, it was determined that the dimensions of the capsules ranged from approximately 150 nm to 400 nm. According to the particle size distribution diagram given in Figure 1, it was determined that capsules exhibited a wide range but a unimodal distribution. The particle size distribution uniformity value was determined as 0.317. The average particle size of 98% of the particles was 127.2 µm.

When the thermal properties of nanocapsules were analysed it was determined that the produced nanocapsules absorbed 101.7 j/g of heat energy at 34 °C and radiated a total of -101.2 j/g of heat for liquid-solid and solid-solid phase transitions at 35 °C and 26 °C, respectively (Figure 2). According to TGA curves, the nanocapsules exhibited two-stage thermal degradation behaviour (Figure 3). The first decomposition step started at 206 °C and ended with a mass loss of 60.3% at 252 °C. This mass loss seen in capsules was due to the thermal breakdown of 1-tetradecanol, which forms the microcapsule core material, due to the increase in temperature and its removal from the capsule wall structure. The second thermal decomposition of the nanocapsules, which started at about 352 °C, was due to the thermal decomposition of the cross-linked PMMA-co-MAA copolymer structure forming the wall structure. Decomposition of encapsulated 1-tetradecanol was delayed due to the presence and thermal resistance of the microcapsule wall structure (decomposition at 206 °C and above).

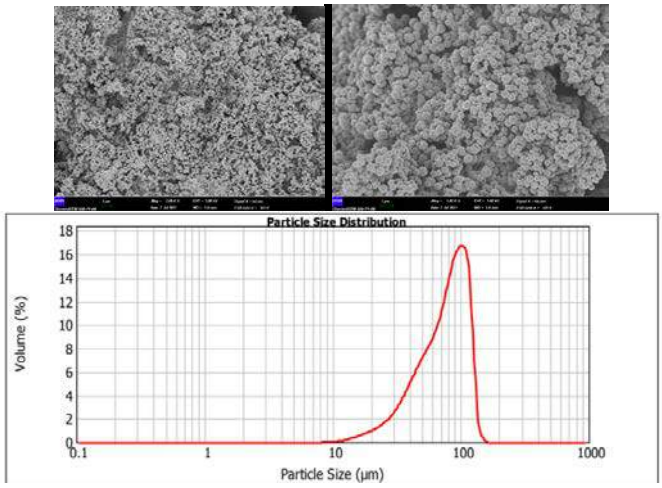

Figure 1. SEM images of the nanocapsules

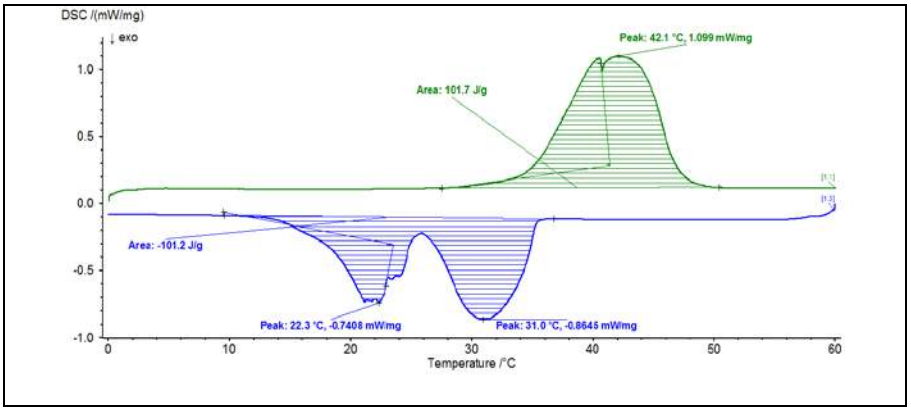

Figure 2. DSC curve of 1-tetradacanol core microcapsules with PMMA-co-MAA wall produced by emulsion polymerization method

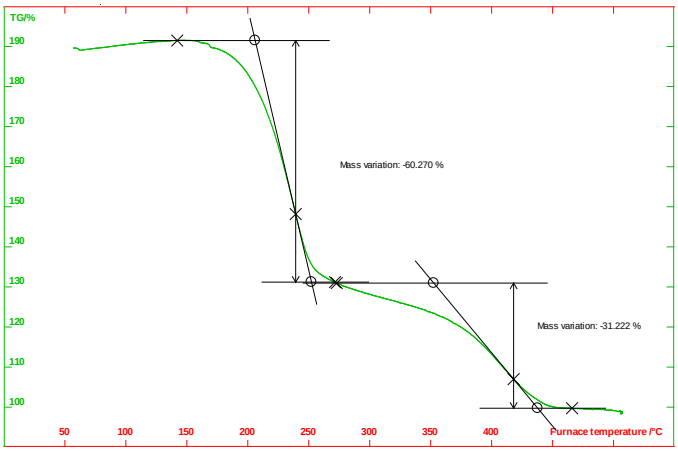

Figure 3. TGA curve of 1-tetradecanol core microcapsules with PMMA-co-MAA walls

3.2. Yarn properties

When the yarn images were examined, it was observed PCM nanocapsules on the surface of all polyester fibres (Figure 4). In particular, presence of capsule in the yarn structure was getting higher as the feeding rate was increased from 62.5 mL/h to 77.5 mL/h (Figure 4b). In addition, capsules were agglomerated and bound to the yarn structure in clusters. Capsule clusters were clearly seen on the

fibre surfaces and between the fibres for 77.5 mL/h feeding rate. The aggregation tendency of the capsules is an inevitable problem especially in applications in the form of dispersion in aqueous media. Particularly, decreasing particle size and size distribution homogeneity increase the aggregation tendency. The capsules produced in this study showed a clustering tendency due to their nano size. In short, SEM images showed that FDM nanocapsules can be integrated into polyester ring yarns.

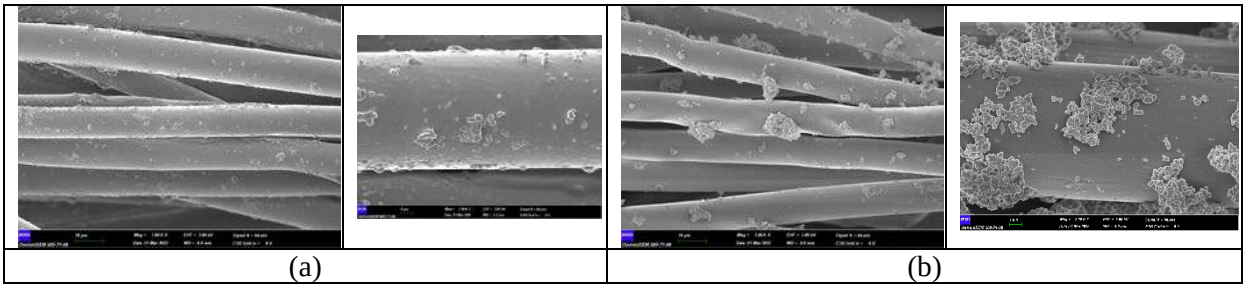

(a) (b)

Figure 4. SEM images of PCM nanocapsule loaded Ne 30/1 polyester ring spun yarns produced at 6% capsule concentration (a: 62.5 mL/h, b: 77.5 mL/h)

Thermal properties of undoped and PCM nanocapsule doped composite polyester ring spun yarns were analysed by Thermal History (T-History) test method. The changes in surface temperatures of yarn samples in variable temperature environments were determined. Undoped and nanocapsule doped yarn samples were firstly conditioned and then temperature changes on the yarn surface were measured with a thermal camera (Fluke TX 100) during the heating of the sample in a warm insulated box. The time-dependent graphs (T-history graphs) of the temperatures measured every 30 seconds with a thermal camera were drawn. In T-History graphs, y-axis shows the temperature measured on the surface of the yarn sample while x-axis shows the measurement time. In the T-history test, the differences on the surface temperatures of the undoped and PCM nanocapsule doped yarns were compared for determination of thermo-regulating effect of the PCM in the yarn structure.

According to the T-History curves of undoped and doped composite yarns, the curves of both yarn types did not overlap and this case indicated that there was a significant difference in the surface temperatures of both yarn types (Figure 5a). Surface temperature of undoped yarn increased very quickly than that of the PCM nanocapsule loaded composite yarns. Therefore, composite yarn had lower surface temperatures during all the measurement process due to the fact that the PCM in the structure absorbed latent heat from the environment during its melting process in a high temperature environment (Figure 5a).

When the undoped and PCM nanocapsule doped yarns were placed in a warm insulated box after the conditioning in a cold environment, their temperatures increased by the time. This case was named as warming-up period. After this point, the rate of increase tended to slow and surface temperature reached to a maximum value at the end of the measurement period. This period was named as saturated surface temperature region. During the warming-up period, surface temperature of the undoped yarn increased rapidly to 21.2 °C in the first 10 minutes while the temperatures were 17.4-15.2 °C for PCM nanocapsule doped yarns at 62.5 and 77.5 mL/h feeding rates. After this point, the rate of increase tended to slow and saturated surface temperature peaked at 38.1 °C at the end of the measurement period (77th minute) for undoped yarns. As to PCM nanocapsule doped yarns, 35.5 °C and 32.7 °C maximum surface temperatures were determined for 62.5 mL/h and 77.5 mL/h, respectively.

Furthermore, mean surface temperatures differences of undoped and PCM nanocapsule doped yarns for different measurement times were found as 2.3 °C for 62.5 mL/h feeding rate and 5.5°C for 77.5 mL/h (Figure 5b).

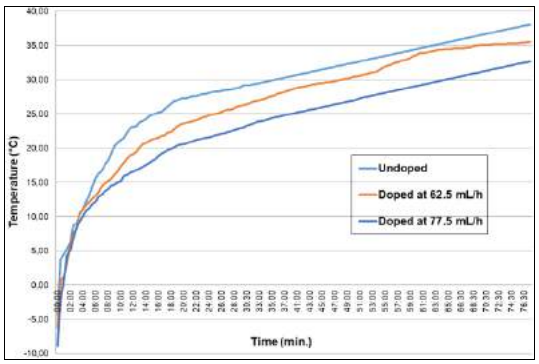

(a)

Time (min.)	Feding rate	
	62.5 mL/h	77.5 mL/h
05:00	1.00 °C	1.90 °C
30:00	2.90 °C	6.20 °C
60:00	0.90 °C	5.40 °C
77:30	2.60 °C	5.40 °C
Mean	**2.3** °C	**5.5** °C

(b)

Figure 5. T-history results of undoped and PCM nanocapsule ring spun yarns (a) and differences in surface temperatures of undoped and PCM nanocapsule doped yarns for different measurement times

4. CONCLUSION

This study focused on the integration of PCM nanocapsules into the polyester staple open fiber bundle before the yarn twisting during the ring spinning process via an alternative nanocapsule application method in order to fabricate thermo-regulating polyester surfaces. SEM images indicated the presence of nanocapsules in yarn structure and time-dependent surface temperature (Thermal-history test) measurements showed that PCM nanocapsules incorporated yarns exhibit temperature differences about 2-5 °C compared to undoped yarns during all the measurement period. Cooling effect of PCM in yarn structure provides nanocapsule-doped composite yarns heat up less in high temperature environment compared to undoped polyester yarns. Alternative application method and the produced spun yarns from staple fibres can be a potential to rival the thermally adaptive textile products produced from specially designed synthetic fibers. Such integrated yarn materials have demonstrated promising potential to be used as thermo-regulating textile material.

ACKNOWLEDGEMENT

This work was financially supported by TÜBİTAK 1505 University-Industry Cooperation Support Program (Project No: 5200098). The authors also wish to express their gratitude to ADIM Tekstil San. Ve Tic. A.Ş. (Isparta).

REFERENCES

Anayurt, R. A., Alkan, C., Alay Aksoy, S., Demirbağ, S., & Tözüm, M. S. (2017). Influence Of Hydrophilic Comoner On Thermal Properties Of Polymethylemethacrylate/N-Alkanes Microcapsules. *Tekstil & Konfeksiyon*, 27(2), 163-172.

Gao, X. Y., Han, N., Zhang, X. X., & Yu, W. Y. (2009). Melt-processable acrylonitrile–methyl acrylate copolymers and melt-spun fibers containing MicroPCMs. *Journal of Materials Science*, 44(21), 5877-5884.

Mattila, H. R. (2006). Intelligent Textiles and Clothing. Woodhead Publishing Limited, The Textile Institute,Cambridge, England.

Mondal, S. (2008). Phase change materials for smart textiles – An overview. *Applied Thermal Engineering*, 28, 1536–1550.

Önder, E., Sarıer, N., & Çimen, E. (2008). Encapsulation of Phase Change Materials by Complex Coacervation to Improve Thermal Performance of Woven Fabrics. *Thermochimica Acta*, 467, 63-72.

Sarıer, N., & Önder, E. (2007). The Manufacture of Microencapsulated Phase Change Materials Suitable for The Design of Thermally Enhanced Fabrics, *Thermochimica Acta*, 452, 149-160.

Tao, X. (2008). Smart Fibres, Fabrics and Clothing, Woodhead Publishing Limited, The Textile Institute, Cambridge, England.

Yılmaz, D., Özen, Ö., Özkayalar, S., Alay Aksoy, S., & Söğüt, B. (2021). An Innovative Method for Microcapsule Based Functional Yarn Production. *Journal of Natural Fibers*, 1-14.

Zhang, X. X., Wang, X. C., Tao, X. M., & Yick, K. L. (2006). Structures and properties of wet spun thermo-regulated polyacrylonitrile-vinylidene chloride fibers. *Textile Research Journal*, 76(5), 351-359.

LAYER BY LAYER SELF-ASSEMBLY APPROACH IN THE UV PROTECTIVE MODIFICATION OF ARAMID-BASED MATERIALS

Yeşim ÜNVAR[1], Ayşe Merih SARIIŞIK[1], Şule Sultan UĞUR[2]

[1] Dokuz Eylül University, Department of Textile Engineering, İzmir, Türkiye
[2] Süleyman Demirel University, Department of Textile Engineering, Isparta, Türkiye

Corresponding author: merih.sariisik@deu.edu.tr

Abstract: *Aramid fibers suffer from poor UV resistance that causes significant loses in their superior characteristics. Therefore, improving UV resistance of aramid fibers is of great importance. However, abrasive pretreatments, high temperature and/or pressure, processes taking long times and consequent fiber damages draw attention in current practices. In this study, considering the limitations and disadvantages of the UV protective modifications, Layer by Layer (LbL) approach was presented to carry out direct coating on aramid yarns without sacrificing fiber integrity. First, pretreatment was achieved by polyethyleneimine with the purpose of obtaining cationic surface charges on aramid fibers then zinc oxide and titanium dioxide nanoparticles were self-assembled on aramid yarns via LbL process. Results proved the nano coatings increased the UV resistance and tensile properties of aramid yarns. This paper revealed that LbL has a strong potential to modify aramid-based materials in a mild condition and capable of exceeding the limitations of earlier works for UV protection.*

Keywords: *Aramid, UV resistance, Layer by Layer, nano coatings.*

1. INTRODUCTION

Aramid fibers have an important position in cutting edge fields owing to outstanding properties like ultra-high strength and modulus, good thermal and chemical stability (Zhu et al., 2014). However, UV light causes deterioration of those properties. This drawback, poor UV resistance of aramid fibers, is unacceptable as it shortens service life and limits applications (Li et al., 2021). Therefore, minimizing these damages with UV protective coatings is of great interest both in academia and industry.

Aramid fibers have inherently inert surface thereby it is generally difficult to prepare coatings directly on aramid fiber with strong adhesion (Chen et al., 2021). For this reason, in most cases, aramid fibers have been pretreated with acid or alkali before any surface treatment (Zhu et al., 2014; Zhou et al., 2017). Yet, abrasive pretreatment with acid or alkali destroys the structure and tensile properties of the aramid fibers (Zhou et al., 2017). As a matter of fact, in current practices long process times, high temperature and/or pressure and special machinery requirements so the difficulties in application and fiber damages draw attention. Thus, main challenge is not only development a robust UV protective coating but also readily integrating it without compromising mechanical properties of aramid fibers.

Layer by Layer (LbL) self-assembly approach, on the other hand, is capable of offering a viable solution to these bottle-necks. Because, LbL is a simple and highly versatile method to modify surfaces and fabricate robust and highly-ordered nanostructured coatings over almost any type of substrate (Borges and Mano, 2014). Interestingly, application of LbL process is quiet rare for the UV protective modification of aramid fibers even though it was proved that enhanced UV resistance (Zhou et al., 2017).

Another issue is that UV protection is mostly developed against UVA (400-315 nm) and/or UVB (315-280 nm) bands corresponding solar exposure. Yet, there are also application areas where aramid-based materials have to be protected from UVC light (100-280 nm). For example, aramid is used in aerospace applications and welding operations (Mäkinen et al., 2004; Karahan et al., 2008). In addition, there is increasing interest UVC irradiation as a new technology in neutralizing various

biological threats such as Corona viruses, biological warfare agents, etc. (Vatansever et al., 2013; Bhardwaj et al., 2021; Olcay et al., 2021). Ultimately, technological developments together with rising concerns about sanitation have required the integration of UVC light into a variety of everyday objects. However, it is still largely unknown today neither protective additives against UVC radiation nor the effects of UVC radiation on materials in our daily lives (McGreer, 2021). Therefore, we foresee that taking into consideration UVC light both in the development and the assessment of UV protective coatings is becoming a need in the near future.

This paper puts emphasis on the strong potential of LbL technology to overcome limitations in the UV protective modifications of aramid-based materials. This preliminary study, calls also attention to the importance of the different UV aging practices by taking into consideration UVC light in the assessment of UV protective coatings.

2. MATERIALS AND METHODS

2.1. UV Protective Coatings by Layer by Layer Self-Assembly Approach

Polyethylene imine (PEI) is a common cationic polyelectrolyte in electrostatic self-assembly with strong adhesion (Xiong et al., 2019) and the recent applications showed that it can be a suitable template to overcome chemically inert surface such as aramid (Yang et al., 2019). On the other hand, zinc oxide (ZnO) and titanium dioxide (TiO_2) were proved the effectiveness on improving UV resistance of aramid fibers (Zhu et al., 2014). Based on these, PEI was employed to obtain cationic surface charges on aramid fibers then to build up self-assembly of nanoparticles on it. Para-aramid (Kevlar 49) yarns were immersed in the PEI solution (1 g/L) for 20 min then dried without any heat treatment. Subsequently, aqueous (anionic and cationic) dispersions of ZnO and TiO_2 (1 g/L) were prepared adjusting pH with sodium hydroxide (NaOH) or hydrochloric acid (HCl). Aramid yarns coated with PEI were dipped into these dispersions of ZnO and TiO_2 separately (20 min) and washed in each sequential step (5 min). As given in the Figure 1, ten bilayers of ZnO and TiO_2 nano coatings were obtained repeating this cycle at room temperature and then LbL nano coatings were dried at 105 °C and fixed for 5 minutes.

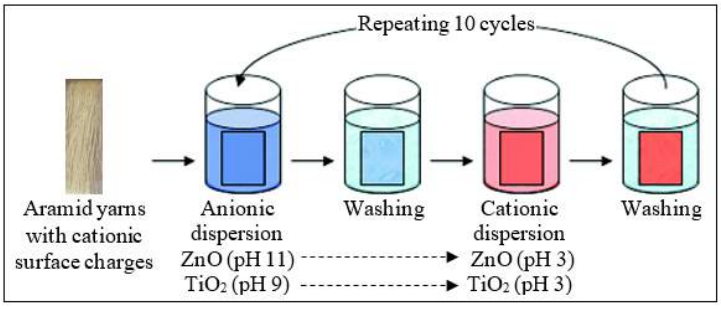

Figure 1. Application procedure of LbL

2.2. UV Aging Procedure

We carried out accelerated UV aging in a box using Philips TUW series UV-C lamp (254 nm, 18 W, 60 V, 0.37 A) for 168 hours.

2.3. Characterizations and Tests of UV Protective LbL Coatings

Scanning Electron Microscopy (SEM) images and Fourier Transform Infrared Attenuated Total Reflection (FTIR-ATR) spectroscopy graphs were examined to confirm the coatings. To reveal UV

protection efficiency of coatings, tensile strength and extension were measured by TS EN ISO 2062 before and after UV aging.

3. RESULTS AND DISCUSSION

When the SEM images were examined (Figure 2), it was seen that a successful coating is achieved by self-assembly nanoparticles with the LbL method on the aramid fiber surface.

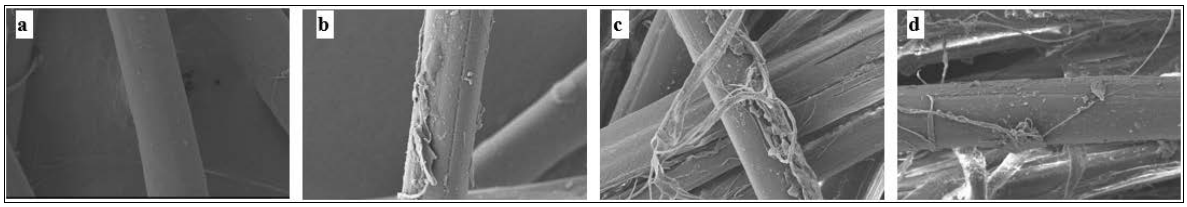

Figure 2. SEM images of aramid yarns a) untreated, b) PEI, c) ZnO, d) TiO_2

Figure 3 gives the FTIR measurement results of aramid yarns before and after UV aging. Similar to previous studies, amide related peaks were at 1644, 1537, 1298, 722 cm^{-1} corresponding amide I, II, III and IV, respectively (Zhang et al., 2006; Azpitarte et al., 2017; Li et al., 2018). The absorption bands at 1509 cm^{-1}, 1015, 820 are due to the C-H of the aromatic ring (Almaroof et al., 2019) while the band located at 1605 cm-1 is due to the C=C tensile vibration of the benzene ring (Cheng et al., 2018, Zhai et al., 2022). After accelerated UV aging, a new peak at 1733 cm^{-1} appeared in untreated samples ("untreated UV"), which is attributed to the breaking of the amide bond and the formation of carboxylic acid group (Zhang et al., 2006; Zhou et al., 2017; Cheng et al., 2018; Li et al., 2021; Zhai et al., 2022). On the other hand, it was not observed any strong peak corresponding cleavage of the amide bond in ZnO and TiO_2 coated samples by UV aging. The unaltered chemical structure of fibers could be interpreted as that LbL nano coatings provide protection to fibers against UVC irradiation.

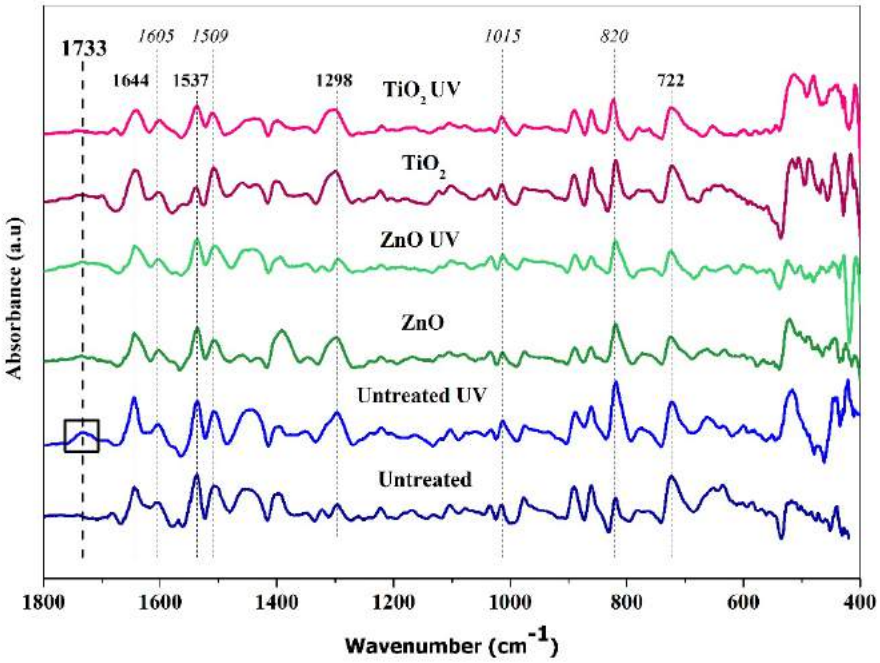

Figure 3. FTIR results of aramid yarns before and after UV aging

The tensile strength and break extension of para aramid yarns before and after UV aging are given in Figure 4 a and b, respectively. Break extension values (%) of yarns appeared to not much affected by

UV aging except for untreated sample. On the other hand, it was found that the tensile properties of aramid yarns are improved thanks to the LbL nano coatings. As seen, it is quite possible to build up nano coatings without the compromising the tensile strength of aramid fibers by LbL approach when used compounds with strong adhesion like PEI, instead of abrasive pretreatments. Furthermore, considered tensile strength values as well as FTIR results after UV aging, high protection levels of LbL nano coatings with ZnO and especially TiO_2 are promising. Since, the findings in this study suggest that the LbL technology among the others can be more simple and easy way to reach desired level of UV protection in a wide range of application fields which required protection against not just UVA/UVB but also high energetic rays like UVC.

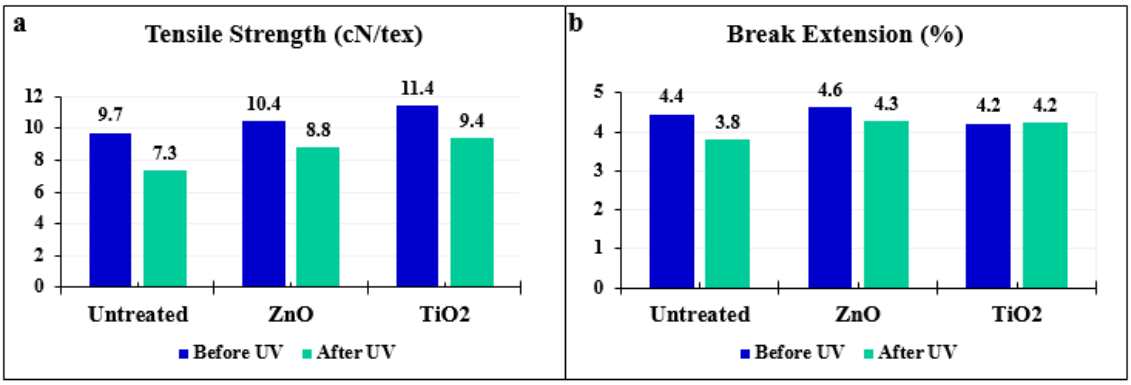

Figure 4. Tensile strength (a) and break extension (b) of aramid yarns before and after UV aging

Tensile strength retentions (%) of aramid yarns after 168 hours of UV irradiation are given in Figure 5 both individually and in comparison with uncoated sample. Uncoated aramid yarns retained only 75% of its original tensile strength. On the other hand, aramid yarns with ZnO and TiO_2 LbL nano coatings could maintain own their original value at least 84% and 82%, respectively. In fact, these retention values were higher compared to the uncoated sample. For instance, tensile strength of TiO_2 coated yarns before and after UV aging are 11.4 cN/tex and 9.4 cN/tex, respectively. When assessed individually, tensile strength retention of those yarns is 82%. However, when compared to the original para-aramid yarns before UV aging (9.7 cN/tex), this value (9.4 cN/tex) corresponds 96%, which is higher relative to retention of uncoated yarns' which is only 75% (7.3 cN/tex).

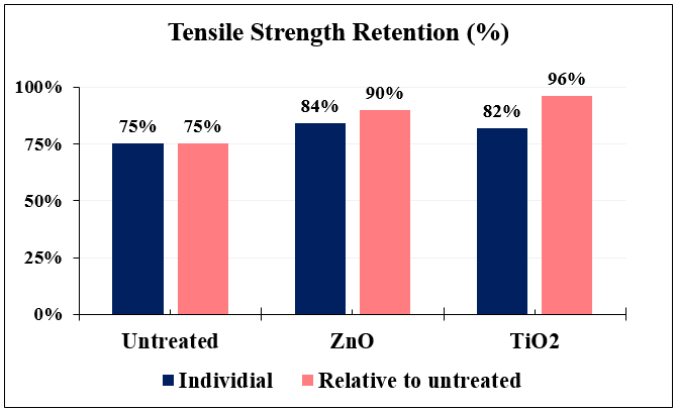

Figure 5. Tensile strength retentions of aramid yarns after UV aging

4. CONCLUSION

In this paper, it was aimed to evaluate Layer by Layer method for UV protective modifications of aramid-based materials. Findings showed that LbL process enables to self-assembly of ZnO and TiO_2

nanoparticles on aramid yarns coated with PEI. Tensile strength values of aramid yarns were significantly increased by LbL nano coatings. After UV aging treatment, LbL nano coated yarns have preserved their tensile properties considerably. It was concluded that LbL self-assembly approach may well exceed limitations of the current coating practices and highly suitable with high protection rates in the UV protective modification of aramid-based materials. Indeed, there are needed to examine comprehensively both the LbL applications with different formulations and the effect of UVC light in the UV aging procedure. Further LbL applications providing protection against the whole UV spectral range are in the development stage and hope to share soon.

ACKNOWLEDGEMENT

Yeşim Ünvar was supported by the Turkish Council of Higher Education 100/2000 doctoral scholarship.

REFERENCES

Almaroof, A., Ali, A., Mannocci, F., & Deb, S. (2019). Semi-interpenetrating network composites reinforced with Kevlar fibers for dental post fabrication. *Dental materials journal*, *38*(4), 511-521.

Azpitarte, I., Zuzuarregui, A., Ablat, H., Ruiz-Rubio, L., Lopez-Ortega, A., Elliott, S. D., & Knez, M. (2017). Suppressing the thermal and ultraviolet sensitivity of Kevlar by infiltration and hybridization with ZnO. *Chemistry of Materials*, *29*(23), 10068-10074.

Bhardwaj, S. K., Singh, H., Deep, A., Khatri, M., Bhaumik, J., Kim, K. H., & Bhardwaj, N. (2021). UVC-based photoinactivation as an efficient tool to control the transmission of coronaviruses. *Science of The Total Environment*, *792*, 148548.

Borges, J., & Mano, J. F. (2014). Molecular interactions driving the layer-by-layer assembly of multilayers. Chemical reviews, 114(18), 8883-8942.

Chen, F., Zhai, L., Yang, H., Zhao, S., Wang, Z., Gao, C., ... & Xu, W. (2021). Unparalleled armour for aramid fiber with excellent UV resistance in extreme environment. Advanced Science, 8(12), 2004171.

Cheng, Z., Hong, D., Dai, Y., Jiang, C., Meng, C., Luo, L., & Liu, X. (2018). Highly improved Uv resistance and composite interfacial properties of aramid fiber via iron (III) coordination. Applied Surface Science, 434, 473-480.

Karahan, H. A., Demir, A., & Toprakçı, O. (2008). Textile materials and structures used for aerospace applications-1. Fibers. *Electronic Journal of Textile Technologies*, *2*, 45-65.

Li, Z., Liu, B., Kong, H., Yu, M., Qin, M., & Teng, C. (2018). Layer-by-layer self-assembly strategy for surface modification of aramid fibers to enhance interfacial adhesion to epoxy resin. *Polymers*, *10*(8), 820.

Li, M., Cheng, K., Wang, C., & Lu, S. (2021). Functionalize aramid fibers with polydopamine to possess UV resistance. *Journal of Inorganic and Organometallic Polymers and Materials*, *31*(7), 2791-2805.

Mäkinen, H., Karkkula, S., Jaakkola, K., & von Nandelstadh, P. (2004). Can laboratory pre-treatment of welders' protective clothing simulate their aging process in normal use?. *Journal of ASTM International*, *1*(5), 1-11.

McGreer, M. (2021). Testing the effects of UV-C radiation on materials. *IST International Surface Technology*, *14*(2), 46-47.

Olcay, A., Albayrak, S. B., Aktürk, İ. F., Akbülbül, M. C., Yolay, O., İkitimur, H., & Bayer, M. Ç. (2021). A new Far-UVC based method for germ free hospitals and travel: Initus-V. *medRxiv*.

Vatansever, F., Ferraresi, C., de Sousa, M. V. P., Yin, R., Rineh, A., Sharma, S. K., & Hamblin, M. R. (2013). Can biowarfare agents be defeated with light?. *Virulence*, *4*(8), 796-825.

Xiong, M., Ren, Z., & Liu, W. (2019). Fabrication of UV-resistant and superhydrophobic surface on cotton fabric by functionalized polyethyleneimine/SiO2 via layer-by-layer assembly and dip-coating. *Cellulose*, *26*(16), 8951-8962.

Yang, X., Tu, Q., Shen, X., Pan, M., Jiang, C., Zhu, P., ... & Hu, C. (2019). Surface modification of Poly (p-phenylene terephthalamide) fibers by polydopamine-polyethyleneimine/graphene oxide multilayer films to enhance interfacial adhesion with rubber matrix. *Polymer Testing*, *78*, 105985.

Zhai, L., Huang, Z., Luo, Y., Yang, H., Xing, T., He, A., ... & Chen, F. (2022). Decorating aramid fibers with chemically-bonded amorphous TiO2 for improving UV resistance in the simulated extreme environment. *Chemical Engineering Journal*, *440*, 135724.

Zhang, H., Zhang, J., Chen, J., Hao, X., Wang, S., Feng, X., & Guo, Y. (2006). Effects of solar UV irradiation on the tensile properties and structure of PPTA fiber. *Polymer degradation and stability*, *91*(11), 2761-2767.

Zhou, L., Yuan, L., Guan, Q., Gu, A., & Liang, G. (2017). Building unique surface structure on aramid fibers through a green layer-by-layer self-assembly technique to develop new high performance fibers with greatly improved surface activity, thermal resistance, mechanical properties and UV resistance. *Applied Surface Science*, *411*, 34-45.

Zhu, X., Yuan, L., Liang, G., & Gu, A. (2014). Unique UV-resistant and surface active aramid fibers with simultaneously enhanced mechanical and thermal properties by chemically coating Ce 0.8 Ca 0.2 O 1.8 having low photocatalytic activity. *Journal of Materials Chemistry A*, *2*(29), 11286-11298.

INSULATION PROPERTIES OF HEMP WASTE REINFORCED POLYURETHANE FOAM COMPOSITES

Betül KALEBAYIR DAĞPARÇASI[1], Ömer Berk BERKALP[1], Gaye KAYA[2],

[1] Istanbul Technical University, Department of Textile Engineering, İstanbul, Türkiye
[2] Kahramanmaras Sutcu Imam University, Department of Textile Engineering, Kahramanmaraş, Türkiye

Corresponding author: kalebayirbetul@itu.edu.tr

Abstract: *In this study, hemp waste reinforced polyurethane (PU) rigid foam composites were produced and characterized to determine the insulation properties. The effect of reinforcement types and amount were investigated on both thermal and sound absorption properties. Hemp shiv (HS) and short hemp fibre (HSF) that produced after combing were used as reinforcements. The composites were prepared with different reinforcement ratios (2, 5 and 10 wt. %). The neat (0%) PU rigid foam composite was also produced for comparison purpose. PU rigid foam composites were moulded by using a press with wooden moulds (300 x 400 x 20 mm). The results showed that heat insulating and sound absorption properties of the 5 wt.% HSF reinforced PU rigid foam composite were comparable with the neat PU rigid foam composite. In conclusion, it is possible to reach insulation properties of PU with 5 wt.% HSF reinforced PU rigid foam composites, so this composite is good candidate for development of a new economic and ecological insulating material.*

Keywords: *Polyurethane foam, hemp waste, thermal conductivity, sound absorption.*

1. INTRODUCTION

The polyurethane (PU) foams are one of the most widely used plastic materials in the world. They represent a wide range of commercial products commonly classified as flexible, semi-rigid and rigid foams depending on the starting ingredients. PU foams are generally used in building insulation, freezers and refrigerators, furniture and bedding, automotive [Oushabi, et al. 2017].

Excellent thermal and acoustic insulation combined with good adhesion, high strength-to-weight ratio and durability make PU rigid foam an indispensable material in the construction industry [Tan, et al. 2011]. However, PU cannot provide enouh thermal, mechanical and corrosion resistance under harsh conditions.

Recent studies clearly demonstrates that organic or inorganic fillers can significantly improve the mechanical, thermal and acoustic properties of rigid polyurethane composites. The use of wastes adds value to an underutilized by-product with excellent properties [Zanini, et al. 2022].

There is an increasing interest in hemp fiber in natural fiber reinforced composites.While hemp fibers are obtained from the hemp plant and hemp yarn is obtained from hemp fibers, a very large amount of hemp stem waste, about 1.2-1.4 tons, is generated for 1 ton of hemp yarn production. The hemp plant stem consists of the hemp fibers, the hemp shiv, the hemp short fibers and the dusts. Hemp stem consists of approximately 20 wt%–40 wt% of hemp fibers and 60 wt%–80 wt% of hemp shiv [Stevulova, et al. 2014]. Hemp wastes have a great potential as sustainable reinforcements for natural reinforced composite. By using hemp waste as reinforcement material in composites, energy and waste management problems and negative environmental effects can be eliminated.

Acoustic properties can be improved with various functional components, particles or reinforcing fibres as they exhibit insufficient sound absorption behaviour, especially in low frequency regions. In

particular, many studies investigating the thermal and sound absorption properties of natural fibers have been conducted on both the awareness created with their environmental advantages and offering an appropriate option in terms of thermal and sound insulation [Olcay, et al. 2020 and Członka, S., et al. 2020].

2. MATERIALS AND METHODS

2.1. Manufacturing of PU rigid foam composites

PU rigid foam composites were reinforced with 2, 5, and 10% wt. hemp shiv and short hemp fibre wastes with respect to the total mass of polyol. Neat (0%) PU rigid foam composite was also produced as a control group. The samples are coded as PU-X (reinforcement type)-Y (reinforcement amount). For example, PU-HS-2 means that 2% wt. hemp shiv reinforcement composite. PU rigid foam composites were manufactured by mixing polyol (Plusol R-103-01, Pluskim, Turkey) and isocyanate (Plusnate-R-100-01, Pluskim, Turkey) compounds in a 1/1.20 weight ratio. Hemp waste and polyol were mixed for 3 min until homogenization, then isocyanate was added to the mixture. The mixture was poured into the mould and placed at a hot press. Moulding was performed at room temperature by using 6 bars pressure for 60 min. After that, the material was removed from the mold and cut to sample sizes.

2.2. Density measurement

The densities of PU rigid foam composites were measured according to ASTM D792-13 using a density meter (Precisa®, XP205) at room temperature. The averages of five specimens were calculated.

2.3. Thermal conductivity test

Thermal conductivity measurements of PU rigid foam composites were conducted by Thermtest (HFM-100, Canada) brand tester according to ASTM C518 standard. The size of each specimen was 200 mm × 200 mm × 20 mm (width × length × thickness).

2.4. Sound absorption test

The sound absorption coefficients were obtained by using two-microphone Bias Engineering TestSENS medium impedance tube based on transfer function method according to ISO 10534–2:1998 and ASTM E1050–98 standards.

2.5. SEM analysis

Scanning electron microscopy (SEM) images were obtained by using Tescan VEGA 3 microscope.

3. RESULTS AND DISCUSSION

It is a well-known the fact that the thermal conductivity (λ) of the insulating foams are highly dependent on the foam density, conductivity of the gas mixture in the cells, matrix polymer conductivity, the radiation between the cells and morphological properties of the cells[Khaleel, et al. 2021] . Table 1 shows the thermal conductivity and density values of PU rigid foam composites. Neat PU rigid foam composite showed the lowest thermal conductivity (0.0394 W/m K). The composite with 10 wt. % short hemp fibre ratio (PU-HSF-10) showed the highest thermal conductivity (0.042 W/m K). It is clear that the thermal insulation properties of hemp waste reinforced PU rigid foam composites are lower than that of neat PU rigid foam. The decreased cells-size and closed cell formation of hemp waste reinforced PU rigid foam composites (Figure 1) compare to neat PU could be caused to reduce thermal insulating properties. As seen in the Tablo 1, the density of all the PU foams increased consistently with increasing in hemp waste percentage.

That is to say increases in the amount of hemp waste in the matrices caused an increase in mass per unit volume, resulting in an increase in the densities of the polyurethane rigid foam composite.

Table 1. Density and thermal conductivity values of the composite samples.

Samples	Density (kg/m^3)	Thermal conductivity (W mK^{-1})
Neat PU	96.10	0.0394
PU-HS-2	98.20	0.0407
PU-HS-5	100.10	0.0410
PU-HS-10	111.20	0.0405
PU-HSF-2	97.30	0.0395
PU-HSF-5	102.8	0.0412
PU-HSF-10	108.9	0.0427

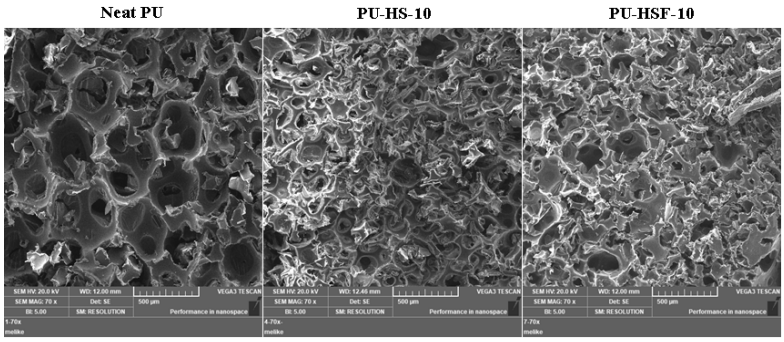

Figure 1. SEM views of neat and 10% wt. hemp shiv (HS) and short hemp fibre (HSF) reinforced PU rigid foam composites.

Sound absorption coefficient values at a frequency range between 400 and 6300 Hz can be seen in Figure 4. When we examine the curves, it has been seen that the sound absorption coefficients of all polyurethane rigid foam composites are lower at low frequency than at high frequency. However, it is clear from the Figure 2 that in a certain frequency ranges, polyurethane rigid foam composites containing hemp waste have better acoustically than neat polyurethane rigid foam composites. The PU-HS-10 composite showed a higher sound absorption coefficient than neat PU in the range of 2000-3000 Hz. The sound absorption coefficient of PU-HS-10 at 2.5 kHz was 0.7 that was the maximum value. In addition, PU-HSF-5 exhibited a higher sound absorption coefficient than the neat PU foam at a frequency of 2000–3150 Hz. The PU-HSF-5 also showed higher sound absorption coefficient than PU-HS-10 at 2000–2500 Hz. The increased density due to hemp waste reinforcement improved sound absorption of PU rigid foam composites at middle and high frequencies.

The acoustic absorption behavior of a porous material depends on the porosity, the tortuosity, and the flow resistivity (Maderuelo-Sanz et al. 2013). Figure 1 shows that compared with the control group, polyurethane rigid foam composites have smaller size cells because of the presence of hemp waste reinforcements. Cell size affects the sound absorption frequency, and large-sized porous cell favored the low frequency sound absorption(Peng et al. 2013).

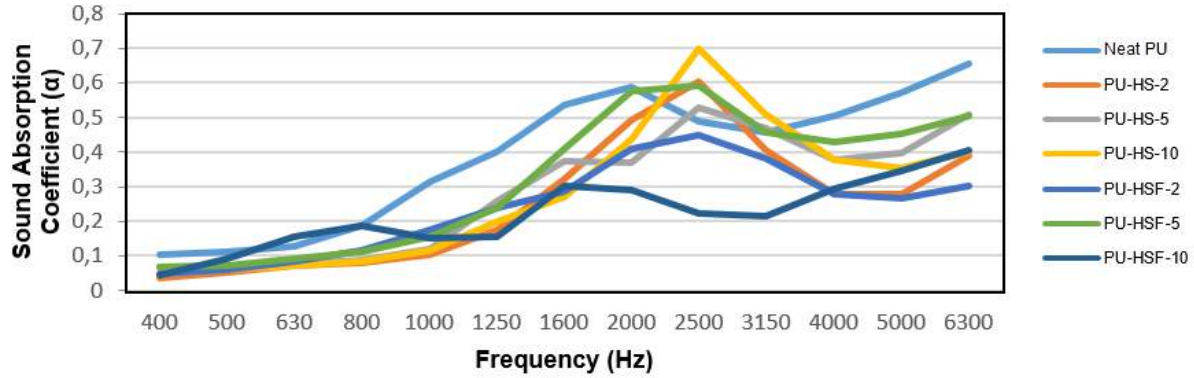

Figure 2. Sound absorption coefficient values of the PU rigid foam composites.

Compared to the sound absorption coefficient, the improvement in the sound transmission loss is more clear. For hemp waste reinforced polyurethane rigid foam composites as shown in Figure 3, there are significant increases in sound transmission loss along with the frequency increasing in the whole frequency range. PU-HSF-10 composites exhibit the best sound insulation with high transmission loss around 32 dB over the entire frequency range (63–6,300 Hz).

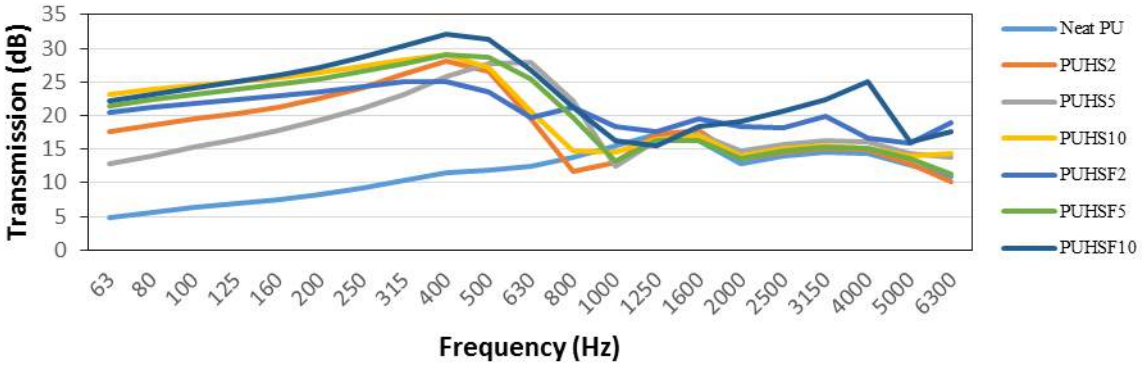

Figure 3. Sound transmission loss values of the PU rigid foam composites.

4. CONCLUSION

In this study, it was aimed to produce PU rigid foam composites reinforced with hemp shiv (HS) and short hemp fibre (HSF) at various weight ratio to investigate the effect of sound absorption and thermal properties. The thermal conductivity values of the hemp shiv (HS) and short hemp fiber (HSF) reinforced PU rigid foams were in the range of 0.040−0.042 W mK^{-1}, revealing that the thermal conductive capacity of the reinforced PU rigid foam was suitable for application as thermal insulation of building. Sound absorption properties of the composites were close to neat PU rigid foam. In future works, the mechanical properties of hemp waste reinforced PU rigid foam composites will be investigated.

REFERENCES

Oushabi, A., Sair, S., Abboud, Y., Tanane, O., & El Bouari, A. (2017). An experimental investigation on morphological, mechanical and thermal properties of date palm particles reinforced polyurethane composites as new ecological insulating materials in building. Case studies in construction materials, 7, 128-137.

Tan, S., Abraham, T., Ference, D., & Macosko, C. W. (2011). Rigid polyurethane foams from a soybean oil-based polyol. *Polymer*, 52(13), 2840-2846.

Zanini, N. C., de Souza, A. G., Barbosa, R. F., Rosa, D. S., & Mulinari, D. R. (2022). Eco-friendly composites of polyurethane and sheath palm residues. *Journal of Cellular Plastics*, 58(1), 139-158.

Stevulova, N., Cigasova, J., Estokova, A., Terpakova, E., Geffert, A., Kacik, F., ... & Holub, M. (2014). Properties characterization of chemically modified hemp hurds. *Materials*, 7(12), 8131-8150.

Olcay, H., & Kocak, E. D. (2020). The mechanical, thermal and sound absorption properties of flexible polyurethane foam composites reinforced with artichoke stem waste fibers. *Journal of Industrial Textiles*, 1528083720934193.

Członka, S., Strąkowska, A., & Kairytė, A. (2020). The impact of hemp shives impregnated with selected plant oils on mechanical, thermal, and insulating properties of polyurethane composite foams. *Materials*, 13(21), 4709.

Khaleel, M., Soykan, U., & Çetin, S. (2021). Influences of turkey feather fiber loading on significant characteristics of rigid polyurethane foam: Thermal degradation, heat insulation, acoustic performance, air permeability and cellular structure. *Construction and Building Materials*, 308, 125014.

Maderuelo-Sanz, R., Morillas, J. M. B., Martín-Castizo, M., Escobar, V. G., and Gozalo, G. R. (2013). "Acoustical performance of porous absorber made from recycled rubber and polyurethane resin," *Latin American Journal of Solids and Structures* 10, 585- 600.

Peng, H. K., Wang, X., Li, T. T., Lou, C. W., Wang, Y., & Lin, J. H. (2019). Mechanical properties, thermal stability, sound absorption, and flame retardancy of rigid PU foam composites containing a fire-retarding agent: Effect of magnesium hydroxide and aluminum hydroxide. *Polymers for Advanced Technologies*, 30(8), 2045-2055.

AN INVESTIGATION ON 3D PRINTED WALNUT SHELL-REINFORCED POLY (LACTIC ACID) COMPOSITE

Murat DEMİR[1], Ayberk SÖZEN[2], Yasemin SEKİ[1], Figen SELLİ[3]

[1] Dokuz Eylül University, Textile Engineering Department, İzmir, TURKEY
[2] Dokuz Eylül University, Marine Sciences and Technology, İzmir, TURKEY
[3] Eskişehir Technical University, Advanced Technologies Research and Application Centre, Eskişehir, TURKEY

Corresponding author: murat.demir@deu.edu.tr

Abstract: *In this current study, the producibility of 3D printed walnut shell composite is investigated. PLA granules and untreated ground walnut shells were mixed priorly and then extruded by using a single screw extruder to produce filaments for 3D printing. Then, pristine and walnut shell doped PLA filaments were 3D-printed by using the fused filament fabrication (FFF) method. The thermal decomposition behaviour of the filaments and the morphology of 3D printed parts are examined by Thermo-gravimetric analysis (TGA) and scanning electron microscopy (SEM), respectively. SEM micrographs presented non-adhesion between the particle and the polymer and also non-homogeneous particle distribution. TGA data revealed that the moisture content of PLA increased, and both pristine and doped PLA filament can resist to extrusion processes which take place at 200C.*

Keywords: *PLA, 3D-printing, walnut shell, extrusion, additive manufacturing, reinforced PLA, Fused filament fabrication.*

1. INTRODUCTION

Additive manufacturing also referred to as 3D printing, has gained a lot of attention and popularity with the help of producing complex geometries without special tools in good accuracy, and ease of production for prototyping. Since the first idea was presented in the 1970s, many different technologies have been presented for additive manufacturing and Fused Deposition Modelling (FDM) is one of the most common used 3D printing technologies (Dip et al., 2020). In the working principle of FDM printers, filament form material is fed through a heated nozzle, and designed parts are produced by the deposition of molten polymers on the printing bed.

In FDM printers, the properties of 3D parts are mainly affected by printing parameters and polymers. Recently, there has been an outbreak of studies that focus on producing reinforced filaments for FDM printers. Most of those studies used different kinds of waste or fibres as additive materials and revealed a cost-effective, sustainable and environmentally friendly production chain for filament production (Balla et al., 2019; Royan et al., 2021).

The cost of filaments can be decreased by the addition of economical filler materials, which may improve the properties of the polymers. The use of fillers especially bio-based materials will assist in mitigating the environmental impact (Ahmed et al., 2020). The aim of this study to manufacture 3D printing of walnut shell reinforced PLA parts. For this purpose, the walnut shells were ground and mixed with PLA pellets. PLA/walnut shell mixture was extruded to produce filament and then 3D printed parts. The composite filaments and 3D printed parts were analysed by thermogravimetric analysis and scanning electron microscopy.

2. MATERIALS AND METHODS

2.1. Materials

FKuR Kunstsoff company's Bio-Flex F7510 PLA product was used as matrix material. The density of the PLA is 1.25 gr/m^3, the melting temperature is 155 °C and the melt flow rate is 2-4 g/10min. for additive material, waste walnut shells are locally provided.

2.2. Preparation of PLA/walnut shell composite filaments

Walnut shells are ground by using Retsch SM 100 grinding device. The grinding process was performed in order to decrease the size of the particle. The ground walnut shells were passed through a 63 µm sieve. No surface treatment has been applied to walnut shells. Laboratory type Flax brand Arya single screw extruder was used to turn PLA pellets and ground walnut shells into filaments. The extruder's zone temperature, screw and production speed are kept as 170 °C, 15 hz/h and 1.5 kg/h (50mm/sec), respectively. Walnut shell reinforced PLA filaments are produced in a diameter of 1.75 mm (±5%) in accordance with the fused filament fabrication technology. Figure 1 illustrates the production of walnut shell reinforced filament production. No surface treatment has been applied to the filament after production. The produced filaments are stored in vacuum bags to protect them from moisture.

Figure 1. PLA-walnut filament making

2.3. Production of 3d printed PLA composite parts

Printed samples were produced using a Creality Cr-200b brand and model printer. The printing temperature was set to 165°. Printing speed was kept as 40 mm/sec. The layer thickness was determined as 0.12 mm. Raft was used to adhere the products to the heated glass plate during printing. As the nozzle width, 0.4 mm was tried first, but because there were blockages. Production was made with 0.6 mm. Production of 3D parts with walnut shell reinforced filaments is illustrated in Figure 2.

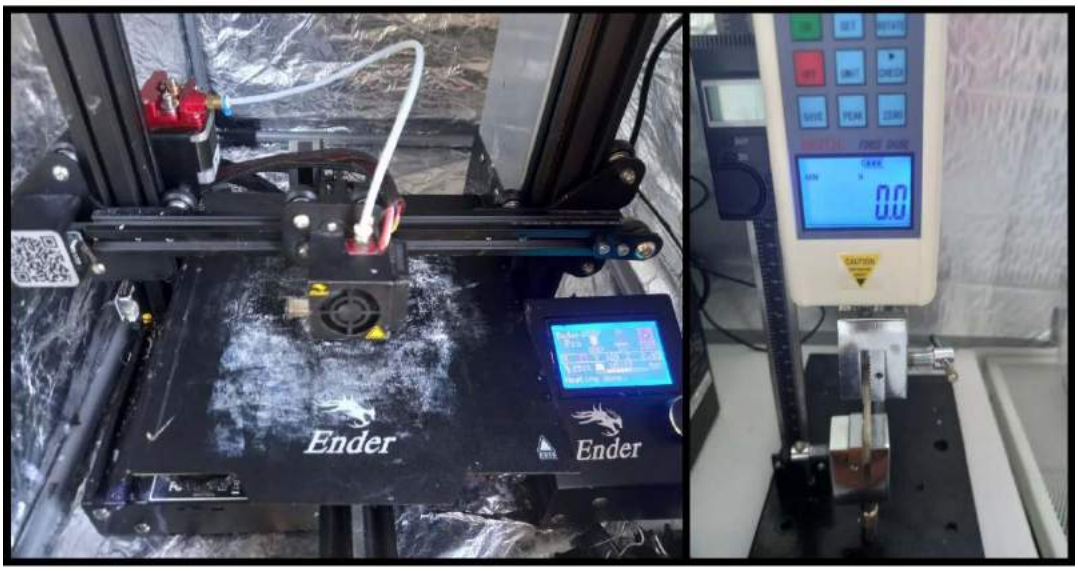

Figure 2. Tensile test printing and testing

2.4. Characterization of the PLA filaments and 3D-printed parts

To investigate the thermal stability of pristine and walnut shell doped PLA filaments, thermogravimetric analysis was conducted by using a Shimadzu DTG-60H instrument. The investigation was performed from room temperature to 600 C at a rate of 10 C/min. To prevent oxidation, the analysis was conducted under a nitrogen atmosphere. The microstructure of the 3D parts was analysed with Zeiss Sigma500 FESEM scanning electron microscope using the SE2 detector. Prior to placement in the microscope, chamber samples were fixed on aluminium stubs with double-sided carbon tape and sputter coated with 10nm gold. Imaging was performed at x500-1000-2500-5000-10000 magnification and 5kV energy.

2.5. Tensile tests

Tensile tests were performed according to the related standard (ASTM D638) with its data acquisition system at a constant crosshead speed of 1 mm/min.

3. RESULTS AND DISCUSSION

SEM micrographs are presented in Figure 3. When the SEM images were examined, it was observed that there was a problem of non-adhesion between the printed layers. Interfacial bonding is unsuccessful. There are gaps in the matrix due to the inability of ground walnut shells to adhere to the PLA matrix during filament production. The distribution of particles in the matrix is not homogeneous. Non-homogeneous structure of reinforced filament for the production of additive manufacturing has also been stated in different studies (Lee et.al., 2021; Singh et.al., 2022; Mazur et.al., 2022). to overcome this problem, some suggestions have been offered as smaller particle size, pre-treatment of reinforcing materials and post-treatment of produced 3D parts (Wang et.al., 2022; Chen et. al., 2022). The mechanical performance of the whole structure decreases due to the above-mentioned reasons.

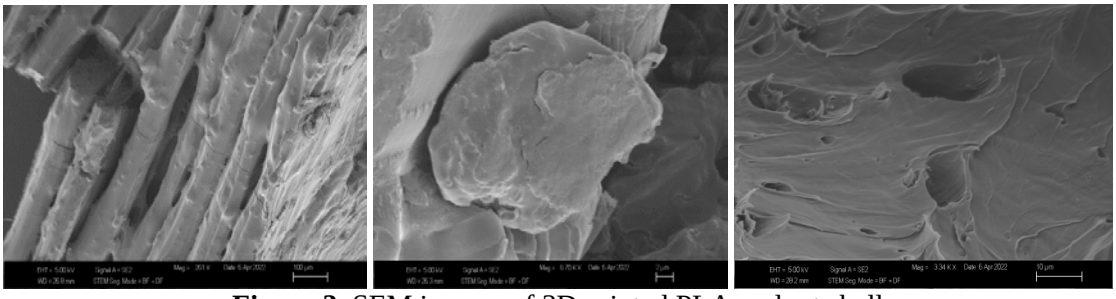

Figure 3. SEM images of 3D printed PLA-walnut shell

Figure 4 and Figure 5 show thermal analysis curves of pristine PLA and walnut shell-loaded PLA filaments. Walnut shell increased mass loss of PLA till 120ºC which can be attributed to the water evaporations present in the filament. It increased by app. 17% due to the incorporation of hygroscopic natural cellulosic waste into PLA. 100% PLA and walnut shell-loaded PLA lost 1% of their mass at 224.58 and 131.95ºC, respectively. The mass losses at 200ºC which is generally extrusion temperature recorded as <1% and 1.5%, respectively. The addition of walnut shells into PLA decreased the maximum decomposition temperature by 11.5%. this is because of the lower thermal decomposition temperature of a walnut shell than PLA (Narlıoglu et al., 2021).

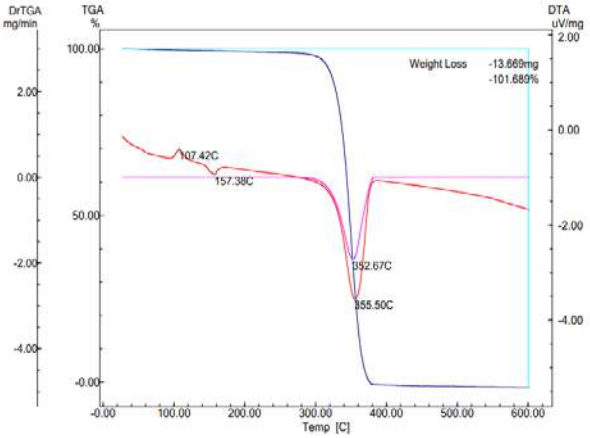

Figure 4. Thermal analysis curves of 100% PLA filament

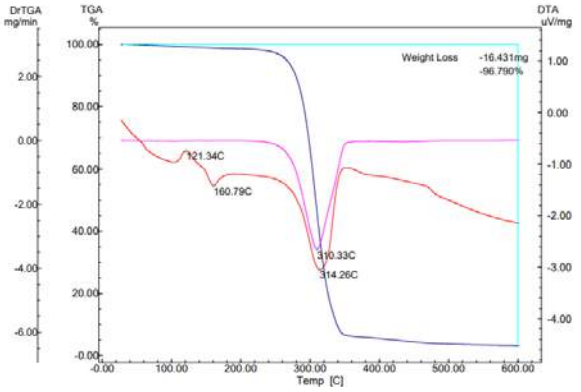

Figure 5. Thermal analysis curves of a walnut shell loaded PLA filament

The tensile test of the 3D parts produced from walnut shell reinforced PLA and pure PLA is illustrated in Figure 6. From figure 6, in accordance with the literature, 3D parts produced from walnut shell-reinforced PLA displayed a smaller tensile test result. Poor adhesion between PLA and walnut shell parts is counted as the main reason for the reduction of mechanical behaviours of 3D parts.

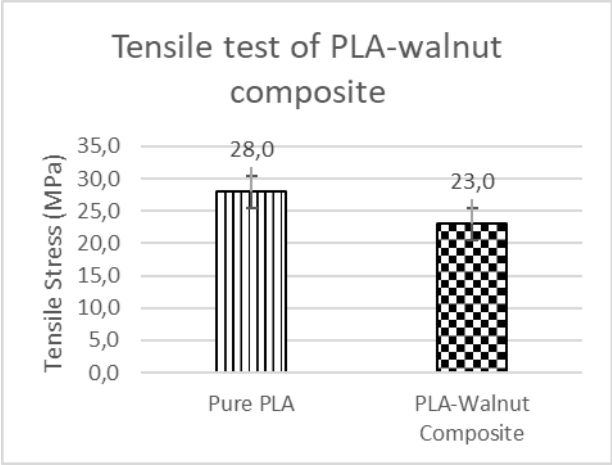

Figure 6. Tensile test results

4. CONCLUSION

This work aims to produce walnut shell reinforced PLA composite filament for 3D-printing. Walnut shells were ground firstly, mixed with PLA granules and then extruded to produce composite PLA filament. Pristine and walnut shell doped PLA filaments were 3D printed via FFF technology. Analysis results revealed that incorporating a walnut shell increased PLA's moisture content and decreased thermal degradation temperature. It is noticed that both of the filaments are thermally resistant to extrusion temperatures at about 200ºC. SEM micrographs delamination of doped PLA parts and non-adhesion between particle and PLA. This is because no surface treatment was applied to the walnut shell. Accordingly, suitable chemical treatment and compatibiliser will be utilised to facilitate producibility and enhance filaments in the later stages of the study. For this reason, the strength values decreased in the tensile tests. While pure PLA was 28 MPa, this value decreased to 23 MPa when walnut was added. In addition, standard deviations in tensile tests are quite high since twin screw extruders are not used. Additives were not mixed homogeneously in the polymer. Despite the mechanical behaviour loss of walnut shell reinforced PLA compared to the pure PLA, including non-industrial wastes in the production process will contribute to the development of eco-friendly production methods. There is a need to improve the mechanical properties of the parts produced for this method, but as such, they can still be used in non-structural structures.

REFERENCES

Ahmed, W., Alnajjar, F., Zaneldin, E., Al-Marzouqi, A.H., Gochoo, M. & Khalid, S. (2020). Implementing FDM 3D Printing Strategies Using Natural Fibers to Produce Biomass Composite. *Materials*, *13*(4065), 1-23.

Balla, V. K., Kate, K. H., Satyavolu, J., Singh, P., & Tadimeti, J. G. D. (2019). Additive manufacturing of natural fiber reinforced polymer composites: Processing and prospects. *Composites Part B: Engineering*,174, 106956.

Chen, F., Ni, X., Liu, Y., Xia, X., & Gao, X. (2022). Preparation and properties of heat-treated esterified wood flour/polylactic acid composites for FDM 3D printing. *Journal of Materials Science*, 1-16.

Dip, T. M.; Emu. A. S.; Nafiz, M. N. H.; Kundu, P.; Rakhi, H. R.; Sayam, A.; Akhtarujjman, Md.; Shoaib, M.; Ahmed, M. S.; Ushno, S. T. et al.. (2020). 3D printing technology for textiles and fashion.*Textile Progress*,52(4), 167-260.

Lee, C. H., Padzil, F. N. B. M., Lee, S. H., Ainun, Z. M. A. A., & Abdullah, L. C. (2021). Potential for natural fiber reinforcement in PLA polymer filaments for fused deposition modeling (FDM) additive manufacturing: A review. *Polymers*, 13(9), 1407.

Mazur, K. E., Borucka, A., Kaczor, P., Gądek, S., Bogucki, R., Mirzewiński, D., & Kuciel, S. (2022). Mechanical, Thermal and Microstructural Characteristic of 3D Printed Polylactide Composites with Natural Fibers: Wood, Bamboo and Cork. *Journal of Polymers and the Environment*, 30(6), 2341-2354.

Narlıoglu, N., Salan, T., Alma, M.H. (2021). Properties of 3D-Printed wood sawdust reinforced PLA composites. *Bioresources*, 16(3), 5467-5480.

Royan, N. R., Leong, J. S., Chan, W. N., Tan, J. R., & Shamsuddin, Z. S. B. (2021). Current state and challenges of natural fibre-reinforced polymer composites as feeder in fdm-based 3D printing. *Polymers*, 13(14), 2289.

Singh, R., Kumar, R., Pawanpreet, Singh, M., & Singh, J. (2022). On mechanical, thermal and morphological investigations of almond skin powder-reinforced polylactic acid feedstock filament. *Journal of Thermoplastic Composite Materials*, 35(2), 230-248.

Wang, J.,Bai, J., Hua, H., Tang, B., Bai, W., & Wang, X. (2022). Characterization and Scalable Production of Industrial Hemp Fiber Filled PLA bio-composites. *Journal of Natural Fibers*, 1-12.

MODELING THE TENSILE PROPERTIES OF FLAX WOVEN REINFORCED COMPOSITE WITH FINITE ELEMENT METHOD

Mehmet KORKMAZ[1], Halis KANDAŞ[2], Melih KORKMAZ[2], Ramazan KARAKUZU[3]

[1] Dokuz Eylul University, Department of Textile Engineering, İzmir, Türkiye
[2] Dokuz Eylul University, The Graduate School of Natural and Applied Sciences, İzmir, Türkiye
[3] Dokuz Eylul University, Department of Mechanical Engineering, İzmir, Türkiye

Corresponding author: mehmet.korkmaz@deu.edu.tr

Abstract: *Man- made fibres reinforced composites are not eco- friendly and hard to recycle in the nature. The growing composite industry demands more fibre and would create bigger risks for nature in the future. For this reason, the natural fibres are seen ecological alternatives for composite industry. However, the physical properties of natural fibres depend on number of parameters like climate, soil fertility or harvesting conditions. This phenomenon makes complex to predict the mechanical properties of natural fibre reinforced composite. In this study, a numerical model, which is based on the representative volume element, was developed to predict the tensile properties of flax woven fabric reinforced polymer composite. As the material model could be correctly settled, the flax yarn and resin were tested. The model results were validated by the test results and good agreement was obtained between the stress- strain graphs and elastic properties.*

Keywords: *Flax fibre, composite, finite element modelling, representative volume element*

1. INTRODUCTION

The textile reinforced polymer composites have outstanding features such as higher strength/ weight ratio, non- corrosion structure and fully customized properties in comparison with the metals and their alloys. The man- made fibres like carbon or glass are mostly preferred to manufacture textile composites. However, these type of fibres are not eco- friendly and hard to recycle in the nature. It was determined that the total glass fibre capacity was 12.9 billion pounds in the world at 2021 (*2022 State of the Industry Report | Composites Manufacturing Magazine*, n.d.). The composite industry is growing day by day and demand more fibre. This phenomenon threatens the nature and would create bigger risks in the future. The natural fibres, which are flax, sisal, hemp and so on, can be used as ecological alternative to man- made fibres in composite production. On the other hand, the physical properties of natural fibres can be varied according to the number of parameters, which are climate conditions, soil fertility, harvesting quality etc. Variable physical properties of natural fibres make complex to predict the mechanical properties of composites. The natural fibre reinforced composites (NFRC) were modelled analytical or numerical in number of studies to estimate their elastic or failure properties (Antony et al., 2018; Beigpour et al., 2021; Sliseris et al., 2016; Xiong et al., 2018). In the most of numerical models (Bambach, 2019; Selver et al., 2018; Xu et al., 2019), NFRC were modelled with shell element and the material properties were assumed as homogeny.

In this study, the tensile properties of flax woven fabric reinforced polymer composite was numerically modelled at mesoscopic level. As the material model could be correctly created, the flax yarn and resin were tested and their elastic properties were detected. Afterward, the representative volume element (RVE) of composite was constituted and analysed via the ABAQUS programme (*ABAQUS CAE - SIMULA™ by Dassault Systèmes®*, n.d.). Thanks to the developed model, the young module and tensile strength of composites were predicted for both directions and validated with the test results. Good agreement was obtained between the model and test results.

2. MATERIALS AND METHODS

2.1. Production of the Flax Fabric and Composite

The flax woven fabric, which is 1x3 Twill, was produced with the CCI Tech Evergreen II sample weaving machine in Textile Engineering Department of Dokuz Eylül University (DEU). Three layers of flax woven fabrics were used to produce the composite material with the vacuum assisted resin infusion moulding method (VARIM) in the Mechanical Engineering Department of DEU. While the flax yarn has 4.8 Nm linear density, the fabric has 10 and 8 yarn densities in warp and weft directions, respectively.

2.2. The Tensile Test of Flax Yarn and Epoxy Resin

The flax yarn and epoxy resin were tested according to the NF EN 2062 and ASTM-D3039/D3039M-14 standards, respectively. While 30 samples were tested for flax yarn, five samples were prepared and tested to determine the elastic properties of epoxy resin.

2.3. Tensile Test of Composite

The tensile test was carried out according to the ASTM-D3039/D3039M-14 standard. The samples have 15 x 250 mm and 25 x 175 mm dimensions in warp and weft directions, respectively. The tests were repeated five times for both directions.

2.4. Numerical Model of Composite

The flax yarn and resin were tested to determine their young modulus. Moreover, the ultimate stress values of tested materials were detected to predict the ultimate stress value of composite. The yarn's cross section was assumed as circular and modelled with solid element. The diameter of yarn was calculated as 0.523 mm by using Equation 1 (Hearle et al., 1969), which is presented in below.

$$d = 4.44\ x\ 10^{-3} \sqrt{\frac{Tex}{FibreDensity}} \qquad (1)$$

Before the RVE of composite was created, the geometrical model of fabric was developed, which is presented in the Figure 1(a). The RVE of composite is 3.552 x 2.844 x 1.046 mm in warp, weft and thickness directions, respectively. The composite model was meshed with the tetrahedral element and its boundary conditions are given in the Figure 1(b).

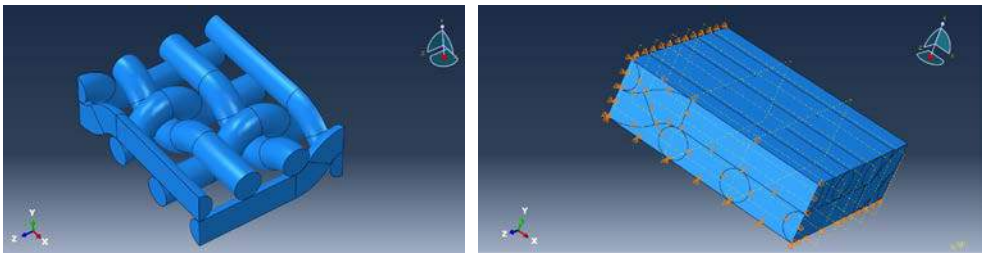

Figure 1. The fabric and composite models (a) the geometrical model of flax fabric (b) the boundary conditions of composite model

3. RESULTS AND DISCUSSION

The elastic module and ultimate stress values of flax yarn and epoxy resin were shown in the Table 1. The obtained results were used to identified material properties of developed model.

Table 1. Tensile test results of flax yarn and epoxy resin

	Elastic Module	Ultimate Stress
Flax Yarn	14.71 GPa	193.62 MPa
Epoxy Resin	2.84 GPa	29.85 MPa

The composite model was loaded in warp and weft directions to obtain stress- strain graphs and elastic properties. The stress distributions of loaded composite were presented in the Figure 2. The tensile load was carried by the yarns and maximum stress was occurred at crossing points as it is shown in the figure.

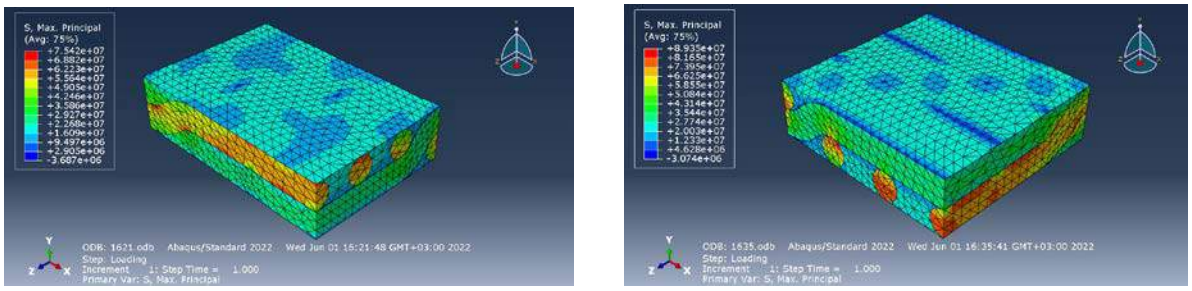

(a) (b)

Figure 2. The stress distributions of composite model (a) loaded in warp direction (b) loaded in weft direction

The stress- strain graphs of composite, which were obtained from the test and model, are given in the Figure 3. In the elastic region, high similarity is seen between the model and test results for both directions.

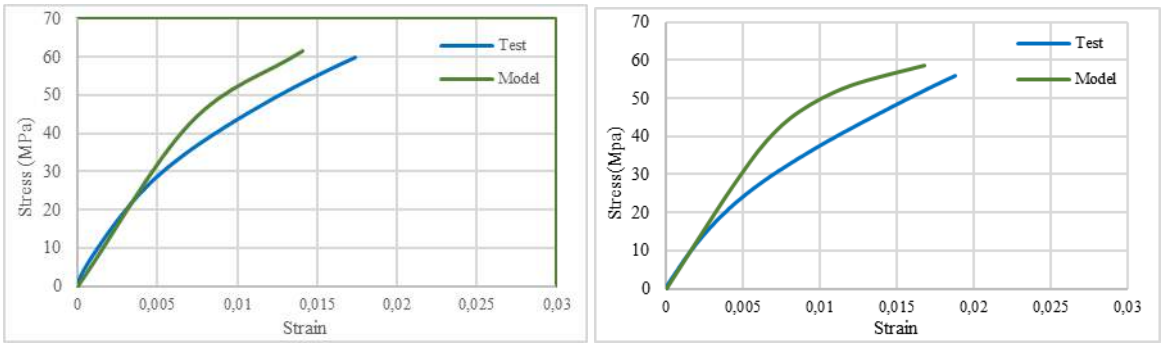

(a) (b)

Figure 3. The tensile stress- strain graphs of composite (a) warp direction (b) weft direction

Predicted and tested young modulus and ultimate stress values of composite are presented in the Figure 4. Higher than 90% agreement could be obtained for both values.

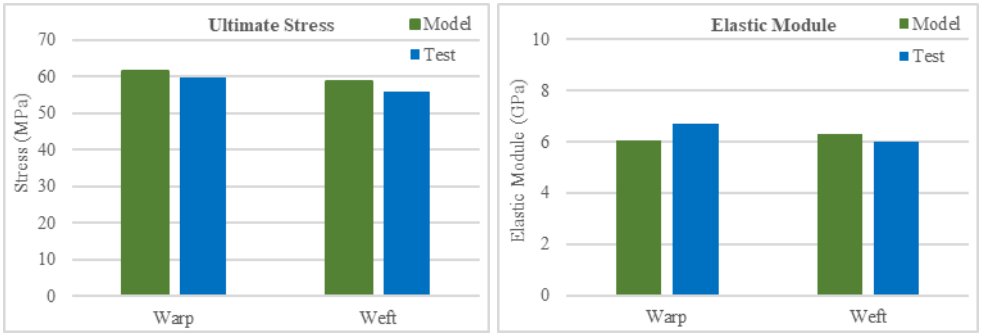

(a) (b)

Figure 4. The predicted and tested elastic module and ultimate stress values of composite (a) ultimate stress (b) elastic module

4. CONCLUSION

The natural fibre reinforced composites have been emerged as good alternatives for man- made fibre reinforced composites according to their eco- friendly structure and recycle abilities. However, their mechanical properties depend on various parameters and hard to characterize. This phenomenon makes complex to predict their mechanical properties. In the study, a numerical composite model was developed at mesoscopic level and its properties were examined with the representative volume element. As the material model could be correctly created, the flax yarn and resin were tested and their elastic properties were determined. Thanks to the developed model, the elastic module and ultimate stress values of composite could be detected as well as the stress- strain graph. Model results were validated with the test results and good agreement could be obtained. The in- plane shear and compressive properties of flax woven fabric reinforced polymer composite will be modelled as the further study of research.

REFERENCES

2022 State of the Industry Report | Composites Manufacturing Magazine. (n.d.). Retrieved June 2, 2022, from https://compositesmanufacturingmagazine.com/2022/02/84417/3/

Abaqus CAE - SIMULA™ by Dassault Systèmes®. (n.d.). Retrieved June 2, 2022, from https://www.3ds.com/products-services/simulia/products/abaqus/abaquscae/

Antony, S., Cherouat, A., & Montay, G. (2018). Experimental, analytical and numerical analysis to investigate the tensile behaviour of hemp fibre yarns. *Composite Structures*, *202*(February), 482–490.

Bambach, M. R. (2019). Experimental and numerical study of the bending strength of natural fibre composite structural channel sections. *Composite Structures*, *210*, 57–69.

Beigpour, R., Shokrollahi, H., & Khalili, S. M. R. (2021). Experimental and numerical analysis of a biodegradable hybrid composite under tensile and three-point bending tests. *Composite Structures*, *273*(May), 114255.

Hearle, J. W. S., Grosberg, P., & Backer, S. (1969). *Structural Mechanics of Fibers, Yarns and Fabrics*. Wiley- Interscience.

Selver, E., Ucar, N., & Gulmez, T. (2018). Effect of stacking sequence on tensile, flexural and thermomechanical properties of hybrid flax/glass and jute/glass thermoset composites. *Journal of Industrial Textiles*, *48*(2), 494–520.

Sliseris, J., Yan, L., & Kasal, B. (2016). Numerical modelling of flax short fibre reinforced and flax fibre fabric reinforced polymer composites. *Composites Part B: Engineering*, *89*, 143–154.

Xiong, X., Hua, L., Miao, M., Shen, S. Z., Li, X., Wan, X., & Guo, W. (2018). Multi-scale constitutive

modeling of natural fiber fabric reinforced composites. *Composites Part A: Applied Science and Manufacturing*, *115*(August), 383–396.

Xu, D., Cerbu, C., Wang, H., & Rosca, I. C. (2019). Analysis of the hybrid composite materials reinforced with natural fibers considering digital image correlation (DIC) measurements. *Mechanics of Materials*, *135*(May), 46–56.

JUTE FIBER REINFORCED COMPOSITES USING TANNIC ACID AS FLAME RETARDANT

Bengi KUTLU[1], Erdem SELVER[2]
[1] Dokuz Eylul University, Department of Textile Engineering, İzmir, Türkiye
[2] Kahramanmaraş Sutcu Imam University, Department of Textile Engineering, Kahramanmaraş, Türkiye

Corresponding author: bengi.kutlu@deu.edu.tr

Abstract: *Flame retardancy processes require sustainable solutions because of their general character as generally high concentrations in phosphorus-nitrogen synergistic compounds and still halogenated chemical usage in some flame retardancy applications. In this study, one of the natural agents, tannic acid, was used to obtain flame retardant jute fabric reinforced thermoset composite material. Sodium ion was used to enhance flame retardant property of tannic acid. Three different combinations of concentrations were used to obtain the flame retardancy. Vertical burning test and limiting oxygen index measurements was used to measure flame retardancy while Scanning Electron Microscopy images of fabrics was taken for distribution of impregnation. Jute fabric reinforced thermoset polymeric biocomposite materials were produced by vinyl ester matrix material and mechanical properties and limiting oxygen index of the composite materials were also investigated.*

Keywords: *biocomposite, flame retardant, tannic acid, sustainable, jute.*

1. INTRODUCTION

Natural fiber-reinforced polymer composites are found being promising products, because of their low cost, lightweight, high specific modulus, renewability and biodegradability. However, these biocomposites show low fire resistancy comparing to glass or Kevlar composites and this limits their final usage areas. The flame resistance of natural fiber reinforced polymer composites can be improved by the addition of flame retardants. The most common flame retardants contain phosphorus or halogen and these have toxic and environmentally hazardous properties. Therefore, alternative substances are needed to have more sustainable, harmless, and nontoxic structures. Tannic acid is one of the choice with its plant-based origin. It is a water soluble, antioxidant, anticarcinogenic and antibacterial polyphenolic molecule. Because of its outer and inner galloyl units, it releases carbon dioxide and forms crosslinked aromatic structures when it is exposed to heat. It has a potential intumescent character. According to literature, the addition of sodium ions in tannic acid solution results in synergistic action to protect cotton fibers (Nam et al. 2016, Nam et al. 2017). Tannin based polyphenols are shown as more effective on ligno-cellulosic polymers compared to the cellulosic polymer like cotton in terms of oxygen index and flame spread time, due to the presence of lignin (ligno-cellulose) in those polymers (Nam et al. 2016, Nam et al. 2017, Nam et al. 2019). The aim of the study is to observe the effects of different recipes of Tannic Acid and NaOH on properties of sustainable flame retardant biocomposites, which were manufactured, from natural lingo-cellulosic fiber (jute) fabric and vinyl ester polymer matrix.

2. MATERIALS AND METHODS

2.1. Preparation of Flame Retardant Jute Fabric and Composite Structure

Unscoured jute fabric was used as received. The jute fabric is plain woven and its areal density is 260.6 g/m^2. In order to obtain the textile base of flame retardant biocomposites, first of all jute fabrics were impregnated with tannic acid-NaOH solutions at room temperature with given ratios in Table 1 with a pressure 10psi and padder speed of 5 rpm. After the impregnation, fabrics were dried at room temperature.

Table 1. Flame Retardant Padding Recipes

Concentrations (m/v)	Recipe 1 (J20-1)	Recipe 2 (J20-5)	Recipe 3 (J25-1)
Tannic Acid	20%	20%	25%
NaOH	1%	5%	1%

2.2. Composite Manufacturing

Pure jute and tannic acid/NAOH impregnated jute fabrics were prepared for vacuum infusion process with [0/90/90/0] stacking sequence. Polives 702 vinyl ester resin mixture was prepared and infused to the jute preforms using vacuum infusion process. For preparation, 0.2% by weight of 6% Cobalt (accelerator) was first added to the vinyl ester resin at room temperature and mixed with a spatula until a homogeneous mixture was formed. Then 1-2% of MEK-P (hardener) was added and mixing continued for another 5 minutes. The prepared resin mixture was given to the preforms under vacuum through the inlet hose as shown in Figure 1. At the end of the process, they were left to cure at room temperature for 2 hours. After the curing, composite samples were kept for 1 day and then removed from the vacuum table.

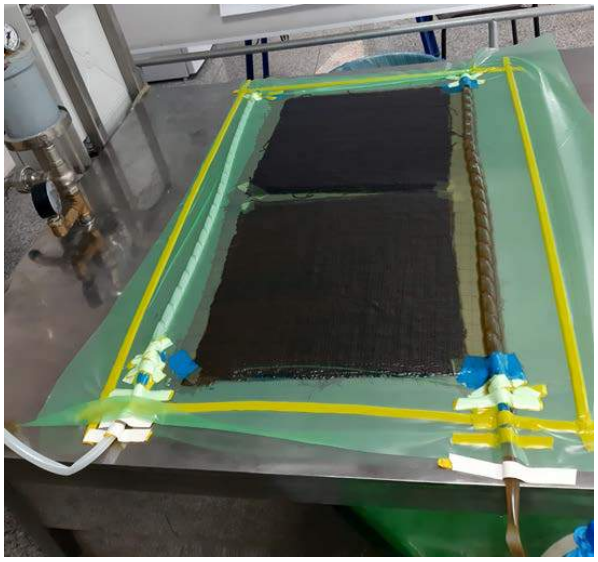

Figure 1. Vacuum infusion process for jute fabric reinforced composites

2.3. Investigation of Burning Properties

To observe flammability characters of fabrics and biocomposites, limiting Oxygen Index (LOI) measurement (ASTM D 2863) was applied in the laboratory of Dokuz Eylül University Textile Engineering.

2.4. Scanning Electron Microscopy

Scanning Electron microscope images of impregnated and untreated fabrics were obtained by Carl Zeiss 300VP device. Samples were gold coatedby Quorum Q150 RES coating device.

2.5. Composite Testing

The densities of the produced composites were measured using ASTM D792 test method using a digital density meter in the Kahramanmaraş Sütçü Imam University Textile Engineering composite laboratory.

Flexural strength tests were carried out according to ASTM D7264 standard using Hounsfield H5KS brand test device located in the Department of Textile Engineering of Sütçü İmam University. The distance between the support points (span) was chosen as 16, and the test speed was determined as 5 mm/min.

3. RESULTS AND DISCUSSION

Sodium hydroxide strongly supports flame retardant character of tannic acid treatment (Nam et al. 2016, Nam et al. 2017). Therefore, in this work, different tannic acid/NaOH combinations were studied. SEM images of untreated and tannic acid/NaOH treated are seen in Figure 2.

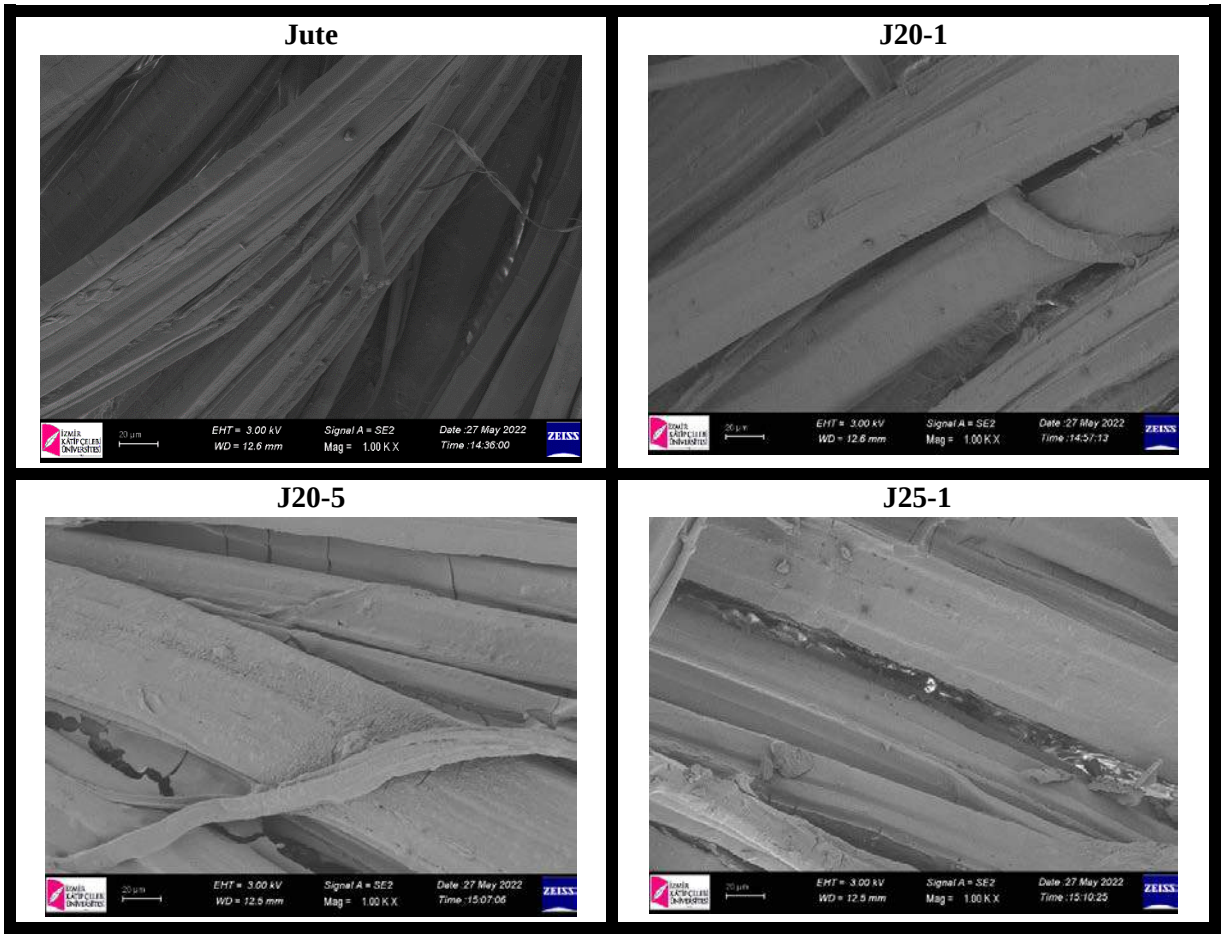

Figure 2. SEM images of fabrics

SEM images were taken from the untreated and tannic acid treated fabrics before limiting oxygen index measurements. Untreated fabric surface did not show any deposition on the surfaces of fibers. However, tannic acid deposits on the fiber surfaces were observed clearly from especially J20-5 coded treated fabric, which has the highest limiting oxygen ratio among all samples.

Limiting oxygen index results of the fabrics and jute composite were given in Table 2. Limiting oxygen index results indicated that tannic acid treatment enhanced flame retardance properties of jute fabric. Before treatments jute fabric was easily burning but after FR treatments all of the fabrics could be classified as flame retardant. LOI value of tannic acid-NaOH treated fabrics were increased by 38-43%.

Table 2. Limiting Oxygen Index of Fabrics and Composites

	Limiting Oxygen Index (%)
Jute	18.2
J20-1	25.1
J20-5	26.1
J25-1	25.1
Jute-C	20.3
JC20-1	21.2
JC20-5	22.0
JC25-1	21.2

The increase in the flame retardancy was found to be result of interactions of tannic acid and sodium ions, increasing adsorption of tannic acid on the fiber, catalysing decarboxylation of tannic acid and dehydration of cellulose. However, increase in limiting oxygen index values was lower than cotton in the literature and the reason may be the scouring pre-treatment of cotton before tannic acid-NaOH application (Nam et al. 2017).

Table 3 presents basic properties of composite laminates. The thicknesses of the composites were increased by addition of tannic acid and NaOH. The thickness of the pure jute composite (Jute-C) is about 2.86 mm whilst the thicknesses of JC20-1, JC20-5, and JC25-1 composites are 3.91, 3.99, and 3.95 mm, respectively. Table 3 also presents the densities of the composites. The densities were slightly decreased after impregnating of jute fabrics with tannic acid and NaOH. This is probably due to increased thicknesses for the tannic acid and NaOH impregnated composites.

Table 3. Composite sample properties

Samples	**Tannic acid (%)**	**NaOH (%)**	**Thickness (mm)**	**Density (g/cm^3)**
Jute-C	-	-	2.86 (±0.08)	1.200 (±0.008)
JC20-1	20	1	3.91 (±0.11)	1.188 (±0.003)
JC20-5	20	5	3.99 (±0.05)	1.178 (±0.002)
JC25-1	25	1	3.95 (±0.13)	1.180 (±0.005)

Table 4 and Figure 3 presents flexural test results of composites. It is clear that flexural strength of jute, JC20-1 and J25-1 composite samples are very similar. Those JC20-1 and JC25-1 composites have 1% of NaOH with %20 and 25% tannic acids. It seems that tannic acid ratio made little effect on flexural strength whilst flexural strength of JC20-1 and J25-1 composites are 61.14 MPa and 59.90 MPa, respectively. On the other hand, jute composite with 5% of NaOH had lower flexural strength compared to other samples. It can be seen from Table 1 that JC20-5 composite has about %20 lower flexural strength than JC20-1 composite. This show that increasing amount of NaOH decreased the flexural strength of composites. This might be due to deteriorating of jute fibers or reducing interfacial strength between jute fabric and vinyl ester after being used NaOH.

Table 4. Flexural test results of composites

Samples	**Tannic acid (%)**	**NAOH (%)**	**Flexural Strength (MPa)**
Jute-C	-	-	62.38 (±3.7)
JC20-1	20	1	61.14 (±4.2)
JC20-5	20	5	48.77 (±4.3)
JC25-1	25	1	59.90 (±5.8)

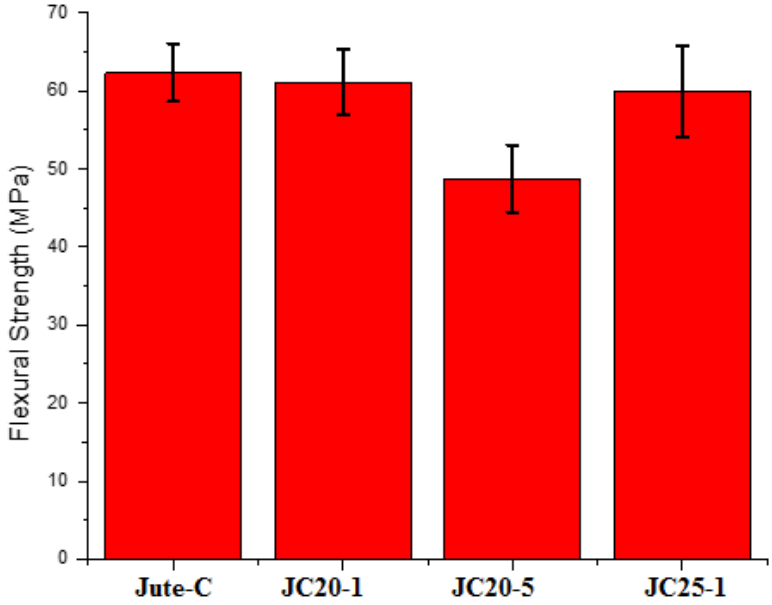

Figure 3. Composite flexural strengths

4. CONCLUSION

This work aimed to create a flame retardant bio based composite product. Tannic acid is a natural chemical giving flame retardancy properties helping to obtain sustainable flame retardant biocomposite materials. As a conclusion, flame retardant property of jute fabric can be obtained by tannic acid solution containing sodium in the reaction medium. Sodium enhances flame resistance property especially when 5% used. This flame retardancy solution can be a sustainable alternative to common flame retardant agents for jute fiber biocomposite materials with keeping the mechanical properties unchanged.

REFERENCES

Nam, S., Condon, B.D., Xia, Z., Nagarajan, R., Hinchliffe, D.C. & Madison, C.A. (2017). Intumescent flame-retardant cotton produced by tannic acid and sodium, *Journal of Analytical and Applied Pyrolysis*, 126, 239-246.

Nam, S. Easson, M.W., Condon, B.D., Hillyer, M.B., Sun, L., Xia, Z. & Nagarajan, R. (2019). A reinforced thermal barrier coat of a Na–tannic acid complex from the view of thermal kinetics, *RSC Advances*, 9, 10914-10926.

Nam, S., Kim, H.J., Condon, B.D., Hinchliffe, D.C., Chang, S.C., McCarty, J.C., Madison, C.A. (2016). High resistance to thermal decomposition in brown cotton is linked to tannins and sodium content, *Cellulose*, 23, 1137-1152.

Ray, D., Sarkar, B.K., Rana, A.K. & Bose, N.R. (2001). The mechanical properties of vinylester resin matrix composites reinforced with alkali-treated jute fibres, *Composites Part A*, 32, 119-127.

Shahinur, S., Hasan, M., Ahsan, Q. & Saha, D.K. (2013). Effect of Fire Retardant Treatment on Thermal Properties of Jute Fiber, *Bangladesh Journal of Physics*, 13, 53-58.

IMPROVING THE IMPACT STRENGTH OF HEMP/EPOXY BIO-COMPOSITES BY POLYDIMETHYLSILOXANE FABRIC COATING

Görkem GEDİK[1], İnan AĞIR[2]

[1]Pamukkale University, Textile Engineering Department, Denizli, Türkiye
[2]Pamukkale University, Mechanical Engineering Department, Denizli, Türkiye

Corresponding author: gorkemgedik@pau.edu.tr

Abstract: *This study aims to investigate and improve impact properties of hemp fiber-epoxy bio composites. For this purpose, hemp fabric reinforcement was coated with polydimethylsiloxane (PDMS) polymer. Different epoxy/fiber volume ratios were carried out. Mechanical and thermal tests were performed to understand the effect of hemp fiber reinforcement and PDMS coating. Notable effect of PDMS coating was observed on the impact strength of the samples, the Izod pendulum impact strength was increased up to 4 times higher by PDMS coating compared to neat epoxy. Thermal characteristics of the samples were evaluated by TGA, DTG and DSC analysis. Surface functional groups and effect of PDMS coating were evaluated by FT-IR measurements.*

Keywords: *Hemp, epoxy, bio-composite, PDMS, impact strength.*

1. INTRODUCTION

Sustainable production methods are the interest of almost all industry branches today, including textile industry (Gedik and Avinc, 2022). For epoxy composite production researchers investigate more eco-friendly alternatives for synthetic reinforcement materials. Hemp fiber is one of the most important candidates for this purpose with its superior environmentally friendly properties (Gedik and Avinc, 2021). The term “bio-composites” is used for these kinds of composite materials which consist of at least one sustainable material (matrix or reinforcement) (Mazzanti et al., 2019).

Epoxy resins offer many advantages such as high strength, low shrinkage, solvent resistance and so on. On the other hand, highly cross-linked structure results in low impact resistance and toughness (Vilcakova et al., 2018). This study aims to overcome this drawback of epoxy composites by using sustainable hemp reinforcement fabric. For this target, hemp fabrics were coated with PDMS polymer for the absorption of the impact energy.

2. MATERIALS AND METHODS

2.1. Alkali Treatment and PDMS Coating of Hemp Fabric

Greige hemp fabric (plain weaved) was alkali treated for the surface improvement in order to enhance the interaction between epoxy matrix and the textile material. The process was carried out with 5 g/L NaOH (Tekkim) and 1 g/L wetting agent (Rudolf) at 95ºC for 60 minutes with 1/20 liquor ratio. Subsequently, the fabric was cold and warm washed, neutralized with 1 g/L acetic acid and finally cold rinsed.

Vinyl terminated PDMS (Wacker Industries) was coated onto hemp fabric by solvent method. PDMS and the hardener (A and B compounds) were mixed in 1:1 weight ratio and dissolved in tetrahydrofuran (THF) (Sigma). The final PDMS concentration in the solution was 25%. Hemp fabric was treated with PDMS solution at 30ºC for 60 minutes in a laboratory type dyeing machine (ATAC). After treatment, fabrics were dried in fume hood for 24 hours. Following this step, the PDMS coated fabric was cured at 165ºC for 10 minutes.

2.2. Composite Production

Hand laying technique was applied for composite production. Diglycidyl ether of bisphenol A (DGEBA) epoxy resin (Hexion) was mixed with amine-based hardener (Hexion) in a 1:0.25 weight ratio to obtain epoxy matrix. PDMS coated and uncoated hemp fabrics were laid 1 or 3 plies which corresponds to 7.5 and 22.5% volume ratio, respectively. Silicon molds with 2 mm depth were utilized for composite production. The composite materials were cured at room temperature for 24 hours and then post cured at 60°C for 12 hours. Produced composite panels were cut with water jet into necessary dimensions for the following tests.

2.3. Fourier-Transform Infrared (FT-IR) Spectroscopy

Thermo Nicolet iS50 Infrared Spectrometer was used in ATR mode. Measurements were done at room temperature between the wavenumber range of 400-4000 cm^{-1}, with a resolution of 4 cm^{-1}.

2.4. Mechanical Tests

The tensile strength and Young's modulus values were determined according to ASTM D 3039 standard utilizing Tinius Olsen H10KT benchtop tester, equipped with 10 kN load cell. The test speed was 1 mm/minute and the gauge length was 50 mm. The impact tests were carried out according to the ASTM D256-10 standard with a pendulum type impact machine. CEAST Resil Izod impact tester with 7.5 joule hammer was used in the experiments.

2.5. TGA, DTG and DSC analyses

TG-DTG and DSC analyses were performed with Setaram SENSYS evo DSC, between 30-1000°C with 10°C/min temperature rise under N_2 atmosphere with 100 ml/min gas flow rate.

3. RESULTS AND DISCUSSION

Impact strength of a composite material can be described as the capacity of the energy absorption under a shock load (Parbin et al., 2019). Although epoxy has a very wide application area in the composite industry and has numerous advantages, in general, epoxy polymers are brittle and exhibit poor impact strength (Gao et al. 2012). From this perspective, the main aim was to overcome this weakness of epoxy composite by the aid of PDMS polymer. The results of Izod pendulum impact strength tests were presented in Figure 1. The impact strength of neat epoxy was 3.5 kJ/m^2. Uncoated hemp fiber reinforcement for 1 and 3 plies improved the impact strength around 60%, elevated to 5.6 kJ/m^2. The effect of PDMS coating is detected for 1 ply reinforcement, impact strength increased 89%. The increase with 3 plies of PDMS coated hemp fabric was dramatic, the impact strength of this sample was 14.8 kJ/m^2 which corresponds to 332% increase.

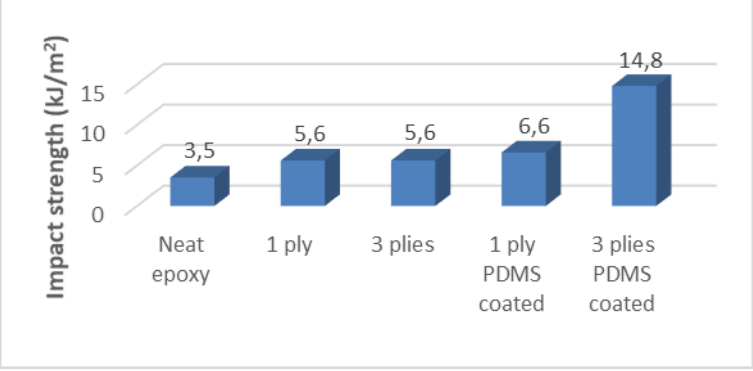

Figure 1. Impact strength values of the samples

Another important mechanical parameter for the composites is the tensile strength. The tensile strength values of the samples are seen in Figure 2. The neat epoxy exhibited tensile strength value of 44.5 MPa. It is expected the tensile strength values to increase with fiber reinforcement due to the new chemical bonding between matrix and reinforcement fiber. Hemp fabric reinforcement increased the tensile strength values up to 53.5 MPa with 1 ply hemp fabric reinforcement. A slight decrease was observed by 3 plies hemp fabric reinforcement compared to 1 ply fabric reinforcement. It is thought that, it would give better results to keep fiber ratio below 22.5%, under these conditions. PDMS coating resulted in a dramatic decrease on tensile strength values. Especially 1 ply PDMS coated fabric reinforcement exhibited the worst result (17.9 MPa) among all samples. It is an indicator that the bonding between epoxy matrix and the fabric weakens after PDMS coating. The increase on the tensile strength value of 3 plies reinforced sample compared to 1 ply reinforced sample, could be explained by the physical attraction between the fabric and the matrix. If impact strength and tensile strength test results evaluated together, it is thought that, the impact strength of PDMS coated samples increased due to the elastic structure and high shock dumping capacity of PDMS polymer, instead of transfer of the force between crosslinking bonds between epoxy and reinforcement fabric.

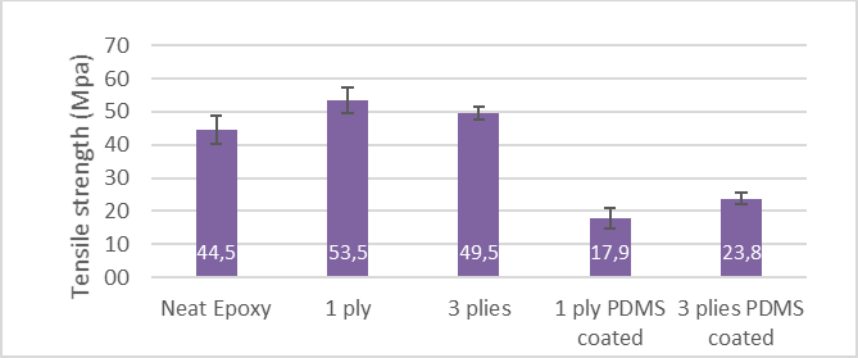

Figure 2. Tensile strength values of the samples

FT-IR spectrum of PDMS coated and uncoated alkali treated hemp fabrics was shown in Figure 3. 3338 cm^{-1} band is characteristic for stretching vibration of cellulose -OH. Coating resulted in a decrease on the intensity of this band. It is thought that the elimination of -OH groups may cause the decline on the tensile strengths due to lower bonding between reinforcement fabric and epoxy matrix. Si-C, S-O, Si-C-H bonds are seen on FT-IR spectrum at 1260, 1010 and 786 cm^{-1} respectively (Hamouni et al. 2019)

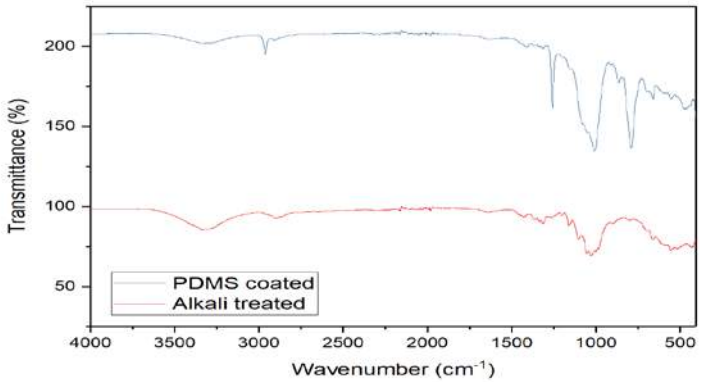

Figure 3. FT-IR Spectrum of PDMS coated and uncoated hemp fabrics

TGA and DTG curves of the samples are seen in Figure 4, DSC results are seen in Figure 5. Compared with neat epoxy, PDMS coating did not caused a distinctive change on the thermal characteristics of the material. The initial degradation of neat epoxy and PDMS coated hemp fiber reinforced epoxy composite started at 286ºC and 298ºC, respectively. Neat epoxy was stable up to 347ºC whereas PDMS coated sample was stable up to 345 ºC. The small initial endothermic peaks (around 0.02mW/mg) on the DSC curves were possibly related with delayed curing reaction of the epoxy resin. As a general trend, PDMS coated hemp fiber reinforcement resulted in higher peak areas which means higher energy take or release depending on the reaction type (endo or exo).

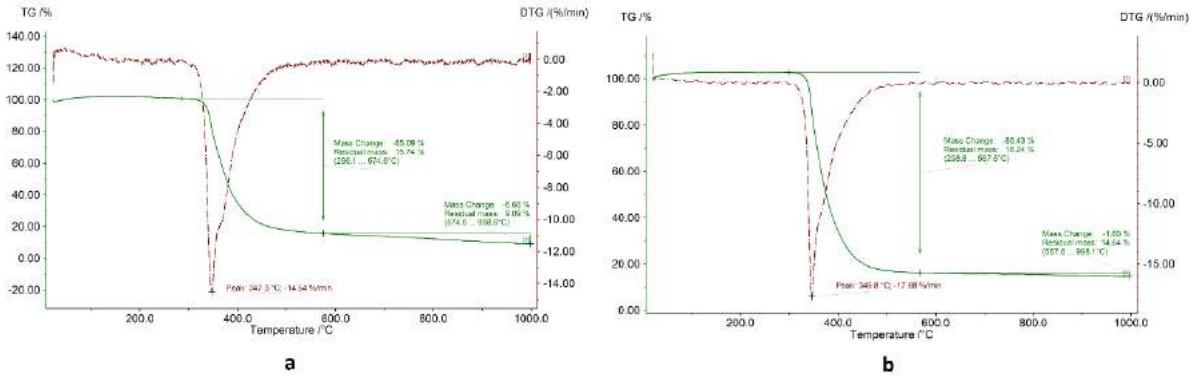

Figure 4. TGA and DTG results of the samples (a: neat epoxy, b: 3 plies PDMS coated hemp fabric reinforced)

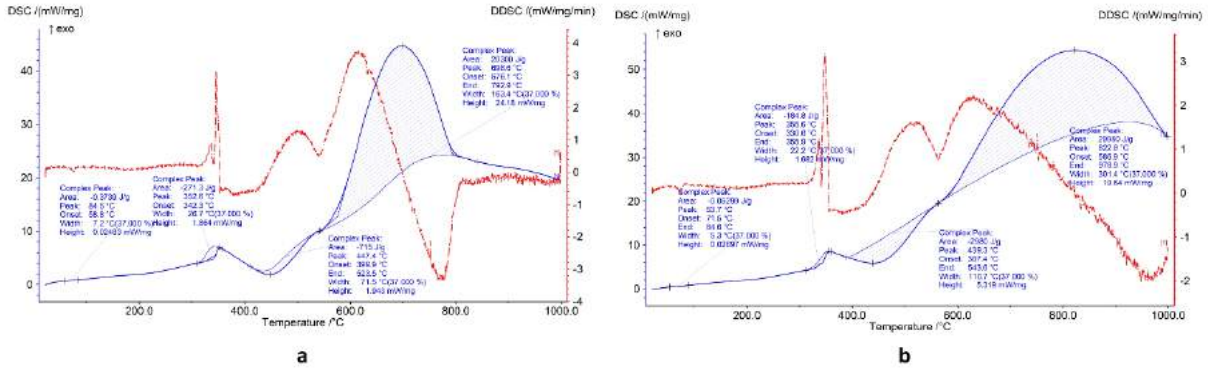

Figure 5. DSC results of the samples (a: neat epoxy, b: 3 plies PDMS coated hemp fabric reinforced)

4. CONCLUSION

In this work, epoxy bio-composite production with hemp fiber reinforcement was carried out. The main aim was to improve impact strength which is generally poor for epoxy composites, of the material. PDMS coating on fabric resulted in dramatic increase on the impact strength. Due to the masking effect of the coating on -OH groups of hemp cellulose, the interaction and bonding between fabric and epoxy polymer decreased, consequently, decrease on tensile strengths (46% for 3 plies reinforcement) was observed for PDMS coated fabrics. This study was successful in the manner of increasing impact strength; however, further studies are required to prevent tensile strength loss.

ACKNOWLEDGEMENT

This study was supported by Pamukkale University Scientific Research Projects Department (PAUBAP) with project number 2020BSP006.

REFERENCES

Gao, J., Li, J., Benicewicz, B.C., Zhao, S. & Hilborg H. (2012) The Mechanical Properties of Epoxy Composites Filled with Rubbery Copolymer Grafted SiO_2. *Polymers, 4*(4), 187-210.

Gedik, G. & Avinc, O. O. (2021) Hemp Fiber as a Sustainable Raw Material Source for Textile Industry: Can We Use Its Potential for More Eco-Friendly Production? In Muthu, S.S. & Gardetti, M. A. (Eds.) *Sustainability in the Textile and Apparel Industries*. Springer.

Gedik, G. & Avinc, O. O. (2022) Hemp Usage in Textile Industry. In Belwal, T. & Belwal, N. C. (Eds.) *Revolutionizing the Potential of Hemp and Its Products in Changing the Global Economy*. Springer

Hamouni, S., Abdessemed, D., Nezzal, G. & Van der Brugen B. (2019) Alcohol and Alkane Organic Extraction Using Pervaporation Process. *Macromoecular. Symposia*, *386*, 1-8.

Mazzanti, V, Pariante, R, Bonanno, A, de Ballesteros, OR, Mollica, F & Filippone, G (2019) Reinforcing mechanisms of natural fibers in green composites: role of fibers morphology in a PLA/hemp model system. *Compos Sci Technol, 180*, 51–59.

Parbin, S., Waghmare N.K., Singh, S.K. & Khan, S. (2019) Mechanical properties of natural fiber reinforced epoxy composites: A review. *Procedia Computer Science, 152*, 375-379.

Vilcakova, J., Kutejova, L., Jurca, M., Moucka, R., Vicha, R., Sedlacik, M., Kovalcik, A., Machovsky, M. & Kazantseva, N. (2018) Enhanced Charpy impact strength of epoxy resin modified with vinyl-terminated polydimethylsiloxane. *Journal of Applied Polymer Science*, *135*, 1-12.

DESIGNING TEXTILE BASED ON CONDUCTIVE POLYMER COMPOSITE FOR HEATING APPLICATIONS

A. CAYLA[1], L. MARISCHAL[1], C. CAMPAGNE[1], E. DEVAUX[1]

[1]Univ. Lille, ENSAIT, ULR 2461 - GEMTEX - Génie et Matériaux Textiles, F-59000 Lille, France

Corresponding author: aurelie.cayla@ensait.fr

Abstract: *Heated textiles have the capacity to relieve patients suffering from Musculoskeletal disorders and/or Raynaud's disease. The objective of this work is the implementation and the characterization of conductive polymer composites (CPC) for the realization of self-regulated heating textile structures. In order to realize this functional textile, several scientific obstacles had to be overcome in the field of formulation and implementation of thermoplastic polymers. A metallic yarn coated with a blend of filler immiscible polymers was developed by extrusion/coating. Indeed, the metallic yarn allowed to ensure the heating of the textile by Joule effect thanks to its high electrical conductivity. On the other hand, the CPC sheath (mixture of filled immiscible polymers) allowed the transfer of electrical charge between the electrodes and the metallic yarn while ensuring the thermal self-regulation thanks to the effect of the positive temperature coefficient (PTC). Indeed, the CPC changes from an electrically conductive state to an insulating state when the CPC temperature reaches its phase transition temperature (melting), caused by the PTC effect. The development of this innovative wire was done in several steps. The first step was the development of a blend of filled immiscible polymers. However, this blend must respect two precise conditions such as a selective localization of the filler in a polymer, but also a co-continuous morphology. Several polymer couples were studied and one of them was selected. The second step was the optimization of electrically conductive fillers in the CPC via a mono- or multi-filler system. Thus, different carbonaceous fillers at different rates were studied in order to obtain an optimized mixture. The last step was the optimization of the extrusion/coating process parameters of the CPC coated yarn*

Keywords: *Carbon fillers, Heating textile, Conductive polymer composite, Melt coating, Polymer blends.*

1. INTRODUCTION

In today's world, textiles are omnipresent. Indeed, textiles have innumerable applications ranging from a simple cloth to an intelligent textile allowing to ensure several properties such as protection, comfort, etc.... These textiles are then used in many fields: sport, luxury, protective equipment, medicine and many others. It is in the medical field that the textile makes it possible to answer needs allowing to cure or prevent certain diseases.

One of the diseases where there are still very few solutions is Raynaud's disease. This disease is still unknown but affects in France between 3 and 12% of men and 6 to 20% of women, that is to say approximately 1.6 to 2 million people in total. In 80% of patients, this phenomenon is not serious and of unknown origin. This disease is a blood circulation disorder that manifests itself in the extremities (mainly fingers, toes and more rarely nose and ears) [Adjavuvu P., 2020; Devulder B., 1998, Hachulla, E. *et al.* 2017, Petit, I., 2009]. It manifests itself in attacks, most often triggered by exposure to cold or more generally to a thermal shock, and causes a narrowing of the blood vessels (vasoconstriction) which leads to a sudden and temporary stop of the arterial circulation. During the attacks, the extremities become white and insensitive, or even blue and swollen.

From the property of electrical conductivity, it is possible to develop heating textiles thanks to the Joule effect (thermal manifestation of the passage of current in a material that is a semi-conductor of electricity, conductor of electricity and/or superconductor of electricity). Thus, these heating products can prevent Raynaud's disease and also alleviate the pain of patients with Muscolo-Skeletal Disorders (MSDs) thanks to heat diffusion. A lot of research has been done on the development of heated textiles, such as the influence of electrical conductivity of the yarns, textile structure (design, sample size), and many others. However, these products are cumbersome because they require adequate electronic equipment: a battery, a voltage variator to adjust the temperature and electrically conductive yarns. In addition, most of these heated textiles use metallic yarns as electrical conductors, which modify the properties of the textile (flexibility, sustainability during washing, ...).

In order to design this self-regulating conductive core, a Conductive Polymer Composite (CPC) is used [Ounaies, Z. *et al.* 2003]. A CPC is an inherently insulating polymer into which electrically conductive fillers have been introduced to provide electrical conductivity in the polymer. A CPC is then electrically conductive when it reaches the percolation threshold of these fillers. Moreover, CPCs have a specific behavior allowing thermal self-regulation thanks to the positive temperature coefficient (PTC) effect [Nakano, H., *et al.* 2012]. This PTC effect allows a modulation of the electrical resistivity of the material according to the temperature. Indeed, when the CPC temperature increases, a modulation of the electrical resistivity takes place at thermal transitions and allows the material to become insulating, following a loss of filler percolation. Then, if the temperature of the CPC decreases, it will return to its initial configuration allowing the electrically conductive fillers to reconnect. To summarize, a CPC is (semi-)electrically conductive at room temperature but once the PTC effect temperature is reached, the material becomes insulating. Thus, the role of the CPC in the electrical circuit is to be a switch that changes its state according to its temperature.

One of the objectives of this study is the development of a self-regulating heating textile in temperature via the use of CPC. Indeed, the creation of a wire from a CPC is possible thanks to several implementation techniques such as melt spinning and melt coating.

2. MATERIALS AND METHODS

2.1. Materials and process

As a reminder, the PTC effect takes place when a phase transition temperature is reached, such as the melting temperature (Tf). Since temperature self-regulation occurs near a temperature of 58°C, the thermoplastic PCL was selected as the polymer for the CPC formulation since the melting temperature of CPC is at 58°C. The PCL used is PCL CAPA 6400 produced by Perstorp (Malmö, Sweden). This PCL has a glass transition temperature of -60°C, a density of 1.1 g/cm^3, and its thermal correction factor (ΔT) is -0.065 mN/m/K. The temperature coefficient allows the processing temperature to be considered when calculating surface energies. This PCL has a molar mass of 37,000 g/mol. In order to ensure the physical structure of the CPC during the PTC effect, the development of filled immiscible polymers blend is necessary. Thus, insulating polypropylene was studied to determine which blend allowed for co-continuity with CPC, noted PCL fillers, and also the selective localization of the fillers in PCL during processing. PP 9069, with a density of 0.905 g/cm^3 and developed by Total, was studied to develop the two-phase PP/PCL filler loaded blend.

There is a large number of electrically conductive fillers. Here, the fillers were only carbon nanofillers (carbon nanotubes and carbon blacks) for reasons of implementation, sustainability and thermal stability:

- Carbon nanotubes (CNT): CNT NC 7000, produced by Nanocyl, have an apparent density of 0.09 g/cm3 for an average diameter of 9.5 nm. They have a length of 1500 nm and their specific surface is between 250 m²/g and 300 m²/g.
- Carbon blacks (CB): CB Printex L6 (CB L6), produced by Orion Engineered Carbons, have a bulk density of 0.09 g/cm^3, specific surface area is 270 m²/g. Their primary diameter is 18 nm and they have a spherical geometry.

In order to implement the two-phase filler blends, a double extrusion is necessary. The first extrusion aims at developing the filled polymer and thus allowing a homogeneity and a dispersion of the fillers within the PCL (noted $PCL_{fillers}$). During this extrusion, the PCL is extruded either with one or a mixture of fillers (CB/CNT) with different ratio. The second extrusion aims at developing the filled biphasic mixtures (PP/$PCL_{fillers}$) with different ratios of polymers, ranging from 30 wt.% of $PCL_{fillers}$ to 70 wt.% of $PCL_{fillers}$ in each of the filled biphasic blends. The extruder used is a ThermoHaake PTW 16/25p co-rotating twin-screw extruder with a screw length of 400 mm and a diameter of 16 mm, giving it an L/D (length/diameter) ratio of 25.

To implement the self-regulating heating textile in temperature, the principle of coating in molten way is used. Indeed, the purpose of the coating principle is to ensure the PTC effect, thus the thermal self-regulation, by the CPC which is in the sheath but also to ensure the heating by Joule effect by the metallic yarn in the core. In the diagram shown in Figure 1, several key elements are noted during the coating process such as: a single screw extruder, a coating head, the yarn and the air cooling. In order to start this pilot, the yarn, which will be in the core, must first be passed through the coating head and then attached to a winder at the end of the process. The purpose of this winder will be to wind the coated yarn at a predefined speed. It is important at this stage to check that the yarn is in the center of the coating head. In a second step, the material is placed in the extruder to be conveyed to the coating head. The coating will then be able to completely cover the yarn before cooling. In our case, in the core there will be a metallic yarn and in the sheath the blend of filled immiscible polymers.

However, in order to be able to implement this coated yarn, different machine parameters are considered such as the speed of the yarn in the coating head, the speed of the extrusion screw, and therefore the flow of material arriving in the coating head. Indeed, this coating pilot uses a single screw extruder with an L/D ratio of 24. In addition, a vacuum pump can be used to create a vacuum of -0.8 bar in the coating head.

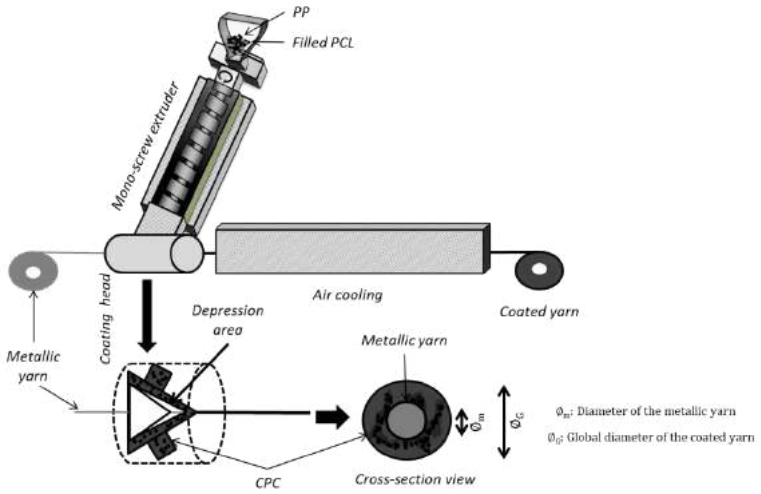

Figure 1: Metallic yarn coating process by CPC

2.2. Electrical characterisations

The measurement of electrical conductivity is performed by a 2-point system with a Keithley 2461. This source-meter allows to deliver a voltage (U) in a system and to measure a current (I). To be more precise, the source-meter delivers a voltage from -0,5 V and goes up to 15 V with a step of 0,5 V. The two clamps connected to the source-meter are spaced one centimeter apart. To improve the contact between the clamps and the sample, silver lacquer is deposited on the sample.

3. RESULTS AND DISCUSSION

Several formulations of the coating, which were an immiscible polymer blend between the PP and the filled PCL, were studied in order to determine their influence on the electrical properties of the coated metallic yarn. Several compounds were developed PP_{50} / $(PCL_{1.25CNT})_{50}$, PP_{50} / $(PCL_{4CNT})_{50}$, and PP_{50} / $(PCL_{0.5CNTC5CB})_{50}$. To understand the influence of the CPC formulation, the electrical conductivity of each CPC formulation was measured on the PP/PCL_{filled} and on the coating yarn $[MF]_c$-$[PP/PCL_{fillers}]_g$ and were illustrated in the Figure 2.

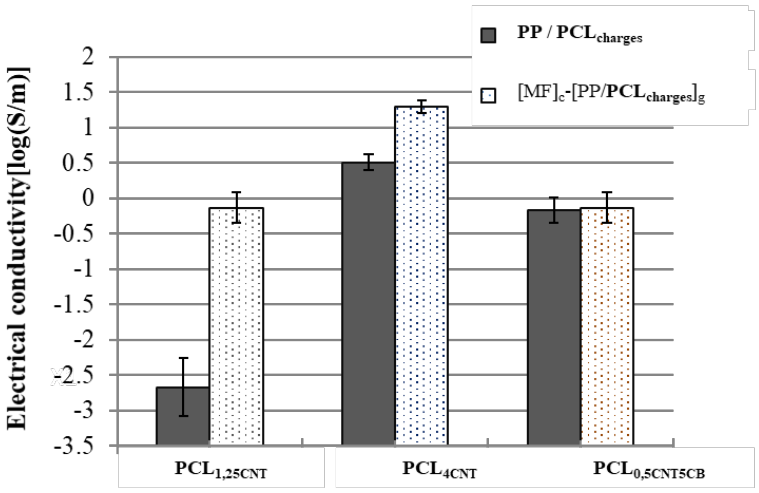

Figure 2 : Electrical conductivity according to the CPC formulation for the PP_{50} / $(PCL_{fillers})_{50}$ and $[MF]c$-$[PP/PCL_{fillers}]g$

The Figure 4 allowed to note several elements. For the blends filled with only CNT, the electrical conductivity had increased with the increase of the filler content. That is more, the electrical conductivity of the PP_{50} / $(PCL_{4CNT})_{50}$ was the highest due to the fact that its filler content was significantly higher than the percolation threshold as opposed to the other blends. The Joule effect of samples were measurement and their were illustrated by the Figure 5.

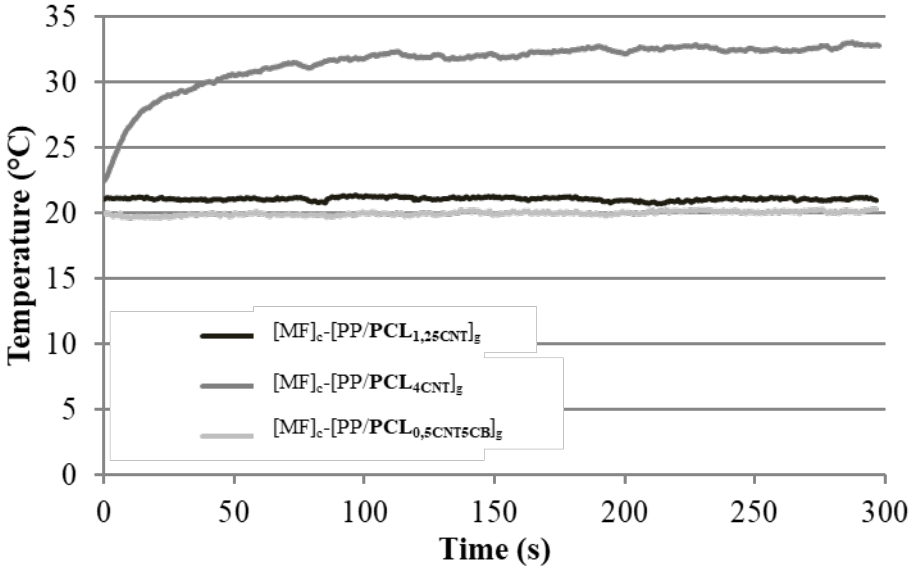

Figure 3 : The temperature according to the time for the $[MF]_c$-$[PP/PCL_{fillers}]_g$ at a voltage of 20 V

In the Figure 3, only the blend $[MF]_c$-$[PP/PCL_{4CNT}]_g$ had a temperature increase as opposed to the others blends which had no temperature increase. The $[MF]_c$-$[PP/PCL_{4CNT}]_g$ was the only one to have Joule effect thank to this high electrical conductivity. However, the electrical values between these blends were close. Thus, between the electrical conductivity of the $[MF]_c$-$[PP/PCL_{4CNT}]_g$ and the two other blends, $[MF]_c$-$[PP/PCL_{1.25CNT}]_g$ and the $[MF]_c$-$[PP/PCL_{0.5CNT5CB}]_g$, there was a threshold of electrical conductivity. In fact, above this electrical conductivty threshold, the heating power was ensured. Thus, it was important, for the development of the heating textile, to be above this electrical conductivity threshold. However, the PTC effect was important in order to have the self-regulating temperature. Thus, the PTC effect was also studied on these samples with the procedure presented. The values of these measurements were illustrated by the Figure 4. In order to have a better display, the sensibilty of the sample according to the increase of the temperature was only represented in the Figure 4.

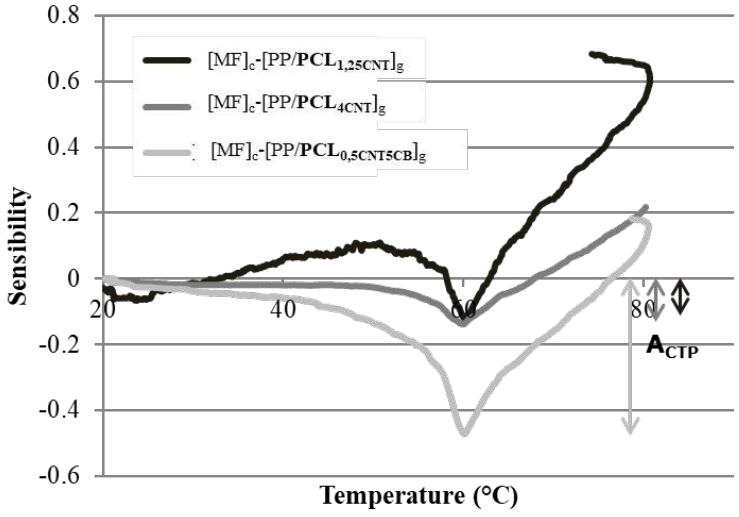

Figure 4 : The sensibility of the second temperature cycle according to the temperature of the $[MF]_c$-$[PP/PCL_{fillers}]_g$

4. CONCLUSION

At first, the CPC formulation was studied to understand her influence on the electrical properties (electrical conductivity, Joule effect and PTC effect). It was noted that the electrical conductivity of the coated yarn was dependant of the filler content of filler and the kind of filler. That is more, it was remarked that it was necessary a minimum of electrical conductivity to have a Joule effect. This minimum was between the electrical conductivity of the $[MF]_c$-$[PP/PCL_{1.25NTC}]_g$ and the $[MF]_c$-$[PP/PCL_{4NTC}]_g$. That is more, it was noted that the filler synergy allowed a sharp increase of the PTC effect as opposed as the other blends which were only with one kind of filler.

REFERENCES

Adjavuvu, P., Le phénomène de Raynaud en médecine générale : enquête auprès des médecins généralistes bordelais To cite this version : HAL Id : dumas-02499546 DIPLOME D ' ETAT de DOCTEUR EN MEDECINE Présentée et soutenue publiquement, 2020.

Devulder, B., Phénomène de Raynaud, Médecine Vasc. 1998, 281–285.

Hachulla, E., L. Mouthon, Sclérodermie Systémique, Protoc. Natl. Diagnostic Soins. 2017, 1–15.

Nakano, H., K. Shimizu, S. Takahashi, A. Kono, T. Ougizawa, H. Horibe, Resistivity-temperature characteristics of filler-dispersed polymer composites, *Polym.* (United Kingdom). 2012, 53, 6112–6117. doi:10.1016/j.polymer.2012.10.046.

Ounaies, Z., C. Park, K.E. Wise, E.J. Siochi, J.S. Harrison, Electrical properties of single wall carbon nanotube reinforced polyimide composites, *Compos. Sci. Technol*. 2003, 63, 1637–1646. doi:10.1016/S0266-3538(03)00067-8.

Petit, I., Phénomène de Raynaud : maladie ou syndrome ?: Questionnaire auprès de médecins généralistes de Nancy, 2009.

CHARACTERIZATION OF MEDITERRANEAN SEAGRASS *POSIDONIA OCEANICA (L.)*

Havva Nur ÖZDEMİR[1], Gizem Ceylan TÜRKOĞLU[2], Yasemin SEKİ[2], Gökdeniz NEŞER[3]

[1] Dokuz Eylul University, Department of Chemistry, Tınaztepe Campus, İzmir, Türkiye
[2] Dokuz Eylul University, Department of Textile Engineering, Tınaztepe Campus, İzmir, Türkiye
[3] Dokuz Eylul University Institute of Marine Sciences and Technology, İnciraltı, İzmir, Türkiye

Corresponding author: gizem.turkoglu@deu.edu.tr

Abstract: *In this current study, Posidonia oceanica (L.) fibers were characterized in order to determine their potential to be used as additive/reinforcement for polymeric materials. Accordingly, fiber chemical composition, fiber density, and fiber surface morphology were analyzed to determine the basic properties of the fiber. Analyses revealed that cellulose, hemicellulose, and lignin amount of Posidonia oceanica (L.) fibers are found to be 45.35, 8.07, and 32.42%, respectively. Fiber density is 1.15g/cm^3. Scanning electron microscopy image to observe the surface morphology of the fiber showed fiber bundle structure and several impurities which are probably saline sand particles and other non-cellulosic components of Posidonia oceanica (L.). These formations create surface roughness which can be accepted as an advantage in reinforced/doped plastic materials.*

Keywords: *Posidonia oceanica (L.), cellulose, fiber, surface morphology, characterization*

1. INTRODUCTION

A Mediterranean indigenous seagrass called *Posidonia oceanica* (Linnaeus) Delile begins in shallow waters on the Mediterranean coast and spreads to a depth of 40 meters (Ferrero et al., 2015). It is very important both economically and ecologically for the marine environment because it prevents sea erosion with its roots, produces oxygen through photosynthesis in the water, provides a home for fish and other species to live in for shelter, food, and reproduction, and serves as the first link in the food chain (Cirik and Cirik, 1999). It has been shown through studies on the economic advantages of seagrass meadows to the ecology that this species contributes 15837 Euro ha^{-1} year^{-1}, which is more than what agricultural lands produce (Terrados and Borum, 2004). *P. oceanica*, which is 0-40 m. fluctuates between depths and can be found in clean, salty waters between 11 °C and 29 °C in the Mediterranean. With the help of currents and waves, dead Posidonia leaves build banks along the shore. Many sea species may survive thanks to these structures, which also shield the coastline from erosion (Ferrero et al., 2015).

The manufacturing of polymeric composite with good mechanical performance and desired properties requires awareness and a search for novel cellulosic natural fibers. In related literature, there are many papers focused on the characterization and extraction of natural fibers (Köktaş et al. 2022; Albayrak et al. 2022; Seki et al. 2018; Erdoğan et al. 2016). To meet the demands for biodegradable, abundant, and ecologically friendly fibers, *P. oceanica* fibers were characterized as a potential cellulose resource for many applications. In accordance with related literature, very limited research has been conducted on the usability of *P. oceanica* in composite manufacturing and its absorption performance. In this study, fiber chemical composition and fiber density were determined. Also, fiber surface morphology was observed by scanning electron microscopy. Furthermore, X-ray diffraction (XRD), thermogravimetric analysis (TGA) and Fourier transform - infrared spectroscopy (FT-IR) are employed to determine crystallographic, thermal, and chemical properties of *P. oceanica* fiber, respectively.

2. MATERIALS AND METHODS

2.1. Materials

P. oceanica fibers were collected from Ayvalık shores (Türkiye) where summer activities are very intensive. NaOH, sulphuric acid, ammonia, acetic acid, sodium chlorite, and EDTA for fiber chemical composition analyses were provided from Sigma.

2.2. Methods

Fiber density was determined by Archimedes' Law (according to ASTM D8171-18 Method B). The density measurement was performed in triplicate. Each sample was oven-dried at 105 °C for 4 hours and then weighed. Afterward, the samples were immersed in boiling water for 24 hours of water absorption. The excess water of the sample was removed and weighed. The density measurement of the fibers was calculated using the formula given in Eq.1,

$$d = \frac{W_d}{W_s - W_d} \qquad \text{Eq.1}$$

where, d indicates the density, W_d and W_s are the dry weight and the actual mass of fibers immersed in the deionized water, respectively (Belaadi et al. 2022; Dalmis et al. 2020).

Fiber chemical composition analysis was performed by using chemical procedures published in the papers of Dalmis et al., 2020 and Erdogan et al. 2017.

The morphological structure of *P. oceanica* was examined by FESEM FEI Nova Nanosem 650 model scanning electron microscope (SEM). SEM images were taken with an accelerating voltage of 5 kV. The average fiber and fibril diameters were calculated from 15 random measurements using ImageJ software on SEM micrographs.

The Rigaku Ultima 3 equipment was used to get the XRD pattern of *P. oceanica* with a copper X-ray radiation source., The power was kept at 40 kV 30 mA with a scan rate of 2°/min. The scanning was carried out in the 2θ range of 5° to 80°. Utilizing the empirical formula found in Eq. 2, the crystallinity index (CI) was determined (Keskin et al., 2020).

$$\text{Crystalline index (CI) (\%)} = \frac{(I_{200} - I_{am})}{I_{200}} \, x\, 100 \qquad \text{Eq.2}$$

where I_{am} denotes the minimum intensity around 18.1°, and I_{200} denotes the peak with the maximum intensity related to the lattice plane (200) at 22.32°. (Seki et al. 2018).

FTIR spectrum of *P. oceanica* fiber was obtained using potassium bromide as standard. This analysis was performed at room temperature using the Perkin Elmer FT-IR spectrometer (Spectrum BX). The wavenumbers were recorded in the range of 4000-450 cm^{1}. Spectra of the samples were obtained from 20 scans and the spectra were measured at a spectral resolution of 2 cm^{-1}.

TGA (Shimadzu DTG-60H) was employed to determine the thermal features of the fiber. The analysis was applied from room temperature to 600 °C at a rate of 10 °C/min under a nitrogen atmosphere.

3. RESULTS AND DISCUSSION

Determination analyses of *P. oceanica* fiber reveal that major components are cellulose, hemicelluloses, lignin, and pectin. The chemical composition is highly effective in thermal decomposition, crystalline structure, mechanical performance, and some other physical properties. The hemicellulose content is found as 8.07 % and the pectin amount is determined as 16.35 %. Cellulose and lignin are 45.35 % and 32.42 %, respectively. In accordance with related literature, cellulose is less but lignin is quite high with similar plant fibers such as *Hierochloe odarata* (Dalmis et al., 2020), *Centaurea solstitialis* (Keskin et al., 2020), *Conium Maculatum* (Kılınç et al., 2018).

The fiber density of *P. oceanica* was determined using the Archimedes principle, Eq. 1. The density of *P. Oceanica* fibers was calculated as 1.15 g/cm3, which is resembling the density of many natural fibers. Also, the density value of *P. Oceanica* fiber is very similar to that of fibers obtained from some new plants. The density of this fiber is slightly lower than cotton, flax, and hemp indicating that this fiber is lightweight.

SEM image of *P. Oceanica (L.)* fibers taken at 500 X magnification is presented in Figure 1. The micrograph presents *P. Oceanica (L.)* fiber consisting of many several elementary fibers bound together by pectin or other non-cellulosic constituents like the other natural cellulosic fibers (Keskin et al., 2020). It was observed that there were some impurities which might be saline and sand particles. These irregularities on the fiber surface increase surface roughness which can be beneficial when utilized as reinforcement material in composite manufacturing. A rough surface can provide mechanical interlocking between fiber and polymer in a composite system (Dalmis et al., 2020).

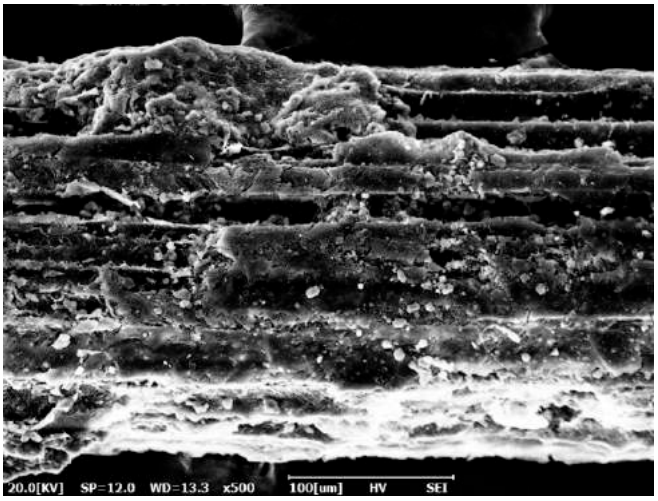

Figure 1. SEM image of *P. Oceanica* fiber

The crystalline structure, mechanical performance, thermal decomposition, and several other physical attributes are all much improved by the chemical composition (Poletto et al., 2012). The hemicellulose content is measured as 8.07% and pectin amount is determined as 16.35%. There are 45.35 and 32.42%, respectively, of lignin and cellulose. According to relevant studies, cellulose is lower but lignin is higher compared to similar plant fibers as *Piliostigma Racemosa* (Ramkumar and Saravanan, 2021), *Corypha taliera fruit* (Tamanna et al., 2021) and *Centaurea solstitialis* (Keskin et al., 2020).

Figure 2 shows the FT-IR spectrum of *P. Oceanica* fiber in a band range of 4000 – 450 cm^{-1}. Generally, absorptions at the characteristic wavelengths are closely associated with the structures of

the chemical components. As seen in Figure 2, several characteristic wavelengths, marked above the spectral lines, are shared by hemicellulose, cellulose, and lignin. The strongest absorption band at 3422 cm^{-1} is associated with the O-H stretching and vibration of cellulose in the fiber (Porras et al. 2015). The peak located at 2924 cm^{-1} is assigned to the C–H stretching vibrations of methyl (-CH_3) and methylene (-CH_2) in cellulose and hemicellulose (Sharma et al. 2021). C=O aromatic stretch of lignin is observed at the peak at 1632 cm^{-1} (Sharma et al. 2021).

The peak found at 1513 cm^{-1} shows aromatic ring vibrations, the characteristic band of lignin (Sharma et al. 2004). The peak at 1428 cm^{-1} is assigned to the symmetrical bending of CH_2 in cellulose (Dalmis et al., 2020). The peak between 1200 – 1300 cm^{-1} indicates the presence of the hemicellulose group (Karakoti et al. 2018). Also, the peak at 1113 cm^{-1} can be attributed to the C-H in-plane deformation of the Syringyl unit of Lignin (Anuchi et al. 2022). The peak at 1035 cm^{-1} occurs as a result of C–O, and O–H stretching in the fiber (Dalmis et al. 2020). The region between 400-800 cm^{-1} can be assigned to the FTIR spectra of cellulose (Gümüşkaya et al. 2007).

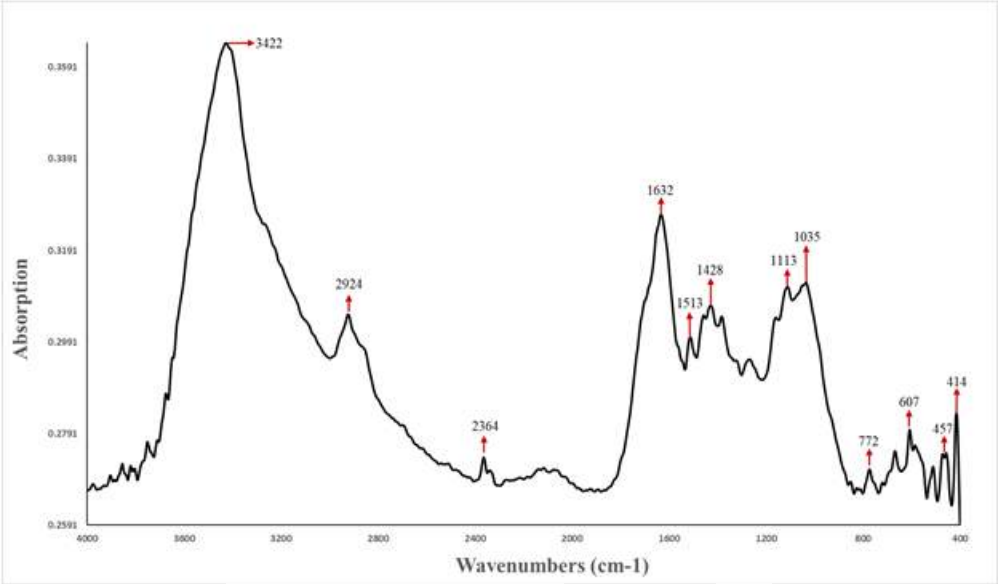

Figure 2. FTIR spectrum of *P. Oceanica* fiber

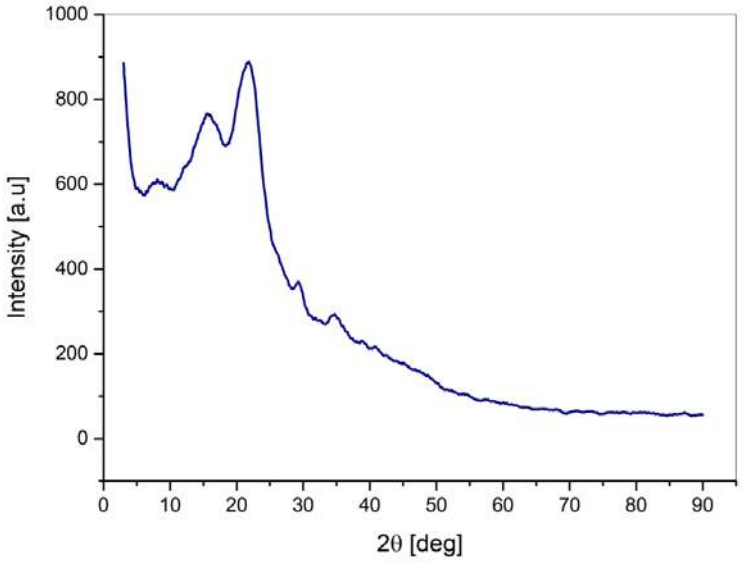

Figure 3. XRD spectra of *P. Oceanica* fiber

The crystallinity index and crystalline structure of the P. oceanica fibers were investigated using XRD analysis. The XRD pattern of the P. oceanica fibers is shown in Figure 3. Three cellulose I crystalline allomorph-specific diffraction peaks were found in the structure of the fibers from *P.oceanica* at approximately 15.42°, 22.0°, and 34.4°, with assigned planes of 1–10, 200, and 004, respectively (Tarchoun et al., 2019). Posidonia's XRD pattern also shows a peak that may be caused by the presence of lignin (Benito-Gonzalez et al., 2018).

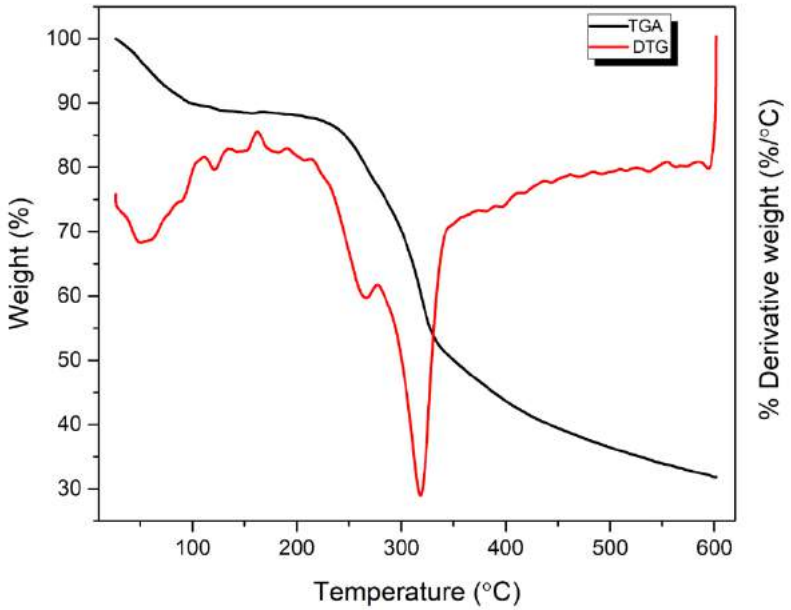

Figure 4. TGA-DTG graph *P. Oceanica* fiber

TGA-DTG was used to evaluate the thermal decomposition of *P. oceanica* fibers. Figure 4. The evaporation of water present in the fibers, which is responsible for the first mass loss till 200°C, which is measured as being about 11%, (Dalmis et al. 2020). The temperature at which deterioration begins is determined to be 173.2 °C with a mass loss of 11.3%, which can also be related to the breakdown of hemicelluloses in the fiber (Keskin et al., 2020). The maximal degradation temperature was reported to be 318.8 °C, with a mass loss of around 40% that can be related to the degradation of lignin and -cellulose.

4. CONCLUSION

P. Oceanica, which has a significant role in the marine ecosystem, is abundant on Turkey's Aegean and Mediterranean coasts. In this work, it is aimed to reveal the elemental properties of fibers of P. *Oceanica* and examine their possible use in the technical textile industry. Although the cellulose content is not very high, (45.4%) with a high lignin ratio (32.4) it can compete with other similar plantal fiber sources such as sweetgrass and hemlock. Therefore, it might be a possible alternative to synthetic fibrous particles in the composite industry as a reinforcement material with its lightweight and rough surface. Also, the economic value of *P. Oceanica* can be increased through these new versatile applications.

REFERENCES

Albayrak, D., Seki, Y., Balcı Kılıç, G., Koktas, S., Keskin, Ö. Y., Dalmış, R., & Karademir, C. (2022). Exploration of alternative cellulosic natural fiber from the stem of Malva Slyvestris. *Journal of Natural Fibers*, 1-18.

Anuchi, S. O., Campbell, K. L. S., & Hallett, J. P. (2022). Effective pretreatment of lignin-rich coconut wastes using a low-cost ionic liquid. *Scientific Reports*, *12*(1), 1-11.

Belaadi, A., Amroune, S., Seki, Y., Keskin, O. Y., Köktaş, S., Bourchak, M., ... & Jawaid, M. (2022). Extraction and characterization of a new lignocellulosic fiber from *Yucca treculeana L.* leaf as potential reinforcement for industrial biocomposites. *Journal of Natural Fibers*, 1-16.

Benito-González, I., López-Rubio, A., & Martínez-Sanz, M. (2018). Potential of lignocellulosic fractions from Posidonia oceanica to improve barrier and mechanical properties of bio-based packaging materials. International journal of biological macromolecules, 118, 542-551.

Cirik, Ş., Cirik, S., (1999). Su Bitkileri (Deniz Bitkilerinin Biyolojisi Ekolojisi yetiştirime Teknikleri) Ege Üniv. Su Ürünleri Fak. Yayın no:58. İzmir.

Dalmis, R., Koktas, S., Seki, Y. & Kılınç, A.Ç. (2020). Characterization of a new natural cellulose based fiber from Hierochloe Odarata. *Cellulose*, *27*, 127-139.

Erdoğan, U. H., Seki, Y., Aydoğdu, G., Kutlu, B., & Akşit, A. (2016). Effect of different surface treatments on the properties of jute. *Journal of Natural Fibers*, *13*(2), 158-171.

Erdogan, Ü.H., Selli, F. & Duran, H. (2017). Banana plant waste as raw material for cellulose extraction. *Fibres and Textiles. 3,* 48-52.

Ferrero, B., Fombuena, V., Fenollar, O., Boronat, T., & Balart, R. (2015). Development of natural fiber-reinforced plastics (NFRP) based on biobased polyethylene and waste fibers from Posidonia oceanica seaweed. Polymer Composites, 36(8), 1378-1385.

Gümüşkaya, E., Usta, M., & Balaban, M. (2007). Carbohydrate components and crystalline structure of organosolv hemp (Cannabis sativa L.) bast fibers pulp. *Bioresource Technology*, *98*(3), 491-497.

Karakoti, A., Biswas, S., Aseer, J. R., Sindhu, N., & Sanjay, M. R. (2018). Characterization of microfiber isolated from *Hibiscus sabdariffa var. altissima* fiber by steam explosion. *Journal of Natural Fibers*, *17*(2), 189-198.

Keskin, O.Y., Dalmış, R., Balci Kılıç, G., Seki, Y. & Koktas, S. (2020). Extraction and characterization of cellulosic fiber from *Centaurea solstitialis* for composites, *Cellulose, 27,* 9963-9974.

Kılınç, A.Ç., Koktas, S., Seki Y. et al. (2018). Extraction and investigation of lightweight and porous natural fiber from *Conium maculatum* as a potential reinforcement for composite materials in transportation, *Composites Part B:Engineering, 140,* 1-8.

Köktaş, S., Keskin, Ö. Y., Dalmiş, R., Seki, Y., & Balci Kiliç, G. (2022). Extraction and characterization of natural cellulosic fiber from Taraxacum Sect. Ruderalia. *Journal of Natural Fibers*, 1-9.

Porras, A., Maranon, A., & Ashcroft, I. A. (2015). Characterization of a novel natural cellulose fabric from Manicaria saccifera palm as possible reinforcement of composite materials. *Composites Part B: Engineering*, *74*, 66-73.

Ramkumar, R., & Saravanan, P. (2021). Characterization of the cellulose fibers extracted from the bark of Piliostigma Racemosa. Journal of Natural Fibers, 1-15.

Seki, Y., Kılınç, A. Ç., Dalmis, R., Atagür, M., Köktaş, S., Göktaş, A. A., ... & Önay, A. B. (2018). Surface modification of new cellulose fiber extracted from Conium maculatum plant: a comparative study. *Cellulose*, *25*(6), 3267-3280.

Sharma, S., Nargotra, P., Sharma, V., Bangotra, R., Kaur, M., Kapoor, N., ... & Bajaj, B. K. (2021). Nanobiocatalysts for efficacious bioconversion of ionic liquid pretreated sugarcane tops biomass to biofuel. *Bioresource technology*, *333*, 125191.

Sharma, R. K., Wooten, J. B., Baliga, V. L., Lin, X., Chan, W. G., & Hajaligol, M. R. (2004). Characterization of chars from pyrolysis of lignin. *Fuel*, *83*(11-12), 1469-1482.

Tamanna, T. A., Belal, S. A., Shibly, M. A. H., & Khan, A. N. (2021). Characterization of a new natural fiber extracted from Corypha taliera fruit. Scientific Reports, 11(1), 1-13.

Tarchoun, A. F., Trache, D., & Klapötke, T. M. (2019). Microcrystalline cellulose from Posidonia oceanica brown algae: Extraction and characterization. International journal of biological macromolecules, 138, 837-845.

Terrados J., & Borum J. (2004). European Seagrasses: An Introduction to Monitoring and Management. "Why are Seagrasses important? – Good and Services provided by seagrass meadows" Ed. J. Borum, CM Duarte, D Krause Jensen and TM Greve Chapter 2 (8-10).

EFFECT OF GRAPHENE-REINFORCED POLYAMIDE 6 FIBER ON STRENGTH AND FUNCTIONAL PROPERTIES OF WOOL BLENDED WOVEN FABRICS

Nazlı CAGLAR CİNPERİ[1]

[1] YÜNSA, R&D Center, Tekirdağ, Türkiye

Corresponding author: ncinperi@yunsa.com

Abstract: *Graphene (GRA) is a material that has been researched in many areas and started to be used in various research areas, combining its unique nanoscale and many functional properties. Having a unique and strong bond structure, two-dimensional graphene gives very good electrical, electrochemical, optical, thermal and mechanical properties. In this study, SEM, TGA, DSC analyses of polyamide 6 fiber containing graphene were performed. Functional and strength properties of the wool blended woven fabrics containing this fiber, such as absorbency, drying speed, UV protection, antibacterial, blade-cut resistance, abrasion, tear strength and breaking strength were tested. Abrasion values of the produced fabrics were obtained as over 100,000 cycles. Good results in absorbency, drying speed, UV protection and blade-cut resistance tests of the fabrics have been obtained.*

Keywords: *Graphene, high performance fabrics, multi-functional fabrics, UV protection, blade-cut resistance*

1. INTRODUCTION

Graphene is a material that has been researched and used in different fields thanks to its many functional properties. The limitations of traditional personal protective equipment were a topic of discussions and it was thought that graphene could be an effective tool to overcome these limitations and improve properties such as mechanical strength, antibacterial activity, flame resistance, conductivity and UV resistance. Methods for incorporating graphene into Personal protective equipment (PPE) fabrics using its unique properties are discussed (Bhattacharjee et al., 2019; Caglar Cinperi, & Yavuzkasap Ayakta, 2018).

A study was conducted to improve the mechanical and thermal properties of recycled polyamide by adding functionalized graphene nanoparticles (GNPs). It has been observed that its thermal conductivity can be increased by 26-59% by adding graphene. It was concluded that 2% graphene content provides improvement in strength and stiffness without significant effect on ductility of the recycled polyamide. It is stated that the obtained fiber will be a promising new advanced material class (Korkees et al., 2021).

After the graphene was produced, it was melted and blended with Polyamide 6. The mechanical, electrical and flame retardant properties of the produced graphene doped PA 6 compounds were investigated. It was seen that the inclusion of graphene in PA 6 delayed the smoke density and increased the flame protection by reducing the combustible gas (Sabet & Soleimani, 2022).

Graphene-reinforced polymeric composites were produced by the electro-spinning method. In the study, primarily polyvinyl alcohol (PVA), poly(vinylidene fluoride) (PVDF), epoxy, polystyrene (PS),

polypropylene (PP), polyimide (PI), polyurethane (PU), polyaniline (PANI), polypyrrole and polythiophene were used and graphene-based composites containing organic and polymeric materials were emphasized. The thermal, mechanical and electrical properties of these graphene-based polymeric composites are discussed (Moharana, 2022).

In this study, effect of graphene-reinforced polyamide 6 fiber on strength and functional properties of wool blended woven fabrics were investigated. After the fibers are supported with graphene, it is aimed to add properties such as strength and functionality to the existing fibers and to make the new fibers suitable for use in different fields such as military and outdoor activity products.

2. MATERIALS AND METHODS

Considering the increase in the demand of stretch fabrics in the market, mono (one-way) and bi (two-way) stretch fabrics were woven in the experiments. The specifications of the fabrics are shown in Table 1. The fabric names are indicated as G1-G4 and in these fabrics, as polyamide, only graphene-reinforced polyamide 6 was used. The woven fabrics were dyed with black metal free reactive dyestuff under the same dyeing conditions and the finishing processes also were carried out under the same conditions.

Table 1. Technical properties of the fabrics

	Unit	G1	G2	G3	G4
Weight	(g/m^2)	198	221	235	163
Width	(cm)	142	142	142	146
Pattern	-	plain	2/1 twill	2/1 twill	2/2 twill
Weft Density	wefts/cm	22	26	24	26
Warp Density	warps/cm	29	36	36	27
Fabric Blend	%	43 Wool	44 Wool	43 Wool	45 Wool
		33 Polyester	34 Polyester	33 Polyester	35 Polyester
		20 Polyamide	20 Polyamide	20 Polyamide	20 Polyamide
		4 Elastane	2 Elastane	4 Elastane	

3. RESULTS AND DISCUSSION

On graphene-reinforced polyamide 6 fiber, TGA and DSC analyses were performed. As can be seen from Figure 1, this fiber started to decompose at 249.7 °C, the remained inorganic materials at 640.7 °C are 11.7% and belongs to graphene.

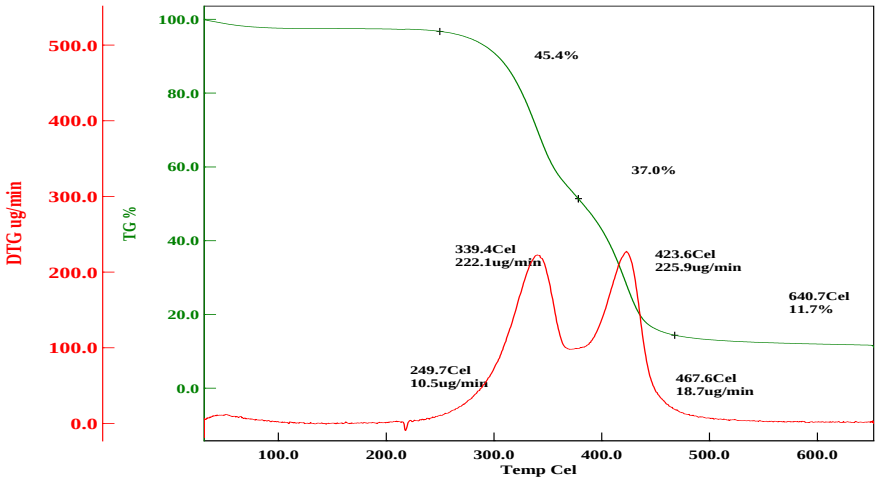

Figure 1. TGA analyse of graphene reinforced polyamide 6 fiber

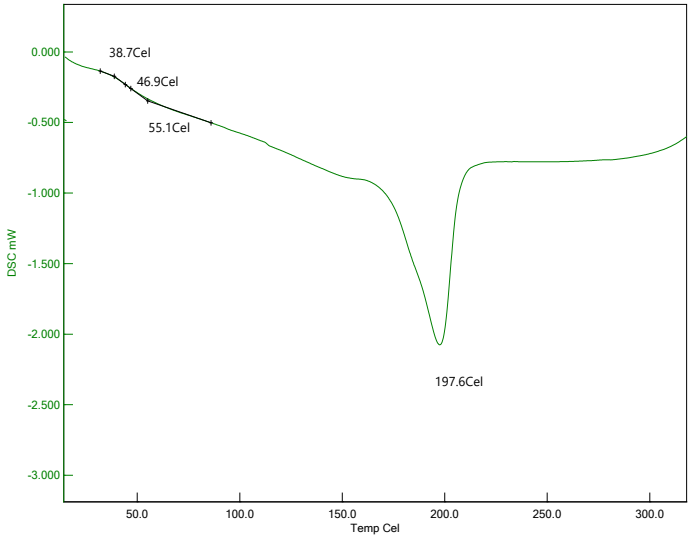

Figure 2. DSC analyses of graphene reinforced polyamide 6 fiber

From Figure 2, it was observed that the material began to soften at 38.7 °C, and the crystalline melting point was 197.6 °C while the expected was around 210 °C. It was thought that the graphene additive in the material may have affected the impurity and lowered the melting point of Polyamide 6.

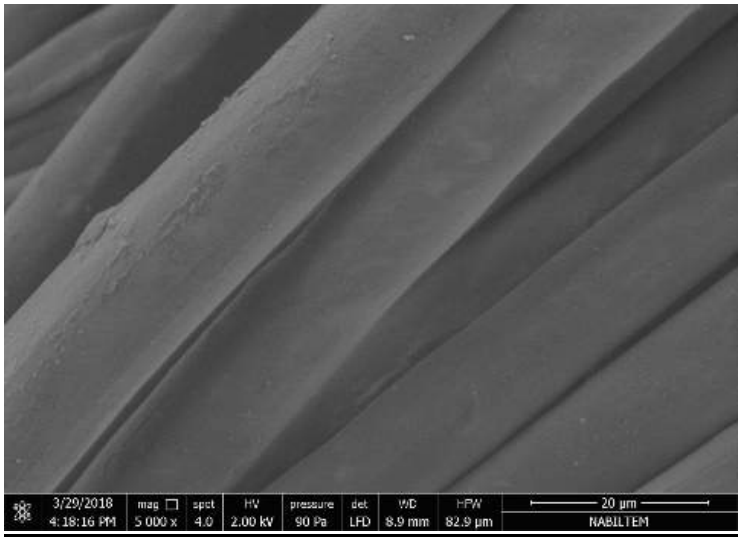

Figure 3. SEM image of graphene-reinforced polyamide 6 fiber

It is expected that the denser fabric is used, the more strength fabric is obtained. As expected, G2 fabrics with the highest warp density have the highest breaking and tear strengths in the warp direction. Since G1 is plain, it is expected to be the most durable fabric, but it gave the least breaking strength values. While the lowest breaking strengths were expected from G4, it was observed that the G4 in 2/2 twill weave was higher than G1 in plain weave. This result can be explained by the strength differences of the yarns occurred during the yarn production. For all these fabrics, tear strengths showed parallel results with breaking strengths.

Since the back of the fabrics were processed at higher pressure in the finishing processes, the fabrics have brighter and more slippery structure. Thus, water permeability capacity decreased. In addition, as the weave factor increases, the water penetration of the fabric decreases. Accordingly, G4 fabric with the highest weave factor gave the worst absorbency value. G3, which has a lower weave factor and density, gave the best absorbency values, as expected. Drying rate of G1 and G4 fabrics were better than the others. These values are similar to fibers which have thermal comfort properties. Excellent UV protection features have been observed for all the fabrics.

Table 2. Test results of the fabrics

Test Name		Std. Number	Unit	Limits	G1	G2	G3	G4
Abrasion (9 Kpa)	-	EN ISO 12947-2	Cycle ($.10^4$)	>2	>10	>10	>10	>10
Breaking Strength	Warp	EN ISO 13934-1	kg	>18	50	92	74	60
	Weft	EN ISO 13934-1	kg	>18	59	59	66	78
Tear Strength	Warp	EN ISO 13937-1	g	>900	2977	4368	3468	4283
	Weft	EN ISO 13937-1	g	>900	2721	2824	3127	5419
Absorbency	Face	AATCC 79:2010	s	<60	26	33	17	35
	Back	AATCC 79:2010	s	<60	32	51	23	53
Drying Rate	-	AATCC 201:2014	ml/h		1.62	1.17	1.16	1.65
UV Protection	-	AS/NZS 4399:2017	UPF	30-50	>50	>50	>50	>50
Antibacterial Activity	S.aureus ATCC 6538	AATCC 100:2012	%	-	86.40	74.09	80.90	68.50
	K.pneumonie ATCC 4352	AATCC 100:2012	%	-	82.77	75.00	83.33	78.09
Blade-Cut Resistance	-	EN 388:2016	Index	≥1	1.29	1.39	1.31	1.30
Dimensional Stability to Hoffman Press	Warp	DIN 53894-2	%	(-3.1)-(1.1)	-3.00	-2.25	-3.00	-2.00
	Weft		%	(-3.1)-(1.1)	-1.50	-2.00	-1.50	-1.00
Dimensional Stability to Wira Steam Cylinder	Warp	TS EN ISO 3005	%	(-3.1)-(1.1)	-2.00	-2.00	-4.50	-1.00
Air Permeability	-	ASTM D737-04	$l/m^2/s$	-	104	55	52	339

Antibacterial activity tests were performed with S.aureus (gram +), K. pneumoniae (gram -) bacteria. Wool also has antibacterial property comes from its nature just like graphene. Since the fabrics contain 43% and 45% wool, it was expected that the test results would be higher. However, it was observed that the use of 20% graphene-reinforced polyamide 6 in the fabrics did not have a positive effect on the antibacterial property. Values were found in the range of 74-86%. In conclusion, all fabrics passed the blade-cut resistance test.

While the Hoffman and Wira shrinkage values remained within the limits in both weft and warp directions, the Wira shrinkage in the warp of G3 fabrics was higher. Fabrics with high knitting factor

and low density value in air permeability are expected to have high air permeability. The test results showed that the air permeability values were as expected. While the air permeability of G4 with the highest knitting factor gave the highest value, G1 with the lowest knitting factor gave the least air permeability values. It has been observed that the effect of the knitting factor affects more than the density.

4. CONCLUSION

In this study, excellent abrasion and UV protection results were obtained in the fabrics woven containing 20% graphene-reinforced polyamide 6. In addition, good results were observed in absorbency, fast drying and blade-cut resistance tests. Graphene-reinforced polyamide fiber can be used in long-lasting military products, extreme sports products suitable for outdoor activities, motorcycle sports due to their high strength and blade-cut resistance; in outdoor applications due to its excellent UV protection property, and in areas that needed multi-functional fabrics.

ACKNOWLEDGMENT

The author would like to thank Assoc. Prof. Berrin Yılmaz for her valuable support of the research.

REFERENCES

Bhattacharjee, S., Joshi, R., Chughtai, A. A., & Macintyre, C. R. (2019). Graphene modified multifunctional personal protective clothing. *Advanced Material Interfaces, 6*, 1900622-1900649.

Caglar Cinperi, N., & Yavuzkasap Ayakta, D. (2018). Development of high performance fabrics with graphene. *7th International Technical Textiles Congress*, İzmir/TURKEY, 10-12 October 2018.

Korkees, F., Aldrees, A., Barsoum, I., & Alshammari, D. (2021). Functionalised graphene effect on the mechanical and thermal properties of recycled PA6/PA6,6 blends. *Journal of Composite Materials, 55*(16), 2211–2224.

Moharana, S., Sahu, B. B., Singh, L., & Mahaling, R. N. (2022). Graphene-Based Polymer Composites: Physical and Chemical Properties. *Defect Engineering of Carbon Nanostructures*, 159–197. DOI: 10.1007/978-3-030-94375-2_7.

Sabet, M., & Soleimani, H. (2022). The influence of graphene on the mechanical, thermal, and flame retardant characteristics of Polyamide 6. *Materials Technology-Advanced Performance Materials*, 37(10), 1251-1262.

MECHANICAL PROPERTIES OF NONWOVEN FABRICS MADE OF BICOMPONENT MICROFILAMENTS

Sukran KARA

Dokuz Eylul University, Engineering Faculty, Textile Engineering Department, Izmir, Turkiye

Corresponding author: sukran.kara@deu.edu.tr

Abstract: *Nonwoven fabrics have wide range of application areas due to their diversity in structure, properties and costs. They are very suitable to be used for disposable products. On the other hand, their advantageous properties can be utilized for durable textile products after improving their some essential properties such as mechanical performance. For this purpose, in the last decades, nonwoven fabric properties are tried to be enhanced by some methods such as combining bicomponent fiber spinning with hydro-entanglement. Within the scope of this study, mechanical properties of nonwoven samples containing bicomponent microfilaments were examined and compared with a woven polyester fabric in order to reveal their usability for durable apparel applications.*

Keywords: *mechanical properties, nonwoven fabrics, bicomponent fibers, PET/PA (polyester:polyamide) microfilaments, apparel application.*

1. INTRODUCTION

INDA (Association of the Nonwoven Fabrics Industry) defines nonwoven fabrics as sheet or web structures that is bonded together by entangling staple fibers or filaments (and by perforating films) mechanically, thermally or chemically (INDA, 2022). The diversity of nonwoven fabric structures and properties provide them usability for various application areas such as automotive textiles, geotextiles, industrial textiles, medical/surgical textiles, and disposable apparels (INDA, 2022; Karthik et al., 2017). Besides their advantageous properties (i.e. low cost, light weight and softness (Kayar et al., 2015; EDANA, 2022), there are some insufficient features of nonwoven fabrics that limit their application for durable/reusable apparels. These properties can be summarized as low drape and low mechanical properties (Karthik et al., 2017). Therefore, in the recent years, there are some attempts to develop mechanical properties of nonwoven fabrics in order to introduce them to durable/reusable apparel applications. For this purpose, bicomponent fiber spinning combined with hydro-entanglement is applied as one of the key solutions (Karthik et al., 2017; Madaline, 2022; Evolon, 2022). If the integration of the nonwoven fabrics to the apparel industry can be successfully achieved by these ways, it can eliminate the complex and costly yarn production and weaving/knitting processes (Cheema, 2016; Tausif and Goswami, 2017).

There are some studies in the literature, which searches the properties of nonwoven fabrics produced via bicomponent fiber spinning and hydro-entangling methods. The most relevant studies to our research are those examining the effects of production parameters on some mechanical properties of bicomponent fiber containing spunlaid (Anantharamaiah et al, 2008; Duo et al, 2021) or carded (Ndaro et al, 2007a, b; Ndaro et al, 2009; Ndaro et al, 2016; Gong et al, 2009, Hollowell et al, 2013) nonwoven fabrics. In addition, there are some studies in the literature subjecting the fiber cross section (Zhao and Liu, 2012; Yeom and Pourdeyhimi, 2011a), fiber orientation and bicomponent fiber splitting degree (Shim et al, 2010; Lu et al, 2011), permeability (Durany et al, 2009) or filtration properties of bicomponent fiber containing hydro-entangled fabrics (Yeom and Pourdeyhimi, 2011b; Heng et al, 2015; Duo et al, 2022).

On the other hand, there are only a few studies subjecting the use of nonwoven fabrics in apparel design and production (Gohar and Mohamed, 2013; Zhao et al 2018; Zhao et al 2019).

The literature search shows that there only limited numbers of researches studying the properties and usability of bicomponent fiber containing nonwovens for the durable applications. Therefore, within the context of this study, mechanical properties of nonwoven fabrics made of bicomponent PET:PA microfilaments were tested and compared with a classical woven fabric. Nonwoven fabric samples with different unit masses were utilized for this purpose.

2. MATERIALS AND METHODS

2.1. Materials

Materials of this study were nonwoven fabrics which were made of bicomponent microfilament PET/PA6 fibers. The fibers were composed of 70:30 PET:PA6 polymers, in the form of 16-segmented- pie splittable microfilaments. Nonwoven fabrics were hydro-entangled for the fixation and splitting process. In this study, fabrics with 5 different unit masses were utilized. The samples were coded from NW1 to NW5, according to their increasing unit masses. All the samples were produced via same machine and raw materials. The woven reference fabric was a plain weave 100 % polyester fabric. Its warp and weft densities were 60 and 35 threads/cm, respectively. It was made of multifilament yarns.

2.2. Methods

Physical and mechanical properties of samples were determined in this study. Unit mass and thickness were determined as physical properties, while tensile strength, tear strength, bursting strength, bending rigidity and abrasion resistance of samples were determined as mechanical properties. Details of the tests are given in Table 1. All the tests were repeated with the required number according to the related standards, and mean values were calculated. Tests were performed under standard atmosphere conditions (20±2 °C, 65±5 % relative humidity) after conditioning at least 24 h.

Table 1. Details of the physical and mechanical testing of samples

Name of the test	Sub-method	Standard	Test machine
Unit mass	-	BS EN 29073-1:1992	Electronic balance
Thickness	Thickness under 5 gf/cm^2 pressure	TS 7128 EN ISO 5084	James Heal RxB Cloth Thickness Tester
Tensile strength	Strip method	BS EN 29073-3:1992	Instron 4411 Universal Tensile Testing Machine (U. T. T. M.)
	Grab method	BS EN ISO 9073-18:2008	
Tear strength	Trapezoid	BS EN ISO 9073-4:1997	Instron 4411 U. T. T. M.
Bursting strength	Ball burst procedure	BS EN ISO 9073-5:2008	Instron 4411 U. T. T. M.
Bending rigidity	Cantilever	BS EN ISO 9073-7: 1998	Shirley Stiffness Tester
Abrasion resistance	Mass loss and visual evaluation	BS EN ISO 12947-3:1998	Martindale Abrasion and Pilling Tester

2. RESULTS AND DISCUSSION

2.1 Physical properties of samples

Unit mass and thickness values of samples are shown in Figure 1. According to results, the reference woven fabric had 93 g/m^2 weight and 0.20 mm thickness. Unit mass of nonwoven samples changed between 110-230 g/m^2. As expected, higher weight samples exhibited higher thickness levels. The unit mass and thickness of nonwoven samples were in the range of apparel applications, corresponding to lightweight and medium weight woven fabrics while corresponding to medium thick and thick woven fabrics.

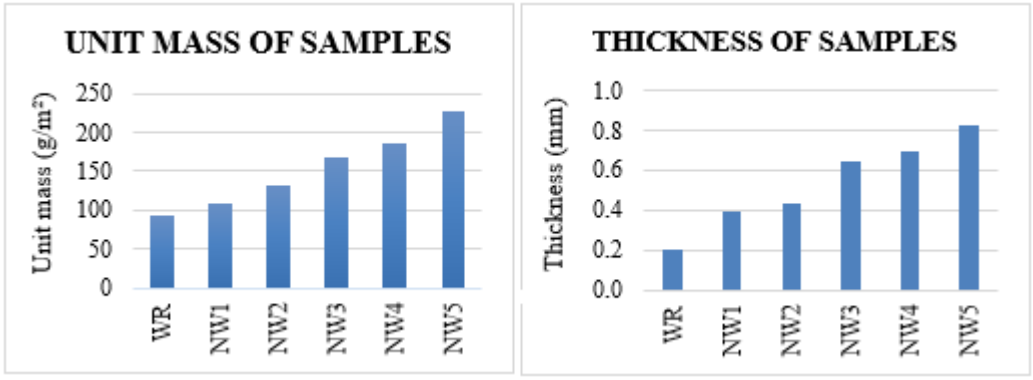

Figure 1. Unit mass and thickness results of samples

2.2 Mechanical properties of samples

Tensile strength and elongation results of samples were obtained according to both strip and grab test methods (Figure 2). According to tensile strength-strip test method, reference woven sample exhibited higher results when compared to nonwoven competitors in both machine and cross directions. Strength of higher weight nonwoven samples were closer to that of reference fabric. In contrary, tensile strength-grab test method yielded closer values for woven reference sample and nonwoven samples in both directions. Unlike the tensile strength results, the elongations of nonwoven samples were higher than that of woven reference sample. It is thought to be a result of entangled fiber structure of the nonwoven fabrics instead of intersected structure of warp and weft yarns of woven fabric.

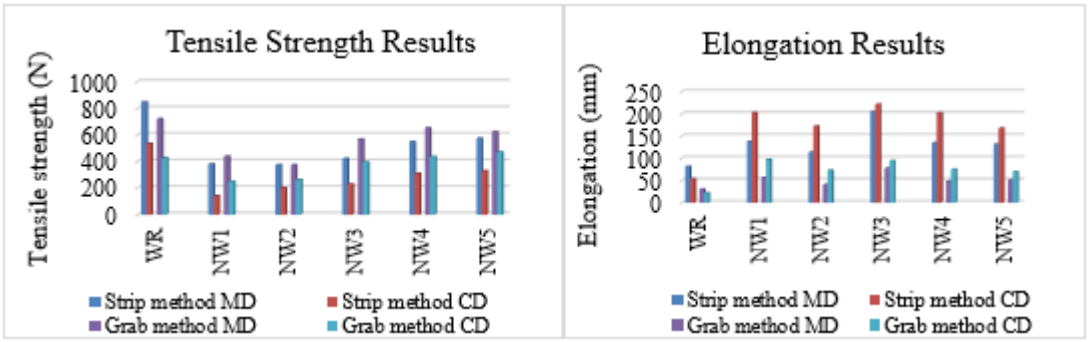

Figure 2. Tensile test results of samples

Tear strength of samples are shown in Figure 3. Tear strength of nonwoven samples were higher than the tear strength of woven reference fabric. During the tests, it was observed that, some microfilaments of the nonwoven samples remained unbroken during the test. They could have supported the nonwoven samples against tearing. For all the samples, tear strength across machine direction were higher than in across cross direction. This can be due to water-jet streaks along the machine direction, that could help the tear propagation across the cross direction (Anantharamaiah et al, 2007).

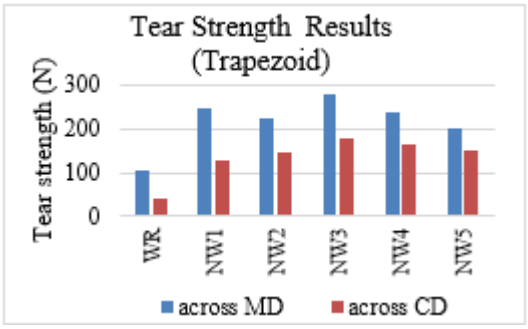

Figure 3. Tear strength results of samples

On the other hand, bursting strength of reference sample was quite high around 1kN. Nonwoven samples showed an increasing tear strength trend with the unit mass increments, reaching 679N (Figure 4). Bursting height of samples did not exhibit a proportional trend with the fabric unit mass or thickness.

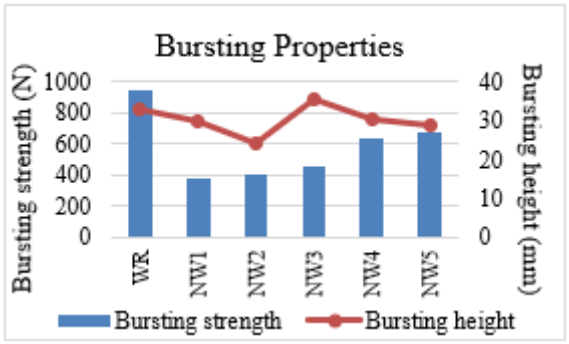

Figure 4. Bursting strength results of samples

Bending rigidity of samples are visualized in Figure 5. Bending rigidity of nonwoven samples especially in machine direction were apparently higher than reference woven sample. This would result with lower drape for the nonwoven samples. Also, higher bending rigidity of samples in machine direction can cause lower formability.

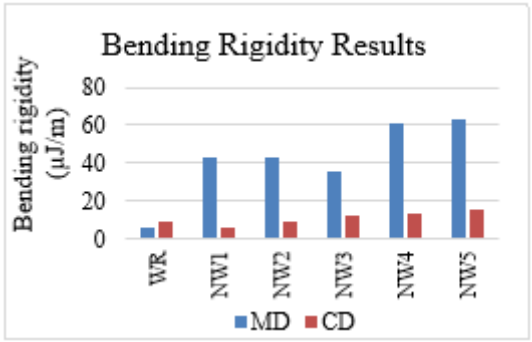

Figure 5. Bending rigidity results of samples

Abrasion test results showed that, nonwoven samples were quite durable against abrasion. After even 25000 abrasion cycles, nonwoven samples maintained their integrity. The maximal mass loss was obtained from NW2 sample after 25000 cycles, around 13%. In spite of this, higher amount of pilling was observed for nonwoven samples when compared to reference woven sample (Figure 6). Some colour changes accompanied the pilling for the coloured samples.

Sample code	VISUAL EVALUATION OF SAMPLES					
	Before abrasion	After 5000 cycle	After 10000 cycle	After 15000 cycle	After 20000 cycle	After 25000 cycle
WR						
NW1			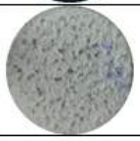			
NW2						
NW3						
NW4						
NW5						

Figure 6. Views of samples after certain abrasion cycles

4. CONCLUSION

In this work, mechanical properties of nonwoven samples containing bicomponent microfilaments were tested and compared to a woven reference in order to reveal their usability for durable apparels. Results show that mechanical properties of nonwoven samples reached to a level, especially when their unit masses increased. In general, tensile, tear and bursting strength properties of nonwoven samples are between 44-110 % when compared to woven reference competitor (in machine direction). Higher bending rigidity of nonwoven fabrics can result with low drape for these samples.

In further studies, drape and other in-use properties of the samples such as breathability and surface properties are planned to be examined.

ACKNOWLEDGEMENT

Nonwoven samples of this study were supplied from Mogul Tekstil San. Tic. A.S. (Gaziantep, Turkey), kindly. Author thanks the company for their supports.

REFERENCES

Anantharamaiah, N., Römpert, K., Vahedi Tafreshi, H., & Pourdeyhimi, B. (2007). A study on the role of hydroentangling waterjets in reorienting fibers in nonwoven fabrics. *Journal of Materials Science*, 42, 6161-6170.

Anantharamaiah, N., Verenich, S., & Pourdeyhimi, B. (2008). Durable nonwoven fabrics via fracturing bicomponent islands-in-the-sea filaments. *Journal of Engineered Fibers and Fabrics*, 3(3).

BS EN 29073-1:1992. Methods of test for nonwovens. Determination of mass per unit area.

BS EN 29073-3:1992. Methods of test for nonwovens. Determination of tensile strength and elongation.

BS EN ISO 12947-3:1998. Textiles. Determination of the abrasion resistance of fabrics by the Martindale method. Determination of mass loss.

BS EN ISO 9073-18:2008 Textiles. Test methods for nonwovens. Determination of breaking strength and elongation of nonwoven materials using the grab tensile test.

BS EN ISO 9073-4:1997 Nonwovens. Test methods. Determination of tear resistance by the trapezoid procedure.

BS EN ISO 9073-5:2008 Textiles. Test methods for nonwovens. Determination of resistance to mechanical penetration (ball burst procedure).

BS EN ISO 9073-7:1998 Textiles. Test methods for nonwovens. Determination of bending length.

Cheema, M. S. (2016). Development of hydroentangled nonwoven structures for fashion garments (Doctoral dissertation, University of Bolton).

Duo, Y., Qian, X., Zhao, B., Gao, L., Guo, X., Zhang, S., ... & Tang, L. (2022). Easily splittable hollow segmented-pie microfiber nonwoven material with excellent filtration and thermal-wet comfort for energy savings. *Journal of Materials Research and Technology*, 17, 876-887.

Duo, Y., Qian, X., Zhao, B., Gao, L., Bai, H., Guo, X., & Song, B. (2021). Preparation and properties of fluffy high-shrinkage polyester/polyamide 6 hollow segmented pie microfiber nonwovens. *Textile Research Journal*, 00405175211062098.

Durany, A., Anantharamaiah, N., & Pourdeyhimi, B. (2009). High surface area nonwovens via fibrillating spunbonded nonwovens comprising Islands-in-the-Sea bicomponent filaments: structure–process–property relationships. *Journal of Materials Science*, 44(21), 5926-5934.

EDANA, "Why use nonwovens in clothing and footwear?". https://www.edana.org/nw-related-industry/nonwovens-in-daily-life/clothing-and-footwear (Access date: 11.01.2022).

Evolon, https://www.freudenberg-pm.com/Materials/evolon (Access date: 11.01.2022).

Gohar, E. E. D. S., & Mohamed, O. S. (2013). Designing and producing women's blouses by using nonwoven fabrics. Internat. Design J, 4(2), 137-151.

Gong, R. H., & Nikoukhesal, A. (2009). Hydro-entangled bi-component microfiber nonwovens. *Polymer Engineering & Science*, 49(9), 1703-1707.

Heng, Z., Xiaoming, Q., Qi, Z., & Zhaohang, Y. (2015). Research on structure characteristics and filtration performances of PET-PA6 hollow segmented-pie bicomponent spunbond nonwovens fibrillated by hydro entangle method. *Journal of Industrial Textiles*, 45(1), 48-65.

Hollowell, K. B., Anantharamaiah, N., & Pourdeyhimi, B. (2013). Hybrid mixed media nonwovens composed of macrofibers and microfibers. Part I: three-layer segmented pie configuration. *Journal of the Textile Institute*, 104(9), 972-979.

INDA (Association of the Nonwoven Fabrics Industry), Nonwovens, https://www.inda.org/about-nonwovens/ (Access date: 11.01.2022).

Karthik, T., Prabha Karan, C., & Rathinamoorthy, R. (Eds.). (2017). Nonwovens: Process, structure, properties and applications. WPI Publishing, India.

Kayar, M., Mistik, S. I., & Inan, D. (2015). Analysing effect of the factors on ultrasonic seam tensile properties of nonwoven fabrics by Nested ANOVA Design. *International Journal of Clothing Science and Technology*, 27(6), 803-817.

Lu, Z. M., & Qian, X. M. (2011). Spunbonded nonwovens made from segmented pie filaments. *Advanced Materials Research*, 194, 726-729.

Madaline, http://www.madalinefabric.com/en/technical-features/process (Access date: 11.01.2022).

Ndaro, M. S., Jin, X. Y., Chen, T., & Yu, C. W. (2007a). Splitting of islands-in-the-sea fibers (PA6/COPET) during hydroentangling of nonwovens. *Journal of Engineered Fibers and Fabrics*, 2(4), 155892500700200402.

Ndaro, M. S., Xiangyu, J., Ting, C., & Yu, C. (2007b). Effect of impact force on tensile properties and fiber splitting of splittable bicomponent hydroentangled fabrics. *Fibers and Polymers*, 8(4), 421-426.

Ndaro S. M., Jin, X. Y., Chen, T., & Yu, C. W. (2009). Optimum water jets inclination angle for better tensile strength in hydroentanglement process. *Fibres & Textiles in Eastern Europe*, 75(4), 82-86.

Ndaro S. M., Mwasiagi J. I., Wangatia L. M. (2016). Tearing strength of hydroentangled non-woven fabrics. *Materials Science*, 14(12), 509-513.

Shim E., Pourdeyhimi B., Latifi M. (2010). Three-dimensional analysis of segmented pie bicomponent nonwovens. *The Journal of The Textile Institute*, 101(9), 773-787.

Tausif, M., & Goswami, P. (2017). Nonwoven fabrics. In Textile and Clothing Design Technology (pp. 259-280). CRC Press, Boca Raton.

TS 7128 EN ISO 5084: 1998.Textiles-Determination of thickness of textiles and textile products.

Yeom B. Y., Pourdeyhimi B. (2011a). Web fabrication and characterization of unique winged shaped, area-enhanced fibers via a bicomponent spunbond process. *Journal of Materials Science*, 46(10), 3252-3257.

Yeom B. Y., Pourdeyhimi B. (2011b). Aerosol filtration properties of PA6/PE islands-in-the-sea bicomponent spunbond web fibrillated by high-pressure water jets. *Journal of Materials Science*, 46(17), 5761-5767.

Zhao B., Qian X., Qian Y., Duo Y., Feng Y., Fan J., Chen Y. (2019). The application of hollow segmented pie bicomponent spunbond hydro-entangled microfiber nonwovens for microfiber synthetic leather apparel. *AATCC Journal of Research*, 6, 45-49.

Zhao B., Qian Y., Qian X., Fan J., Liu F., Duo Y. (2018). Preparation and properties of split microfiber synthetic leather. *Journal of Engineered Fibers and Fabrics*, 13(2), 15-21.

Zhao Y., Liu Y. (2012). The preparation of spunbonded PA6/PET segment bicomponent fiber. *Journal of Textile Science and Engineering*, 2(1).

COMPARISON OF THE FABRICS WOVEN WITH THREE DIFFERENT THERMAL FUNCTIONALIZED POLYESTER FIBERS

Nazlı CAGLAR CİNPERİ[1]

[1] YÜNSA, R&D Center, Tekirdağ, Türkiye

Corresponding author: ncinperi@yunsa.com

Abstract: *Technologies that keep the human body at a comfortable temperature for all seasons increase the performance and comfort of the user by quickly removing the sweat from the body. In this study, microencapsulated fiber containing carbon and volcanic minerals added from the melt, four channeled scalloped oval structured fiber, hollow and four channeled scalloped oval structured fiber and standard polyester fiber as a reference were used. Four different fabrics were woven in the same construction; fabric dyed in black with the same dyeing conditions; were subjected to parallel finishing processes. As a result of the evaluations, it has been determined that "hollow and four channeled scalloped oval structured fiber", which can be used in hot and cold weather and can combine "heat insulation and fast drying" features, may be equivalent to fiber containing microcapsules.*

Keywords: *Thermal comfort, fast drying, thermal insulation, functional fibers.*

1. INTRODUCTION

One of the most important morphological features of textile fibers is the cross-sectional shape. It is possible to change many properties of yarn and fabric by changing the fiber cross-section shape. The effect of fiber cross-section shape and fiber diameter on the moisture transmission properties of the fabric has been studied. It has been observed that the increased fiber specific surface area as a result of the change in shape factor and fiber diameter increases the wicking speed along the fabric and decreases the water vapor permeability of the fabric (Bueno, et al. 2004; Das, et al. 2008).

Fibers are produced by varying their cross-sectional shapes for many reasons such as increasing performance, providing comfort, improving pilling tendency, etc. PET with two different cross-section shaped filaments, circular and cruciform, was produced by melt spinning method; the effects of cross-section geometries on fiber properties were investigated; The thermal and thermomechanical properties of both sections of the filament yarn were investigated and revealed by DSC and TMA methods, respectively (Badrul Hasan, et al. 2009).

Thermal comfort properties like thermal conductivity, thermal absorption and thermal resistance, and the water vapour and air permeabilities of fabrics woven with different cross sectional shaped (round, hollow round, trilobal and hollow trilobal) polyester fibres were investigated. Fabrics consisting of hollow fibers have higher thermal conductivity and thermal absorption values than solid fibers. It was observed that the thermal resistance, water vapor and air permeability values were lower (Karaca, et al. 2012).

The water/moisture vapor permeability and thermal wear comfort of woven fabrics containing Coolmax®/bamboo/tencel were investigated. It has been observed that Coolmax® in the core region plays a very important role with its high fabric porosity by incorporating a capillary absorption into the wicking property. It was determined that the fast-drying rate of fabrics containing high porosity

composed of Coolmax® sheath/core yarns, and spun yarns with non-circular cross-sectional fibers (Coolmax®) was strongly affected by moisture vapor diffusion (Kim, 2020).

Properties of trilobal, flat and hollow shaped polyester filaments such as tensile strength, elongation, breaking load, unevenness etc., were investigated. The results showed that cross-sectional shape of the filaments directly affected the yarn properties (Toydemir & Vatansever Bayramol, 2021).
The effect of cross-section shape on the properties of profiled polyester (PET) fibers and their fabrics was investigated. It has been observed that the air permeability, heat retention and wrinkling resistance of fabrics containing fat-shaped and hexagonal-shaped profiled PET fibers are better than circular-section PET fiber fabrics, while circular-section PET fabric is softer than profiled PET fiber fabrics (Ge, et al. 2021).

Thermal conductivity (Alambeta Parameters), permeability and liquid management properties of double-face knitted fabrics in which functional yarns such as Thermosoft®, Nilit Heat®, Viloft® are combined with wool were investigated. Nilit Heat®/PP (inner/outer) fabric has been determined to have advantages for breathability, warmer feelings as a result of minimal thermal absorption, conductivity and diffusion (Kaplan & Yılmaz, 2022).

In this study, microencapsulated fiber containing carbon and volcanic minerals added from the melt, four channeled scalloped oval structured fiber, hollow and four channeled scalloped oval structured fiber and standard polyester fiber as a reference were used in woven fabrics by blending with wool. The physical, chemical and thermal properties of the fabrics were compared with each other.

2. MATERIALS AND METHODS

2.1. Properties of Fibers

In the trials, fibers with thermal property in three different structures and standard polyester fiber as a reference were used. Properties of the fibers named as F1, F2, F3 are detailed below.

Fiber 1 (F1): Microencapsulated fiber containing active carbon and volcanic minerals added to the melt keeps the body cool in hot weather and warm in cold weather, keeping the body in the comfort range. Being suitable for all seasons use, it increases the performance and comfort of the user, thanks to its rapid removal of sweat from the body. In this technology, there are active particles that are protected by microencapsulation dispersed in and on the polyester fibers. Active particles trap the moisture inside and at the same time absorb the near-IR energy emitted from the human body and use it to remove moisture faster.

Fiber 2 (F2): The four-channeled, scalloped oval fiber can remove moisture from its upper and lower parts, due to its channeled structure.

Fiber 3 (F3): This fiber consists of a mixture of 50% four channels with scalloped oval cross-section and 50% hollow structure. By the help of its channeled structures, it can remove moisture and breathe easily. In addition, it provides thermal insulation due to hollow structures.

Fiber 4 (F4): The last fiber is a standard round cross-section polyester fiber with no thermal properties. It was used as a reference for comparison in the trials.

2.2. Construction of Fabrics

Fabrics with the construction specified in Table 1 were produced by using polyesters with different thermal comfort properties (all polyesters in the fabrics have thermal properties). After dyeing fabrics to black color, 40 g/L ethoxy carboxylic acid based hydrophilic finish was applied to all fabrics.

Table 1. Technical properties of the fabrics

Property	Unit	Value
Weight	g/m^2	255
Width	cm	150
Pattern Type	-	Plain
Weft Density	wefts/cm	30
Warp/Weft Yarn Number	Nm/ply	80/2
Fabric Blend	%	60/40 Wool/Polyester
Dyeing Type	-	Fabric

3. RESULTS AND DISCUSSION

The names of the fabrics indicated in Table 2 are named according to the polyester fiber type used in its content (For example: F1F for the fabric using F1 fiber).

Table 2. Physical, chemical and thermal test results of the fabrics

Tests		Standard	Unit	F1F	F2F	F3F	F4F
Abrasion Resistance (9 KPa)	-	TS EN ISO 12947-2	break	15000	27000	26000	30000
Breaking Strength	Warp	TS EN ISO 13934-1	kg	48	50	59	64
	Weft	TS EN ISO 13934-1	kg	51	43	55	76
Tear Strength	Warp	TS EN ISO 13937-1	g	1416	1463	2084	2354
	Weft	TS EN ISO 13937-1	g	1583	2193	2300	2354
Slim Slippage	Weft	TS 1619 EN ISO 13936-1	kg	20	20	20	20
Pilling (2000 cycle)	-	TS EN ISO 12945-2	-	4.5	4.5	4.5	4.0
Spray Rating	-	M&S Test Standard	-	50	50	50	50
Vertical Wicking/Capillary Rise (After 30 minutes)	Warp	ITM 348	cm	4.5	6.5	6.5	8.6
	Weft	ITM 348	cm	7.3	7.6	7.1	8.1
Vertical Wicking/Capillary Rise (After 30 minutes after washing)	Warp	ITM 348	cm	4.9	8.7	7.3	6.9
	Weft	ITM 348	cm	8.4	8.1	9.2	5.9
Transplanar Wicking (Wetted Area)	-	-	cm^2	0	0	0	0
CLO (Thermal Test)	-	ITM 374	-	0.26	0.14	0.16	0.14
Air Permeability	-	ASTM D737-04	l/m^2/s	116	135	125	153
Absorbency	Face	AATCC 79:2010	s	>60	38	>60	>60
	Back	AATCC 79:2010	s	>60	37	>60	>60
Drying Rate	-	AATCC 201:2014	ml/h	2.03	1.88	1.62	1.60

When the test results of the finished fabric were evaluated among thermal propertied fabrics, it has been observed that the tear strength of the F3F fabric gives the highest results (Table 2). Considering the breaking strengths among thermal propertied fabrics again, the highest value in both directions was obtained for F3F. No differences were observed between seam slippage values.

Vertical wicking values of F2F and F3F were observed higher than F1F; this is an expected result due to their channeled structure. When transplanar wicking and absorbency tests were evaluated; it has been observed that hydrophilic finishing application to fabrics was not sufficient. Increasing the hydrophilic finishing chemical ratio or using a different chemical that will not block the channels can be tested.

As a result of the CLO thermal test, F1F gave the highest heat holding capacity. The closest results to this value was obtained with F3F fabrics. Here, it is an expected result due to the ability of F1F to absorb near-IR rays emitted from the human body and use this heat for drying. F3F, on the other hand, shows heat retention feature due to the 50% hollow fibers in it.

Table 3. Color fastness test results of the fabrics

Tests		Standard	F1F	F2F	F3F	F4F
Color Fastness To Perspiration-Acid	Change	TS EN ISO 105 - E04	5.0	5.0	4.5	5.0
	Acetate		3.5	3.5	3.5	3.5
	Cotton		4.5	4.5	4.5	4.5
	Nylon		3.0	3.5	3.0	3.0
	Polyester		4.5	4.5	4.0	4.0
	Acrylic		4.5	4.5	4.5	4.5
	Wool		4..5	4.5	4.0	4.5
Color Fastness To Perspiration -Alkali	Change	TS EN ISO 105 - E04	5.0	5.0	4.5	5.0
	Acetate		3.5	3.5	3.5	3.5
	Cotton		4.5	4.0	4.5	4.5
	Nylon		2.5	2.5	3.0	2.5
	Polyester		4.0	4.0	4.0	4.0
	Acrylic		4.5	4.5	4.5	4.5
	Wool		4.5	4.0	4.0	4.0
Color Fastness To Dry Cleaning	Change	TS 473 EN ISO 105 D01	5.0	5.0	5.0	5.0
	Acetate		4.5	5.0	5.0	5.0
	Cotton		4.5	5.0	5.0	4.5
	Nylon		4.5	5.0	5.0	4.5
	Polyester		4.5	5.0	5.0	4.5
	Acrylic		5.0	5.0	5.0	5.0
	Wool		5.0	5.0	5.0	5.0
Color Fastness To Water	Change	TS EN ISO 105 - E01	5.0	5.0	4.5	5.0
	Acetate		3.5	3.5	3.5	3.5
	Cotton		4.5	4.5	4.5	4.5
	Nylon		3.5	3.0	3.0	3.0
	Polyester		4.5	4.5	4.0	4.0
	Acrylic		4.5	4.5	4.5	4.5
	Wool		4.5	4.5	4.5	4.5
Color Fastness To Rubbing	Dry	TS EN ISO 105 X12	4.5	4.5	4.5	4.0
	Wet	TS EN ISO 105 X12	2.5	3.5	3.0	3.0

Among the four fabrics with the same construction, the air permeability of F2F and F3F fabrics was better than F1F. It is expected that the absorbency value is good and fast absorbing in fibers with fast drying feature. Absorbency property was observed only for F2F; but it is thought to be caused by the finishing application. Therefore, it was not taken into account in the evaluations. Considering the drying rates, it was observed that F2F fabrics were close to F1F. At F3F, on the other hand, it can be interpreted that the hollow structures keep the heat inside to a certain extent, and drying takes place with the remaining heat.

It has been determined that F3, which combines heat insulation and fast drying features, can be used as a product that can be used in hot and cold weather, equivalent to F1 fiber.

No big differences were observed between the fastness values of the fabrics. For the rubbing fastness of fabrics dyed black with the same recipe, the best values were observed in F2F, while the second best value was observed in F3F (Table 3).

Table 4. Color fastness test results of the fabrics

Tests		Standard	Unit	F1F	F2F	F3F	F4F
Dimensional Stability to Hoffman Press	Warp	DIN 53894-2	%	-2.00	-2.50	-1.75	-2.00
	Weft	DIN 53894-2	%	-1.50	-3.00	-1.75	-1.50
Dimensional Stability to Wira Steam Cylinder	Warp	TS EN ISO 3005	%	-0.25	-0.50	0.00	-0.50
	Weft	TS EN ISO 3005	%	-2.25	-3.25	-2.50	-1.50

When we examined Hoffman Press and Wira Steam Cylinder tests, we saw that the shrinkage values of the F2F fabric were close to the 3% limit. Other fabric shrinkage was achieved within limits.

Table 6. Spectrophotometer test results

	DL*		Da*		Db*		DE*	Decision
F1F	1.16	lighter	-0.11	more green	-0.14	more blue	1.17	Fail
F2F	0.70	lighter	-0.06	more green	-0.32	more blue	0.77	Pass
F3F	0.61	lighter	-0.05	more green	-0.20	more blue	0.64	Pass

Spectrophotometer measurements were made by taking F4F fabric as a reference. Color measurements were performed by using the CIE L*a*b* difference – D65 10 Deg method. It was observed that F3F fabrics caused the least color change.

4. CONCLUSION

Finished fabric tests were evaluated comparatively. Accordingly, it has been determined that "hollow and four channeled scalloped oval structured fiber", which can be used in hot and cold weather and can combine "heat insulation and fast drying" features, may be equivalent to fiber containing microcapsules. The result of 0 in the transplanar wicking test; showed that hydrophilic finishing application to fabrics is not sufficient. It is recommended to try different chemicals instead of chemicals with ethoxy carboxylic acid functional groups. Since the F2 and F3 fibers have channel structure, in the finishing processes chemicals that will not block the channels (Ex. non-ionic or anionic softener with silicon or nano-sized silicon) should be used. Hydrophilic finishing chemicals

can be applied to increase absorbency; but cationic softeners should not be used as they reduce absorbency.

ACKNOWLEDGMENT
The author would like to express their gratitude to Cem Karaboğa from The LYCRA Company that provide some of thermal tests of the fabrics to the research. Also, the author would like to thank Assoc. Prof. Berrin Yılmaz for her valuable support of the research.

REFERENCES

Badrul Hasan, M. M., Dutschk, V., Brünig, H., Mäder, E., Häussler, L., Hässler, R., Cherif, Ch., & Heinrich, G. (2009). Comparison of Tensile, Thermal, and Thermo-Mechanical Properties of Polyester Filaments Having Different Cross-Sectional Shape, *Journal of Applied Polymer Science, 111*, 805–812.

Bueno, M.A., Aneja, A.P., & Renner, M. (2004). Influence of the shape of fiber cross section on fabric surface characteristics. *Journal of Materials Science, 39*, 557-564.

Das, B., Das, A., Kothari, V.K., Fanguiero, R., & de Araújo, M. (2008). Effect of Fibre Diameter and Cross-sectional Shape on Moisture Transmission through Fabrics. *Fibers and Polymers, 9*(2), 225-231.

Ge, Y., Deyan, Q., Hongfang, W., Jianhong, T., Xuefei, W. & Bojun, X. (2021). Study on Special Shaped Polyester Fibers and Development of Products. *AATCC Journal of Research*, *8*(3): 17-22.

Kaplan, S., & Yılmaz, B. (2022). Thermal Comfort Performances of Double-face Knitted Insulation Fabrics. *Fibers and Polymers*, *23*: 537–545.

Karaca, E., Kahraman, N., Omeroglu, S., & Becerir, B. (2012). Effects of Fiber Cross Sectional Shape and Weave Pattern on Thermal Comfort Properties of Polyester Woven Fabrics. *Fibres & Textiles in Eastern Europe*, *3*(92): 67-72.

Kim, A. H. (2020). Water/moisture vapor permeabilities and thermal wear comfort of the Coolmax®/bamboo/tencel included PET and PP composite yarns and their woven fabrics. *The Journal of The Textile Institute, 112*(12): 1940-1953.

Toydemir, Y., & Vatansever Bayramol, D. (2021). Properties investigation of polyester yarns with different cross-sections. *BEU Journal of Science, 10*(1), 170-176.

14 OCTOBER 2022

ORAL PRESENTATIONS

A STUDY ON ACOUSTIC PERFOMANCE OF BLACKOUT CURTAINS

Hacer Merve BULUT[1], Merve KÜÇÜKALİ ÖZTÜRK[2], Cevza CANDAN[1], Banu NERGİS[1], Tuğba ZENGİN[3], Aysun YENİCE[3], Rasim BOYACIOĞLU[4]

[1] Istanbul Technical University, Department of Textile Engineering, Istanbul, Turkey
[2] Bilgi University, Department of Textile and Fashion Design, Istanbul, Turkey
[3] Kucukcalik Tekstil San. ve Tic. A.S., Bursa, Turkey
[4]KFS Kucukcalik Filament ve İplik San. ve Tic. A.S., Sakarya, Turkey

Corresponding author: merve.bulut@itu.edu.tr

Abstract: *Indoor environmental quality (IEQ) covers the combined impact of the surrounding conditions (such as temperature, noise, lighting, etc.) inside a building and their effects on the health and well-being of people. An accurate design and control of indoor sound and light environment would positively influence the comfort, health and working performance of the occupants. This study is conducted in an attempt to observe the dependence of acoustic performance of blackout curtains on their constructional properties and to establish a roadmap for further acoustical improvement studies. For doing so, six blackout curtains were studied in terms of their acoustic properties.*

Keywords: *acoustic textile, blackout curtain, sound absorbption, sound transmission loss.*

1. INTRODUCTION

Indoor environmental quality (IEQ) refers to the conditions inside a building and their effects on the health and well-being of occupants or residents. The term covers the combined impact of the surrounding conditions in terms of temperature, noise, air quality, lighting, as well as odour, drinking water, ergonomics, electromagnetic radiation, and many related factors. A better indoor environment quality (IEQ) can noticeably improve the occupant's health, mood and, productivity (Angelova, 2016; Aydın & Mıhlayanlar, 2017; Noor et al., 2021; Priniotakis et al., 2022).

Acoustics is one of the cornerstones within the concept of IEQ and noise control is essential in residential, commercial, automotive, and industrial areas (Nayak & Padhye, 2016). Room acoustics describes how sound propagates in a room while building acoustics is related with sound propagation between rooms through walls, doors, and floors. The main focus of room acoustics is on easy communication and high speech intelligibility. The building acoustics, on the other hand, is concerned with unwanted disturbing sound coming from other rooms. The volume and geometry of a room, source of the sound, airborne noise transmission, and the acoustic properties of the interior surfaces are the parameters that affect the acoustic comfort (Mujeebu, 2019). In a room, sound is either reflected from the surfaces or absorbed by them. Sound absorption and sound transmission loss are decisive criteria among common acoustic parameters that can be used to evaluate the effects of room acoustics on speech intelligibility (Blaurock C et al., 2019; Lopez et al., 2021). The most common application of textiles that impact the IEQ are the ones used for the control of acoustics. Home textiles such as wall coverings, curtains, chairs, carpets, etc. can be designed to absorb sound, decrease reverberation times, and prevent echoes inside a room (Memon et al., 2015). Different restrictions and requirements apply for each application of acoustic textiles. This becomes more critical when a textile having some other functional properties, such as curtains, is modified to increase its acoustic performance. For instance, blackout curtains are expected to be UV resistant, non-transparent, foldable, or rollable while a porous sound absorber requires a voluminous, open structure (Blaurock C et al., 2019).

Blackout fabrics, blind or shading fabrics as they are also called, might be in the form of coated or multi-layered structures and provide barrier properties against visible light and are expected to darken a room completely (Szkudlarek et al., 2017). A study on acrylic coated polyester blind fabrics showed that acrylic content in the coating material, fabric type, and occurrence of viol structures due to the coating process were found to be effective parameters on sound absorption properties of these fabrics (Demiryürek & Aydemir, 2017). In another one, several commercially available curtain fabrics' acoustic performance has been investigated. The results showed that the PVC-coated polyester fabric exhibited better sound insulation properties, in the 600-1600 Hz frequency range and the multi-layered curtains have superior acoustic properties than those of the single-layered ones (Kumar et al., 2021).

Keeping the effect of noise and intensity of light on people's comfort in mind, this article presents a study on determination of sound absorption performance of a "bi-functional" home textile in the form of blackout curtain.

2. MATERIALS AND METHODS

2.1. Blackout Curtain Samples

Six commercial woven foldable blackouts from textured warp polyester yarns having weft-faced satin construction have been studied. Summary of the sample specifications is given in Table 1. Although the samples are apparently homogeneous, their structures varied from one another.

In the table, rPET refers to recycled polyester, and FR refers to flame retardant polyester.

Table 1. Sample specifications

Sample	Weight (g/m^2)	Thickness (mm)	Fabric density (kg/m^3)	Loop Density ($yarn/cm^2$)	Yarn Material	Warp Yarn Count (dtex)	Weft Yarn Count (dtex)
1	220	0,42	528	6972	rPET	75F72	150F48
2	236	0,51	467	3855	PET	75F72	300F96
3	232	0,54	429	7055	One face PET, opposite face cationic PET.	75F72	150F48
4	227	0,43	527	7179	FR PET	75F72	150F48
5	231	0,48	484	6992	FR rPET	75F72	150F48
6	229	0,48	478	7264	PET	75F72	150F48

The warp yarns in all samples are chosen as intermingled polyester yarns. This decision is given due to the previous research showing that the fabrics made with intermingled yarns have shown better sound absorption properties than the ones made with textured and staple polyester yarns. (Küçükali, 2010).

2.2. Acoustic Properties

Sound absorption and sound transmission loss were measured by Testsens impedance tube in accordance with the ISO 10534 standard. The tests were conducted in three ways; in the first test, the measurements were taken without leaving any air gap in the tube. Then the test is repeated two more times by leaving an air gap of 20mm and 50mm behind the fabrics, respectively. This is because when the curtain is hung, there will be a gap between the wall and the fabric, so it is a more realistic approach.

3. RESULTS AND DISCUSSION

The graph of sound absorption coefficients without air gap, with 20mm of air gap, and 50mm of air gap can be seen in Figure 1, Figure 2 and Figure 3, respectively.

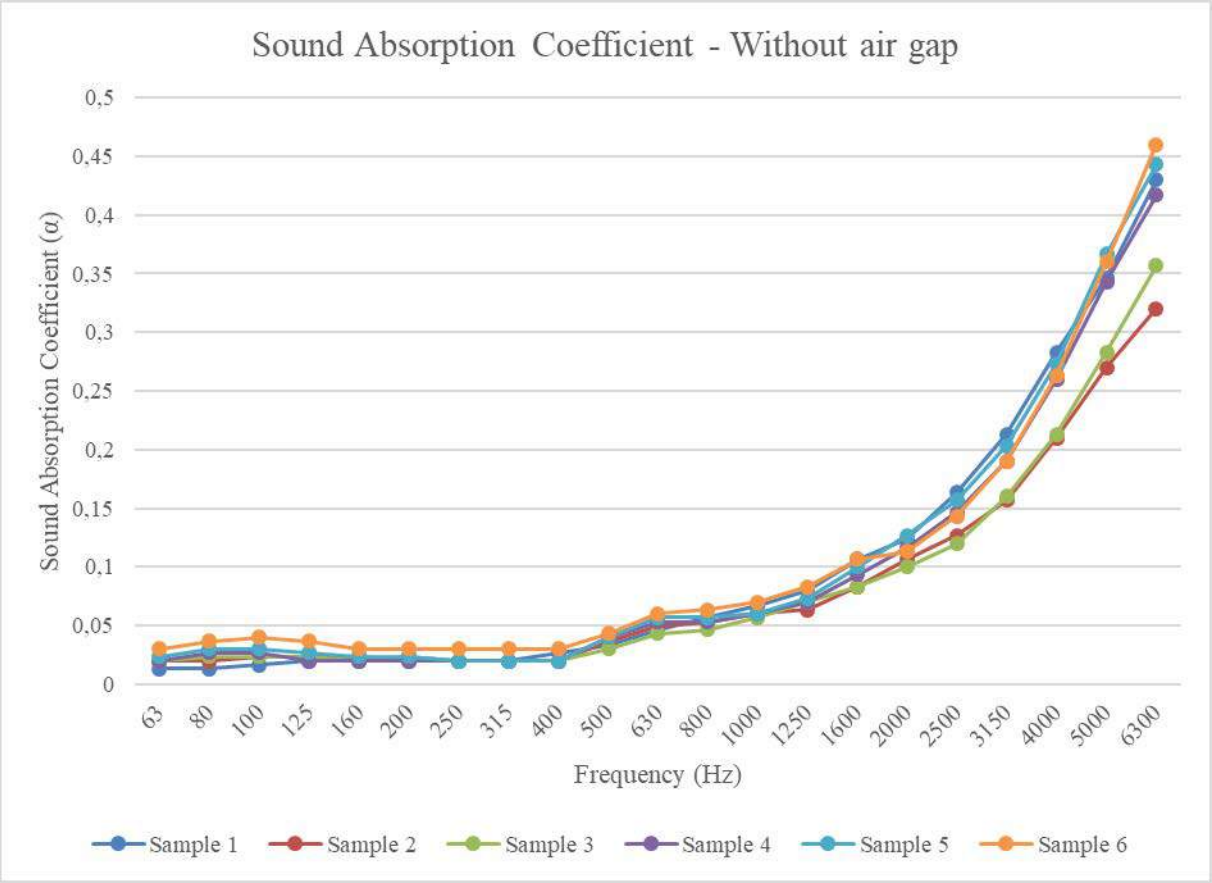

Figure 1. Sound absorption coefficients without air gap.

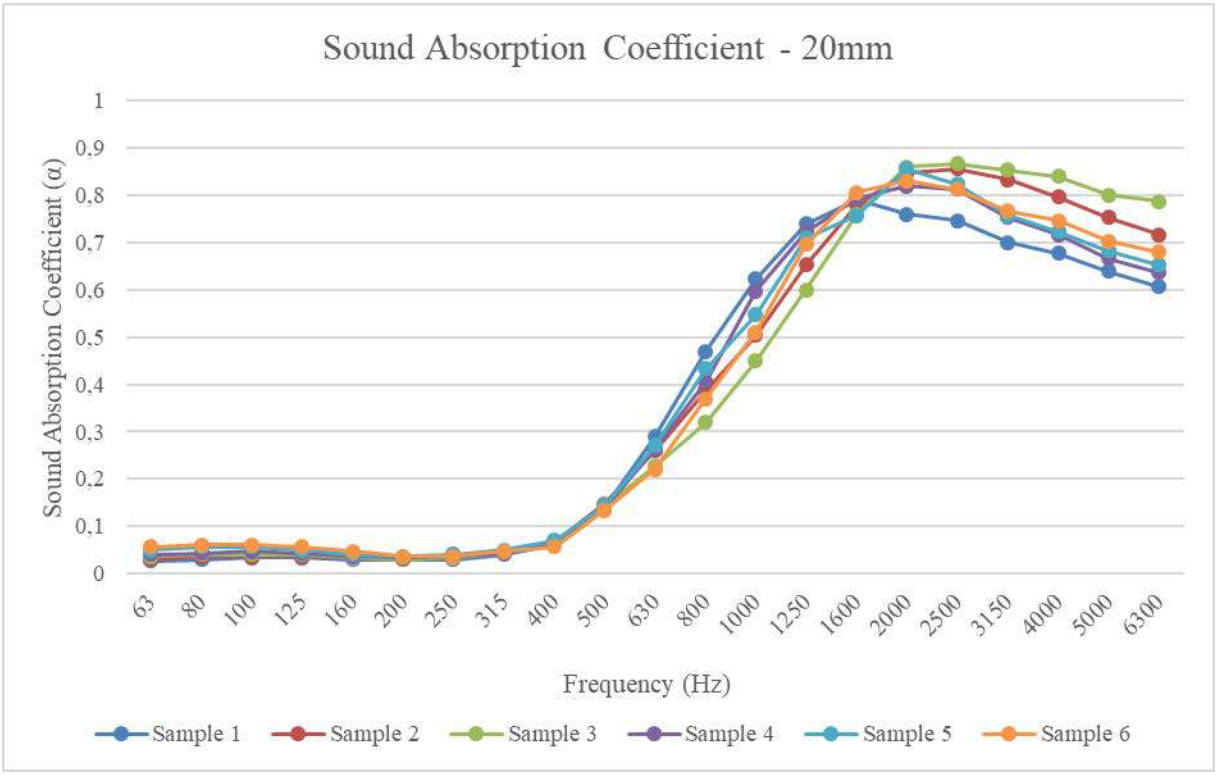

Figure 2. Sound absorption coefficients with 20mm of air gap.

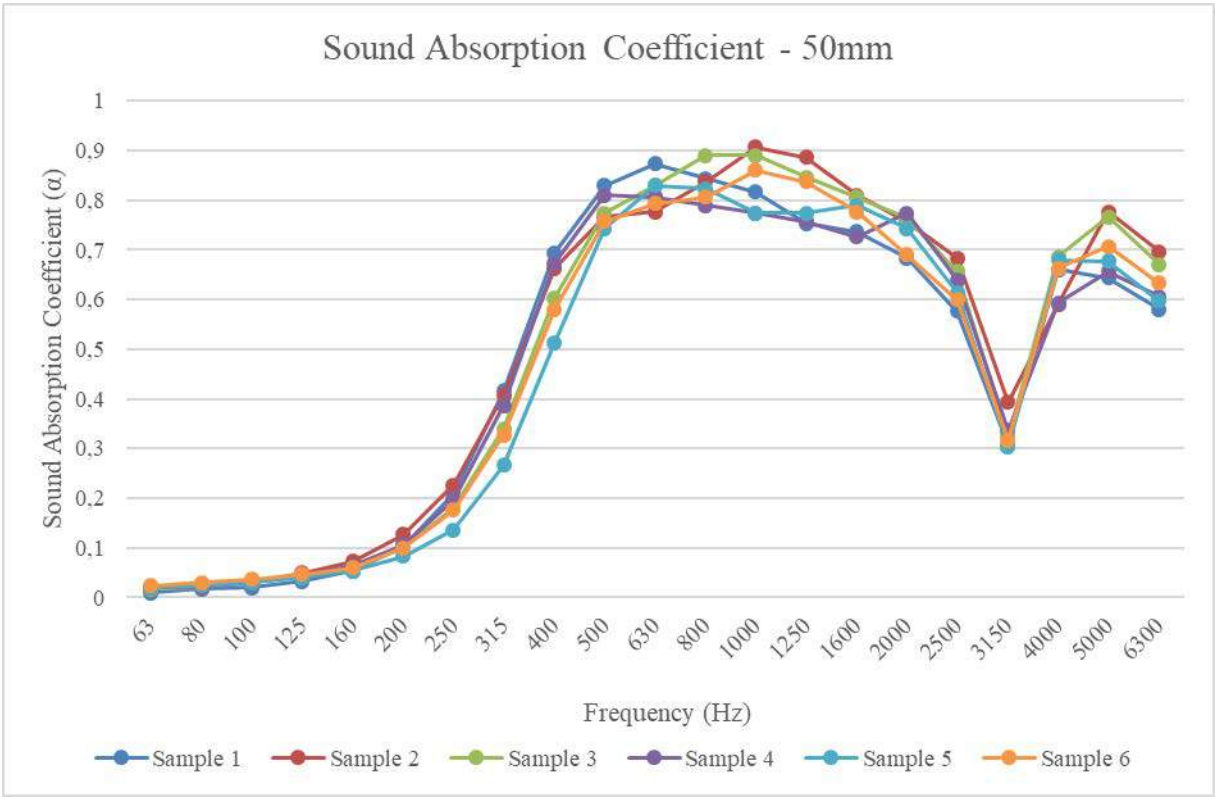

Figure 3. Sound absorption coefficients with 50mm of air gap.

Regardless of the PET fiber type, no significant difference was observed in terms of sound absorption results. This means that rPET can be used successfully without compromising the sound absorption performance for a more sustainable approach, or fibers with enhanced functionality such as flame-retardant PET and cationic PET can be used, which is a positive result. The sound absorption curve of samples behaved like a porous material and their sound absorption performances were observed to be low especially in low and medium frequency ranges. As can be seen in Figure 1, sound absorption of all samples increases similarly after 500 Hz. Sample 2 and Sample 3 showed the lowest sound absorption amongst all samples. For Sample 2, this may be due to the fact that the weft yarn count is double in Sample 2 compared to other samples. This leads to a reduction in loop density, and an increase in the fabric porosity. As the porosity increases, the area within the fabric where the soundwave can hit and get absorbed will decrease, and therefore the sound absorption of the fabric will also decrease. In addition, the fact that Sample 3 had the lowest density may have caused this result. Although all samples except the second sample were produced in similar construction from yarns of the same number, the different structural properties measured may be due to the different behavior of yarns from different fibers to weaving and dyeing processes.

In order to analyze the effect of the air gap size on the sound absorption behavior of the sample, the distance forming an air gap between the sample and the rigid wall was changed such that 20mm and 50mm air gaps were left while testing the samples. By leaving air gap and increasing the air gap between the sample and the rigid wall sound absorption performance increases, and also the resonance absorption frequencies of the samples tended to shift to the lower frequency range as the air gap was increased, both results are consistent with previous studies (Hanna & Kandil, 1991; Rubino et al., 2019). When a 20mm air gap is left, the sound absorption coefficient increases after 500 Hz, while it starts to increase after 200 Hz when a 50mm air gap is left. In fact, at 500Hz there is almost no sound absorption when there is no air gap, but the coefficients go up to around 0,8 at 50mm air gap. Same trend continues in mid frequencies, the sound absorbing coefficients are around 0.075 at no air gap but goes up to 0.9 at 50mm. Sound absorption coefficients up to 0.9 is especially a very promising result, it indicates that the curtain fabrics dissipate a very significant amount of the incoming soundwaves. This is both a desirable and a more realistic result, since when a curtain is hanged, there is almost always an air gap left between the fabric and the window or wall behind it. It is also consistent with previous findings on the acoustic properties of woven fabrics (Segura Alcaraz et al., 2021).

Sample 2 and Sample 3 are the thickest and low-density samples which can be seen in Table 1. Their relatively higher thickness hasn’t been enough to show the best performance without leaving an air gap behind samples, but the air gap and the thickness might contribute to their acoustic performances. As the fabric density and fabric thickness increase, there is more space within the fabric to absorb and dissipate the soundwaves. By using air gap behind the samples, the sound absorption coefficient was improved at low frequencies, which is a problem with commercial structures. The sound absorption coefficient of the samples was improved almost as much as three times at 500Hz by using 20mm air gap, while it was improved almost as much as sixteen times by using 50mm air gap.

4. CONCLUSION

This work aims to serve the studies that will be conducted to improve the acoustic properties of blackout curtains without comprising their opacity and light permeability performance. With this intention, 6 different commercial blackout curtain samples having different constructional parameters were tested and evaluated with different amounts of air gap left behind. The results were then interpreted and compared among themselves in terms of their fiber materials, fabric properties, and

different test parameters. It is shown that there is no tangible difference between fabrics that were made with different fiber types. This is a promising result for both manufacturers and users because it indicates that the desired functionality or aesthetic appearance can be given to the fabric without any loss in its sound absorption performance. It is also shown that leaving an air space behind the fabric drastically influences the sound absorbency of the fabrics positively. Leaving the air gap allowed all the samples to show better performance at low and middle frequencies, as well as increasing their sound absorption coefficients. These results are promising since these results are also more realistic for daily life use. In the later stages of the study, the effect of yarn structure on sound absorption properties of blackout curtains, as well as different methods to increase the sound absorbency of the fabrics without compromising from the blackout effect will be studied.

ACKNOWLEDGMENT

The authors gratefully acknowledge the funding by The Scientific and Technological Research Council of Turkey (TUBITAK) 1505 Program under the grant number 5210113.

REFERENCES

Angelova, R. A. (2016). Non-Woven Textiles in the Indoor Environment. In *Non-woven Fabrics*. InTech. https://doi.org/10.5772/61324

Aydın, D., & Mıhlayanlar, E. (2017). Investigation of indoor environmental quality in high-rise residential buildings. *Megaron*, *12*(2), 213–227. https://doi.org/10.5505/megaron.2017.07830

Blaurock C, Koeppe G, Kloeckner M, & Gries T. (2019). TEXTILE NOISE REDUCTION-REQUIREMENTS; OPTIONS AND RESTRICTIONS FOR INTERIOR DESIGN. *AUTEX2019 – 19th World Textile Conference on Textiles at the Crossroads*.

Demiryürek, O., & Aydemir, H. (2017). Sound absorbing properties of roller blind curtain fabrics. *Journal of Industrial Textiles*, *47*(1), 3–19. https://doi.org/10.1177/1528083716631332

Hanna, Y. I., & Kandil, M. M. (1991). Sound Absorbing Double Curtains from Local Textile Materials. In *Applied Acoustics* (Vol. 34).

Küçükali, M. (2010). *Akustik Özellikleri Geliştirilmiş Örme Kumaşlar*. İstanbul Teknik Üniversitesi.

Kumar, S., Aow, J. W., Dexuan, W., & Lee, H. P. (2021). *Investigation of lightweight acoustic curtains for mid-to-high frequency noise insulations*.

Lopez, P. S., Callens, P., & Cernak, M. (2021). A Universal Deep Room Acoustics Estimator. *2021 IEEE Workshop on Applications of Signal Processing to Audio and Acoustics (WASPAA)*, 356–360. https://doi.org/10.1109/WASPAA52581.2021.9632738

Memon, H., Abro, Z. A., Arsalan, A., & Khoso, A. N. (2015). Considerations while designing Acoustic Home Textiles: A Review. *Journal of Textile and Apparel, Technology and Management*, *9*(3), 1–29. https://www.researchgate.net/publication/317083985

Mujeebu, M. A. (2019). Introductory Chapter: Indoor Environmental Quality. In *Indoor Environmental Quality*. IntechOpen. https://doi.org/10.5772/intechopen.83612

Nayak, R., & Padhye, R. (2016). Acoustic Textiles: An Introduction. In R. Nayak & R. Padhye (Eds.), *Acoustic Textiles* (pp. 1–32). Springer Science+Business Media. https://doi.org/10.1007/978-981-10-1476-5_1

Noor, S. N. A. M., Ding, H. H., Saharuddin, S., Yusof, N. F. M., Roshdi, F. R. M., & Namandadin, N. A. (2021). Indoor environment quality (IEQ): Lighting and acoustics factors toward occupants satisfaction. *AIP Conference Proceedings*. https://doi.org/10.1063/5.0051620

Priniotakis, G., Stachewicz, U., & van Hoof, J. (2022). Smart textiles and the indoor environment of buildings. *Indoor and Built Environment*, *31*(6), 1443–1446. https://doi.org/10.1177/1420326X211067596

Rubino, C., Aracil, M. B., Gisbert-Payá, J., Liuzzi, S., Stefanizzi, P., Cantó, M. Z., & Martellotta, F. (2019). Composite Eco-Friendly Sound Absorbing Materials Made of Recycled Textile Waste and Biopolymers. *Materials 2019, Vol. 12, Page 4020*, *12*(23), 4020. https://doi.org/10.3390/MA12234020

Segura Alcaraz, M. P., Bonet-Aracil, M., Julià Sanchís, E., Segura Alcaraz, J. G., & Seguí, I. M. (2021). Textiles in architectural acoustic conditioning: a review. *Https://Doi.Org/10.1080/00405000.2021.1976483*, *113*(1), 166–172. https://doi.org/10.1080/00405000.2021.1976483

Szkudlarek, J., Snycerski, M., & Owczarek, G. (2017). Proposal of Objective Assesment of the Phenomenon of Light Passage Through Blackout Fabrics. *Fibres and Textiles in Eastern Europe*, *25*(0), 50–58. https://doi.org/10.5604/01.3001.0010.2663

EFFECTS OF PATTERN AND RAW MATERIAL ON SOFTNESS AND SMOOTHNESS PROPERTIES OF NONWOVENS

Gonca BALCI KILIC[1], Ebru CELİKTEN[2], Tülin KAYA NACARKAHYA[2], Doğu Fırat AYDOGAN[2]

[1] Dokuz Eylul University, Department of Textile Engineering, İzmir, Türkiye
[2] KaraFiber Textile and Trade Co. Inc. Research and Development Center, Gaziantep, Türkiye

Corresponding author: gonca.balci@deu.edu.tr

Abstract: *In this study, the effects of pattern and raw material on softness and smoothness properties of nonwovens were investigated. For this reason, spunlaced nonwoven fabrics with three different patterns (plain, dots and apertured) were produced. 100% polyester, 100% viscose, 50%-50% polyester-viscose, 50%-50% lyocell-viscose and 100% Ecocell fibres were used as raw materials for nonwoven fabrics. Within the scope of the study, in addition to synthetic fibres, biodegradable fibres and their mixtures have been preferred as raw materials due to the increasing importance of biodegradability and recycling in recent years. Softness and smoothness properties of nonwoven fabrics were measured by EMTEC TSA Softness Analyzer. Statistical analyzes (ANOVA and pairwise comparison) were performed using the SPSS 24 program with a confidence interval of 95%.*

Keywords: *spunlaced nonwoven, smoothness, softness, Ecocell, biodegradable fibre.*

1. INTRODUCTION

Nonwoven textile surfaces have been used for years, especially in disposable products. With the COVID 19 pandemic, the use of disposable products (especially masks and wet wipes) has increased even more. According to EDANA's data, the use of nonwovens for medical increased by 118%, wipes personal care by 22% and for hygiene by 9.6% in 2020. Parallel to this growing, the production of nonwovens also increased: drylaid-hydroentangled: 16.7%, spunlaid: + 12.4 % and wetlaid: + 6.2% (Edana, 2022).

Production of nonwoven is dominated by man-made fibre made from synthetic, natural, and inorganic materials with proportion polypropylene 63%, polyester 23%, viscose rayon 8%, acrylic 2%, polyamide 1.5%, and other specialty fibre 3% (Melani&Kim, 2021). The increase in environmental awareness in recent years has also led to the production of recyclable and environmentally friendly nonwoven products. Short-length viscose and short-length lyocell are among the main biodegradable fibres used in the production of nonwovens. Ecocell (Lyocell) is another natural, and biodegradable fibre, made from wood pulp sourced from sustainable plantations and forests, are used in nonwoven production.

Considering the usage area of spunlaced nonwovens, since these products usually contact the skin directly (such as surgical masks: inner and outer layer, wet wipes etc.), softness and surface smoothness are among the most important parameters that affect the handle characteristics and therefore purchasing behaviour.

The literature review shows that most of the studies focused on performance properties of nonwovens (Leucker et al., 2018; Motaleb et al., 2020; Korkmaz et al., 2022). However, there are few studies which analyze the softness and smoothness (surface roughness) properties of nonwovens. The vast majority of the studies in this field are related to the surface roughness of nonwovens (Roedel at al,

2003; Sul et al, 2006; Wei et al., 2008), whereas the studies to examine softness (Melani&Kim, 2021, Yin et al., 2020), which is more subjective parameter, is limited.

The most important parameters affecting the softness and smoothness (surface roughness) properties of nonwovens are raw material, pattern and production technology. In this study, it was aimed to analyze the effects of pattern and raw material on softness and smoothness properties of spunlaced nonwovens.

2. MATERIALS AND METHODS

2.1. Material

Within the scope of the study, synthetic (polyester) and recyclable (viscose, lyocell, Ecocell) fibres and their blends were used as raw material and nonwoven fabrics were produced with three different patterns: plain, dots and apertured. Due to the increasing environmental awareness in recent years, the use of biodegradable fibres in the production of recyclable and environmentally friendly nonwoven products has also increased. Lyocell is one of the biodegradable fibres used in the production of nonwovens. KaraFiber was established in 2020 as the first Lyocell factory of Turkey in Gaziantep with it's brand Ecocell. Ecocell is manufactured using latest closed-loop technology, requiring minimal chemical input during the production process, and utilising an organic solvent that is non-toxic and harmless which can be 99.5% recovered and recycled (KaraFiber, 2022).

Structural properties of spunlaced nonwovens are given in Table 1.

Table 1. Structural properties of nonwovens

Material	Pattern	Unit Weight (g/m^2)	Thickness (mm)
100% Polyester (PET)	Plain	40	0.60
100% Polyester (PET)	Dots	40	0.72
100% Polyester (PET)	Apertured	42	0.65
50%-50% PET-Viscose	Plain	45	0.55
50%-50% PET-Viscose	Dots	40	0.65
50%-50% PET-Viscose	Apertured	40	0.57
100% Viscose	Plain	40	0.41
100% Viscose	Dots	45	0.60
50%-50% Lyocell-Viscose	Plain	40	0.40
50%-50% Lyocell-Viscose	Dots	44	0.57
100% Ecocell	Apertured	40	0.47

The production parameters of spunlaced nonwovens as follows: temperature: 120-140 ºC, production speed: 180-220 m/min and pressure of water jet: 60-80 bar, which change according to material and pattern.

2.2. Method

To determine structural properties of nonwoven fabrics, unit weight and thickness were measured according to NWSP 130.1.R0 (15) and NWSP 120.6.R0 (15), respectively. Softness and smoothness (roughness) properties of nonwoven fabrics were measured by EMTEC TSA Softness Analyzer. Micro-surface variations (softness) and macro-surface variations (roughness) are measured via sound analysis in TSA softness analyzer (EMTEC, 2022). The TSA was developed to mimic the interaction of the hand with the fabric by measuring the light brushing of the surface by mechanical lamella

(Pawlak et al., 2022). While, smooth material surface gives light vibration, rough material surface gives strong vibration. Therefore, lower test results indicate higher smoothness and softness values. Measuring principle of smoothness and softness are given in Figure 1.

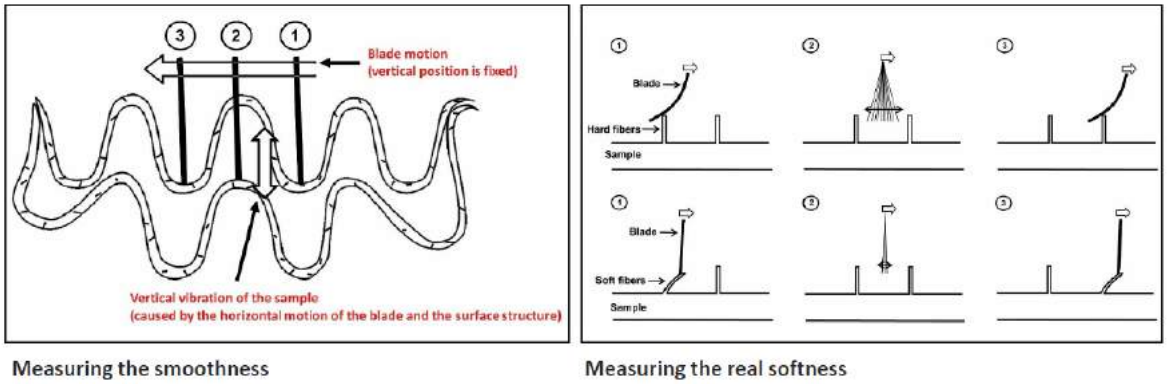

Figure 1. Smoothness and softness properties measuring principle for TSA (EMTEC, 2022)

In EMTEC TSA test device, to measure smoothness and softness, the measuring head includes rotor and blades (mechanical lamella) moves down to the sample until a load of 100 mN is applied. Once the load is reached, the rotor starts to rotate over the sample with a constant load of 100 mN. The rotation of the blades over the material cause two different types of vibrations. One is the vibration of the sample and the other one is the vibration of the blades. The vibration of both, the sample and the blades, causes a sound. This sound is recorded by a microphone, which is located underneath the sample. Both parameters are measured at the same time in two different frequency areas. The first peak (TS750 peak) represents the macro-surface variations (roughness) of the material, normally it can be found between 200 and 2000 Hz. The peak at approximately 6500 Hz is called TS7 and represents the micro-surface variations (softness). The examples of sound spectrum, TS750 (smoothness-roughness) and TS7 (softness) are given in Figure 2. When the blades move over the fibers and other micro-surface variations, they will get into vibration according to the stiffness or flexibility of these fibres (stick-slip principle). Stiff and hard fibres cause a strong vibration of the blades and thus more sound. Soft and flexible fibres cause much less vibration and thus less sound (EMTEC, 2022).

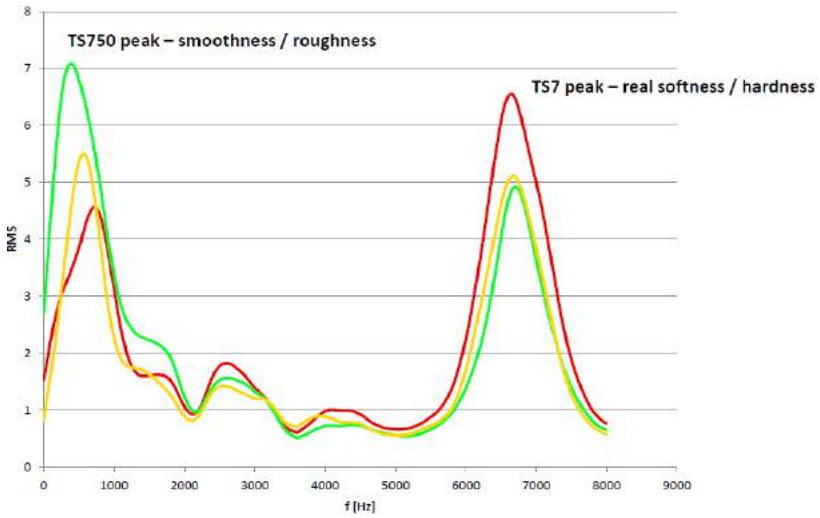

Figure 2. Sound spectrum, TS750 and TS7 parameters (EMTEC, 2022)

Within the scope of the study, in addition to smoothness and roughness properties, mechanical properties (tensile strength and breaking elongation) of nonwoven fabrics were measured according to NWSP 110.4.R0 (15) test method.

3. RESULTS AND DISCUSSION

The softness and roughness values of nonwoven fabrics are shown in Figure 3. According that, the softness values change between 3.9-6.5 dB, and roughness values change 80-285 dB for nonwovens used in the study. When an evaluation was made in terms of pattern, whereas fabrics with dots pattern structure have the best softness values, they have the worst smoothness values.

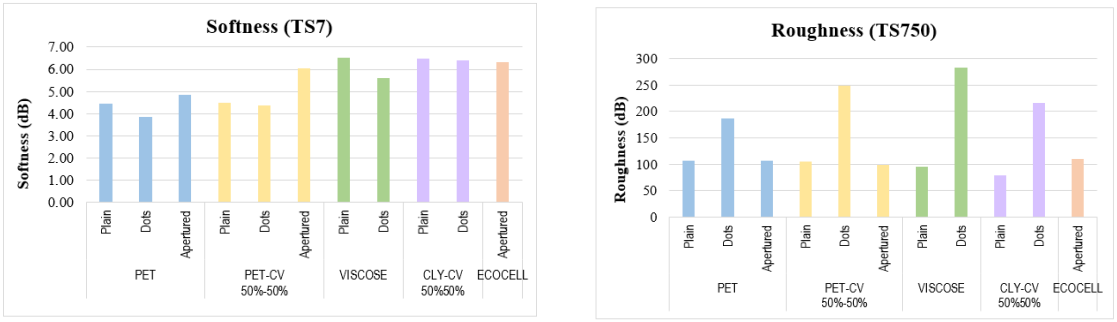

Figure 3. Softness and roughness values of nonwoven fabrics

ANOVA results for softness and roughness (smoothness) properties are given Table 2 and Table 3, respectively.

Variance analyzes showed that the effects of pattern and raw material are statistically significant on both parameters: softness and roughness ($p<0.05$) (Table 2 and Table 3). When comparing different materials separately, it was seen that the best softness values belong to dots pattern. The pairwise comparison of softness values revealed that, while the differences between plain and dots pattern are not statistically significant ($p>0.05$) for PET-CV and CLY-CV raw materials, the differences are statistically significant for others. For smoothness, it was concluded that nonwoven fabrics with dots pattern have the lowest smoothness values (higher roughness (TS750) peak) generally, as opposed the softness. According to pairwise comparison of smoothness values, the differences between plain and apertured pattern are not statistically significant ($p>0.05$) for PET and PET-CV raw materials.

Table 2. ANOVA results for softness

Tests of Between-Subjects Effects

Dependent Variable: Softness

Source	Type III Sum of Squares	df	Mean Square	F	Sig.	Partial Eta Squared
Corrected Model	51.061[a]	10	5.106	33.214	.000	.883
Intercept	1605.354	1	1605.354	10442.459	.000	.996
Pattern	10.634	2	5.317	34.586	.000	.611
Material	44.333	4	11.083	72.094	.000	.868
Pattern * Material	2.535	4	.634	4.122	.006	.273
Error	6.764	44	.154			
Total	1664.294	55				
Corrected Total	57.825	54				

a. R Squared = .883 (Adjusted R Squared = .856)

Table 3. ANOVA results for roughness (smoothness)

Tests of Between-Subjects Effects

Dependent Variable: Roughness

Source	Type III Sum of Squares	df	Mean Square	F	Sig.	Partial Eta Squared
Corrected Model	255733.944[a]	10	25573.394	24.799	.000	.849
Intercept	1108078.080	1	1108078.080	1074.545	.000	.961
Pattern	211041.853	2	105520.926	102.328	.000	.823
Material	11567.686	4	2891.922	2.804	.037	.203
Pattern * Material	17318.936	4	4329.734	4.199	.006	.276
Error	45373.082	44	1031.206			
Total	1520357.707	55				
Corrected Total	301107.026	54				

a. R Squared = .849 (Adjusted R Squared = .815)

Tensile strength (N) and breaking elongation (%) values showed that the effects of pattern and raw material were also important for tensile properties (Figure 4).

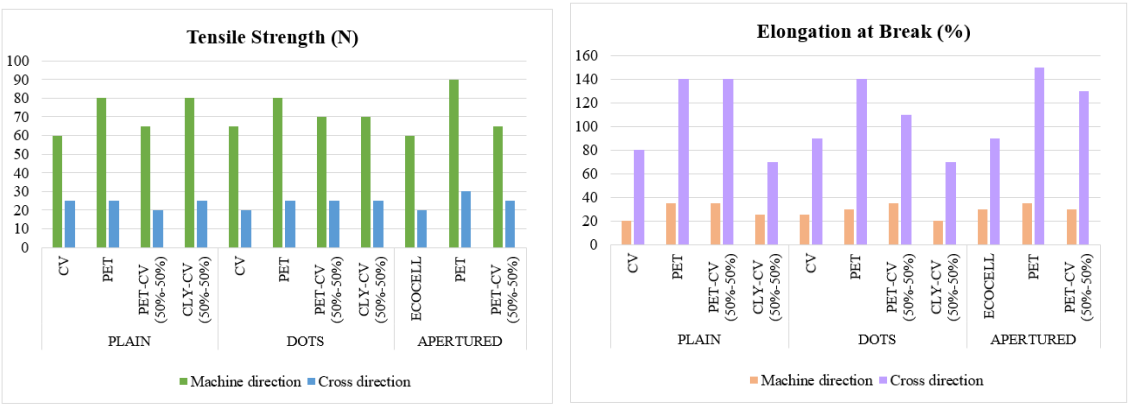

Figure 4. Tensile strength and breaking elongation values

4. CONCLUSION

In this work, it is aimed to analyze the effect of pattern and raw material on the softness and smoothness properties of spunlaced nonwoven fabrics. Test results showed that there are significant differences between smoothness and roughness properties depending on the pattern and raw material. In the later stages of the study, the softness and smoothness properties of nonwoven fabrics will be measured by subjective test method (fabric handle test) and the correlations between objective and subjective test results will be examined.

REFERENCES

Edana (European Disposables and Nonwovens Association), The Voice of Nonwovens, www.edana.org, May 2022.

EMTEC TSA Tissue Softness Analyzer Booklet, 2022, Emtec Electronic GmbH.

Karafiber, Ecocell, https://www.karafiber.com/ensingle-service-v2.html, July 2022.

Korkmaz, G., Kılınç, M., Razak, S. A., Ocak, M., Korkmaz, S., & Kut, Y. D. T. (2022). Comparison of the performance properties of spunlaid non-woven fabrics used as face mask. *The Journal of The Textile Institute*, 1-7, online published.

Leucker, K., Amtmann, J., & Schubert, D. W. (2018). Novel objective test method for the abrasion and pilling behaviour of low basis weight spunbond polypropylene nonwovens. *Polymer Testing*, 69, 175-181.

Melani L.& Kim, H. J. (2021). The surface softness and mechanical properties of wood pulp–lyocell wet-laid nonwoven fabric. *The Journal of The Textile Institute*, 112(8), 1191-1198.

Motaleb, K. Z. M., Mizan, R. A. & Milašius, R. (2020). Development and characterization of eco-sustainable banana fiber nonwoven material: surface treatment, water absorbency and mechanical properties. *Cellulose*, 27(14), 7889-7900.

Pawlak J. J., Frazier, R., Vera, R. E., Wang, Y. & Gonzalez, R. (2022). Review: The softness of hygiene tissue, *BioResources*, 17(2), 3509-3550.

Roedel, C. & Ramkumar, S. S. (2003). Surface and Mechanical Property Measurements of H Technology Needle-Punched Nonwovens. Textile research journal, 73(5), 381-385.

Sul, I. H., Hong, K. H., Shim, H., & Kang, T. J. (2006). Surface roughness measurement of nonwovens using three-dimensional profile data. *Textile Research Journal*, 76(11), 828-834.

Wei, Q., Yu, L., Hou, D. & Huang, F. (2008). Surface characterization and properties of functionalized nonwoven. *Journal of Applied Polymer Science*, 107(1), 132-137.

Yin, L., Shim, E. & DenHartog, E. (2020). A study of skin physiology, sensation and friction of nonwoven fabrics used in absorbent hygiene products in neutral and warm environments. *Biotribology*, 24, 100149, 1-12.

DEVELOPMENT AND PRODUCTION OF BREATHABLE ARTIFICIAL LEATHER WITH MICROPORES

İffet AKKUŞ ALTINDAĞ[1], Berrak Buket AVCI[2], Gökhan ERKAN[2]

[1] Güzelcan Suni Deri Tekstil Tic. San. A.Ş. , İzmir, Türkiye
[2] Dokuz Eylul University, Department of Textile Engineering, İzmir, Türkiye

Corresponding author: iffetakkus@egesunideri.com

Abstract: *Despite the increasing ethical and social opposing views, genuine leather continues to be preferred due to its air and water vapour permeability. In this study, Poly(vinyl) chloride (PVC) coated fabric, artificial leather, with high air permeability and optimum water vapour permeability was developed as an alternative to genuine leather. Thanks to the formulation and process developed for the PVC coated fabric, which is normally not air-permeable, a coating with micropores has been obtained, thus providing a product that is higher than standard products and close to real leather in terms of comfort of use. The air permeability, water vapour permeability and micropore structure of the developed product were evaluated by comparing it with real leather and standard PVC coated fabric.*

Keywords: *PVC coated fabric, artificial leather, breathable PVC film, microporous, transfer coating*

1. INTRODUCTION

Genuine leather is a material that has been widely used in many areas such as clothing, upholstery, shoes, automotive for centuries (Harmon, 2020). It is more preferred than artificial leather, as it provides comfort to the user due to its air and water vapour permeability. On the other hand, the high water vapor permeability of real leather causes it not to be easily cleaned and gets wet quickly, which makes it uncomfortable to use (Träubel, 2012). Due to the recent increase in global warming and the decrease in biodiversity, as well as the formation of ethical awareness, genuine leather use is not considered correct. However, in addition to increasing global warming, decreasing biodiversity, it is also on the agenda to restrict or even terminate its use due to ethical, environmental and social effect (Payne et al., 2016; Minh & Ngan, 2021; Choi & Lee, 2021). On the other hand, real leather continues to be preferred because of the comfort it offers to the user due to its air and water vapor permeability, and a material that will fulfill these functions has not been fully developed yet (Saha, 2020).

Artificial leather is a material developed as an alternative to genuine leather, and its use is becoming more and more common. It can be also expressed as coated fabric, where different polymers are used to increase the strength of a fabric. The main polymers for coating are polyurethane (PU) and poly (vinyl) chloride (PVC). PVC coated fabrics are often preferred because they are more advantageous than PU coated ones due to their high stability, mechanical properties and price advantage (Altindag & Akdogan, 2021). However, since standard PVC coated fabrics do not have air permeability, they cannot offer the comfort of real leather to the user.

Although air permeability in PVC coated fabric is commonly achieved by mechanical punching, it causes a loss of strength in product due to deformation of the support fabric during perforation. Also there are some breathable film production example in the literature without mechanical punching, but they use additional chemicals to develop these materials. In this study, breathable artificial leather is developed using only water which is homogenously emulsified in the plastisol by mechanical mixing, and these emulsified water droplets were evaporated in the controlled manner during pre-gelification

stage. The evaporated water left empty space behind, and full gelification was achieved around this spaces. Although some pores are not fully open, they are completely opened after vacuum embossing process is applied, which increases the air and water vapor permeability of the produced artificial leather. This full work is patented under application number PCT/TR2021/051045.

2. MATERIALS AND METHODS

2.1. Preparing and Transfer Coating of Microporous PVC

The plastisol, which is formed according to the area of use and basically contains PVC, plasticizer, filler material, stabilizer and pigment, is mixed until it becomes a homogeneous mixture. As a result, pure water (1-30 phr) is added at the rate determined according to the targeted pore amount and dispersed in Transfer coating method is a method that is frequently used in the production of artificial leather. Its basic principle is to spread a certain amount of plastisol on a special transfer paper coated with silicone and gelify this plastisol at 180-190 °C. In this way, the selected fabric lamination after a single or repeated coating is achieved by combining the spread plastisol with the fabric and providing gelification.

For the obtaining of microporous PVC coating, transfer coating is applied. For a smooth pore structure, the gelification process is carried out by gradually increasing the oven temperature from 100 °C to 200 °C. It has been determined that the pores that will provide air permeability are formed just before gelification. For this, first of all, homogeneous distribution of the water to be added into the formulation was ensured. To achieve that the mixing is even in all parts of the plastisol, the mixing was ensured not to fall below 1800 rpm. The PVC film, which underwent surface deformation due to high temperatures under standard PVC production conditions, became porous and gelified in a stable structure when heated gradually. The support fabric was chosen sparsely knitted in order not to adversely affect the air permeability of the film. The breathable film production principle is shown in the figure below (Figure 1).

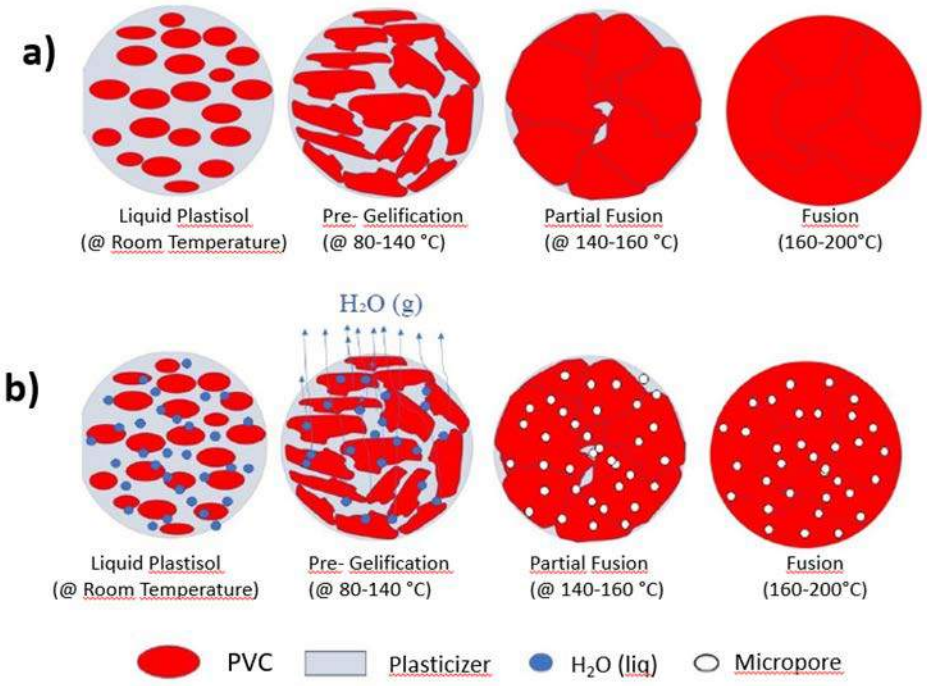

Figure 1. Gelification Principle: (a) Normal Condition (b) With Water

To obtain different air and water vapor permeable artificial leather, four different sample were prepared by changing their coating mass and fabric backing. By emulsifying 8 % water in the plastisol, transfer coatings were applied based on the parameter in the Figure 1. The type of backing and total mass of artificial leathers are shown in the table below.

Table 1. The total mass and type of backing of artificial leather samples.

Sample	Weight (g/sqm)	Backing Type
Non-porous Artificial Leather	680	Tricot Cotton-Polyester
Porous Artificial Leather 1	680	Tricot Cotton-Polyester
Porous Artificial Leather 2	680	Brushed Polyester
Porous Artificial Leather 3	400	Brushed Polyester
Porous Artificial Leather 4	300	Brushed Polyester

2.2. Examination of Micropores under the Microscope

The surface of leather, non-porous artificial leather and porous artificial leather were examined with light microscope and stereo microscope. Light microscope images were taken by Olympus BX 43, stereo microscope images were taken by Olympus SZ61. In addition, the presence of porous structure was investigated in microscope images.

2.3. Water Vapour Permeability

The ability of fabrics to pass water vapour is related to their breathability. Water vapour permeability of samples was determined by using Shirley M261 (SDL Atlas International, USA) model water vapour permeability tester according to BS 3424-34:1992-Method 37. The amount of water vapour that the fabrics pass through; after the 1st and 25th hours, the results were determined and the water vapour permeability indexes were calculated. The test was repeated two times for each sample type.

2.4. Air Permeability

The air permeability of the samples was measured to examine the effect of the treatments on the air permeability of the fabrics. Textest FX3300 air permeability tester was used in the all measurements. Measurements were made using 500 Pa air pressure according to ISO 9237. Measurements were made from 20 cm^2 of the fabrics and the average was taken by making 5 repetitions for each fabric in total

2.5. Smoothness/Roughness of Materials

The surface smoothness/roughness values were measured with Emtec TSA Softness. Emtec TSA Softness Analyzer measures the surface smoothness/roughness with sound analysis. A lower value in measurement results means higher smoothness.

3. RESULTS AND DISCUSSION

3.1. Examination of Micropores under the Microscope

Stereo microscope images of samples were given at Figure 2 and Figure 3. Moreover, light microscope images of porous artificial leather was given at Figure 4. When the stereo microscope images of the samples were looked at, porous were seen on the surface of the porous artificial leather depending on the direction of the light. In addition, it had been observed that there was no porous structure in genuine leather and non-porous artificial leather. The porous on the porous artificial leather were examined with a light microscope at x20 magnification and the presence of the porous structure was observed.

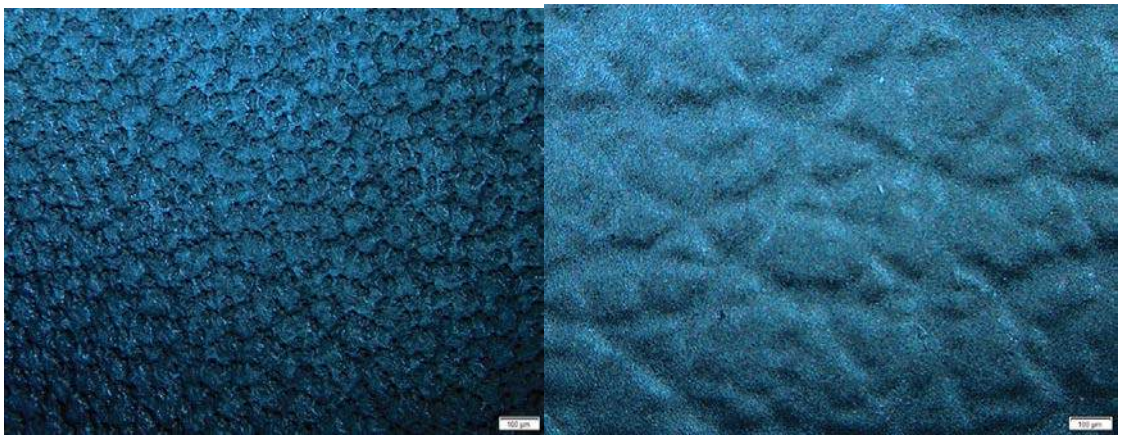

(a) (b)

Figure 2. Stereo microscope image of (a) genuine leather, (b) non-porous artificial leather

(a)

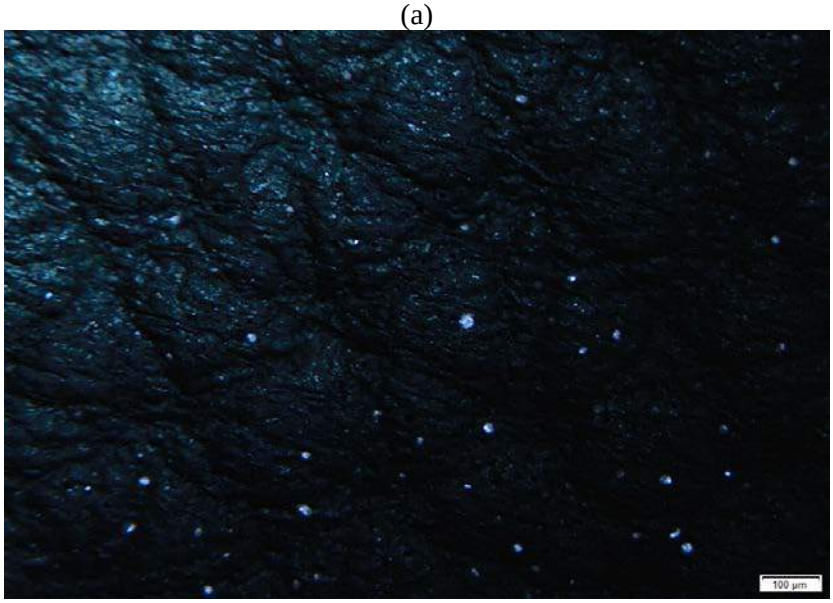

(b)

Figure 3. Stereo microscope images of porous artificial leather: (a) bottom lighting and (b) both top and bottom lighting

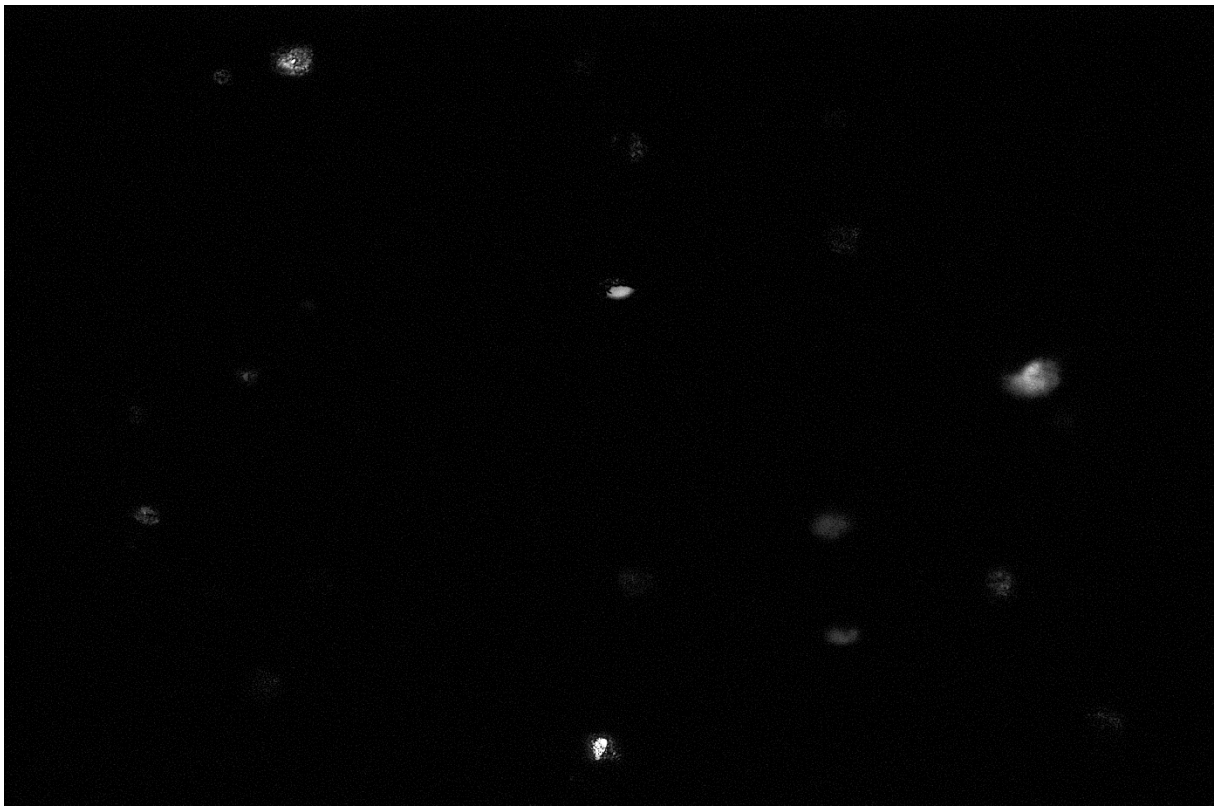

(a)

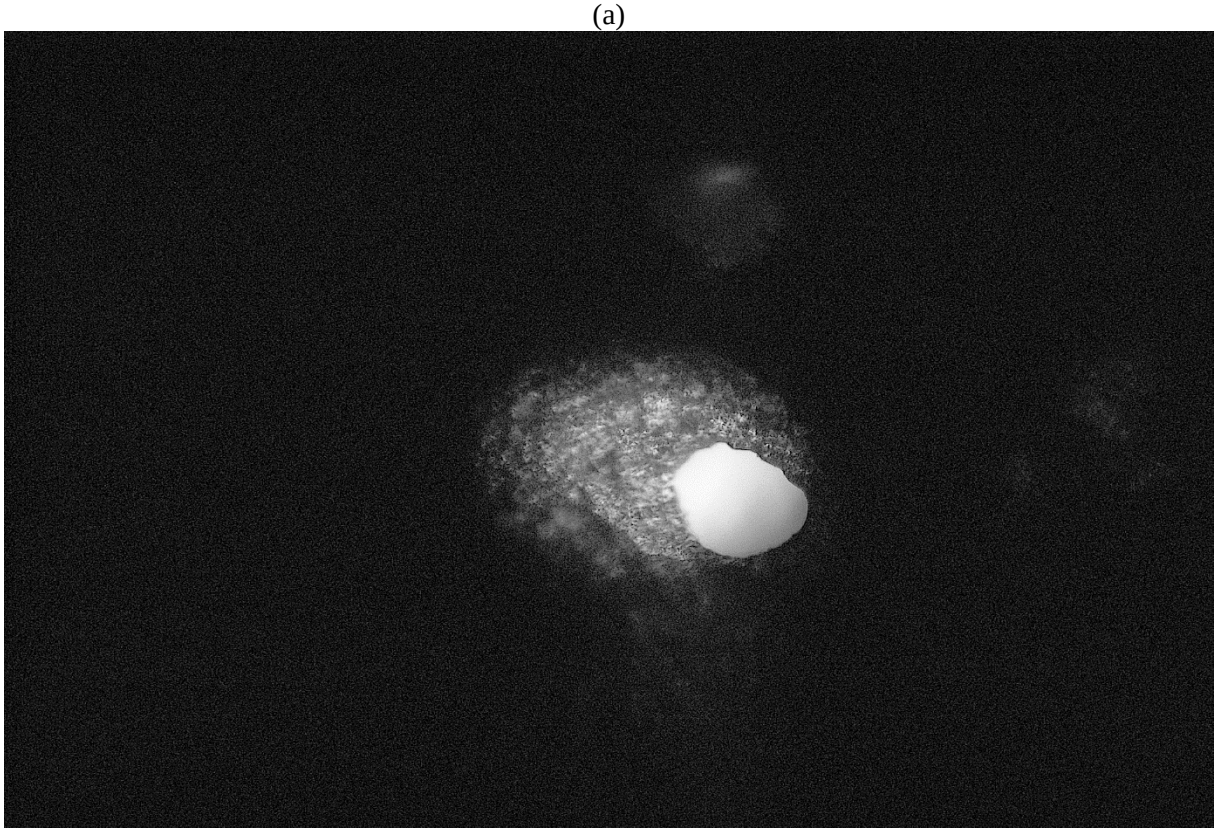

(b)

Figure 4. Light microscope images of porous artificial leather: (a) x4 magnification (b) x20 magnification

3.2. Water Vapour Permeability

Water vapour permeability analysis was carried out to examine the comfort properties of the fabrics obtained. Water vapour permeability of samples are tabulated in Table 2. The highest water vapour permeability was obtained from leather with 497.48 g/m^2 per 24 h permeability value. The skin is a semipermeable membrane, which manages the oxygen and moisture transport that regulates the vital functions of the cells (Türkoğlu et al., 2021). The lowest water vapour permeability was observed with the 17.28 g/m^2 per 24 h value in non-porous artificial leather. It has been observed that the water vapour permeability of porous artificial leathers are 160.31, 32.56, 60.87 and 144.33 per 24 h, respectively. Although porous artificial leather is not as water vapour permeable as leather, it has been found that porous artificial leather has a much higher water vapour permeability than non-porous artificial leather's water vapour permeability. The permeability can be changed by changing the backing and total weight of the sample. The backing of artificial leather has critical role for permeability, because the brushed structure of backing fabric effect the water vapor movement in negative way. Even the most breathable coating polymer applied to the samples would add a resistance to vapour flow by closing the pores and creating an additional layer (Song, 2011). The water vapour permeability of a material plays an important part in evaluating the physiological wearing comfort of clothing systems or determining the performance characteristics of textile materials used in technical applications (Uyar et al., 2022).

Table 2. Water vapour permeability of genuine leather, non-porous artificial leather and porous artificial leathers

Sample	Water Vapour Permeability, g/m^2 per 24 h
Genuine Leather	497.48
Non-porous Artificial Leather	17.28
Porous Artificial Leather 1	160.31
Porous Artificial Leather 2	32.56
Porous Artificial Leather 3	60.87
Porous Artificial Leather 4	144.33

3.3. Air Permeability

The air permeability of prepared artificial leather samples are shown in the table above. According the measurements, the air permeability value of the same fabric backing samples is increasing with decreasing the total mass. It is because of the applying more coating influences the micro pore quality and quantity of the samples. Considering same weighted samples, Artificial leather 1 and 2, the backing affected the air permeability.

Table 3. Air permeability of genuine leather, non-porous artificial leather and porous artificial leathers

Sample	Air Permeability of Samples (mm/sec)
Genuine Leather	1.75
Non-porous Artificial Leather	0.0
Porous Artificial Leather 1	46.42
Porous Artificial Leather 2	14.72
Porous Artificial Leather 3	28.16
Porous Artificial Leather 4	62.56

3.4. Smoothness/ Roughness of Materials

Emtec TSA Softness Analyzer measures the surface smoothness/roughness with sound analysis. According to the technical bases of TSA, the first peak of the graph gives the smoothness/roughness measurement of the samples. When Figure 5 was examined, it was seen that the first peak in the graph was 376,905 for non-porous artificial leather, and 340.940 for porous artificial leather. A lower value in measurement results means higher smoothness in Emtec TSA. Therefore, it was seen that the porous artificial leather (with a value of 340.940) was more smoothness than the non-porous artificial leather (with a value of 376.905).

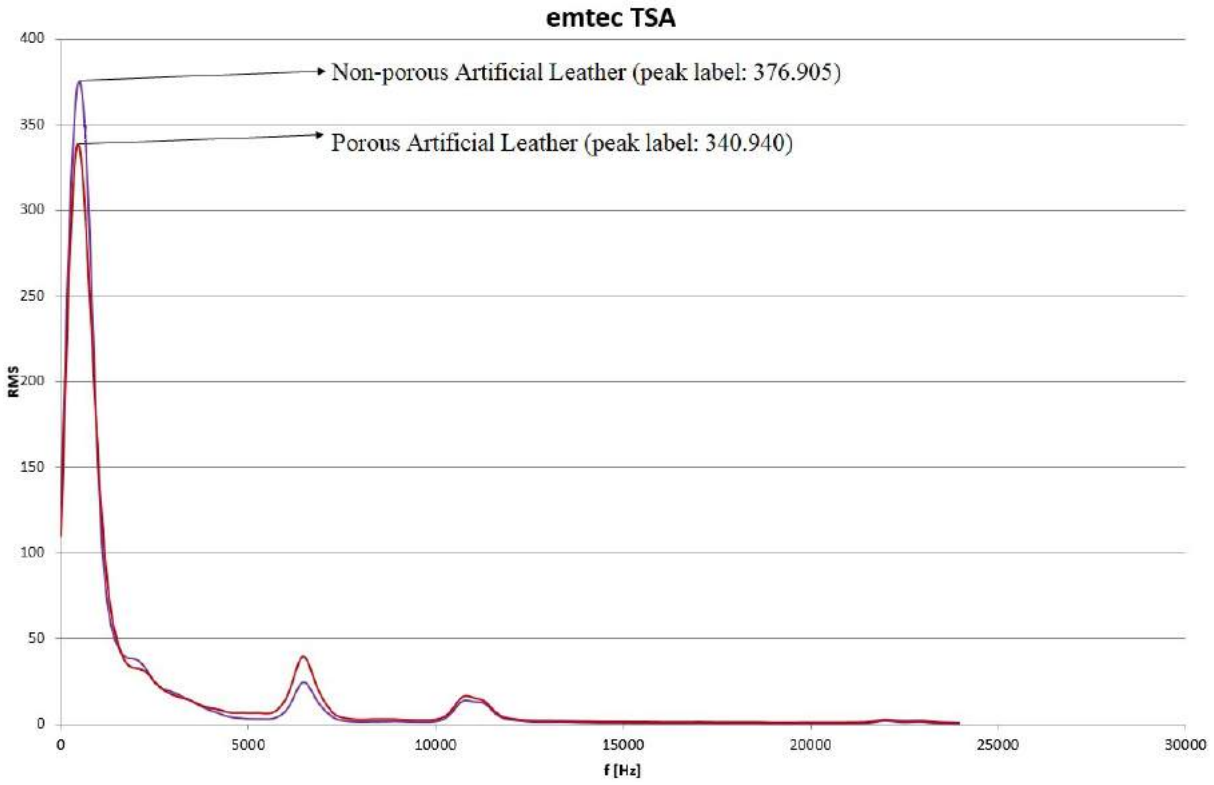

Figure 5. Smoothenss/Roughness values of non-porous and porous artificial leather

4. CONCLUSION

In this work, it is aimed to develop air and water vapor permeable artificial leather, which normally does not have enough of these features. When the results were evaluated, it was clearly seen that the developed artificial leather with high air permeability was affected by the backing and the weight of the coating. The properties of the fabric to be selected for backing also directly affected the air and water vapor permeability. The selected fabric not only affected these properties, but also made a difference in the ability to view the pores with a microscope. It has been understood that by combining different coating amount and backing fabrics, artificial leather can be developed with the closest comfort to real leather.

ACKNOWLEDGEMENTS

Support from the Scientific and Research Council of Turkey (TUBITAK) (Project Number: 3210892) is gratefully acknowledged.

REFERENCES

Altindag, I. A. & Akdogan, Y. (2021). Spectrophotometric characterization of plasticizer migration in poly (vinyl chloride)-based artificial leather. *Materials Chemistry and Physics*, 258, 123954.

Choi, Y. H. and Lee, K. H. (2021). Ethical consumers' awareness of vegan materials: Focused on fake fur and fake leather. *Sustainability*, 13, 1, 436.

Harmon, J. (2020). *Bacterial Cellulose Product Development: Comparing Leather and Leather Alternatives*. In *International Textile and Apparel Association Annual Conference Proceedings*. Iowa State University Digital Press.

Minh, N. T. & Ngan, H. N. (2021). *Vegan leather: An eco-friendly material for sustainable fashion towards environmental awareness*. In *AIP Conference Proceedings*, AIP Publishing LLC.

Payne, A., D. Brough, & P. Musk. (2016). Will we soon be growing our own vegan leather at home? *The Conversation*, November, 1-4.

Saha, N., Ngwabebhoh, F. A., Nguyen, H. T., Saha, P. (2020). *Environmentally friendly and animal free leather: fabrication and characterization*, AIP Conference Proceedings, 2289, 020049, 1-6.

Song, G. (2011). *Improving Comfort in Clothing*. Woodhead Publishing Limited, Cambridge, UK.

Träubel, H. (2012). *New materials permeable to water vapour*. Springer Science & Business Media.

Türkoğlu, G. C., Sarıışık, M., Karavana, S. Y., Aydın Köse, F. (2021). Production of wheat germ oil containing multilayer hydrogel dressing, Carbohydrate Polymers, 269, 118287.

Uyar, M. N., Sarıışık, A. M., Kartal, G. Erkan. (2022). Examination of the coating method in transferring phase changing materials, Johnson Matthey Technology Review, 66, 2, 177–185.

INVESTIGATION OF THE EFFECTS OF FABRIC STRUCTURE ON PEDOT COATED CONDUCTIVE POLYESTER TEXTILE SURFACES

Aysun YENİCE[1], Aslı HOCKENBERGER[2]

[1] Küçükçalık Tekstil San. ve Tic. A.Ş., Bursa, Türkiye
[2] Uludag University, Department of Textile Engineering, Bursa, Türkiye

Corresponding author: aysuns@kcalik.com

Abstract: *In this study, it's aimed to examine the effect of number of filaments and weave type on the conductivity performance of these surfaces. PEDOT polymer was chosen due to its conductivity performance, and vapor phase polymerization method was chosen due to its ease of application and industrial adaptability. Polyester has been preferred because of its cost, wide usage area and durablity of the polymer. Plain and 3/1 twill fabrics were woven with 150 Den 48, 144 and 288 filament yarns, keeping the weft and warp densities constant. A cabinet suitable for the horizontal flow of textile fabrics was designed for polymerization and laboratory-scale steaming was done in sets to compare the results.*
With the study, it was determined that the polymerization in the vapour phase can be applied homogeneously to the fabric and there is no difference in electrical resistance between the front and the back side of the fabric.

Keywords: *Conductive fabrics, conductive polymers, PEDOT, vapor phase polymerization, smart textiles.*

1. INTRODUCTION

The increase in our use of technology aroused the need of smart textiles. So that the electronic circuits became smaller and lighter to be carried easily. Textile surfaces can be used in different areas such as computers, electromagnetic shielding or sensors to react to various mechanical, thermal, chemical, electrical or magnetic effects in their location (Qu & Skorobogatiy, 2015).

Making textile surfaces conductive is in the focus of these issues. Fabric structures, which have both strength features to support technical needs and comfort features such as lightness and flexibility during use, have been one of the most popular subjects in academic studies. The process, which started with the use of metal wires in weaving (Schwarz-Pfeiffer & Van Langenhove, 2013), accelerated with the discovery of conductive polymers in 1977. In 1988, Bayer Ag reached a higher level with the production of PEDOT Poly(3,4-ethylenedioxythiophene), one of the most successful polymers in terms of processability, stability and conductivity (Elschner et al., 2010).

Although there are many different application methods for coating textile surfaces with conductive polymers, polymerization in the vapour phase is seen as one of the most preferred methods in terms of surface smoothness, conductivity level and ease of application (Truong et al., 2008).

In the coating of textile surfaces with conductive polymers, the surface properties of the fabric are important parameters to provide a homogeneous coating and therefore to obtain a good conductivity. The weave type of the fabric and the number of filaments of the yarns are the basic parameters that change the fabric surface properties.

The aim of this study therefore is to examine the effect of weave type and number of the filaments on conductivity. For this reason, yarns with 48, 144 and 288 filaments were woven with plain and 3/1

twill weaves using the same weft and warp densities. PEDOT polymer was chosen due to its high conductivity potential and vapour phase polymerization method was chosen due to its ease of application. The fabrics were coated with polymerization process under laboratory conditions.

2. MATERIALS AND METHODS

2.1. Properties of Yarns and Fabrics

For the experiments, the fabric constructions (Table 1) were created using 150 Den PET yarns with 48, 144 and 288 filaments to investigate the effects of number of the filaments and the weave types on the vapour phase polymerization method. The yarns used in this study were not twisted but texturized in order to increase the surface coverage.

Table 1. Fabric constructions

Article Number	Type of Weave	Warp Yarns	Weft Yarns	Warp Density (ends/cm)	Weft Density (picks/cm)	Weight (gr/sqm)	Thickness (mm)
38198	Plain	150F48 Texturised	150F48 Texturised	31	31	121	0,21
38191	Plain	150F144 Texturised	150F144 Texturised	31	31	118	0,21
38193	Plain	150F288 Texturised	150F288 Texturised	31	31	118	0,21
38197	3/1 Twill	150F48 Texturised	150F48 Texturised	31	31	120	0,21
38194	3/1 Twill	150F144 Texturised	150F144 Texturised	31	31	117	0,21
38195	3/1 Twill	150F288 Texturised	150F288 Texturised	31	31	115	0,21

The production of yarns, weaving of fabrics and dyeing processes were carried out in the weaving plant of Küçükçalık Tekstil. Before the conductivity process, the fabrics were washed with an oil remover in the dyehouse to ensure that no residue was left on them and to ensure surface cleanliness.

2.2. Chemicals

The samples first put into the dopant solution (Table 2) in order to start the polymerization. Then the sample fabrics were placed in the unit in the polymerization cabinet and the EDOT monomer was placed on the heating plate. When the lid of the cabin was closed, Argon gas was started to be fed simultaneously with the air release valve with speed and time control.

After the samples were kept in the cabinet for a total of 1 hour, the samples were taken out and their electrical resistance was measured with a 4-Point Probe Conductivity Measuring Device. The samples were washed afterwards with 50% ethanol- 50% distilled water mixture and dried in oven for 15 minutes at 100^0C and their conductivity was measured again.

Table 2. Chemicals used in the experimental study and their properties

Chemical	**Content**	**Formula**	**Molar Mass (gr/mol)**
3,4- Ethylenedioxythiophene (EDOT)	96.5% (GC)	$C_6H_6O_2S$ 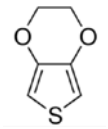	142,18
Iron(III) p-toluenesulfonate hexahydrate	Carbon 30.9-43.5% Sulphur 11.8-16.6% Clorid ≤10 %	$[C_{21}H_{21}FeO_9S_3 \cdot 6(H_2O)]$ 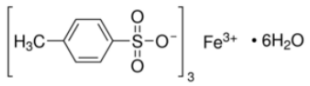	677,52
n-butanol	≥ 99.4 % A.C.S. Reagent	$CH_3(CH_2)_3OH$ 	74,12
PEG		$H(OCH_2CH_2)_nOH$ 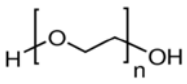	400
Pyridine	≥99.8 A.C.S Reagent	C_5H_5N 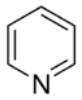	77
Argon	≥99.998%	Ar	39,95
Ethanol	≥ 99.5 A.C.S Reagent	C_2H_5OH	46,069

2.3. Polymerization Cabinet

The polymerization cabinet (Figure 1) designed in such a way that the fabrics are placed horizontally, so that the applied solution does not drain from the fabric surface that may cause unevenness. Inside there is a unit with needle frames to accommodate the samples whose height can be adjusted. In order to heat the cabinet to the desired degree, the heating plate is centred under the sample frame, a fan is placed inside to keep the temperature homogeneous, and the temperature is kept constant by thermostat control. A digital display is attached to the device that allows reading the target temperature and the instantaneous temperature. There is an inlet valve at the bottom of the cabin for feeding argon gas and an air outlet valve at the top for air evacuation. Since the cabin requires air evacuation, it is placed inside the fume hood. All experiments made at Uludağ University Textile Engineering Laboratory.

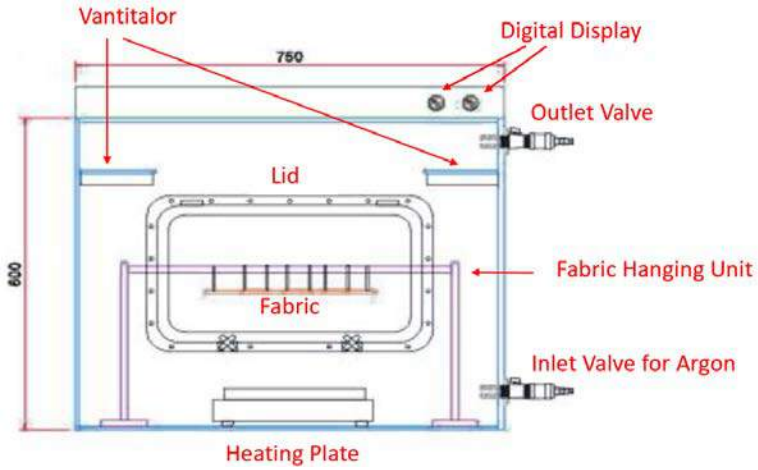

Figure 1. Polymerization cabinet

2.4. Applied Tests

The Surface Electrical Resistance of the sample fabrics before polymerization was measured in Mesdan brand Static Lab device in accordance with the EN 1149-1 test standard, since resistance value was out of the measuring range of the 4-Point Probe Conductivity Measuring Device. After polymerization and ethanol washing, the electrical resistance values were examined in 4-Point Probe Conductivity Measuring Device.

SEM images of the fabrics (Figure 2) before polymerization and after polymerization were taken using the ZEISS EVO 40 device to evaluate the evenness of the polymerization.

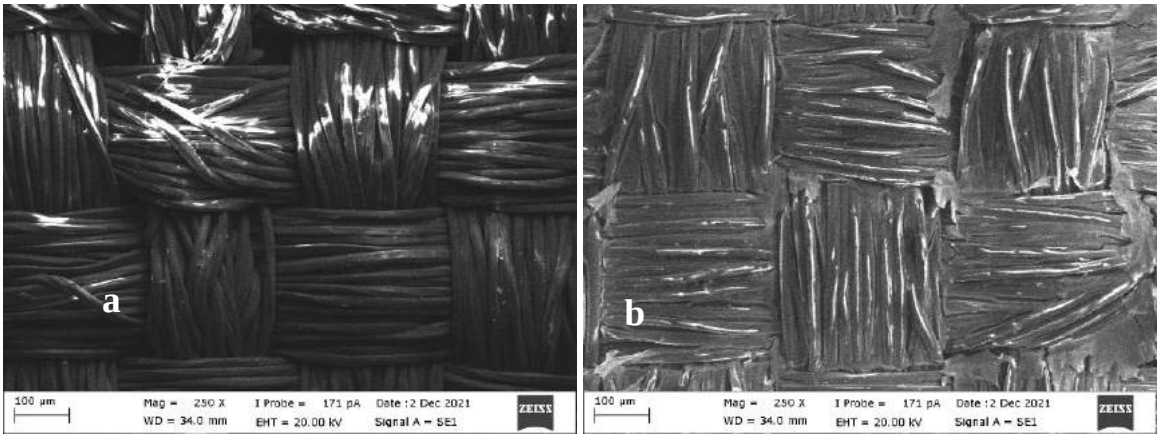

Figure 2. SEM pictures of samples a) Raw fabric b) After vapour phase polymerization

3. RESULTS AND DISCUSSION

Optimization is carried out with plain woven fabrics with 48 filaments. 50^0C was found to be the optimum temperature for the polymerization in our earlier studies. The effect of duration time of the samples in the cabinet before the polymerization temperature reached and the effect of distance between the sample and the heating plate were evaluated. The electrical resistance values were measured after polymerization indicated as PLM, and after the ethanol washing indicated as YKM.

It has been observed that the lowest resistance value for both the front and back of the fabric is obtained when the samples were placed into cabin after it is heated to 50^0C and when the samples are in the lowest position to heating plate (Figure 3)

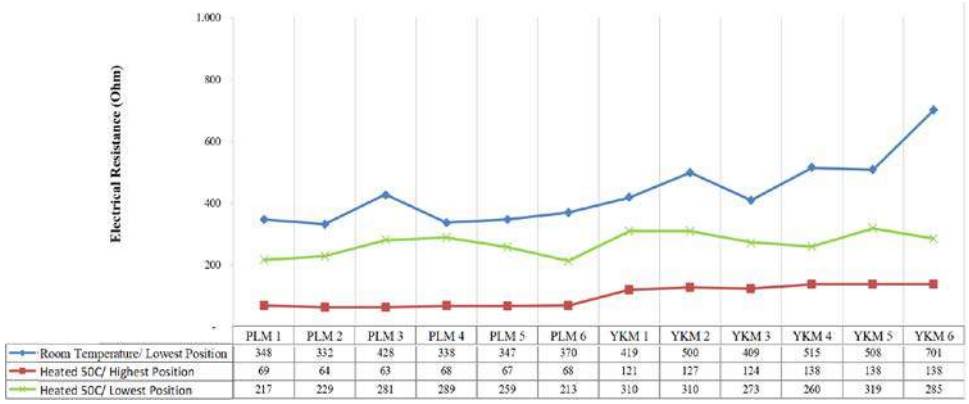

	PLM 1	PLM 2	PLM 3	PLM 4	PLM 5	PLM 6	YKM 1	YKM 2	YKM 3	YKM 4	YKM 5	YKM 6
Room Temperature/ Lowest Position	348	332	428	338	347	370	419	500	409	515	508	701
Heated 50C/ Highest Position	69	64	63	68	67	68	121	127	124	138	138	138
Heated 50C/ Lowest Position	217	229	281	289	259	213	310	310	273	260	319	285

Figure 3. Cabinet optimization measurements

While applying the dopant solution, the weft faces of all fabrics were considered as the front surfaces and the electrical resistance values after polymerization and washing were measured from both the front surface and the back surface to evaluate the effect (Figure 4)

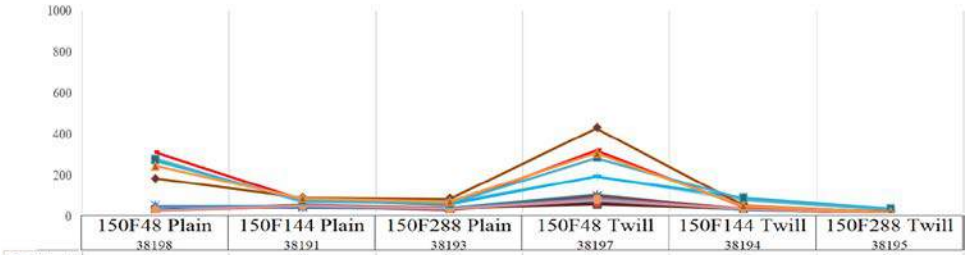

	150F48 Plain 38198	150F144 Plain 38191	150F288 Plain 38193	150F48 Twill 38197	150F144 Twill 38194	150F288 Twill 38195
Front1	48	44	38	70	36	24
Back1	32	56	41	60	40	18
Front2	50	50	41	105	33	19
Back2	28	52	34	100	40	12
Front3	49	47	40	88	35	22
Back3	30	54	38	80	40	15
Front4	285	70	68	196	80	33
Back4	311	82	58	323	48	23
Front5	271	83	60	195	91	40
Back5	185	92	85	429	55	20
Front6	278	77	64	286	86	37
Back6	248	87	72	308	52	22

Figure 4. Electrical resistance of front and back sides of all types of fabrics

Fabrics were stored closed 90 days in plastic bags and it was observed that the resistance values increased but still less than 10^3 Ohm (Figure 5)

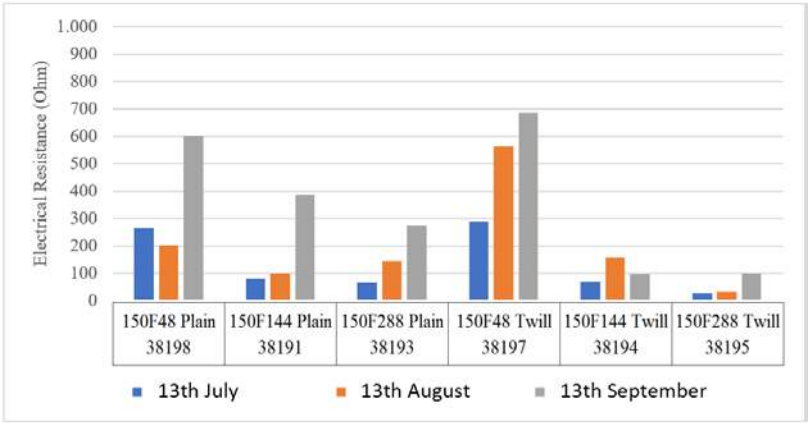

Figure 5. The electrical resistance of the stored fabrics in plastic bag

4. CONCLUSION

In the study, it was determined that the resistance values of 3/1 twill samples were lower than the plain samples. When the effect of filament number is examined, 288 filament yarns give lower resistance values. The structure of the twill weave and the large surface area of the microfilaments, has enabled a better penetration of the solution and increased the conducting performance.

The fact that the coated 3/1 twill samples with 150f288 filament yarns allow for bidirectional use and show electrical resistance below 50 Ohm and that there is no significant change in performance at the end of 90 days supports the idea that they can be converted into industrial production in the next stage.

ACKNOWLEDGMENT

The authors would like to express their gratitude to Küçükçalık Tekstil for the support to this research.

REFERENCES

Elschner, A., Kirchmeyer, S., Lovenich, W., Merker, U., ve Reuter, K. (2010). The discovery and development of conducting polymers. In *PEDOT: Principles and Application of an Intrinsically Conducting Polymer* (s. 1–20). Boca Raton: Taylor and Francis Group, LLC.

Qu, H., ve Skorobogatiy, M. (2015). Conductive polymer yarns for electronic textiles. In *Electronic Textiles* (s. 21–53). Elsevier. https://doi.org/10.1016/B978-0-08-100201-8.00003-5

Schwarz-Pfeiffer, A., ve Van Langenhove, L. (2013). Types and processing of electro-conductive and semiconducting materials for smart textiles. In *Multidisciplinary Know-How for Smart-Textiles Developers*. Woodhead Publishing Limited. https://doi.org/10.1533/9780857093530.1.29

Truong, T. Le, Kim, D. O., Lee, Y., Lee, T. W., Park, J. J., Pu, L., ve Nam, J. Do. (2008). Surface smoothness and conductivity control of vapor-phase polymerized poly(3,4-ethylenedioxythiophene) thin coating for flexible optoelectronic applications. *Thin Solid Films*, *516*(18), 6020–6027. https://doi.org/10.1016/j.tsf.2007.10.114

THERMOCHROMIC MICROCAPSULE APPLICATION IN POLYESTER DYEING PROCESS

Saadet MIHÇI[1], Sennur ALAY AKSOY[2]

[1] Başyazıcıoğlu Tekstil San. ve Tic. A.Ş., Kayseri, Türkiye
[2]Süleyman Demirel University, Department of Textile Engineering, Isparta, Türkiye

Corresponding author: mihci.saadet@gmail.com.tr

Abstract: *In this study, it was aimed to apply microcapsule containing thermochromic system (TS) to 100% polyester knitwear twisted yarns in the bobbin dyeing process. For this aim, thermochromic system containing 1-tetradecanol as solvent, 2´-(Dibenzylamino)-6´-(diethylamino) as color former and phenolphthalein as color developer was prepared and microcapsulated in poly(methyl methacrylate-co-glycidyl methacrylate) wall by emulsion polymerization method. The morphology of the microcapsule was analyzed by SEM. Heat storage capacity and temperatures were determined with DSC and thermal resistance were determined with TGA. Produced microcapsules were exhausted to cationized polyester yarn during bobbin dyeing process. The presence and homogeneous distribution of microcapsules in the structures of dyed and simultaneously microcapsule-appied yarns were confirmed by SEM images. According to the spectrophotometer color measurement results of thermochromic microcapsule applied yarns, the average L value increased from 74.35 to 87.92 when the temperature increased from 25ºC to 50ºC indicating the color of the yarns lighten with the increase in temperature.*

Keywords: *Thermochromic microcapsules, polyester, bobbin dyeing, poly(methyl methacrylate-co-glycidyl methacrylate).*

1. INTRODUCTION

Chromic materials respond to the stimuli by showing reversible changes in their colors. They are classified as thermochromic, photochromic, etc. according to temperature, light, etc. stimulus. The two types of thermochromic materials arisen in the production of color sensing smart textile structures are ternary systems and liquid crystals. Ternary systems change reversibly their color in a solid-liquid phase changing solvent medium. Color change occurs with the interaction of a color former (generally a leuco dye) with a color developer in a solvent (Bourque, 2014). pH sensitive dyes are often referred to as leuco dyes or color formers (Crano and Guglielmetti, 2002). Color formers used in organic thermochromic systems are N-acyl lycomethylene blue derivatives, fluoran dyes, diarylphthalide compounds, diphenylmethane compounds or spiropyran compounds. The most commonly used are crystal violet lactone analogs (diarylphthalide compounds) and fluoran dyes (Crano and Guglielmetti, 2002; İbrahim, 2012).

These compounds are colorless when they are in closed ring form, they become colored when the ring structure is opened. The opening of the ring structure of the color former in pH sensitive dyes is achieved by structural modifications in the presence of hydrogen ions (acids) or hydroxyl ions (bases). Acidic or basic color developer are used to create the colored form of the dye in thermochromic systems. For example, the open ring structure can be achieved by protonation (creation of conjugate acid by adding H+) using a weakly acidic developer such as a phenolic compound (İbrahim, 2012; Bourque, 2014). The ring opening of the colorless lactone as a result of protonation with a weak acid developer gives the colored form. While it is possible to use many components as color developer, especially phenols have come to the fore, and the most important commercial phenol compound is Bisphenol A. Because it creates high contrast changes and bright colors. In thermochromic systems,

organic hydrophobic solvents are used to create a medium for the interaction of color former and color developer and to enable reversible color change. Alcohols, hydrocarbons, esters, ethers, ketones, fatty acids, amides, acid amides, thiols, sulfides and disulfides are generally used as solvents. Generally, aliphatic solvents are preferred as solvents because of their high efficiency at low concentration. The solid-liquid phases of the solvent determine the interaction of the color former with the color developer. While the solvent, in which the color former and color developer are dissolved in, is solid state, the color former and color developer interact and the thermochromic system becomes colored. However, when the solvent melts, the interaction between the color former and developer ceases and the system becomes colorless. The melting temperature of the solvent determines color change temperature of the system (Crano and Guglielmetti, 2002; İbrahim, 2012; Bourque, 2014).

Ternary systems should be encapsulated in a non-permeable shell before application to textiles in order to prevent leakage of the liquid system. When current research and industrial applications are examined, it is seen that microcapsules are generally applied to fabrics by the impregnation method due to its high application efficiency. Microcapsule application to textile structures by exhaustion method has been investigated in limited numbers (Monllor et al., 2007; Aydın vd., 2011; Bonet et al., 2012; Bonet et al, 2015; Öner et al., 2019; Tözüm et al., 2021; Tözüm et al., 2021; Tözüm et al., 2022). In the studies on the application of microcapsules to fabrics by exhaustion method, it has been revealed that it is possible to apply microcapsules with different contents to yarn or fabrics by exhaustion method, but for this, it is necessary to prepare microcapsule wall structure having affinity to the fiber molecules. On the other hand, it is stated that the application of thermochromic microcapsules by exhaustion method would be more beneficial since both the fibrous structure and the liquor are mobile, in order to distribute the microcapsules on the fibrous structure homogeneously to give a homogeneous color effect to the structure. An important point to be emphasized is that the binder materials used to ensure the permanent bonding of microcapsules to the fibers in the application by the impregnation method adversely affect the properties of the fabrics such as handle and permeability.

In this study, prepared thermochromic microcapsules were applied to polyester yarn by exhaustion process during bobbin dyeing. In this study, microcapsules were able to applied to the polyester yarn by exhaustion method because of their reactive shell having affinity to cationic polyester fibers. In the study, the morphologies, chemical structures, thermal properties, as well as thermochromic performance of the produced microcapsules were characterized. Furthermore, morphology, color changing, color fastness and yarn quality properties of the microcapsule applied yarn were investigated.

2. MATERIALS AND METHODS

2.1. Preparation and Characterization of Microcapsules

To prepare thermochromic system, 2’-(Dibenzylamino)-6’-(diethylamino) (green) dyestuff as color former, phenolphthalein (FF) (Carlo Erba) as color developer and 1-tetradecanol (TD, Alfa Aesar, 97%) as solvent were used. In the production of microcapsules, methyl methacrylate (MMA, Sigma Aldrich, 99%) and glycidyl methacrylate (EGDM, Sigma Aldrich, 97%) 98% were used as cross-linker, 2,2’azobis(2-methylpropionamidine) dihydrochloride (Aldrich, 97%) was used as initiator and polyethylene glycol 1000 (PEG1000) was used as emulsifier. A UV light absorber (2,4-Dihydroxybenzophenone was also added to the system in order to improve the resistance of the paint to UV light.

The core/wall material ratio was used as 1:0.5. Production stages:

- 100 mL of deionized water was heated to 50ºC, 6,5 g of three component TS and 2 g of PEG1000 were added, and an oil in water emulsion was formed by mixing at 2000-3000 rpm for half an hour.
- A 3.25 g of monomer (MMA and 10% of its GMA mixture), 1.35 g of EGDM crosslinker and 1 g of initiator were added to the prepared emulsion. The temperature was increased to 80ºC, the mixing speed was adjusted to 1000-2000 rpm and stirring was continued for about three hours. At the end of this period, the microcapsules produced were washed several times with hot water around 70ºC, rinsed, filtered and stored in the refrigerator (Özkayalar et al., 2020).

The morphology of the microcapsules was analyzed by SEM, and their chemical structures were analyzed by FT-IR spectroscopy. Heat storage capacity and temperatures were determined with DSC, and thermal resistance were determined with TGA (Mıhçı, 2022).

2.2. Polyester Yarn Pre-treatment, Dyeing and Characterization

100 % polyester yarns were pretreated for 30 minutes at 60 °C in a bath containing polyester acid and dispersant before dyeing. Subsequently, cationization was carried out at using cationize agent concentration of 20 g/L at 90 °C during 40 minutes. The dyeing process on polyester yarns and the application of thermochromic microcapsules were carried out with bobbin dyeing processes. After the bobbins pretreated were washed two times, dyeing process was started at 60°C by heating with a slow temperature rise to 90°C. When required amount of dispersing was added, the temperature was raised to boil and dyeing was continued 30 min. After the dyeing process, the bobbins were washed 2 times and then subjected to the squeezing process. The dyed bobbins were kept at room temperature for 3 hours in the laboratory environment and then dried in a drying machine (T 608 SF Fast & Easy Drying) at 60°C for 20 minutes. Microcapsule application was carried out by adding microcapsules at 8 g/l concentration and 1 g/L binder (CHT acrylic binder) to the dye bath instead of dyestuff.

2.3. Analysis of Microcapsule Applied Yarns,

The morphology of the yarn was analyzed by SEM. In addition, washing, water, perspiration and rubbing color fastness of the yarns and the yarn strength and unevenness properties were tested according to the related standard. The color values of the yarn at room temperature and heated 50 °C was measured by spectrophotometer.

In this study, the strength tests of the yarns used were carried out with the Uster Tensorapid 5 yarn strength tester. The speed of the measuring device was used as 5000 mm/min. Ten tests for each yarn were carried out according to the TS EN ISO 2062 test standard. As a result of the test, the breaking strength (cN/tex) and elongation at break (%) values were taken. Evenness tests of the yarns were carried out on the Uster Tester 6 yarn unevenness test device. The test speed of the device was set as 800 m/min. Three tests were carried out for each yarn test, and the tests were carried out in accordance with ASTM 1425 test standards. As a result of the unevenness test, unevenness (% CVm), thin place (-40%), thick place (+50%), neps (+200%) and hairiness (H) results were obtained.

The washing fastness test of the dyed yarns produced in the study was carried out according to ISO 105 C01-C02-C03-C04-C05 standards. Color change was evaluated with gray scale. The sweat fastness test was carried out according to the ISO 105 E04 standard. Acidic and basic test solution was prepared for the experiment. The water fastness test is based on measuring whether the colors of dyed yarns kept in cold water for a short or long time are resistant to water. This test is according to ISO 105-E01 2013 standard.

3. RESULTS AND DISCUSSION

In Figure 1, photographs taken below and above the melting temperature of the solvent (1-tecradecanol) and SEM images are given. Microcapsules, which are dark green in color when heated to a temperature above the melting temperature of the solvent (approximately 50 °C), turn gray when cooled to room temperature. According to the SEM image, it is seen that microcapsules with homogeneous particle sizes and spherical morphology were obtained. According to the size scale on the SEM images, it was determined that the capsules had nano dimensions and their sizes ranged from approximately 150 nm to 400 nm.

Figure 1. Photos (cold and heated) and SEM image of microcapsules

According to the results of the DSC analysis (Figure 2), the TS contained in the microcapsules stored 41.54 j/g of latent heat energy during melting at 28.6 °C, and emitted a total of 39.32 j/g of heat at 26.2 °C during solidification. According to the TG analysis (Figure 2), the microcapsules exhibited two-stage thermal degradation behavior. The initial degradation ended with a mass loss of 82%. This mass loss was due to the thermal breakdown of the thermoch :e material due to the temperature increase and its evaporat :d in a mass loss of 13%.

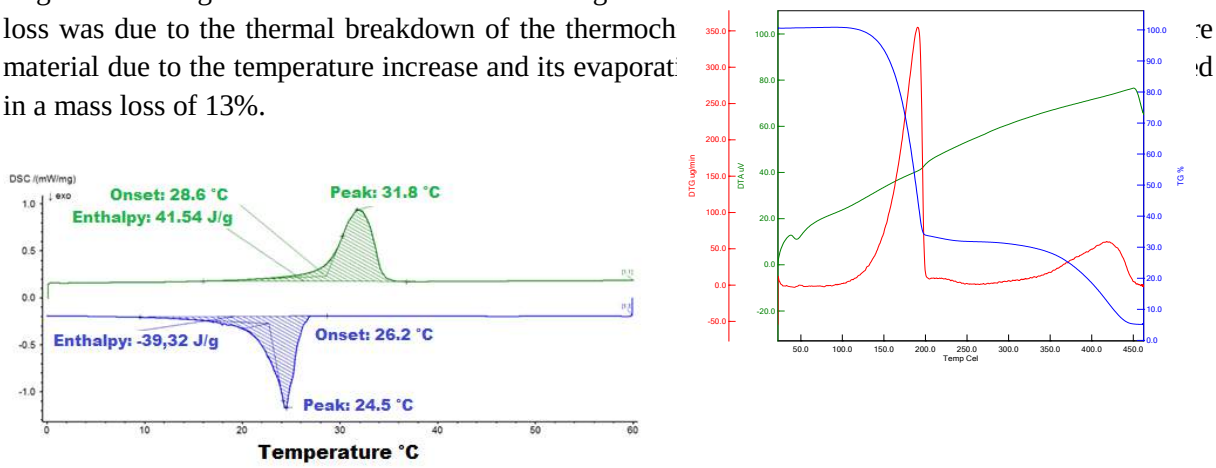

Figure 2. DSC and TGA curves of the microcapsules

In Figure 3, SEM image of polyester yarn sample applied with thermochromic microcapsule by bobbin dyeing process was given. According to the image, there was a dense microcapsule presence in the yarn structure and they exhibited a homogeneous distribution.

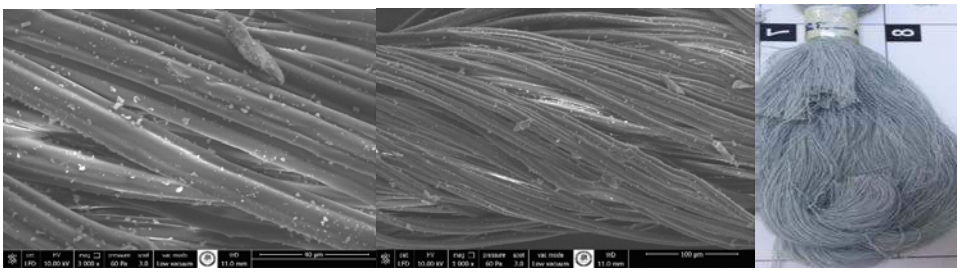

Figure 3. Yarn images and photo SEM

According to the spectrophotometer color measurement results of thermochromic microcapsule applied yarns, the average L value increased from 74.35 to 87.92 when the temperature increased from 25 °C to 50 °C. This increase shows that the color of the yarns lightens with the increase in temperature. The results of the perspiration, washing and watercolor fastness tests of the yarns were given in Table 1. Dry and wet rubbing fastness values were determined as 5 and 4/3, respectively.

Table 1. Yarn color fastness test results

PES yarn	**Fading**	**Staining**					
		Acetate	Cotton	Nylon	Polyester	Acrylic	Wool
Washing	5	5	4/5	5	5	5	5
Perspiration (acidic)	5	5	4/5	5	5	5	5
Perspiration (basic)	5	5	5	5	5	5	5
Water	5	5	5	5	5	5	5

The strength value of the yarn after microcapsule application decreased from 30.44 RKM to 27.5 RKM compared to the raw yarn, and the elongation at break decreased from 12.51% to 11.3%. According to the yarn unevenness measurement results, it was determined that there was no significant difference in the unevenness, thin place (-40), thick place (+50) and neps (+200) values of the microencapsulated yarns compared to untreated yarn results.

4. CONCLUSION

In the study, nano-sized, spherical morphology TS capsules with 41.54 j/g latent heat storage property were produced. They were exhausted to cationized polyester yarn by bobbin dyeing process. T he presence and homogeneous distribution of microcapsules in the structures of the yarns were confirmed by SEM images. The yarns exhibited thermochromic function depending on change in temperature. Their L values measured by spectrophotometer increased from 74.35 to 87.92 when the temperature increased from 25 °C to 50 °C. As a result, in the study, TS microcapsule application to the yarns was successfully carried out with the bobbin dyeing process.

ACKNOWLEDGMENT

The authors would like to thank Süleyman Demirel University Scientific Research Projects Coordination Unit (BAP) for financial support of this study with the project number FYL-2020-7974. Additionally, the authors would like to express their gratitude to BAŞYAZICIOĞLU TEKSTİL SAN.TİC.&A.Ş for experimental study opportunity.

REFERENCES

Bourque, A.N. (2014). Investigations of reversible thermochromism in three-component systems", PhD thesis, Dalhousie University, Halifax, Nova Scotia.

Crano, J.C., Guglielmetti, R.J. (2002). Organic photochromic and thermochromic compounds volume 2: physicochemical studies. Biological Applications, and Thermochromism, USA: Kluwer Academic Publishers.

İbrahim, W. (2012). An investigation into textile applications of thermochromic pigments, PhD thesis, Heriot-Watt University, UK.

Aydın, N., Öztürk, G., Karaboyacı, M., Alay, S. (2011). Characterization of fragrant microcapsules incorporated fabrics knitted from acrylic hand knitted yarns, *SDÜ Fen Bilimleri Enstitüsü Dergisi*, 15(1), 67-74.

Bonet, M. Á., Capablanca, L., Monllor, P., Díaz, P., & Montava, I. (2012). Studying bath exhaustion as a method to apply microcapsules on fabrics. *Journal of the Textile Institute*, 103(6), 629-635.

Bonet Aracil, M., Monllor, P., Capablanca, L., Gisbert, J., Díaz, P., & Montava, I. (2015). A comparison between padding and bath exhaustion to apply microcapsules onto cotton. *Cellulose*, 22(3), 2117-2127.

Öner, E., Saraç, E., Kahraman, M. (2019). A study on developing thermo-regulating denıım fabric by integrating of microencapsulated phase change material using exhaustion method. *Annals of The University of Oradea, Fascicle of Textiles-Leatherwork*, 20(1).

Tözüm, M.S., Alay-Aksoy, S., ve Alkan, C. (2021). Manufacturing surface active shell and bisphenol A free thermochromic acrylic microcapsules for textile applications, *International Journal of Energy Resear*ch, 45:7018–7037.

Tözüm, M. S., Alay Aksoy, S., & Alkan, C. (2021). Development of reversibly color changing textile materials by applying some thermochromic microcapsules containing different color developers. *The Journal of The Textile Institute*, 1-10, DOI: 10.1080/00405000.2021.1972645.

Tözüm, M. S., Alkan, C., & Aksoy, S. A. (2022). Developing of thermal energy storing visual textile temperature indicators based on reversible color change. *Journal of Industrial Textiles*, 51(2_suppl), 1964S-1988S.

Özkayalar, S., Adıgüzel, E., Aksoy, S. A., & Alkan, C. (2020). Reversible color-changing and thermal-energy storing nanocapsules of three-component thermochromic dyes. *Materials Chemistry and Physics*, 252, 123162.

Mıhçı, S. (2022). An investigation on developing microcapsule application processes in the yarn dyeing process, Süleyman Demirel University, Graduate School of Natural and Applied Sciences, M.Sc. Thesis, Isparta, Turkey.

THE EFFECTS OF USING NONWOVEN STRUCTURES IN AUTOMOTIVE SEAT COVER ON RESILIENCE PROPERTIES

Semih OYLAR, Osman AYDIN, Diren MECİT, Nur Ceyda UYANIKTIR
Martur Fompak International/ Textile R&D Department

Corresponding author: ceyda.uyaniktir@marturfompak.com

Abstract: *Automotive seat cover fabrics are traditionally produced by 3 main components. Face fabric as the upper layer, scrim fabric as the backing layer and polyurethane foam as the middle layer creates this 3 structured composite material which are laminated by flame lamination method. PET fibres which meet automotive requirements such as high strength, heat aging, light fastness etc. are generally used in the production of face fabric and scrim fabric. The use of polyurethane foam has many purposes, but the most important purpose is the feeling of comfort gained by its resilience property. By the latest developments of nonwoven industry, added properties in non-woven products allows to be used as lamination material instead of PU foam. In parallel, environmental concerns in automotive industry is increasing day by day. In order to create recyclable mono-polymer composites, the usage of 100% PET based non-woven structures as lamination material starts to take place for automotive seat cover fabrics. In this study, different kind of nonwoven structures which are able to be used as lamination material on back side of automotive seat cover fabrics were evaluated in terms of their resilience properties. These properties were compared with PU lamination foam.*

Keywords: *Automotive seat covers, mono-polymer, recycling, polyurethane foam, nonwoven*

1. INTRODUCTION

An average of 20 kg of textile material is used in the automotive interiors. Approximately 3.5 kg of 20 kg consists of seat cover fabrics which are 3 structured composite material. Since the textile industry is constantly developing, this ratio is also increasing (Fung and Hardcastle 2001). During the production of this material, high amount of carbon emission occurs. Waste accumulation is created in the environment when their lifetime ends. Therefore, it has become important to improve the recyclability of seat cover fabrics. In order to gain more recyclability options, polyurethane lamination foams can be replaced with nonwoven structures (Sunhilde 2017).

Nonwoven surfaces are the structures produced by combining fibres with physical, chemical or thermal processes (Çelikkanat 2002). Nonwoven surfaces can be formed in many structures according to the bonding methods. Needlepunched, malivilies, kunit and multiknit nonwoven structures are commonly used in automotive industry. Needle punched nonwoven structures are based on a method of bonding the web form by needling the fibres. Malivilies, kunit and multiknit structures are based on a method of stitching the web form by simulating warp knit process. Nonwoven production technologies are constantly developing; thus, these structures are becoming more feasible to replace PU foam as lamination material. (Russell 2007).

In the production of automotive seat cover fabrics, regarding car producer's requests, PU foam which has 3-5 mm thickness is used in fabric structure as lamination material. By the flame lamination technique, the foam is melted by applying flame and the face fabric, foam and scrim are bonded to each other by melting process (Oylar, Mecit et al. 2021). During flame lamination process, approximately 1mm of the lamination foam is burned and melted, heavy smoke and toxic fumes such as hydrogen chloride and/or cyanides are occurred (Smith 2001). Today, with the development of

nonwoven fabric production technologies, nonwoven structures can be produced in thickness and weight that can be competitive with PU foam (Chen 2010).

The suitable method for laminating face fabric and nonwoven structures is the hot-melt technique. By using this lamination technique, toxic fumes caused by the flame lamination process is eliminated and by using PET-based adhesives and 100% PES recyclable automotive seat cover constructions can be produced. While these environmental advantages are achieved by using hot-melt lamination technic and non-woven material usage, nonwoven materials should be compatible in terms of resilience properties which is related to comport expected from traditional seat cover fabrics. (Oylar 2021). In this study, the impact elasticity test and the compression set after heat tests were performed on multiknit, kunit and needlepunch nonwoven structures and the traditional lamination foam. According to the test results, the resilience properties of 3 different nonwoven fabrics relative to each other and to PU foam were compared.

2. MATERIALS AND METHODS

2.1. Materials

Three different 100% recycled PES based nonwoven structures kunit, multi-knit and needle punch were supplied from nonwoven manufacturers which serve to the automotive industry. Nonwoven materials supplied from outsource companies have been selected with recycled content with considering environmental concerns. To compare non-woven structures, PU lamination foam which is produced in Martur Sünger ve Koltuk Tesisleri A.Ş.is used.

Figure 1. Multiknit nonwoven fabric, kunit nonwoven fabric, needle-punched nonwoven fabric and PU lamination foam

2.2. Physical Properties of the Materials

The materials to be performed test were preferred with similar thicknesses in order to make an accurate comparison. The thickness and weight information of each material is given in the table below.

Table 1. Mass, density, and thickness information of the used materials

Materials	**Mass** (g/m²) / **Density** (g/dm³)	**Thickness** (mm)
Multi-knit nonwoven	185 g/m²	3 mm
Kunit nonwoven	200 g/m²	3.2 mm
Needlepunched nonwoven	400 g/m²	3 mm
Traditional Lamination Foam	30 g/dm³	3,5 mm

2.3. Method

In order to determine the resilience properties of four different materials, the impact elasticity test and the compression set after heat tests were performed according to the TSM 7100G specification. Each test was performed five times and average values were calculated.

2.3.1. Impact Elasticity Test

The foam test specimen is prepared in 100*100 mm width and length dimensions and 50mm thickness. That specimen preparation is possible for block foam to take as one piece. Due to the final product thickness of nonwoven which was used within this study is much less that 50mm, each non-woven layer located over each other to reach 50 mm thickness. The test specimen is compressed 10 times with the palm of the hand to a depth of approximately 75% the thickness of the test specimen. A steel ball is dropped on the test specimen from a height of 460 mm by gravity. The maximum vertical height of steel ball's rebound is measured. The impact resistance is determined by the equation.

2.3.2. Compression Set After Heat Test

The foam test specimen is prepared in 50*50 mm dimensions and 30 mm thickness. That specimen preparation is possible for block foam to take as one piece. Due to the final product thickness of non-woven which was used within this study is much less that 30mm, each non-woven layer located over each other to reach 30 mm thickness. The test specimen is compressed 10 times with the palm of the hand to a depth of approximately 75% the thickness of the test specimen. The thickness of the sample is then measured. As the second part of the test, using two parallel compression plates made of metal, the test specimen is compressed to 50% of its thickness. The sample is kept in this state and heated in a controlled thermostatic chamber at 70°C ± 2°C for 22 hours continuously. The sample is then removed from the thermostatic chamber and on the compression plates. After the test sample is left in a certain environment for 30 minutes, residual thickness is measured. Compression set value is determined with the help of equations.

3. RESULTS AND DISCUSSION

According to impact elasticity test results, the values show that except needle punch product non-woven surfaces meet the requirement.

According to the compression set after heat test results, nonwoven structures could not give results in the required range. As results shown in table 2. the most durable structure against compression is traditional PU lamination foam. Kunit and multiknit structures were shown similar behaviour when needle punch structure is more durable than these two structures.

Table 2. Resilience Test Results of the Materials

Performed Resilience Tests	Required Range of Values	Multi-knit Nonwoven	Kunit Nonwoven	Needle punched Nonwoven	Traditional Lamination Foam
Impact Elasticity	min. 20%	35,40%	30,60%	2,08%	22,43%
		33,30%	32,50%	2,12%	26,05%
		32,10%	25,75%	1,90%	25,12%
		31,00%	26,20%	2,01%	22,88%
		33,18%	31,44%	1,91%	28,54%
	Average value	**33,00%**	**29,30%**	**2,00%**	**25,00%**
	%CV	1,63%	3,11%	0,10%	2,49%
Compression Set After Heat	max. 15%	36,04%	37,95%	30,04%	7,10%
		37,12%	38,90%	30,12%	10,50%
		39,90%	34,90%	31,90%	10,40%
		29,90%	28,80%	27,01%	8,20%
		39,96%	39,90%	32,86%	8,80%
	Average value	**36,58%**	**36,09%**	**30,39%**	**9,00%**
	%CV	4,11%	4,48%	2,24%	1,46%

4. CONCLUSION

Within the scope of this study, the resilience properties of nonwoven structures, which are able to be an alternative to polyurethane foam used in automotive seat covers as lamination surface, were compared with polyurethane lamination foam. When the results are evaluated, the resilience properties of nonwoven structures do not meet the required values. Compared to other nonwoven structures, the most promising structure is multi-knit.

Within the scope of that study, non-woven materials which are commonly used in industry are not competitive when compression set after heat test results are observed. That disadvantage shows that even the multi-knit and kunit structures meets the impact resiliency requirements, they will lose their thickness during long lasting usage.

REFERENCES

Aksoy, S. , Işılak, C. , Ertürk, S. , Oylar, S. & Mecit, D. (2021). Investigating the Effect of Fabric and Lamination-Foam Properties on the Air Permeability of Laminated Headrest Fabrics . *Textile and Apparel* , 31 (4) , 235-241 . DOI: 10.32710/tekstilvekonfeksiyon.812489

Çelikkanat, A.B. (2003). Teknik Tekstiller (Yüksek lisans tezi). İTÜ, Tekstil Mühendisliği Ana Bilim Dalı, İstanbul.

Fung, W., Hardcastle, M. (2001). *Textiles in Automotive Engineering*. Woodhead Publishing Limited, Cambridge, England

https://www.textileworld.com/textile-world/textile-news/2001/01/laminate-faster-more-competitive/

J.Y. Chen (2010). In Applications of Nonwovens in Technical Textiles

Oylar, S. (2021) Tamamen Geri Dönüştürülebilir Otomotiv Koltuk kılıfı Tasarımı ve Geliştirilmesi (Yüksek lisans tezi), Uludağ Üniversitesi, Tekstil Mühendisliği Ana Bilim Dalı, Bursa.

Sunhilde, C. (2017). Recycled textiles used in automotive interiors. Case study-Ford Motor Company. Annals of the University of Oradea: Fascicle of Textiles, Leatherwork, vol XVIII(2):171–176.
S.J. Russell (2007). *Handbook of nonwovens*. A volume in Woodhead Publishing Series in Textiles

PREPARATION AND CHARACTERIZATION of ELECTROSPUN SURFACES FROM PHB AND ITS BLENDS (PHB/PBS, PHB/PHBV)

Hatice Aybige AKDAĞ ÖZKAN[1], Aslı HOCKENBERGER[2]

[1] Bursa Uludag University Graduate School of Natural and App. Science, Bursa, Türkiye
[2] Bursa Uludag University, Department of Textile Engineering, Bursa, Türkiye

Corresponding author: aybigeakdag@uludag.edu.tr

Abstract: *PHB (Polyhydroxy Butyrate) and its blends, PHB/PBS (Polybutylene Succinate), PHB/PHBV (Polyhydroxybtyrate-co-valerate) electrospinning surfaces were studied to produce new biodegradable products and enhance physical properties of P3HB. Morphological properties such as fiber diameter, uniformity, beadings were investigated with SEM. Miscibility, thermal behaviors and crystallinity of blends were characterised with DSC.*

Keywords: *Biopolymers, PHB, electrospinning. Nonwovens, textiles.*

1. INTRODUCTION

It is necessary to use the right renewable resources to reduce the environmental waste load, minimize the consumption of fossil resources and reduce the greenhouse effect (Nova Institute, 2020). At this point, it is important to choose which renewable resources are, their life cycles and their usage areas as final products. Biopolymers, whose raw materials are obtained from nature and can degrade without leaving toxic residues by microorganisms in environments containing water, soil, and sunlight at the end of their useful life, are the best alternatives to replace petroleum-based conventional polymers, especially in disposable products (Nova Institute, 2021). Polyhydroxyalkanoates are biopolymers that are polyesters of hydroxyalkanoic acids and are synthesized and stored in the cell by most bacteria under growth conditions where growth factors such as nitrogen, phosphorus, oxygen, magnesium are limited but carbon source is abundant (Koller et al, 2013). Due to its linear chain structure and regulated crystal forms, it can be processed as fiber and nonwoven surface (Hufenus et al., 2015). However, the high crystallinity, smaller number of nuclei and brittleness of PHB limits its processability and usage areas (Correira et al., 2014). In some areas of use, it is also included in the literature to work with mixtures of PHA to improve thermal stability and improve mechanical properties. The elongation and processing window of PHBV can be improved by copolymer with the hydroxyvalerate (HV) groups. The presence of HV PHBV reduced crystallinity of PHB (Conti et al., 2004, Ublekov et al., 2017). PHB enhances PBS crystallinity, and at the same time, PBS improves mechanical properties of PHB (Arrieta et al., 2015, Ma et al., 2014).

In this study, PHB, PHB, PHB/PBS, PHB/PHBV fibers obtained by electrospinning method were produced and characterized.

2. MATERIALS AND METHODS

2.1. Preparation of solutions and production of samples

P(3HB) extrusion form Biomer (Germany) and PHBV (2% Valerate) will be supplied by Tianan Biologic (China). PLA and PBS, rPET and PET will be available from suitable suppliers. The polymers were vacuum dried at 60°C for 48 hours before use. PHB Solutions were prepared by mixing in 99.98% Sigma-Aldrich Chloroform at a speed of 500-1000 rpm in a heated mixer set at 60°C. Viscosity measurements of polymers were made according to ASTM D2857 standard using ubbelohde viscometer based on intrinsic viscosity. Surface tension, viscosity and electrical conductivity of the solutions will be measured.

The production of surfaces was carried out in the Nano Spinner brand NE300 model electrospinning mechanism in Uludag University Textile Engineering Laboratory. PHB and PHBV (%100), PHB/PHBV (90:10), PHB/PBS (90/10) blends were prepared by dissolving 7 wt% in a solvent of chloroform, stirred at 60°C, 1000 rpm during 2 hours. The applied voltage was -17, -17, -17,6 and 13,5 kV respectively with a fixed flow rate of 0,8 mL/h. Viscosity of solutions were measured 112-115 cP. The fibers were deposited on the collector spinner roller connected to the ground with velocity of 300 rpm. The distance between the nozzle and the collector was of 15 cm.

2.2. Surface Characterisation

Thickness measurements of the samples were investigated by Electronic Digital Micrometer, fibrous structure formation, fiber fineness and homogeneity across the cross-section by SEM imaging, and the flow rate of the air passing under pressure by air permeability test. The morphology of the produced surfaces was analyzed using Carl Zeiss Evo 40 model scanning electron microscope in Uludag University Faculty of Science with 20kV voltage and 500- and 2500-times magnification.

2.3 Thermal Characterization

The thermal properties of the surfaces with positive morphological analyzes (homogeneous distribution, non-adhesive fibrous surfaces) were determined by differential scanning calorimeter (DSC) Mettler Toledo Stare System DSC 823E under nitrogen atmosphere (30 cm3/min) from room temperature to 300°C at a rate of 10°C/min. in Korteks inc. The differences of the mixtures with respect to pure P3HB surfaces were interpreted through the changes in the melting peaks. The degree of crystallinity, Xc, is estimated from the area under the endotherm by the equation:

$$\%Xc: \left(\frac{\Delta Hf - \Delta Hc}{\Delta Hf}\right) \times 100$$

ΔHf is the variation of the melting enthalpy for PHB 100%crystalline (142Jg−1)

3. RESULTS AND DISCUSSION

3.1 Surface Characterisation

SEM micrographs of P(3HB), P(3HB-HV), PBS blends electrospun fibers in surface were shown in Figure 1. Well distributed surface with low pore network was observed. Blends created tighter, poreless surfaces. The fibers have smooth surfaces and relatively uniform fiber diameter distributions without any beads or spindle-like units. Additionally, the surfaces of fibers quite perfect and had not visible cracks and pores.

During electrospinning, polymer concentration and applied voltage are influential in fibers or beads are produced. Fiber average diameter was near to 400nm, while the fiber average diameter for P3HB, PHBV and P3HB/PHBV blend were in the range of 3-4 µm, 3-4 µm, 1.3-1.5 µm respectively, without beads formation, P3HB/PBS blend created 0.8-1.3 µm beaded fibers. Production of P3HB/PBS surface was carried out lower (-13,8 kV) voltage because of formation of multi jet at -17 kV. Higher voltages were needed to achieve a stable jet from PHB. So, from -17 to -20 kV voltages had been studied to gain a stable jet.

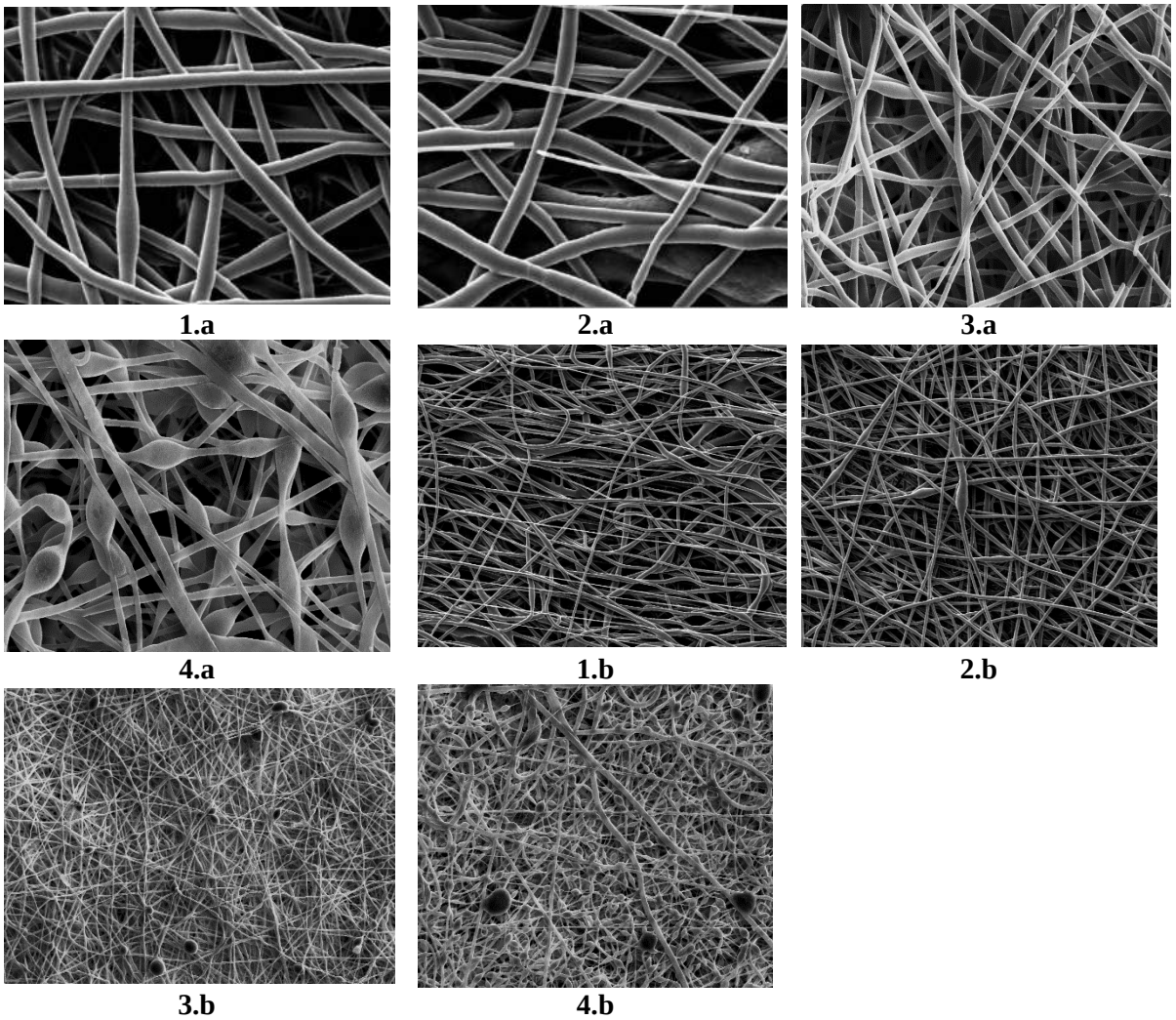

Figure 1. SEM images of electrospun surfaces 1) P(3HB) 2) P(3HB-HV) 3) P(3HB)/PBS 4) P(3HB)/ P(3HB-HV) a) ×2500 b) ×500

3.2 Thermal Characterization

PHB/PBS blend showed an additional melting peak before the main melting peak as shown in Fig.2. A melting peak of PHB was observed at 173°C and PBS melted at 112°C in blends. Multiple melting temperatures are observed due to phase separation, indicating that P(3HB) is immiscible with PBS. PBS is a type of ductile polyester but is not miscible with PHBV and PHB (Ma et al., 2012). Electrospun PHB presents a broad exothermic peak between 40 and 100°C corresponding with the cold crystallization of PHB. The pure PHB shows high crystallinity degree obtained by DSC normally but as seen at Fig. 3 PHB/PBS blend presented highest crystallinity degree. Broad exothermic peak often indicates that distribution of polymer crystallites perfectness. As we know that PHB has large, low density imperfect spherulites and crystallinity of PHBV is lower than P3HB due to presence hydroxyvalerate (HV) units in its molecular structure. However, both crystallinity ratio and the formation of the peak showed exact opposite in this study. Nevertheless, crystallization of polymer under varied processing conditions is a very complicated process and cannot to be described by any single-valued effect and this behaviour need to investigation with different process parameters, especially voltage and distance between nozzle and collector.

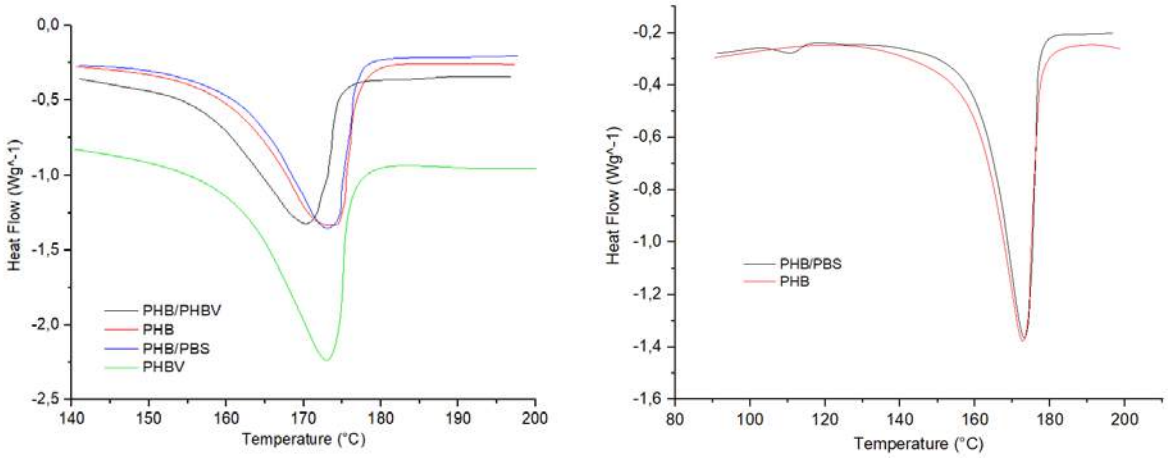

Figure 2. Melting thermogram of surfaces

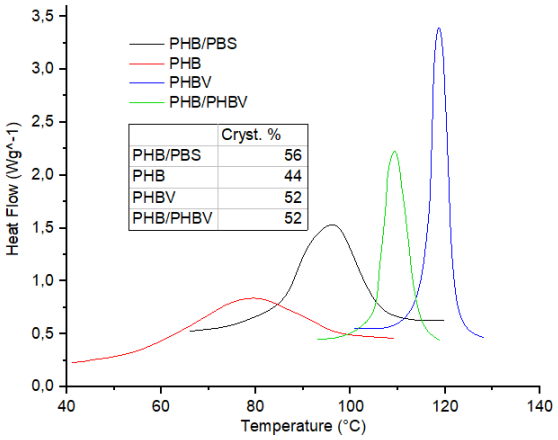

Figure 3. Crystallization behaviour of surfaces

4. CONCLUSION

Formation of surface of P3HB and its blends were studied by electrospinning method in this study. These surfaces will be investigated at usability of disposable mask filter. Productions of samples have been continued yet. Limited results showed us that although homogeneous nonwoven surfaces can be obtained from P3HB polymers, it has some disadvantages such as low thermal stability and hard brittleness. These properties can be improved by selecting suitable plasticizers or by mixing or blending with other natural polymers. Aim of further studies are obtain nonbeaded fibers surface with homogene pores and improving the tensile strength. The influence of the applied electric field and concentration of solution will be continued to study. Filter capacity of surfaces will be analysed later.

The most important point to consider when mixing biopolymers is to make the polymer modification by ensuring the compatibility of the fully biodegradable system, without compromising the rate of degradation, P3HB is biodegradable in nature without need any industrial degradation process so effect of each different product added on the degradation of PHB will be examined.

ACKNOWLEDGEMENT

This work is supported by Tübitak 118C040 and Uludağ University BAP unit FGA-2022-911 projects.

REFERENCES

Arrieta, M. P., López, J., López, D., Kenny, J. M., & Peponi, L. (2015). Development of flexible materials based on plasticized electrospun PLA–PHB blends: Structural, thermal, mechanical and disintegration properties. *European Polymer Journal*, 73, 433-446.

Carus, M., Dammer, L., Raschka, A., & Skoczinski, P. (2020). Renewable carbon: Key to a sustainable and future-oriented chemical and plastic industry: Definition, strategy, measures and potential. *Greenhouse Gases: Science and Technology*, 10(3), 488-505.

Conti, D. S., Yoshida, M. I., Pezzin, S. H., & Coelho, L. A. F. (2007). Phase behavior of poly (3-hydroxybutyrate)/poly (3-hydroxybutyrate-co-3-hydroxyvalerate) blends. *Fluid Phase Equilibria*, 261(1-2), 79-84.

Correia, D. M., Ribeiro, C., Ferreira, J. C., Botelho, G., Ribelles, J. L. G., Lanceros-Méndez, S., & Sencadas, V. (2014). Influence of electrospinning parameters on poly (hydroxybutyrate) electrospun membranes fiber size and distribution. *Polymer Engineering & Science*, 54(7), 1608-1617.

Global Markets and Trends of Bio-based Building Blocks and Polymers 2020 –2025 (2021). Nova-Institute

Hufenus, R., Reifler, F. A., Fernández-Ronco, M. P., Heuberger, M. (2015). Molecular orientation in melt-spun poly (3-hydroxybutyrate) fibers: Effect of additives, drawing and stress-annealing. *European Polymer Journal*, 71,12-26.

Koller, M., Salerno, A., Braunegg, G (2013). *Polyhydroxyalkanoates: Basics, Production and Applications of Microbial Biopolyesters. Bio-based plastics*. John Wiley & Sons Ltd, Chichester, 137-140.

Ma, P., Cai, X., Wang, W., Duan, F., Shi, D., & Lemstra, P. J. (2014). Crystallization behavior of partially crosslinked poly (β-hydroxyalkonates)/poly (butylene succinate) blends. *Journal of Applied Polymer Science*, 131(21).

Ma, P., Hristova-Bogaerds, D. G., Lemstra, P. J., Zhang, Y., & Wang, S. (2012). Toughening of phbv/pbs and phb/pbs blends via in situ compatibilization using dicumyl peroxide as a free-radical grafting initiator. *Macromolecular Materials and Engineering*, 297(5), 402-410.

Thomas, S., Shanks, R., & Chandran, S. (Eds.). (2013). *Nanostructured polymer blends*. William Andrew, 1-14

Ublekov, F., Budurova, D., Staneva, M., Natova, M., & Penchev, H. (2018). Self-supporting electrospun PHB and PHBV/organoclay nanocomposite fibrous scaffolds. *Materials Letters*, 218, 353-356.

DEVELOPMENT OF BIOBASED WORSTED FABRICS WITH PLA FIBER

Büşra EROĞLU

Yünsa Yünlü Sanayi ve Ticaret A.Ş., Tekirdağ, Türkiye

Corresponding author: beroglu@yunsa.com

Abstract: *Polylactic acid (PLA) fiber is a biodegradable fiber with mechanical properties closest to polyester fiber (PES). PES which is a synthetic fiber does not degrade in nature for hundreds of years. In this study, PLA fiber which is a biodegradable fiber was used instead of polyester fiber in wool fabric qualities. Thus, 100% biodegradable fabric qualities have been developed. Developed fabric qualities contains different ratio wool, PLA and polyester fibre. Fabric qualities were also produced by using polyester fiber instead of PLA in the same blends. Fabric tests were performed and the results were compared.*

Keywords: *PLA, wool, bio-based fabrics, worsted fabrics*

1. INTRODUCTION

Polylactic acid (PLA) fibers are used many different textiles applications because of several factors. One of the factors is environmentally friendly chemicals and processes used in production. In Japan and Europe were focused the manufacturing of PLA/ cotton blend t-shirts, golf shirts, and women's lingerie. [Scheyer & Chiweshe,2001]

Polyester fiber (PES) is a petroleum-based fiber and it causes a global warning because of its life cycle. Therefore, bio-based polyester fiber has been develeoped to produce for yarn and fabric. Poly (lactic acid), PLA, is accepted as the eco-polyester fiber. It is derived from renewable materials e.g. corn, sugar and starch. [Azubuike & Esiaba,2012]

2. MATERIALS AND METHODS

Tops form of PLA, polyester and wool fiber were used in this study. Strength of PLA fiber in the form of tops is 8.29 cN. The average strength of polyester fiber is 11.71 cN. First of all, blend of PLA / wool and polyester / wool fiber were used in different blends to produce yarn. After that these yarns are wovened. The fabrics have different ratio. Also, fabrics were produced same ratio with polyester fiber instead of PLA fiber. Then, they are compared. In the finishing department, fabrics washed and drye. After that it is used decatizing machine.

2.1. Fiber Tests

Breaking strength of PLA fiber and polyester fiber were tested using Prowite E002-B-V350 tester. They were determined in accordance with TS EN ISO 5079.

2.2. Fabrics Tests

Dimension stability, tear strength, seam slippage, martindale pilling, colour fastness, weight, breaking strength were determined.

Table 1. The list of standards of tested fabrics

FABRIC TESTS	STANDARD
Breaking Strength (kg) warp/weft	STRIP METODU ISO 13934 - 1
Tear Strenght -Elmendorf Metod-warp (gram)	ISO 13937 - 1
Tear Strenght -Elmendorf Metod-weft (gram)	ISO 13937 - 1
Seam Slippage 6mm-Weft	ISO 13936 - 1
Martindale Pilling Test - 2000 Cycles	2000 Cycle ISO 12945 - 2
Colour Fastness to Rubbing-dry-warp	ISO 105 - X12
Colour Fastness to Rubbing-wet-warp	ISO 105 - X12
Dımension Stabılıty to Hofmann Press-warp	DIN 53894-2
Dımensıon Stabılıty to Hofmann Press-weft	DIN 53894-2
Dımensıon Stability to Wira Steam Cyclinder-Warp	ISO 300
Dımensıon Stability to Wira Steam Cyclinder-Weft	ISO 300
Dımensıon Stability to Dry Cleanıng-warp	ISO 3175
Dımensıon Stability to Dry Cleanıng-weft	ISO 3175
Weight (g/m2)	-

3. RESULTS AND DISCUSSION

The breaking strength tests results were evaluated of PLA fiber and PES fiber (Figure 1). According that, breaking strength of PLA fiber is lower than breaking strength of PES fiber.

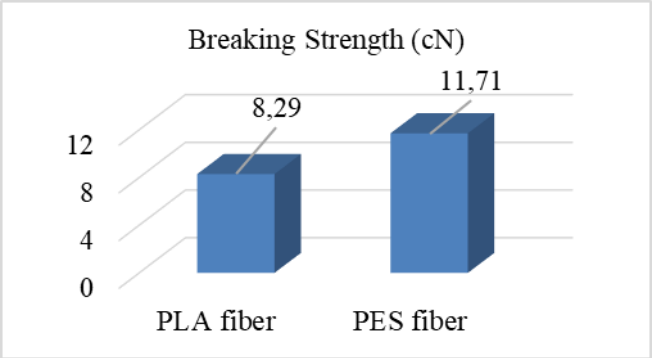

Figure 1. Breaking strength values of fibers

The fabrics composition and fabrics code were shown Table 2. The fabrics were prepared in different ratio.

Table 2. Fabrics definitions

Fabric code	Fabric blend	Fabric weight	Ratio of fiber in fabric (%)	Weft densities	The fabric structure
1	Wool /PLA	159	70/30	330	2:2 Twill
1-a	Wool /PES	153			
2	Wool /PLA	165	60/40	360	2:2 Twill
2-a	Wool /PES	168			
3	Wool /PLA	183	50/50	280	2:2 Twill
3-a	Wool /PES	195			

The yarn used in the fabrics were shown in Table 3. The yarns in the fabric have different properties.

Table 3. The yarn used in the fabrics

Fabric code	Fabric blend	Yarn Blend, Thickness, Twist (Warp)	Yarn Blend, Thickness, Twist (Weft)
1	Wool /PLA	45/55:Wool/PLA, Nm 80/2 750 S	100 %: Wool, Nm 48/1 667 Z
1-a	Wool /PES	45/55:Wool/PES, Nm 80/2 750 S	100 %: Wool, Nm 48/1 667 Z
2	Wool /PLA	60/40: Wool/PLA, Nm 80/2 750 S	60/40: Wool/PLA, Nm 56/1 700 Z
2-a	Wool /PES	60/40: Wool/PES, Nm 80/2 750 S	60/40: Wool/PES, Nm 56/1 700 Z
3	Wool /PLA	50/50: Wool/PLA, Nm 76/2 667 S	50/50: Wool/PLA, Nm 76/2 667 S
3-a	Wool /PES	50/50: Wool/PES, Nm 76/2 667 S	50/50: Wool/PES, Nm 76/2 667 S

Firstly, after woven fabrics were worked in finishing department. Optimum conditions were researched in this department. The fabrics were washed at 60 ºC and dried at 80 ºC. Decatizing process was used for hand feeling. After these processes, the fabrics were tested and the results (Table 4) were compared. According to test results, for in the warp direction when PLA fibre in fabric increased, breaking strength value is increased. For weft direction although PLA fiber is changed in the fabric, results are near.

The difference in fiber breaking strength test results was also reflected in the fabric strength test results. When analyzed according to the standard, the results were greater than 18, passing the standard.

Table 4. The test results of fabrics

Fabric Tests	Fabric Code						Standard
	1	2	3	1-a	2-a	3-a	
Breaking Strength (kg) warp/weft (KG)	34/28	47/24	50/29	56/28	58/40	92/70	Greater than 18
Tear Strenght - Elmendorf Metod-warp (Gram)	3308	2926	3177	4850	2347	6000	Greater than 900
Tear Strenght - Elmendorf Metod-Weft (Gram)	1164	1244	1529	1586	1872	6000	Greater than 900
Seam Slippage 6mm-Weft (KG)	20	20	20	20	19	20	Greater or equal 12
Martindale Pilling Test- 2000 cycles	4.5	4.5	4.5	4.5	4.5	4	Greater or equal 3.5
Colour Fastness to Rubbing-dry-warp	4.5	4.5	4	4.5	5	4.5	Greater or equal 3.5
Colour Fastness to Rubbing-wet-warp	4	4	4	3	4.5	4	Greater or equal 2
Weight (g/m2)	159	165	183	153	168	195	-

4. CONCLUSION

In this study, 100 % biodegradable fabric production was studied. Thermal properties, breathability, fire-resistant and odorless properties of wool fiber, which is biodegradable on its own, are combined with environmentally friendly PLA and transferred to fabrics. When compared to fabrics containing synthetic fiber, the results pass the standard.

ACKNOWLEDGMENTS

This work has been supported by HORIZON 2020 project no: 737882

REFERENCES

Chiweshe, L.S and Scheyer, A. (2001). Application and Performance of Disperse Dyes on Polylactic Acid (PLA) Fabric. Aatcc Review, 48.

Azubuike C. P., Esiaba J. (2012). Investigation into some physico-technical and tableting properties of low-crystallinity powdered cellulose prepared from corn residues. Journal of Pharmaceutical Research and Opinion 2: 8 94 – 98.

POLYVINYL ALCOHOL (PVA) / CELLULOSE ACETATE (CA) BASED ENVIRONMENTALLY FRIENDLY HYBRID FILTER PRODUCTION

Dicle Ayça ERTEK[1], Metin YÜKSEK[1]

[1] Marmara University, Department of Textile Engineering, İstanbul, Türkiye

Corresponding author: ayca.ertek@marmara.edu.tr

Abstract: *In this study, the development of filters made of spunbond fabric coated with nanofiber surface was studied. With Covid 19, filters have gained importance in terms of human health. In this study, it is aimed to produce filters by using cellulose acetate and polyvinyl alcohol materials with the help of solution blowing method. The purpose of choosing polyvinyl alcohol (PVA) raw material is that it is not toxic and not polluting the environment, has high chemical stability, high abrasion resistance and low cost.*
Cellulose acetate (CA) material was chosen because it is a renewable, biodegradable, low-cost and high-quality fiber source that can be used in many manufacturing processes. These two materials were chosen in order to make the produced filter environmentally friendly and biodegradable. For the samples produced; tensile strength and FT-IR tests were carried out.

Keywords: *Hybrid Filter, Cellulose acetate (CA), Polyvinyl alcohol (PVA), Nanofiltration, Solution Blowing Method*

1. INTRODUCTION

As a result of the rapid increase in industrialization and urbanization, especially air pollution increases with the pollution of natural resources. This pollution is caused by macro and micro particles in the air. These particles, which can be in solid and liquid phase, enter the human body through the air and cause various respiratory diseases. In order to be protected from the effects of living things such as bacteria, which are harmful to human health and are about 100 nm in size, the air must be filtered effectively. It is aimed to reduce the number of material layers used in the filters and to provide better filter performance through the lower fiber diameter and porosity, by adding a low-thickness nanofiber layer that will perform the same or better than the filter materials obtained from traditional nonwoven surfaces. Since the costs of filters with high particle holding capacity are high, low-cost hybrid filter production is aimed in this project. (Graham K.)

In this study, nano surface coating was applied on the nonwoven surface to increase the filtration amount. The main thing in filtering is the size of the pores in the material. There are two methods for reducing the pore size. These;

Obtaining a more voluminous surface by increasing the number of fiber layers,
It is the production of low diameter fibers with the number of layers and a low volume/thickness structure.

Depending on the size of these pores, the efficiency of the filter class and production standards change. It is aimed to make more precision filtering by using nano surface. In this work, the straining effect, one of the filtering methods, was used. (Gundogdu, N. A. S.)
In air filtration, submicron size fibers provide higher filter efficiency at the same pressure drop compared to others. Although the pressure drops increases, the higher diffusion, interception and

inertial effects of nanofibers will increase more than the pressure drop, so this will positively affect the filter performance. (Kosmider and Scott)

2. MATERIALS AND METHODS

2.1. Preparation of PVA and CA solutions for the air blow method

The solution was prepared in 2 steps. In the first step, PVA and CA were dissolved separately. 9% (w/v) PVA and 9% (w/v) CA solutions were prepared separately in a mixture of AA and distilled H_2O at 80°C for 3 hours. In the second step, the dissolved PVA and CA solutions were combined at 80/20, 65/35 (v/v) ratios and mixed for 1 hour at 80°C. After 1 hour, it was stirred for 30 minutes at room temperature. (Felgueiras H.P.)

Mixture of soluble PVA and CA was produced in a solution blowing machine at a rotation speed of 100 RPM, a flow rate of 2mL/hour, a constant pressure of 2.5 bar, using air at a constant pressure of 2.5 bar, at 30 cm between the collector needle tip, at a temperature of 23-25°C, in an environment of 34-46% relative humidity. The viscosity values of the solutions produced are given in the table below.

Table 1. Viscosity Value

Viscosity was measured with a 100 RPM S21 spindle.		
	cP Value	% Value
%100 PVA	198.0	%39.6
%80 PVA / %20 CA	184.0	%36.8
%65 PVA / %35 CA	186.5	%37.3

2.2. Physical Properties

Tensile strength test was carried out with Instron 4411 brand universal test device according to TS EN 20-9073-3 standard. The tests were carried out by cutting the nonwoven textile surface structure in 20x5cm (length x width) dimensions and setting the piston speed to 100mm/min. The results are read in MPa (megapascal).

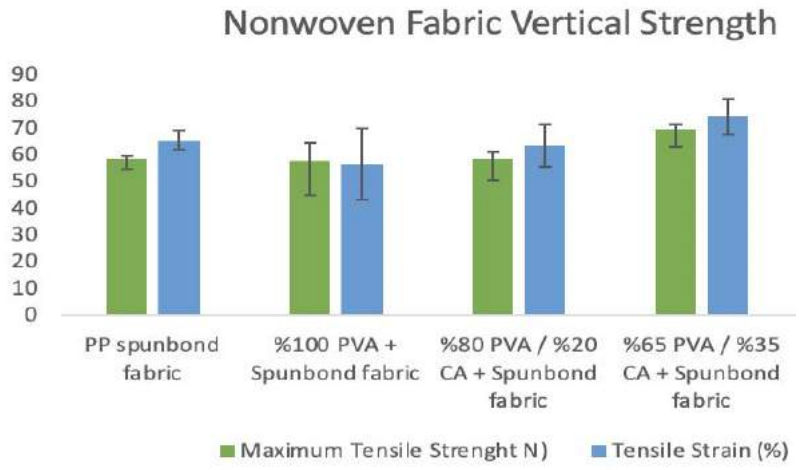

Figure 1. Vertical Strength Graph

According to the graphic given above, when the effect of nano-surfaces obtained with productions made in 5 minutes on spunbond fabric tensile strength was analyzed, it was determined that 65% PVA

/ 35% CA ratios increased the tensile strength by 19%. It has been determined that 100% PVA added and 80% PVA / 20% CA coated fabrics have similar strength values with the nano surface uncoated spunbond fabric. The flexibility of the filter structure increased with the increase of the CA ratio.

3. RESULTS AND DISCUSSION

Air permeability test was made out with SDL Atlas M021S test device according to TS 391 EN ISO 9237 (Determination of permeability of fabrics to air) standards. Testing area was 5cm^2, air pressure 50 Pa and 100 Pa (Pascal). Results are read in L/min (Liter/minute). (Dincer K.)

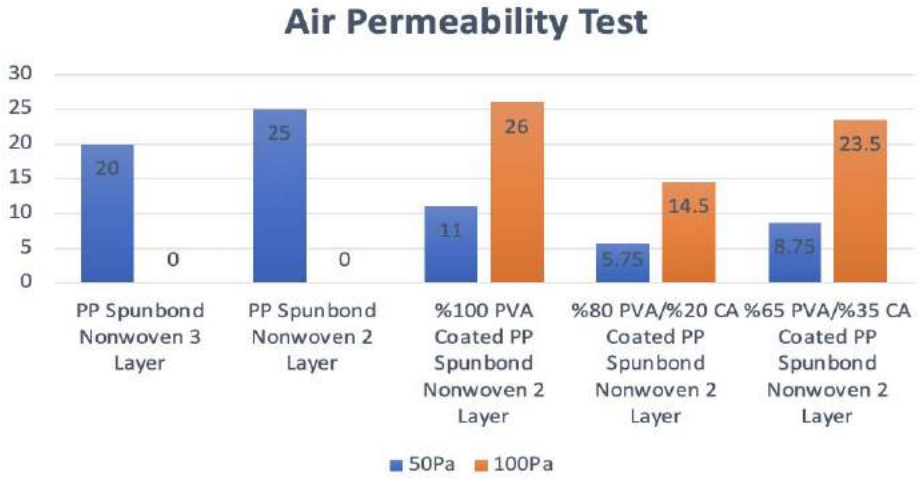

Figure 2. Air Permeability Test

In the air permeability test, the results of two and three layers of raw spunbond fabric were compared with nano surface coated fabrics. Considering the test results, no results were obtained for uncoated fabrics under 100 Pa air pressure. (Akıncı F.C.)

Under 50 Pa air pressure, air permeability decreases by 50% when nano-coated fabrics and raw fabrics are compared. The lowest air permeability value was measured at 5.75 L/min under 50 Pa pressure of the spunbond fabric coated with 80% PVA 20% CA.

It was determined that the fabrics coated with nano surface decreases the air permeability.

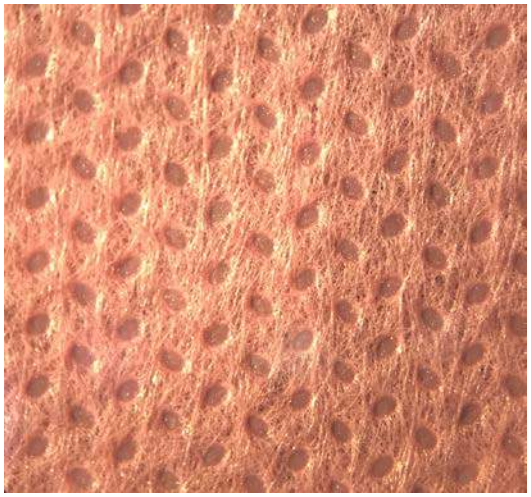

Figure 3. Non coated PP spunbond fabric

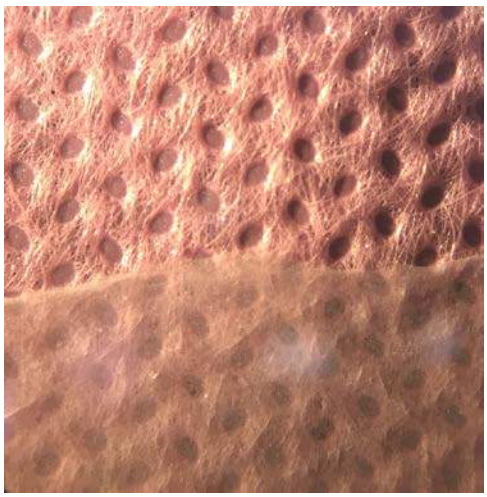

Figure 4. % 100 PVA coated spunbond fabric

Nano-coated and uncoated nonwoven fabrics can be seen at 60x magnification under the fabric microscope. For Figure 4.-5.-6., the upper area is uncoated, the lower area is the nano-surfaced.

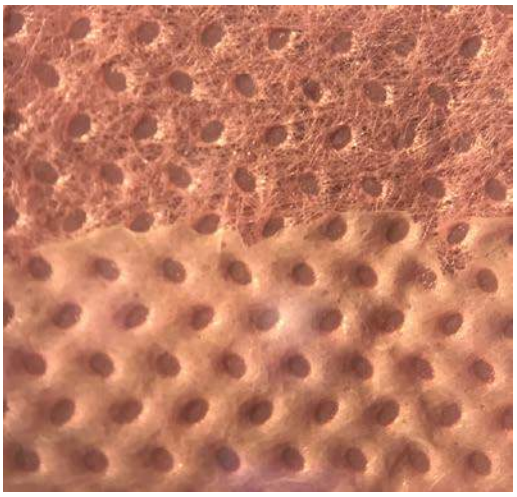

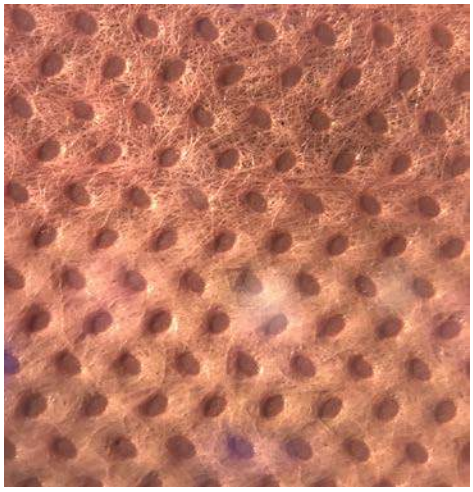

Figure 5. %80PVA /%20CA coated spunbond fabric **Figure 6.** %65PVA /%35CA coated spunbond fabric

There are specific peaks (Figure 7) for CA at 1735cm^{-1} (C=O), 1375 cm^{-1} (C-CH3) and 1254cm^{-1} (C-O-C). (Zeeshan Khatri) For CA, the peaks at 1735cm^{-1} (C=O), 1254cm^{-1} (C-O-C) peaks in 65% PVA/35% CA sample, in FTIR measurements, these peaks were stronger than 80% PVA/ 20% CA mixture. Also, it was determined that these peaks were not detected in the 100% PVA sample. (Song J.)

The characteristic peaks for PVA are 2900cm^{-1} (C−CH2), 1450cm^{-1} (-OH), 1375cm^{-1} (C-CH3). The vibrational band observed between 2840 and 3000 cm^{-1} refers to the stretching C–H from alkyl groups and the peaks between 1750–1735 cm^{-1} are due to the stretching C-O and C–O from acetate group remaining from PVA. (Mansur H. S.)

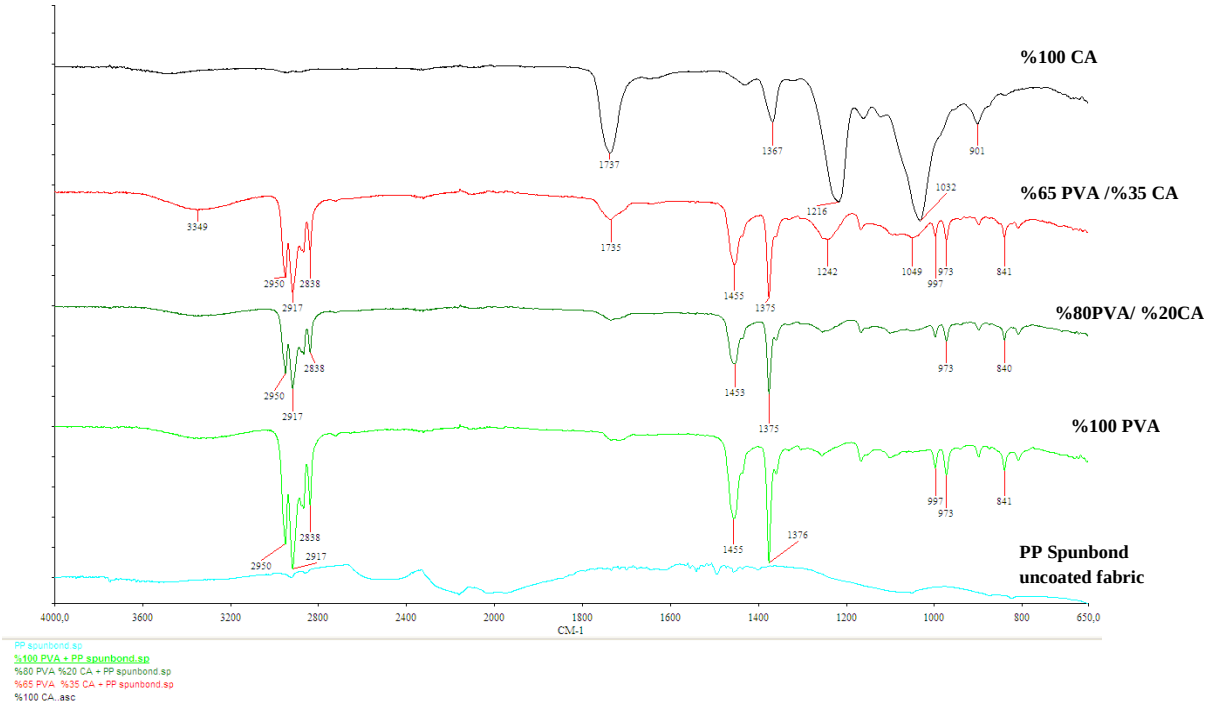

Figure 7. FT-IR Spectra

4. CONCLUSION

In This study includes preliminary results of studies on improving the performance of spunbond fabrics used for filter purposes with nanofiber surface. PVA stands out with its low cost and biodegradable material, while CA was chosen for its properties such as flexibility, hardness, tensile strength, and its resistance to bacteria. As a result of the selection of these materials, nano fiber production was made by solution blowing. In the later stages of the study, the filter class of the produced filter will be determined by measuring the filtration degree with the TS EN 1822-1 test and SEM (scanning electron microscope). According to the tensile strength test result, it is expected that the air flow resistance will be high because the fabric coated with 65% PVA/35% CA solution increases its tensile strength by 19%.

ACKNOWLEDGMENT

The authors would like to express their gratitude to Micrononwoven Tekstil San & Tic. A.Ş. that provide PP Spunbond Nonwoven to the research.

REFERENCES

Gündoğdu, N. A. S., (2016) Aerosol filtration performance of nanofibrous webs produced via centrifugal spinning technique, ITU institute of science master thesis.

Felgueiras H. P., Teixeira M. A. , M., Tavares T. D.,Amorim T. P. , (2019) New method to produce poly(vinyl alcohol)/cellulose acetate films with improved antibacterial action, Elsevier.

Graham, K., Ouyang, M., Raether, M., Grafe, T., McDonald, B., Knauf, P., (2002), Polymeric nanofibers in air filtration aplplication, *15. Annual Technical Conference&Expo of the American Filtration & Separations Society*, Galveston, Texas, USA, 17p.

Zeeshan Khatri, Kai Wei, Byoung-Suhk Kim, Ick-Soo Kim, (2011) Effect of deacetylation on wicking behavior of co-electrospun cellulose acetate/polyvinyl alcohol nanofibers blend, Elsevier.

Mansur H. S., Sadahira C. M., Souza A. N., Mansur A.A.P., (2008) FTIR spectroscopy characterization of poly (vinyl alcohol) hydrogel with different hydrolysis degree and chemically crosslinked with glutaraldehyde, *Materials Science and Engineering C* 28 (2008) 539–548 Elsevier.

Song J., Birbach N. L., Hinestroza J. P., (2012) Deposition of silver nanoparticles on cellulosic fibers via stabilization of carboxymethyl groups, *Cellulose* 19:411–424 Springer.

Kosmider, K., Scott, J., **(**2002), Polymeric nanofibers exhibit an enhanced air filtration performance, *Filtration and Separation*, doi:10.1016/s0015-1882(02)80187-2

Dincer K, .Önal G., Selbes B., Akdemir A.(2018), Nanofiber Tabakalı Hava Filtrelerinin Partikül Yakalama Performanslarının İncelenmesi, *Journal of Natural and Applied Sciences* Volume 22, Special Issue, 32-41, doi:10.19113/.sdufbed.45779

Akıncı F.C., Kaynak H.K., Kkorkmaz Y.(2018): Filament İnceliği ve Atkı Sıklığının Mikrofilament Dokuma Kumaşlarda Geçirgenlik Özelliklerine Etkileri, *Tekstil ve Mühendis*, 25: 111, 234-240.

SMART TEXTILE pH SENSOR BASED ON CURCUMIN MICROCAPSULES

Fabien SALAÜN[1]

[1] Univ. Lille, ENSAIT, ULR 2461 - GEMTEX - Génie et Matériaux Textiles, F-59000 Lille, France

Corresponding author: fabien.salaun@ensait.fr

Abstract: *In this study, pH-sensitive textile systems are developed for use in the field of detection of alkaline media variations. The product is designed based on the surface functionalization of cotton fabric by semi-porous microcapsules containing curcumin. The capsules synthesized by interfacial polymerization from MDI and xylitol serve as micro-reactors where a modification of the chemical form of curcumin takes place, allowing to observe a change of color. This change of color is linked to the acidity constant of this molecule. The objective is also to correlate the visual observation to an evaluation of the color code via image capture by a smartphone of the textile structure and simplified processing of the image color. The analyses have shown that the product obtained is well sensitive to pH variations and easy to use.*

Keywords: *Curcumin, microencapsulation, chemical grafting, smart textile, pH sensor.*

1. INTRODUCTION

pH tests are commonly used in chemistry laboratories to measure the acidity or alkalinity levels of solutions. There are various technologies for measuring pH values, but the most accurate pH measurements can be obtained with a pH meter. For these reasons, many researchers have begun to look for new methods to determine pH values. With the help of computer technology, many processes can be simplified and performed in a shorter time. Today, digital image processing and analysis methods have gained popularity in these applications.

The most common and convenient way to use pH paper is to measure acidity, basicity and pH concentration by changing the color. A pH paper is a paper made by infiltrating an indicator into a filter paper with a color change occurring as a result of the reaction depending on the hydrogen ion concentration of the solution. The pH of the solution can be determined by observing the color change and comparing it to the standard discoloration table. This method has the following advantages: simple and fast measurement Colorimetric indicators such as pH sensitive dyes provide visual information. The pH value is an important parameter in many circumstances and therefore a halochromic textile could be used for various applications (De Clerck, Geltmeyer, Steyaert, & Van der Schueren, 2012). In this context, the textile structure can also be used to detect the pH of an environment.

Curcumin (1,7-bis(4-hydroxy-3-methoxyphenyl)-1,6-heptadiene-3,5-dione) is a bioactive component and a low molecular weight polyphenol of turmeric (Curcuma longa L.) which is widely used as a food colorant. Curcumin has a yellow color, and the chemical structure presents two o-methoxy phenols attached symmetrically through α, β-unsaturated β-diketone linker, which also induces keto-enol tautomerism (Pourreza & Golmohammadi, 2015). This compound is practically insoluble in water at acidic and neutral pH, and this stability is attributed to its conjugated diene structure. Furthermore, curcumin has three ionizable protons, one from the enolic proton and the two last from the two phenolic OH groups. The pKa values for dissociating the three acid protons have been estimated from 7.7 to 8.5, 8.5 to 10.4, and 9.5 to 10.7, respectively. Thus, when the pH increases to neutral-basic conditions, a proton is removed from the enolic form and afterward from the phenolic group leading to the destabilization of the structure. Even if the solubility can be enhanced under

alkaline conditions resulting in a color change of the chromophore groups to deep red, the pH modification caries to the instability and the destruction of this structure.
This paper studies the conventional finishing method to as possible approaches to obtain textile pH-sensors. Since curcumin can interact with the environment, it is necessary to protect it with a semi-porous polymeric membrane allowing the diffusion of the liquid into the core of the capsule to modify its chemical form, while ensuring the reversibility of the effect (Salaün, Bedek, Devaux, & Dupont, 2011). In addition, the chemical grafting method of the microcapsules was preferred to ensure the permeation of the membrane. The objective of this study is to investigate the influence of the rate of microcapsules required for pH detection, and to couple the visual measurement with simple image processing from capturing the functionalized media with a smartphone to edit the color code, as a simple alternative approach to determine pH values of different, was investigated.

2. MATERIALS AND METHODS

2.1. Reagents and Materials

1,7-Bis(4-hydroxy-3-methoxyphenyl)-1,6-heptadiene-3,5-dione (curcumin) was purchased from Aldrich (France) and used as core matarial, Diphenyl methylene diisocyanate (MDI) (Suprasec 2030, Hüntsman ICI), and xylitol (Roquette Frères, content >99%) ($C_5H_{12}O_5$), a polyhydric alcohol, were employed as shell-forming monomers for the interfacial polycondensation. Ethyl acetate (EtAc) (Fluka, France) and acetone (Merville, France) were used as solvents. Nonionic surfactant, Tween® 20 (Polyethylene glycol sorbitan monolaurate) was purchased from Aldrich and used as emulsifier. Sodium Dodecyl Sulfate (SDS) purchased from Aldrich (France) was used as surfactant. A 100% cotton twill fabric (TDV Industries, France) (296 g/m^2, air permeabilty 156 L/m^2/s, thickness 0.67 mm) was used as textile substrate.

2.2. Preparation of Curcumin Microcapsules

Curcumin microcaparticles were prepared by emulsion–diffusion technique, which is divided in four steps, i.e. mutual saturation, emulsification, diffusion and purification (Souguir, Salaün, Douillet, Vroman, & Chatterjee, 2013). First, continuous (distilled water) and dispersed (ethyl acetate, EtAc) phases (2:1 v/v) were mutually saturated for 24 h to ensure thermodynamical equilibrium. The obtained solutions, aqueous and organic phases, contain 8.7% w/v of EtAc and 3% of water, respectively. Second, for the emulsification step, 0.5 g of curcumin and 2.9 g of MDI were dissolved in 30 ml of a binary mixture of acetone/ethyl acetate (1/2 v/v) saturated with water, and then this phase was emulsified with 60 ml of the aqueous phase containing 1.5 wt.% of Tween 20 at 4 °C, with the use of a high speed homogenizer (Ultra-Turrax® T25 basic, Germany) at 6500 rpm during 50 min. After 25 min, when the expected droplet size of the emulsion was reached, the polymerization reaction was carried out by drop-wise addition of 10 ml of aqueous solution containing 5.1 g of Xylitol. Third, to induce the formation of polymeric shell, the solution was transferred into a double walled four-necked vessel, the microparticles were maintained in suspension under a stirring speed of 500 rpm for 3 h. A large quantity of distilled water was subsequently added to the microemulsion inducing the diffusion of EtAc from the inner to the outer phase for the microsuspension. A volume equal to twice the volume of the emulsion was used for dilution. Finally, the resultant microparticles were recovered by filtration and washed twice with water, and then dried at 50 °C overnight, before being redispersed in water for further uses.

2.3. Preparation of Textile Based Curcumin Microparticles

In order to obtain the textile based Curcumin microparticles, microcapsules were applied to the surface of the fabric by bath exhaustion with a liquor ratio about 1:20, during one hour at 70°C before being

dried in an oven at 130°C during 3 minutes. The solutions were prepared with different concentration of the microencapsulated curcumin, 60 g/L of Mikracat B and 10g/L of Mikrafix (obtained from Devan Chemcals, Belgium).

2.4. Color Measurement

In this paper, we utilize a Datacolor International SF 600 plus interfaced with a personal computer to determine the reflectance and CIELAB values of the textile samples, a pH meter to control the value of the pH buffer solutions, a Android smart phone.

3. RESULTS AND DISCUSSION

In this study, we observed the color change of the pH sensitive textile with different pH solutions. The average of the repeated data was obtained and analyzed. The first part of the study consisted in analyzing the influence of the weight of microcapsules deposited on the surface of the surface to determine the optimum concentration according to the response, and thereafter the response according to the pH of the solution (Figure 1).

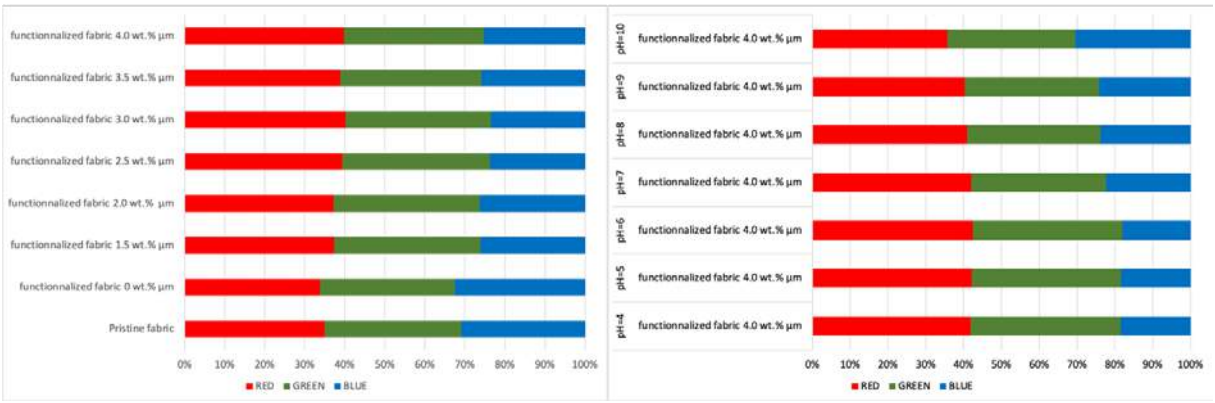

Figure 1. Ratio of RGB according to the microcapsules concentration at neutral pH (left) and at various pH value in buffer solution with 4.0 wt.% (right)

From 2.5 wt.% of microcapsules, there is no more varitation of the RGB ratios, the amount of curcumin is sufficient to obtain a uniform hue. The variations of the RGB ratios are minimal for acidic pH, but notable changes are observed at the first change of pKa of the dye, and the ratio of R decreases while that of B increases at the change of the second and third pKa, showing that the textile structure is well reactive to the change of pH of the medium. The measurements indicate that the RGB ratio obtained from the Smartphone image processing is sufficiently sensitive to estimate the pH of a solution, making the system easy to use, and also reusable.

4. CONCLUSION

In this work, the objective is to create pH sensitive textile structures based on textile containing curcumin microcapsules. In the evaluation of the results, it is believed that the products have sufficient activity and sensitivity to detect the pH of the surrounding liquid medium, and that the exploitation of photographic images is a simple way to determine the pH value. In the later stages of the study, the improvement of the sensitivity of the system will be investigated to improve the performance.

REFERENCES

De Clerck, K., Geltmeyer, J., Steyaert, I., & Van der Schueren, L. (2012). Halochromic textile materials as innovative pH-sensors. Advances in Science and Technology, 80, 47-52. doi:10.4028/www.scientific.net/AST.80.47

Pourreza, N., & Golmohammadi, H. (2015). Application of curcumin nanoparticles in a lab-on-paper device as a simple and green pH probe. Talanta, 131, 136-141. doi:10.1016/j.talanta.2014.07.063

Salaün, F., Bedek, G., Devaux, E., & Dupont, D. (2011). Influence of the washings on the thermal properties of polyurea-urethane microcapsules containing xylitol to provide a cooling effect. Materials Letters, 65(2), 381-384. doi:10.1016/j.matlet.2010.10.041

Souguir, H., Salaün, F., Douillet, P., Vroman, I., & Chatterjee, S. (2013). Nanoencapsulation of curcumin in polyurethane and polyurea shells by an emulsion diffusion method. Chemical Engineering Journal, 221, 133-145. doi:10.1016/j.cej.2013.01.069

INVESTIGATION OF TEXTILE BASED ELECTRODES FOR MONITORING sEMG MUSCLE SIGNAL

Elif GÜLTEKİN, Halil İbrahim ÇELİK, Hatice Kübra KAYNAK

Gaziantep University, Department of Textile Engineering, Gaziantep, Türkiye

Corresponding author: elfgultekin30@gmail.com

Abstract: *Wearable electronics are technological devices that are incorporated into garments with embedded systems and provide constant interaction with the user performing a specific task. This technology often focuses on devices to monitor physiological variables and seeks the most convenient and portable form for continuous monitoring. Although sEMG has emerged as a tool used in laboratory research for many years, with the development of technology in the fields of electricity, electronics, computers, and biomedicine, it has been used for different purposes in kinesiology (the branch of science dealing with human movements), rehabilitation, sports medicine, sports sciences, and many sports branches. In this study, textile based sEMG electrodes were produced by using knitting technology with silver plated polyamide conductive yarn with different densities. Then resistivity and sEMG signals of the produced samples and conventional disposable electrode were compared.*

Keywords: *Smart textile, textile-based electrode, medical textiles, sEMG signal, physiological monitoring.*

1. INTRODUCTION

The role of technology in healthcare is gaining importance day by day. The research and development studies on smart garments for monitoring physiological condition is growing very rapidly in scientific and technological areas. Such smart garments, popularly also known as electronic textiles, find applications in varied fields like civilian, medical, military etc.

Surface Electromyography (sEMG) is an assessment tool that is frequently used in many areas of medical science today and is used to analyse muscle function. With the help of this measurement technique, which contains important information about the contraction of our body muscles, it is determined which muscles are activated in which movement. sEMG provides information on which stage the muscles are active, especially in activities that contain important data such as walking movement. In addition, it allows evaluating muscle fatigue and making muscle strength estimates. Surface electromyography (sEMG) is one of the most common methods used to measure muscle activity in athletes and patients. Textile-based electrodes cover a larger area to acquire the sEMG signal, thus achieving muscle stimulation from all muscle groups. Real-time measurement of textile-embedded EMG electrodes has been shown to significantly improve clinical outcomes after rehabilitation. Scientific studies show that sEMG muscle signals can be obtained from muscle groups in the human body with conventional electrodes (Giggins et al.,2013; Pehlivan, 2006) or textile-based electrodes (Catarino et al., 2012; Pani et al., 2019; Colyer et al., 2018) integrated on a garment. When the studies in this field are examined, it is seen that textile-based electrodes can be created by various methods.

Biopotential monitoring has been greatly facilitated by advances in wearable technologies and textile electronics has become an important technology. The human body itself is a critical signal “source” in wearable applications. The material type and production technology have important effects on the performance and functionality of the textile-based electrodes. Textile-based electrode production is

fundementally based on the integration of conductive materials in the form of fabric. Commonly used conductive materials include metals and conductive polymers. With these materials, electrode fabric form is applied using knitting, weaving, embroidery techniques or using various other methods such as printing, electroplating, physical vapor deposition (PVD), chemical coating and chemical polymerization (Stoppa et al., 2014; Takamatsu et al., 2015).

Knitting, weaving, and embroidery technology are the most known and widely used techniques in wearable technology. Using various conductive fibers and yarns, electrode surfaces can be created by knitting, weaving and embroidery techniques directly. Woven textiles are produced by interlacing two perpendicular yarn groups. In contrast, the knitting technique uses a needle that constantly connects a series of thread chains. The embroidery method is a kind of decoration method for creating a pattern by including different sewing forms on a fabric surface. Among these methods, knitted fabrics, provide consumers skin comfort, low weight, and great flexibility, and the knitting process is a well-established approach that allows a whole garment to be made on a single machine (An et al., 2018; Xu et al., 2008). Electroless plating is a technique that involves spontaneous reactions in an aqueous solution without requiring the application of an external electric field, unlike galvanic plating, which uses an electrode current to reduce metal cations for plating (Mallory et al., 1990). Electrodeposition techniques and physical vapor deposition (PVD) are the most prominent techniques for metal coating on non-conductive yarns and textiles. PVD techniques such as thermal/e-beam evaporation and sputtering depend on the formation of conductive layer on the textile material, similar to electrodeposition in the microelectronic process industry. Metals are evaporated and deposited to form a thin film layer on various textile products (Mattox et al., 2010; Silva et al., 2012). Dip coating is one of the simplest methods of coating yarns or fabrics and is still used in the textile industry. Upon application of a conductive solution to textiles, excess material is removed, and a drying step known as curing is performed to evaporate the solvent and fix the conductive particles on the fiber surfaces (Shang et al., 2013; Garcia-Breijo et al., 2015). Printing techniques such as inkjet and screen printing are widely used to create conductive patterns on textile substrates and are already being used on a large scale to print stickers/images on textiles (Ujiie, 2006).

In the scope of this study, knitted fabric samples with different loop densities were produced using conductive yarn in order to obtain textile based sEMG electrodes. Different loop densities were applied to samples to investigate the effect of fabric tightness on resistivity and signal reception capability. Then, resistivity and signal reception capability of textile-based electrodes were inspected in comparison to conventional electrodes.

2. MATERIALS AND METHODS

In this study, it is aimed to produce a textile-based electrode samples for measuring sEMG signals. For this purpose, it is planned to produce electrode surface by using silver-coated polyamide yarns (Statex/Shildex Group, 117/17 dtex) via circular knitting technology. Since the conductivity and measurement accuracy of the produced textile-based electrodes is affected by the structural parameters, it is aimed to evaluate the textile-based electrode samples with different loop densities. The produced textile-based electrodes have a voluminous structure and form a surface area in contact with the body, conductivity levels were determined by resistivity measurements. The resistivity measurements were done by using a digital multimeter device. Three knitted fabric samples were produced with different levels of fabric density as loose, medium and tight, as single jersey structure. For this aim, a sample circular knitting machine with 3.5” gauge, 22 fein was used at 20±2 rev/min production speed. All fabric samples were conditioned according to TS EN ISO 139 before the tests

and the tests were performed in the standard atmosphere of 20±2ºC and 65±4% relative humidity. Fabric mass, thickness, loop density and loop length properties of samples were determined according to TS EN 12127:1999, TS 7128 EN ISO 5048:1998, TS EN 14971:2006 and TS EN 14970:2006 respectively. All measurement results were given in Table 1. The produced fabric samples images were illustrated in Figure 1.

Table 1. Structural properties fabric samples

Samples	Resistance, ohm/10 cm	Thickness, mm	Course density, course/cm	Wale density, wale/cm	Loop length, mm
Dense	1.4	0.34	11	16	2.9
Medium	1.4	0.35	10	14	2.7
Loose	1.5	0.36	9	12	2.5

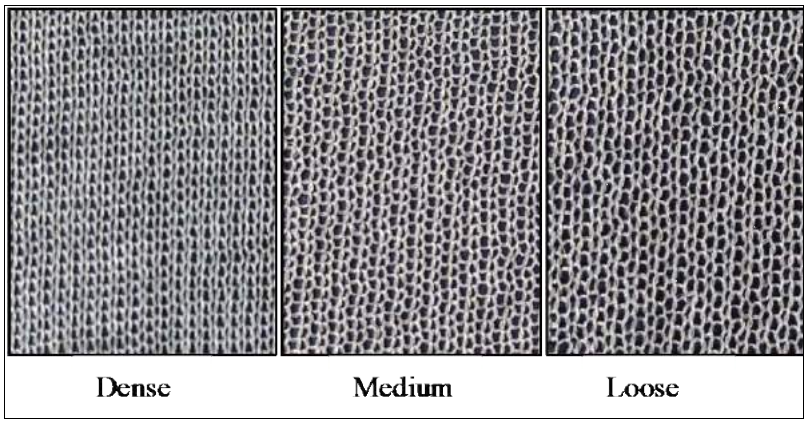

Figure 1. Knitted fabric images

After the knitted fabric samples were produced and the necessary measurements were completed, the fabric samples were sewn on the torniquet in order to get the muscle signal. The knitted fabric samples with 1x1 cm size were prepared and sewn on the torniquet using conductive yarn. Arm muscle signals were obtained with the prepared torniquet as in Figure 2. Muscle signals captured using the Arduino sEMG sensor were displayed on the computer screen.

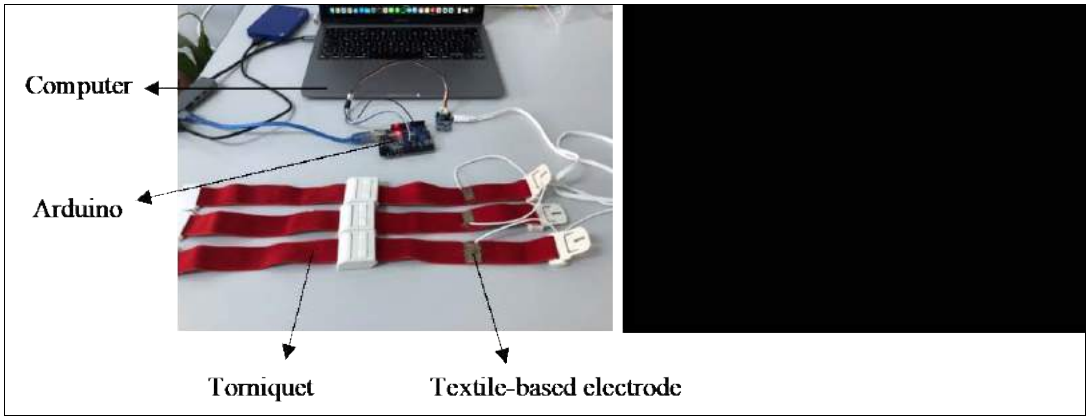

Figure 2. Conductive fabric placed on the torniquet

3. RESULTS AND DISCUSSION

Surface resistivity measurements of the knitted fabric samples were carried out as shown in Figure 3. The fabric sample is placed in a hoop to keep the fabric tension constant and regular. The resistivity

value of the fabric was measured at a certain distance by placing the probes of the digital multimeter device on the fabric surface. After that a square signal was created using Arduino and the characteristic of the signal transmitted through the fabric sample was analyzed via oscilloscope device. The signals acquired from each sample was compared. It was observed from the oscilloscope device that there was no loss in the generated square signal (Figure 4).

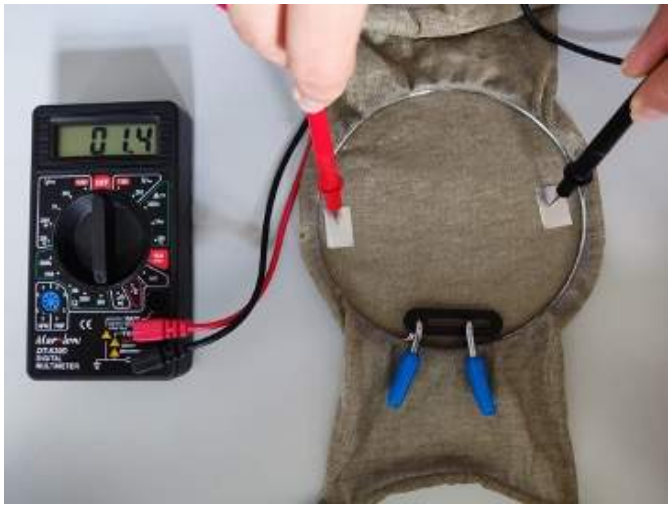

Figure 3. Surface resistivity measurement of knitted fabric sample

Figure 4. Signal measurement of knitted fabric sample

Muscle signals were acquired from three textile-based electrode samples and conventional disposable electrodes. In order to compare the signals, they were captured from the same person and same muscle group. The person made the same arm movement during the signal acquisition. When the muscle signals were analyzed, it was seen that all three fabric samples have similar results with disposable electrodes. It is clearly seen in Figure 5 that the signals received from the arm muscle have a similar characteristic. This result can be attributed to the close resistance values of the fabric samples. The disposable electrodes and all textile-based electrodes used in the experimental setup captured signals in the range of 200 to 800 millivolts. The obtained findings as a result of this study are also similar to the literature. It has also been stated in previous studies that textile-based electrodes and disposable electrodes perform similar measurements (Lee et al., 2018; Babusiak et al., 2018).

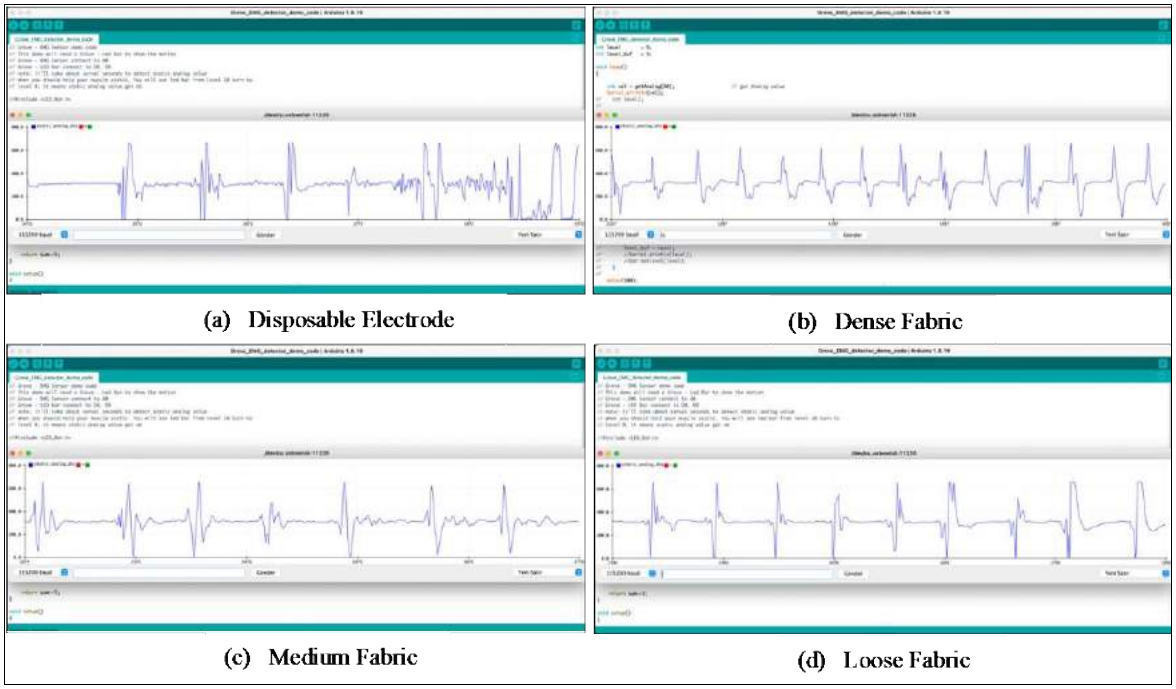

Figure 5. Comparison of sEMG signals captured from (a), (b), (c), (d) samples

4. CONCLUSION

In this work, it is aimed to submit information about textile-based electrode properties and to create textile-based electrode structures containing silver-plated polyamide conductive yarn. By producing knitted fabrics with three different densities with conductive yarn, textile based sEMG electrodes were produced. Then, surface resistivity and signal transmission levels of textile based and conventional sEMG electrodes were observed. It was seen that sEMG signals acquired from textile-based electrodes and conventional electrodes are very close to each other. It shows that the electrode structures produced by using conductive yarns, can be used in sEMG measurements. As a result, it is seen that textile-based electrodes can be used as an alternative to disposable electrodes. Thus, it can be concluded that the reliability of smart textiles to be used in the medical field is very high.

It is possible to collect clinical and behavioral data using wearable technology, which may be categorized under broad categories such real-time monitoring of health status in the medical area, diagnosis, and therapy. Numerous application examples highlight this benefit of wearable technology. As a result of this study, it can be demonstrated that smart clothing made with textile-based sEMG electrodes is adequately accurate for real time health monitoring. The smart clothes allow it to analyze muscle signals during active exercise, which is superior to measurements in medical environment. Smart clothes produced with textile electrodes provide comfort to the user in terms of both ease of measurement and comfort. As technology advances, consumers' perceptions of computers are changing from desktop computers to smart phones, tablets, and eventually wearable devices. According to market studies, this technology is becoming more and more prevalent in our daily lives. It has established itself as a significant player in the market with a wide range of products as a result of users' growing awareness of its benefits.

REFERENCES

An, X., Stylios, G. (2018). A Hybrid Textile Electrode for Electrocardiogram (ECG) Measurement and Motion Tracking. *Materials, 11*, 1887.

Babusiak, B., Borik, S., & Balogova, L. (2018). Textile electrodes in capacitive signal sensing applications. *Measurement, 114*, 69-77.

Catarino, A. P., Carvalho, H., Barros, L., & Dias, M. J. (2012). Surface electromyography using textile-based electrodes. *The Fiber Society 2012 Fall Meeting and Technical Conference*.

Colyer, S. L., & McGuigan, P. M. (2018). Textile electrodes embedded in clothing: A practical alternative to traditional surface electromyography when assessing muscle excitation during functional movements. *Journal of sports science & medicine, 17(1),* 101.

Garcia, B. E., Prats, B. G., Lidon, R. J. V., Ye L. Y., Garcia, C. J. (2015). A comparative analysis of printing techniques by using an active concentric ring electrode for bioelectrical recording. *Microelectron. Int., 32,* 103–107.

Giggins, O. M., Persson, U. M., & Caulfield, B. (2013). Biofeedback in rehabilitation. *Journal of neuroengineering and rehabilitation, 10(1),* 1-11.

Lacerda S. N., Goncalves, L. M., Carvalho, H. (2012). Deposition of conductive materials on textile and polymeric flexible substrates. *J. Mater. Sci. Mater. Electron*, 635–643.

Lee, S., Kim, M. O., Kang, T., Park, J., & Choi, Y. (2018). Knit band sensor for myoelectric control of surface EMG-based prosthetic hand. *IEEE Sensors Journal, 18(20),* 8578-8586.

Mallory, G.O., Hajdu, J.B. (1990). *Electroless Plating: Fundamentals and Applications*. William Andrew: Norwich, NY, USA.

Mattox, D.M. (2010). *Handbook of Physical Vapor Deposition (PVD) Processing*. William Andrew: New York, NY, USA.

Pani, D., Achilli, A., Spanu, A., Bonfiglio, A., Gazzoni, M., & Botter, A. (2019). Validation of polymer-based screen-printed textile electrodes for surface EMG detection. *IEEE Transactions on Neural Systems and Rehabilitation Engineering, 27(7),* 1370-1377.

Pehlivan, Y. S. (2006). Elektromiyografik biyofeedback ile kombine edilen elektrik stimülasyon ve egzersiz uygulamalarının inme sonrası üst ekstremite rehabilitasyonunda motor ve fonksiyonel gelişim üzerine etkisi.

Shang, S., Zeng, W. (2013). *Conductive nanofibres and nanocoatings for smart textiles. In Multidisciplinary Know-How for Smart-Textiles Developers*. Woodhead Publishing: Cambridge, UK, pp. 92–128.

Stoppa, M., Chiolerio, A. (2014). Wearable Electronics and Smart Textiles: A Critical Review. *Sensors, 14*, 11957–11992.

Takamatsu, S., Lonjaret, T., Crisp, D., Badier, J.-M., Malliaras, G.G., Ismailova, E. (2015). Direct patterning of organic conductors on knitted textiles for long-term electrocardiography. *Nature, 5*, 15003.

TS EN ISO 139: 2008 Textiles-*Standard atmospheres for conditioning and testing.*

TS EN 12127: 1999 Textiles- Fabrics - *Determination of mass per unit area using small samples*.

TS 7128 EN ISO 5048:1998-Textiles - *Determination of thickness of textiles and textile products.*

TS EN 14971:2006 Textiles - Knitted fabrics - *Determination of number of stitches per unit length and unit area*.

TS EN 14970:2006 Textiles – Knitted fabrics - *Determination of stitch length and yarn linear density in weft knitted fabrics.*

Ujiie, H. (2006). *Digital Printing of Textiles*; Woodhead Publishing: Cambridge, UK.

Xu, P., Zhang, H., Tao, X. (2008). Textile-structured electrodes for electrocardiogram. *Text. Prog., 40,* 183–213.

A SMART TEXTILE SENSOR THAT CAN ANALYZE BODY MOVEMENT MEASURING SLEEP QUALITY

Gizem AYDEMİR[1], Murat YILDIRIM[1], Levent ÖZTÜRK[2]

[1] Research & Development, Zorluteks Tekstil Ticaret ve Sanayi A.S. Kırklareli, Türkiye
[2] Trakya University, Faculty of Medicine, Department of Physiology, Edirne, Türkiye

Corresponding author: Gizem.Aydemir@zorlu.com

Abstract: *Nowadays, the increase in the pace of life and stress brought by technology and industrialization negatively affect the sleep pattern and sleep quality in human life. In this study, the development of a portable, underpad home textile sensor and integrated mobile application suitable for home use, which provides information about the sleep patterns and quality of individuals by creating a personalized sleep performance report, were carried out. Textile-based sensor creation studies were applied to the fabric surface with the embroidery technique. For the first time in Turkey, the sensor structure was developed using the flexible home textile-based embroidery method.*

Keywords: *Textile-based sensor, sleep quality, home textile*

1. INTRODUCTION

On average, humans spend one-third of their lives asleep. Accumulating evidence suggest that sleep is indispensable and necessary for optimal health, but modern life dictates a life with lesser sleep due to factors such as round-the-clock services (i.e., health, security, transportation, etc), shift work, and social life. As a result, Almost two-thirds of adult people in developed countries fail to obtain a sufficient amount of sleep. The so-called “sleep debt” has become a kind of public insomnia associated with daytime impairment. Furthermore, the total annual cost of insomnia in one study was estimated to be $6.6 billion Canadian dollars. (Skaer TL. Sleep deprivation and economic burden. In: Bianchi MT (ed). Sleep deprivation and disease: effects on the body, brain and behavior. Springer Science 2021, p.269-279) Thus, it is important to prevent sleep-related disorders and inform people about their sleep quality.

Nowadays, the increase in the pace of life and stress brought by technology and industrialization negatively affect the sleep pattern and sleep quality in human life. Studies have shown that sleep deprivation caused by irregular and low-quality sleep plays a major role in traffic and work accidents. In the United States, approximately 110,000 people are injured in motor vehicle accidents each year, and more than 5000 people die. Drowsy driving and napping at the wheel are responsible for 1-3% of these accidents. (Lyznicki JM, Doege TC, Davis RM, Williams MA, for the Council on Scientific Affairs, American Medical Association. Sleepiness, driving, and motor vehicle crashes. JAMA 1998;279: 1908- 1913)

2. MATERIALS AND METHODS

The experimental plan carried out in this study is given in Table 1.

Table 1. Experimental Plan

Trial Name	Trial Code	Trial Parameter	Number of Trials
A trials	a1	9 patterns+1 conductive thread	9
	a2		
	a3		
	a4		
	a5		
	a6		
	a7		
	a8		
	a9		
B Trials	b1	2 patterns+2 conductive thread	4
	b2		
	b3		
	b4		
	c1	1 patterns+2 conductive thread	2
	c2		
	d1	1 patterns+1 conductive thread	12
	d2		
	d3		
	d4		
	d5		
	d6		
	d7		
	d8		
	d9		
	d10		
	d11		
	d12		

2.1. Material

Sensor design studies to be designed with the brode embroidery technique were made with conductive threads. The conductive threads used are 100% steel. The properties of the conductive materials used for the sensor design made with the brode embroidery method are given in Table 2.

Table 2. Conductive thread properties

Thread Resistance Number	Thread Number	Thread Resistance (ohm/m)
1	2044 tex	a
2	44 tex	b
3	96 tex	c
4	235/36 dtex	d

2.2. Method

Studies within the scope of trial A were carried out using the Juki LZ-391-N Zigzag Embroidery machine. Technical information of machine Juki LZ-391-N Zigzag Embroidery is given in Table 3.

Table 3. Technical information of machine Juki LZ-391-N Zigzag Embroidery

Model	LZ-391N
Maximum Sewing Speed	2,000 sti/min
Needle Bar Stroke Length	33.4mm
Needle Bar Stroke Length	DB×1B (#14) #9～#16

Studies within the scope of trial B were carried out on the Epoca Embroidery machine. Within the scope of A trials, 9 different sensor designs were developed using the number 4 conductive thread. Electrical characterization tests were carried out for the developed patterns and no signal difference or

voltage change was observed in contact with the fabric. The images of the studies performed in the A trials are given in Figure 1.

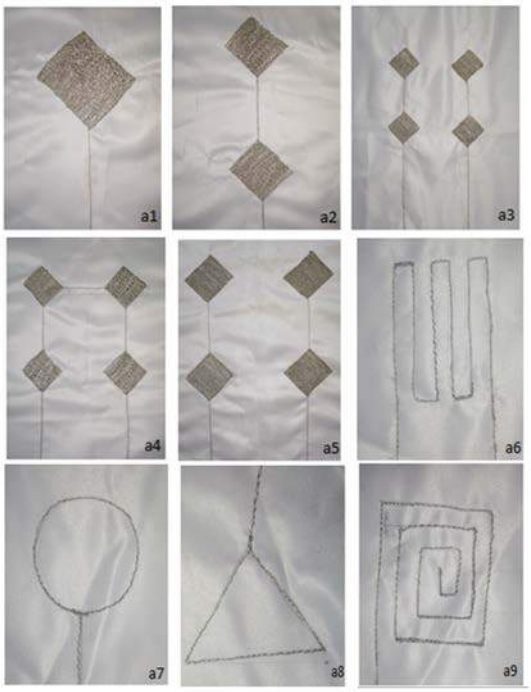

Figure 1. Studies carried out in trials A

B1, b2, b3, and b4 pattern studies were conducted to investigate the effect of angular patterns on the perception of capacitive change. Threads numbered 1 and 4 were used. Studies of b1, b2, b3, and b4 coded trials are given in Figure 2.

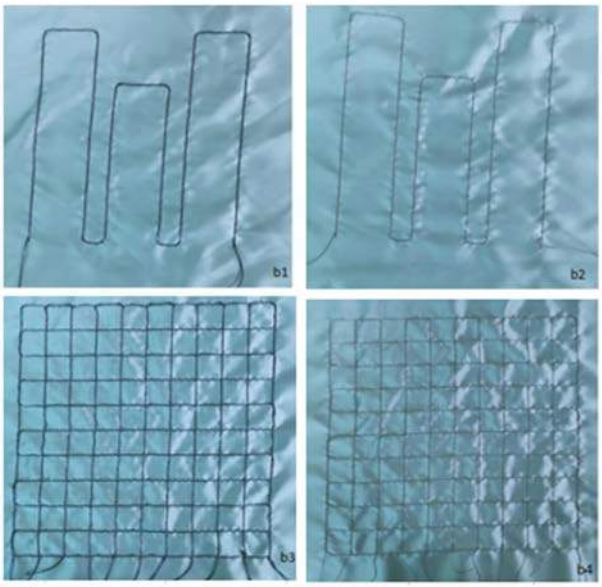

Figure 2. Studies of b1, b2, b3, and b4

In the c1 and c2 trials, studies were carried out with circular patterns. Conductive threads numbered 1 and 4 are used in patterns c1 and c2. Trials of c1 and c2 design studies are given in Figure 3.

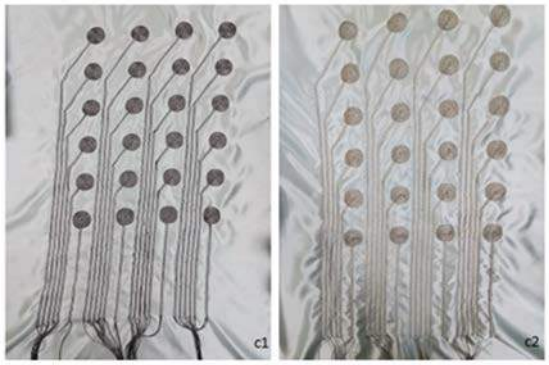

Figure 3. C1 and c2 design studies

D1-d12 pattern studies were carried out using 1. 2 and 3 numbered conductive yarns. Trials of d1- d12 design studies are given in Figure 4.

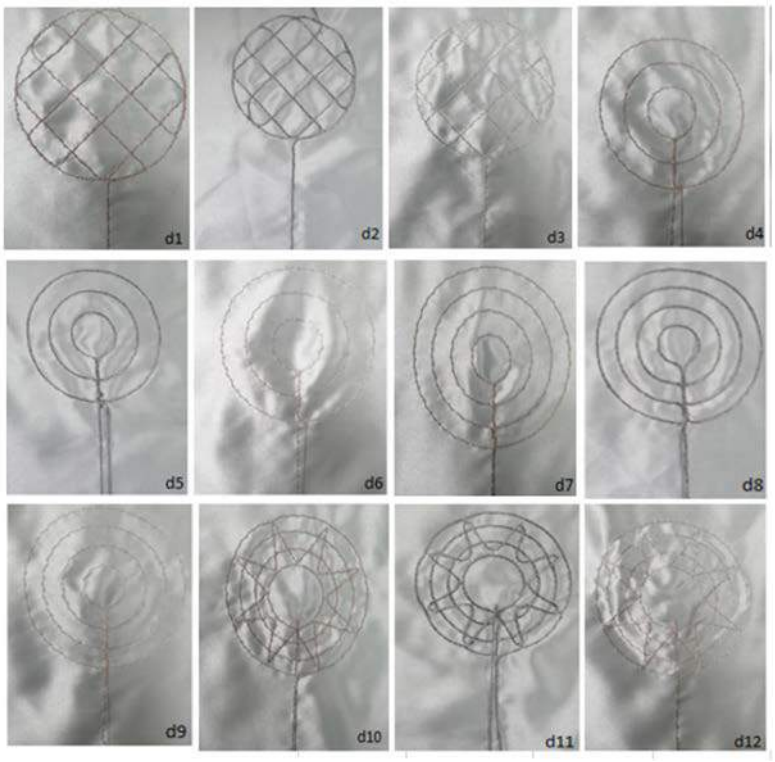

Figure 4. d1-d12 design studies

Studies within the scope of textile-based sensor trials were carried out on Epoca Brode machines. Patterns made on Epoca Embroidery machines are given in Figure 5.

Figure 5. Patterns made on Epoca Embroidery machine

3. RESULTS AND DISCUSSION

Electrical characterization tests were carried out for the patterns developed in the A trials and no signal difference (Figure 6) or voltage change (Figure 7) was observed in contact with the fabric. The first is that the angular patterns reduce the capacitive detection threshold due to the antenna function, and the second is that the specific properties of the conductive thread no 4 in the designs are not strong enough to detect the capacitive change.

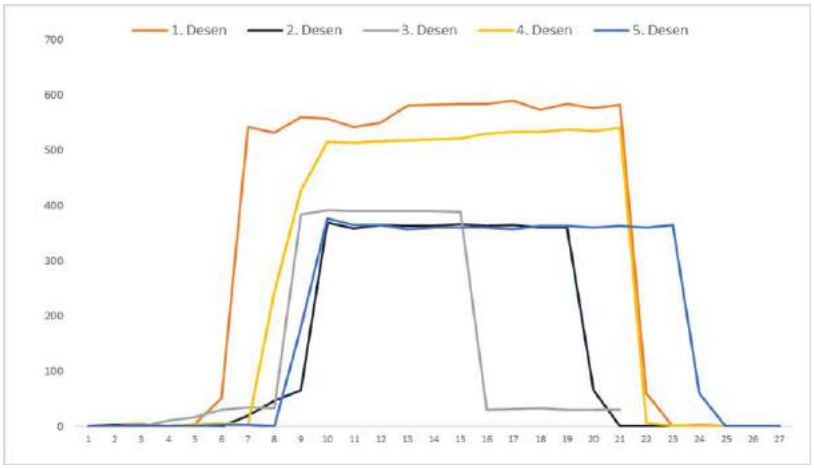

Figure 6. Capacitive Variations for Sensor Designs Number 1-5

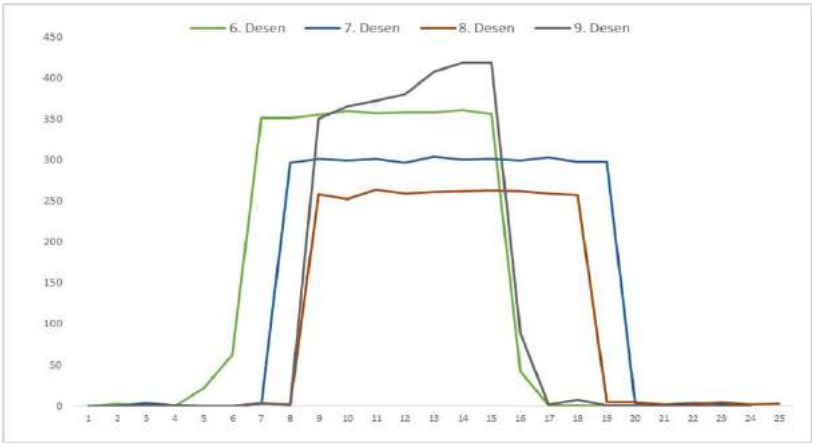

Figure 7. Capacitive Variations for Sensor Designs Number 6-9

B1-b4 pattern studies were carried out to investigate the effect of angular patterns on the perception of capacitive change. Two different pattern studies were made using different threads. Trial results on the detection of capacitive change of angular patterns were unsuccessful.

Electrical characterization tests (Figure 8 and 9) were carried out on the sensor structure formed by using the numbers 1 and 4 conductive threads in c1-c2 patterns. In the contacts made to the created sensor structures, the values that could observe the movement sufficiently could not be obtained. Pattern studies made with the number 1 conductive yarn were found to be more successful.

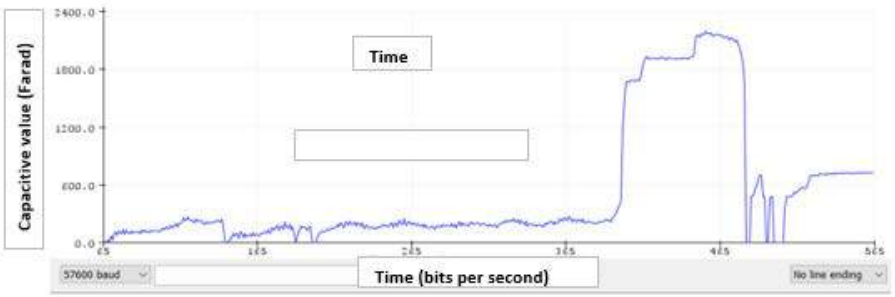

Figure 8. Sensor Design Developed Using Conductive Thread Number 1 and Capacitive Change in Pattern at Contact

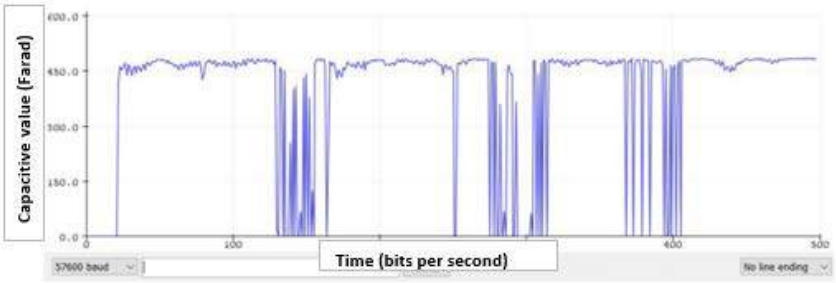

Figure 9. Sensor Design Developed Using Conductive Thread Number 4 and Capacitive Change in Pattern at Contact

Conductive threads numbered 1, 2, and 3 were used in d1-d12 pattern works (Figure 10, 11 and 12).

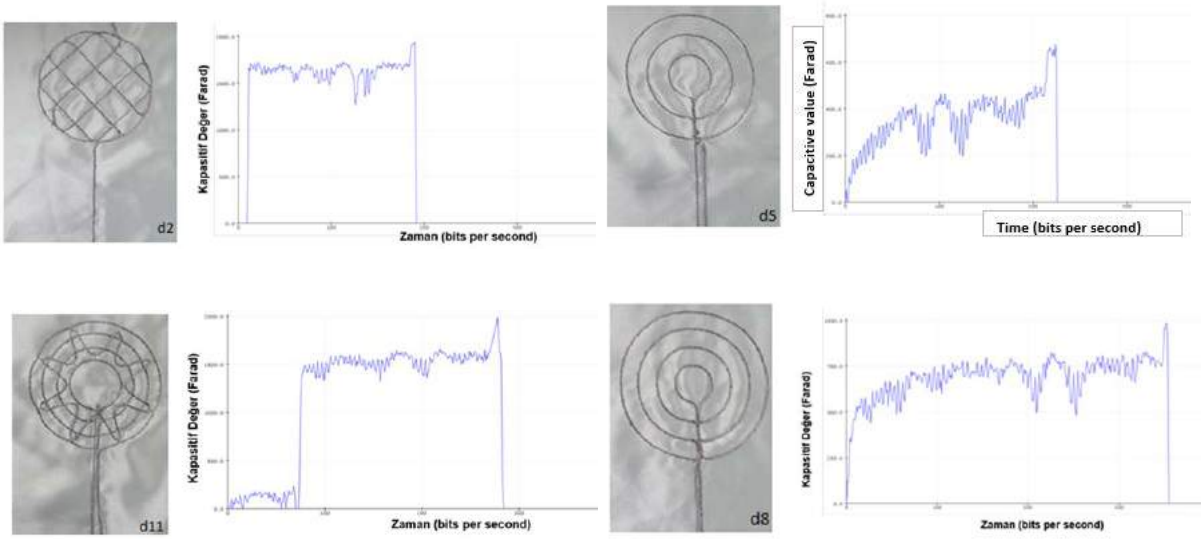

Figure 10. Analysis Results For Sensor Design Created Using The Number 1 Conductive Thread

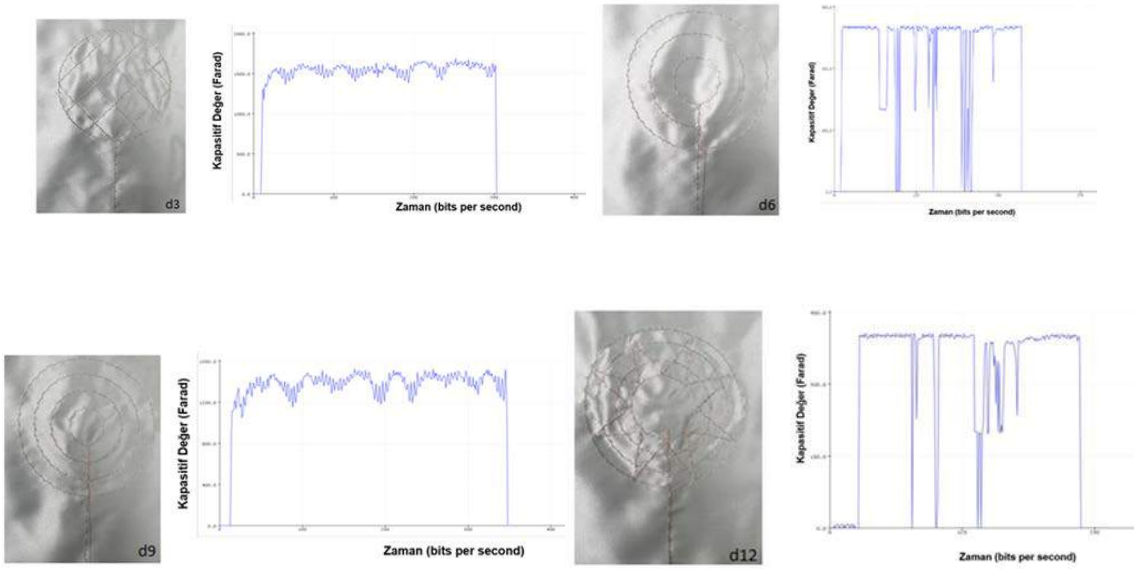

Figure 11. Analysis Results For Sensor Design Created Using The Number 2 Conductive Thread

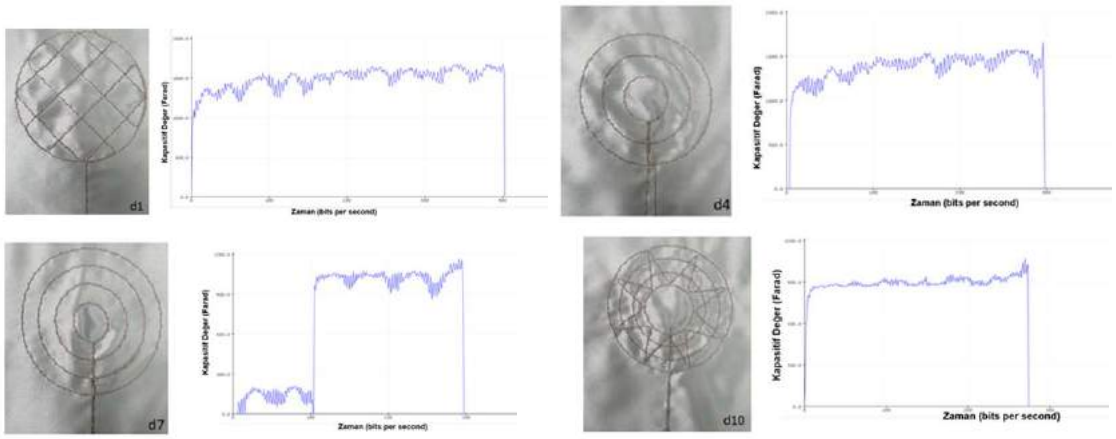

Figure 12. Analysis Results For Sensor Designs Created Using The Number 3 Conductive Thread

The most efficient pattern images determined as a result of the analyzes are given in Figure 13. The most productive thread was determined as the number 1 thread.

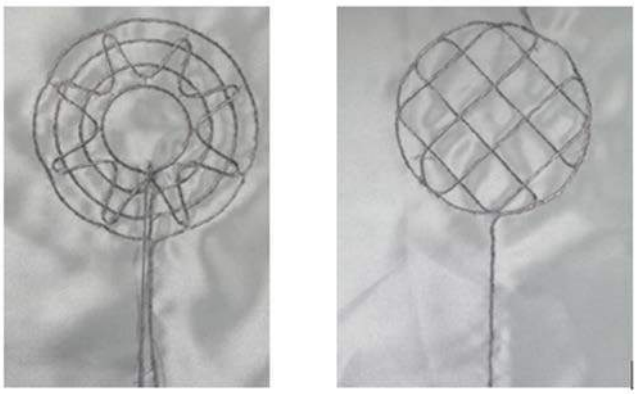

Figure 13. The most efficient pattern image determined as a result of the analyzes

4 different pattern studies were done by using the number 1 conductive thread in the embroidery machine. Electrical characterization tests were carried out for each pattern, and the capacitive changes in contact are given in Figure 14.

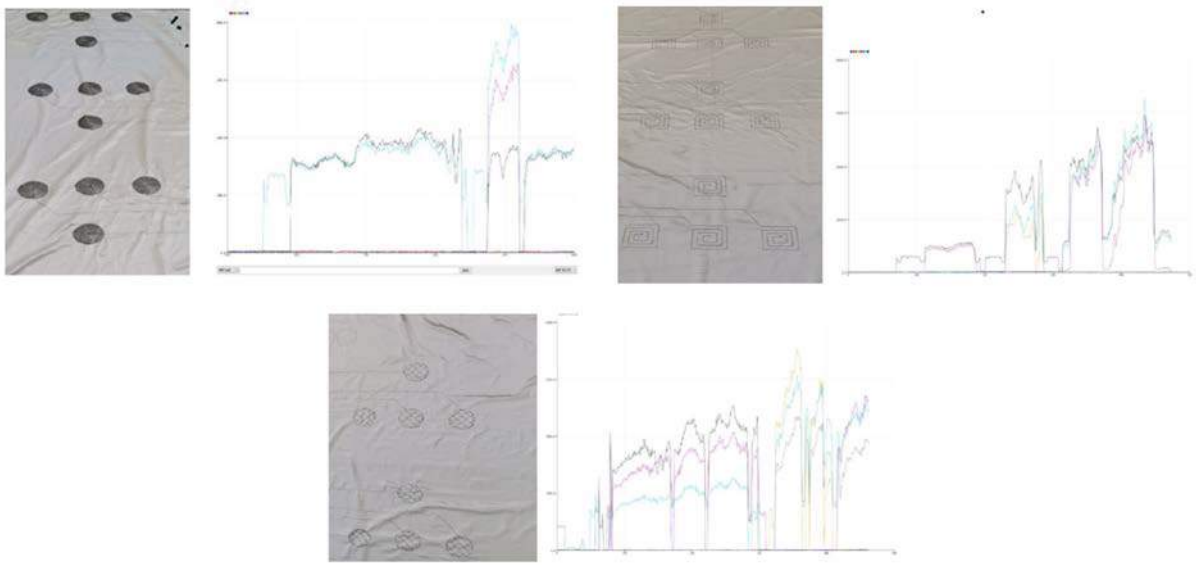

Figure 14. Capacitive change graphs of a9, c1, and c2 patterns

As a result of the analyzes and measurements made with the fabric of the a1 pattern, data could not be obtained due to the excessive contact of the conductive threads with each other.

4. CONCLUSION

Since the angular patterns act as antennas and lower the capacitive detection threshold, the studies were mostly carried out on round patterns. It was concluded that another important point for capacitive sensing is the specific properties of the conductive thread. Therefore, studies have been carried out by taking into account the specific properties of conductive threads. In this study, a flexible fabric-sensor structure used in the field of home textiles, which creates a signal from the mobility of people, has been developed.

ACKNOWLEDGMENT

This study is funded by the Zorluteks Textile Trade and Industry Inc. Scientific Research Project under grant no. TUBITAK TEYDEP 1501. (Project Number: 3181383)

REFERENCES

Skaer TL. Sleep deprivation and economic burden. In: Bianchi MT (ed). Sleep deprivation and disease: effects on the body, brain and behavior. Springer Science 2014, p.269-279

Lyznicki JM, Doege TC, Davis RM, Williams MA, for the Council on Scientific Affairs, American Medical Association. Sleepiness, driving, and motor vehicle crashes. JAMA 1998;279: 1908- 1913)

PREPARATION OF PVDF MICROSPHERES BASED ELECTROSPRAYING METHOD WITH HIGH CONTENT OF ELECTROACTIVE PHASE

Zhongchen HE[1], Elham MOHSENZADEH[1], François RAULT [1],Fabien SALAÜN [1]

[1] Univ. Lille, ENSAIT, ULR 2461 - GEMTEX - Génie et Matériaux Textiles, F-59000 Lille, France

Corresponding author: fabien.salaun@ensait.fr

Abstract: *Adding microspheres to poly (vinylidene fluoride) (PVDF) is a way to improve the piezoelectric properties of a PVDF membrane. This study prepared PVDF microspheres with the electrospraying method using PVDF/DMF/acetone solution. We discussed the influence of process parameters on the morphology and crystal structure of PVDF nanofibers. The morphology and crystal structure of PVDF nanofibers was determined by using SEM, DSC, and FTIR. The electrosprayed PVDF microspheres formation is affected by entanglement between polymer chains, solvent evaporation rate, crystallization rate, and electric field stretching. The optimized PVDF microspheres are obtained through the discussion of these four factors. The average diameter of microspheres is 546.0±190.9 nm, the F_{EA} is 92.1 %, and the Xc is 35.1 %.*

Keywords: *PVDF, electrospray, piezoelectric property, microsphere.*

1. INTRODUCTION

PVDF nanofibrous membranes (PVDFNM) with excellent piezoelectric performance can transfer daily mechanical energy into electrical energy, a new clean energy resource with huge potential. The piezoelectric performance of PVDF increases with the content of the electroactive phase (β+γ phase, F_{EA}). Thus, it is feasible to improve the F_{EA} by optimizing parameters (solvent properties, process parameters, nanoparticles, etc.) to enhance the piezoelectric performance of PVDFNM (Damaraju et al., 2013; Gee et al., 2018).

In addition, recent studies have shown that adding another layer to PVDFNM increases the piezoelectric properties of PVDFNM. The added layer is ceramic nanoparticles or a PVDF membrane doped with ceramic nanoparticles (Hu et al., 2013; Kalani et al., 2020). The ceramic nanoparticles have higher piezoelectric properties than PVDF but are toxic (PZT) or expensive ($BaTiO_3$). And the interface compatibility between ceramic materials and PVDF is not good. In this study, we prepared a kind of PVDF microspheres with high F_{EA}, which is a possible way to replace the ceramic materials and increase the piezoelectric performance of PVDFNM.

2. MATERIALS AND METHODS

2.1. Preparation of PVDF microspheres

PVDF pellets (Mw=220,000, Arkema Kynar 705, France) were used as the polymer. N, N-Dimethylformamide (DMF, CARLO ERBA, Mw=73.1 g/mol, assay≥99.9%), and acetone (CARLO ERBA, Mw=58.01 g/mol, assay≥99.8%) were used as the solvents.

The electrospinning machine (CAT000002, Electrospraying Instrument Kit Instruction Manual, Spraybase®, AVECATS, Kildare, Ireland) was used to prepare PVDF microspheres. The PVDF solutions with DMF/acetone=4:6 (volume ratio) were loaded into a 10 mL syringe and connected for injection to a 20-gauge needle. The parameters during the electrospinning process were fixed as fellow: feed rate of 1 $ml.h^{-1}$, tip-to-collector distance (TCD) was 18 cm, and the applied voltage was 16 kV. The nanofiber samples were collected on a metal plate wrapped in aluminum foil.

2.2. Thermal Properties

Differential Scanning Calorimetry (DSC 3+, Mettler Toledo, Columbus, OH, USA) was used to determine the crystallinity of the PVDF samples. The samples were heated up from 10 ℃ to 200 ℃ at a rate of 10 ℃/min and then cooled from 200 ℃ to 10℃ at a rate of 30 ℃/min in a nitrogen atmosphere.

Fourier-transform infrared spectroscopy (FTIR, Nexus-560 spectroscopic, Nicolet, Madison, USA) analysis was performed under 64 scans with a resolution of 4 cm^{-1}, and the wavenumber ranged from 400 to 1600 cm^{-1}.

2.3. Morphology

Scanning Electron Microscopy (SEM, Phenom ProX, ThermoFischer Scientific, US) was used to characterize the morphology of PVDF nanofibers. The average diameter of PVDF microspheres was automatically determined by Image J (National Institutes of Health, MD, USA).

3. RESULTS AND DISCUSSION

The SEM images show that the PVDF microspheres were obtained when the PVDF concentration was 4 % to 10 %. Nanofibers appeared when the PVDF concentration was higher than 12 % (Figure 1). This phenomenon is attributed to the entanglement between polymer chains. As the PVDF concentration decreases, the entanglement between the macromolecular polymer chains decreases, an advantage in forming microspheres (Gupta et al., 2005).

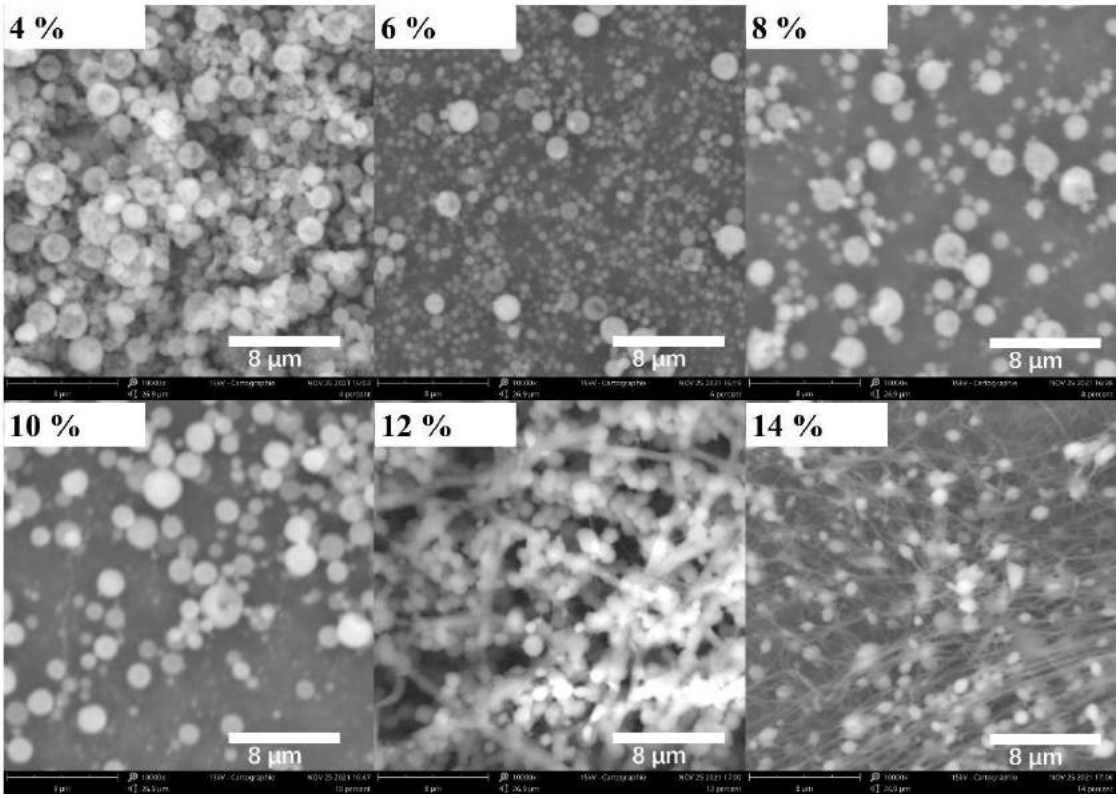

Figure 1. The SEM images of PVDF samples under different PVDF concentrations

Table 1. The diameter, F_{EA}, F_{β}, $F_{\gamma,}$ and Xc of PVDF microspheres under different PVDF concentrations (Adhikary et al., 2015; Barrau et al., 2018)

Concentration	Diameter of	FTIR			DSC
(%)	microspheres (nm)	F_{EA} (%)	Fβ (%)	Fγ (%)	Xc (%)
4	1036.3±500.7	89.7	53.2	25.9	39.5
6	546.0±190.9	92.1	53.8	30.7	35.1
8	1156.9±456.4	90.3	54.2	23.5	35.6
10	1681±765.5	88.4	52.0	26.3	33.8
12	-	89.5	44.4	33.9	37.6
14	-	89.6	46.1	31.9	39.1

With the increase in PVDF concentration, the average diameter of electrospray microspheres decreased to a minimum of 6 %. And F_{EA} increased to the maximum value of 6 % (Table 1). When the PVDF concentration increased from 4 % to 6 %, the solvent content in the PVDF solution decreased. This leads to the complete volatilization of the solvent during the electrospray process, and the PVDF is solidified before it is wholly crystallized, resulting in a decrease in Xc. However, the stretching of the electric field on the microspheres is enhanced, causing a decrease in the average diameter of the microspheres and an increase in F_{EA}. As the concentration increased from 6 % to 10 %, the solvent evaporated faster, causing faster solidification of the microspheres. It was manifested as a decrease in Xc and an increase in the average diameter of microspheres. Moreover, the molecular chains inside the microspheres were not stretched and polarized by the electric field, resulting in a decrease in F_{EA}. It further increased the PVDF concentration, the $F_{EA,}$ and Xc increase, which is attributed to the formation of nanofibers.

4. CONCLUSION

This work prepared electrospraying PVDF microspheres with a high electroactive phase from DMF/acetone=4/6 solution. The minimum average diameter of microspheres is 546.0±190.9 nm, and the maximum of FEA is 92.1 %, Xc is 35.1 %. We pointed out that four factors affect the electrospray results: entanglement between polymer chains, solvent evaporation rate, crystallization rate, and electric field stretching. In the later stages of the study, the influence of PVDF microspheres on multilayer PVDF membranes will be discussed.

REFERENCES

Adhikary, P., Garain, S., & Mandal, D. (2015). The co-operative performance of a hydrated salt assisted sponge like P(VDF-HFP) piezoelectric generator: An effective piezoelectric based energy harvester. *Physical Chemistry Chemical Physics*, *17*(11), 7275–7281.

Barrau, S., Ferri, A., Da Costa, A., Defebvin, J., Leroy, S., Desfeux, R., & Lefebvre, J. M. (2018). Nanoscale Investigations of α- And γ-Crystal Phases in PVDF-Based Nanocomposites. *ACS Applied Materials and Interfaces*, *10*(15), 13092–13099.

Damaraju, S. M., Wu, S., Jaffe, M., & Arinzeh, T. L. (2013). Structural changes in PVDF fibers due to electrospinning and its effect on biological function. *Biomedical Materials (Bristol)*, *8*(4).

Gee, S., Johnson, B., & Smith, A. L. (2018). Optimizing electrospinning parameters for piezoelectric PVDF nanofiber membranes. *Journal of Membrane Science*, *563*(2), 804–812.

Gupta, P., Elkins, C., Long, T. E., & Wilkes, G. L. (2005). Electrospinning of linear homopolymers of poly (methyl methacrylate): Exploring relationships between fiber formation, viscosity, molecular weight and concentration in a good solvent. *Polymer*, *46*(13), 4799–4810.

Hu, P., Wang, J., Shen, Y., Guan, Y., Lin, Y., & Nan, C. W. (2013). Highly enhanced energy density induced by hetero-interface in sandwich-structured polymer nanocomposites. *Journal of Materials Chemistry A*, *1*(39), 12321–12326.

Kalani, S., Kohandani, R., & Bagherzadeh, R. (2020). Flexible electrospun PVDF-BaTiO3hybrid structure pressure sensor with enhanced efficiency. *RSC Advances*, *10*(58), 35090–35098.

PRODUCTION OF MULTILAYER MICROCAPSULES CONTAINING N-EICOSANE AND TEXTILE APPLICATION

Berrak Buket AVCI[1], Gökhan ERKAN[1]

[1] Dokuz Eylul University, Department of Textile Engineering, İzmir, Türkiye

Corresponding author: gokhan.erkan@deu.edu.tr

Abstract: *This study aimed to investigate the production of multi-layered capsules containing two different active substances and the possibilities of using the obtained capsules in the textile sector, thereby balancing the body temperature with the phase changing material to be used, and to provide a second feature in addition to balancing the body temperature with the other active substance. In this study, a phase change material as the first core material was microencapsulated with melamine formaldehyde prepolymer, then the resulting microcapsules were subjected to a second microencapsulation process to form the mandarin oil as a second core material and ethyl cellulose as a second capsule wall. Single layer microcapsules were produced according to the in-situ polymerization method, and multilayer microcapsules were produced according to the coaservation method. Particle size and distribution analysis, DSC, FT-IR and SEM were performed to single layer and multilayer microcapsules. Also, imaging with a thermal camera were applied to detect the capsule effectiveness of microencapsulated fabrics.*

Keywords: *n-eicosane, mandarin oil, phase change materials, multilayer microcapsule, in-situ, textile*

1. INTRODUCTION

Energy storage technologies are increasing attention due to the trend towards renewable energy sources. Energy storage technologies are very promising tools in terms of providing the low carbon emission needed in the future (Turan & Yönetken, 2016). Thermal energy storage is a method of storing energy by raising the temperature of the object or changing its phase (Esgel, 2014).

Phase change materials are materials that have the ability to store a high amount of energy during phase change and to release the stored energy to the environment. The most suitable phase change agents for textile products are solid-liquid phase change agents (Demirbağ, 2014). Phase change materials with melting temperatures in the range of 15-35 °C are the most suitable materials for use in textile materials. The reason for this is that these temperatures are the most suitable values for body temperature (Alay, 2010).

Microencapsulation technology finds wide use in food, medicine, cosmetics, agriculture and other industries (Enginar & Çayır, 2016). Many methods such as coacervation, spray drying, emulsion polymerization, *in-situ* polymerization are used for the microencapsulation of the core material (Bansode et al., 2010; Eyüpoğlu & Kut, 2016). *In-situ* polymerization, interfacial polycondensation, emulsion polymerization, spray-drying and coacervation methods are mostly used in the encapsulation of phase change materials (Yataganbaba et al., 2017).

2. MATERIALS AND METHODS

2.1. MATERIALS

Mandarin oil (Sigma Aldrich) and n-eicosane (Merck) were used as the core materials. Melamin (Sigma Aldrich), formaldehyde (>34.5 %, Sigma Aldrich) and ethyl cellulose (viscosity 4 cp, Sigma Aldrich) were used as the shell materials. Tween 20 (Merck) was used as a surfactant and ethyl acetate (≥ 99.5 %, Merck) was used as a solvent. Pericoat Crosslinker MV (Dr. Petry) was used as binder. 100

% cotton fabric was used as textile material. All other chemicals used during this study were laboratory commercial grades.

2.2. METHODS

2.2.1. Production of Single Layer and Multilayer Microcapsules

Single Layer Microencapsulation: Melamine-formaldehyde prepolymer was used as the shell material and n-eicosane was used as the core material in single-layer microcapsules by *in-situ* polymerization method. For this purpose, melamine-formaldehyde prepolymer was produced at 1:3 molar ratio. Melamine:formaldehyde/n-eicosane ratio was produced at 1:3/0.035 molar ratio, it was used for the production of single-layer microcapsules. Single layer microcapsules was producted to modified method according to reference (Erkan et al., 2010).

Multilayer Microencapsulation: Single layer microcapsules and mandarin oil were used as a core material and ethyl cellulose was used as a second shell material by coaservation method. For this purpose, A ratio 1:2 (w/w) was used for the ethyl cellulose:core materials. The core materials were mixed according to the ratio of 1:1 (w/w). In addition, this method had been modified according to reference (Türkoğlu et al., 2017).

2.2.2. Application to Textile Material

The produced microcapsules were transferred to 100% cotton fabric by impregnation method. The pH of the impregnation liquor was adjusted to pH 5.5 with acetic acid. Impregnation of microcapsules on textile material were given in Table 1.

Table 1. Impregnation of microcapsules on textile material

Microcapsule (g/l)	Binder (g/l)	Pick Up (%)	Drying + Fixation	
			Temperature (℃)	Time (min)
40	10	75	150	5

2.2.3. Experimental Analysis

Particle size and distribution analysis, DSC, FT-IR and SEM were performed to single layer and multilayer microcapsules. And also, imaging with a thermal camera were applied to detect the capsule effectiveness of microencapsulated fabrics.

3. RESULTS AND DISCUSSION

3.1. Particle Size and Distribution Analysis

When Figure 1 were examined, it was seen that the dimensions of single layer microcapsules were between 1.98-17.38 μm and the peak value was 6.01 μm, multilayer microcapsules were owned dimensions between 2,60 -116.21 μm and the peak value was 10.27 μm. According to the results of the analysis, it was observed that the multilayer microcapsules had a larger particle size than the single layer microcapsules. This was thought to be due to the fact that a multilayer was formed on top of the single layer microcapsules.

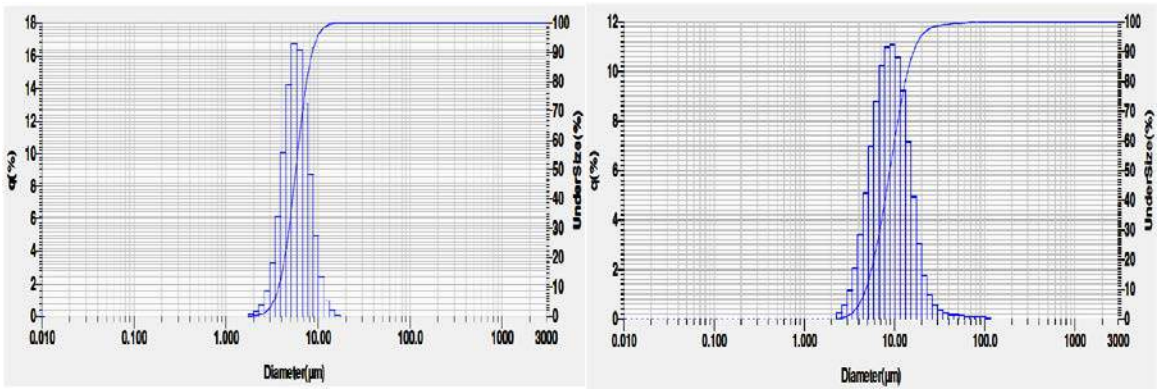

(a) **(b)**

Figure 1. Partical size and distribution analysis of (a) single layer and (b) multilayer microcapsules

3.2. DSC Analysis

When investigation of DSC analysis of single layer and multilayer microcapsules (Figure 2 and Figure 3), phase change had been observed in both microcapsules. Phase changes in both microcapsules occurred in the body temperature range. However, it had been observed that the ΔH value occuring during the phase change of the single layer microcapsule was higher compared to the multilayer microcapsule. It was thought that the reason for the small amount of enthalpy change (ΔH) in the multilayer might be due to the small amount of single layer microcapsule used during microencapsulation. Therefore, it had been concluded that the ΔH value might increase by increasing the amount of single layer microcapsule used.

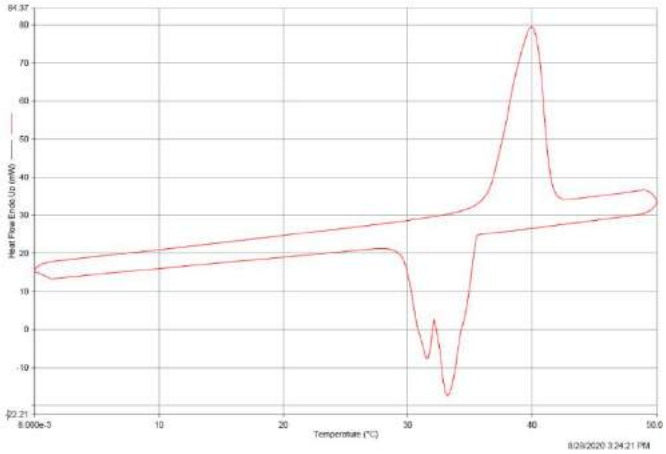

Figure 2. DSC analysis of single layer microcapsules (melting temperature range 36.5 – 41.5 ºC and enthalpy change (ΔH) of melting 90.64 J/g, freezing temperature range 31.5 – 35.5 ºC and enthalpy change (ΔH) of freezing 88.06 J/g)

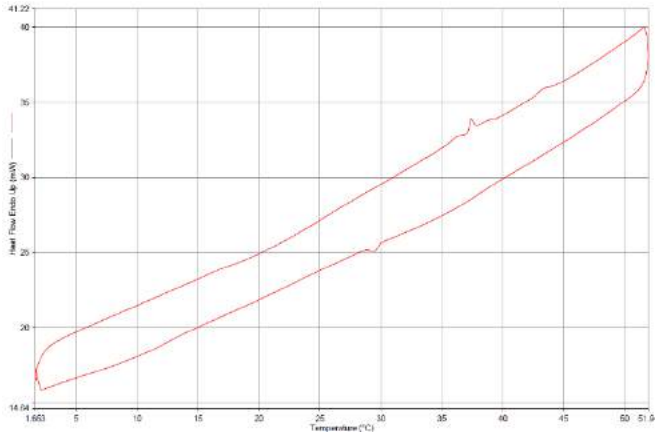

Figure 3. DSC analysis of multilayer microcapsules (melting temperature range 37.1 – 37.9 ºC and enthalpy change (ΔH) of melting 1.78 J/g, freezing temperature range 29.6-30.33 ºC and enthalpy change (ΔH) of freezing 4.00 J/g)

3.3. FT-IR Analysis

FT-IR spectra of single and multilayer microcapsules were given in Figure 4. When the FT-IR spectra of the two samples were examined, the peaks for the N-H, C-N, –C=N- bonds originated from the melamine formaldehyde prepolymer and the multilayer capsules peaked at the same places in the FT-IR analysis, it was showed that the microencapsulation was successful. It was observed that the area under the peaks was less. In the spectrum of the multilayer microcapsule, it was seen that the peaks originating from the ester carbonyl functional groups of triglycerides, which the main components of oils, and the peaks were originating from the terpene in mandarin oil. In addition, there were peaks originating from the pyran ring of cellulose in the spectrum of multilayer microcapsules. When the two spectra were compared, the peaks of single layer capsules, the peaks of mandarin oil and the peaks of cellulose in the spectrum of multilayer microcapsules were observed in all spectrum. According to the FT-IR spectra, it was concluded that the microencapsulation was successful.

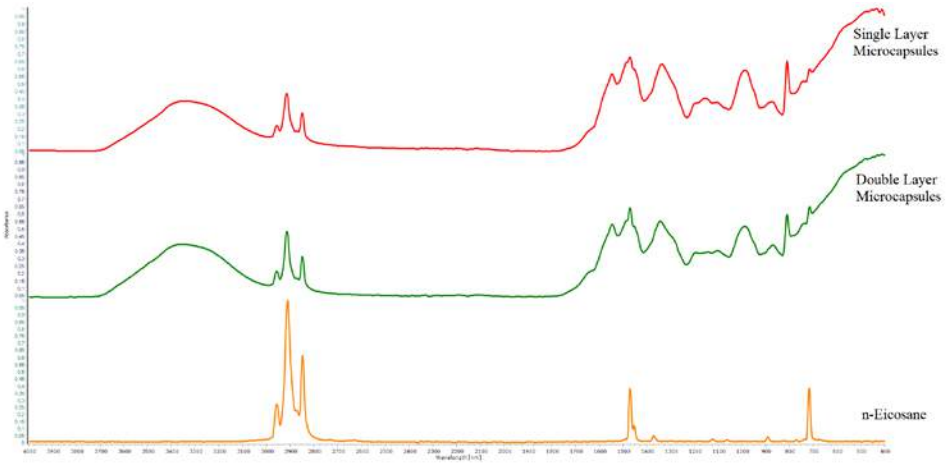

Figure 4. FT-IR analysis of single layer microcapsules, multilayer microcapsules and n-eicosane

When the FT-IR results of single layer (melamine formaldehyde/n-eicosan) microcapsules were examined, it was observed that 3343 cm^{-1} peak in the hydrogen bond region was caused by N-H stretching vibration, 2954 cm^{-1}, 2919 cm^{-1}, 2848 cm^{-1} peaks were caused by C-H stretching. It has been observed that the peaks of 1547 cm^{-1}, 1487 cm^{-1}, 1471 cm^{-1} occured as a result of stresses

originating from aliphatic and aromatic double bonds. The 1547 cm^{-1} peak was thought to be due to in-plane –C=N- vibrations for a triazine ring system. The 1341 cm^{-1} peak could be attributed to in-plane C-H deformations of heterocyclic rings. 1159 cm^{-1}, 1000 cm^{-1} peaks were considered to be C-N and C-O stretching vibrations. The 811 cm^{-1} peak was thought to be related to the out-of-plane deformation vibration of the triazine ring system. It was estimated that the 716 cm^{-1} peak originates from the C-H bonds in the fingerprint region. When the FT-IR spectrum of the single layer microcapsules was examined, it was seen that the melamine formaldehyde prepolymer and n-eicosan were successfully microencapsulated and it was consistent with the information available in the literature (Moheddes et al., 2014). When the FT-IR spectrum of the multilayer microcapsules was examined, it was caused by the 3473 cm^{-1} N-H stretching vibration in the hydrogen bond region, the 2973 cm^{-1} and 2869 cm^{-1} peaks were observed the asymmetric/symmetric stretching vibration of the aliphatic C-H bond in the CH_2 groups and the –OH stretching in alcohol and phenol. It was determined that the 1736 cm^{-1} peak was caused by the ester carbonyl functional groups of triglycerides. Triglycerides are the main components in oils. It was determined that 1552 cm^{-1} occurred as a result of stresses originating from aromatic and aliphatic double bonds. 1457 cm^{-1}, 1374 cm^{-1}, 1353 cm^{-1} peaks were thought to be caused by C-O-C stresses originating from the pyran ring in cellulose. It was thought that the terpene content in 1055 cm^{-1} peak mandarin oil may be due to alkane groups. The 920 cm^{-1},883 cm^{-1},812 cm^{-1} peaks were thought to be caused by the stresses in the C-H bonds in the fingerprint region. When the FT-IR spectra of multilayer microcapsules were examined, it was seen that the FT-IR spectra of mandarin oil and ethyl cellulose capsules in the literature were examined (Öge, 2017; Carbajal-Valdez et al., 2017), and when the spectra of single layer and multilayer microcapsules were examined together, the microencapsulation of multilayer microcapsules was found to be successful.

3.4. SEM Analysis

SEM images of the single layer and multilayer microcapsules were given in Figure (5-6). When the Figure 5 was examined, it was seen that the single layer microcapsules were smooth and spherical, and the microencapsulation was successful and also it had been observed that the microencapsulation of multilayer microcapsules could be achieved by coaservation method.

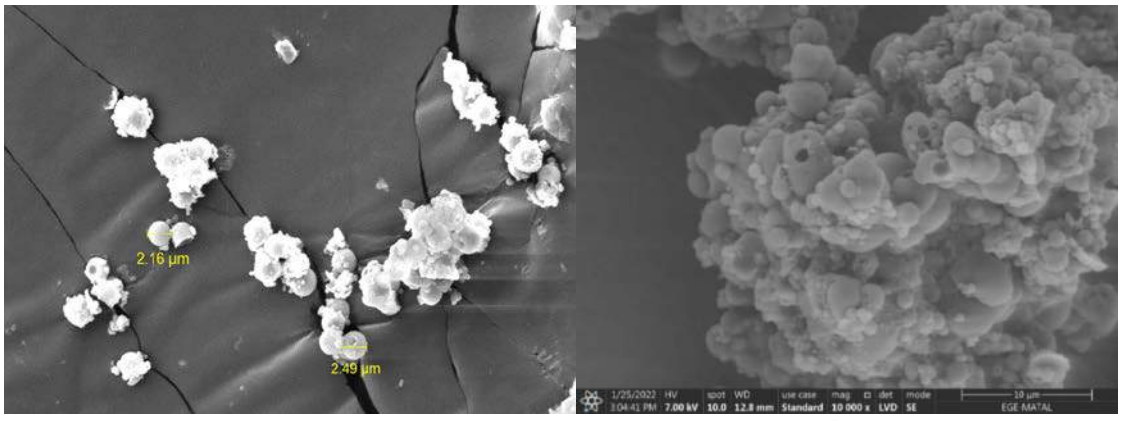

(a) **(b)**

Figure 5. SEM image of (a) single layer microcapsules and (b) multilayer microcapsules before impact force

When Figure 6 was examined, the presence of a multilayer in the microcapsules broken after the impact force has been detected.

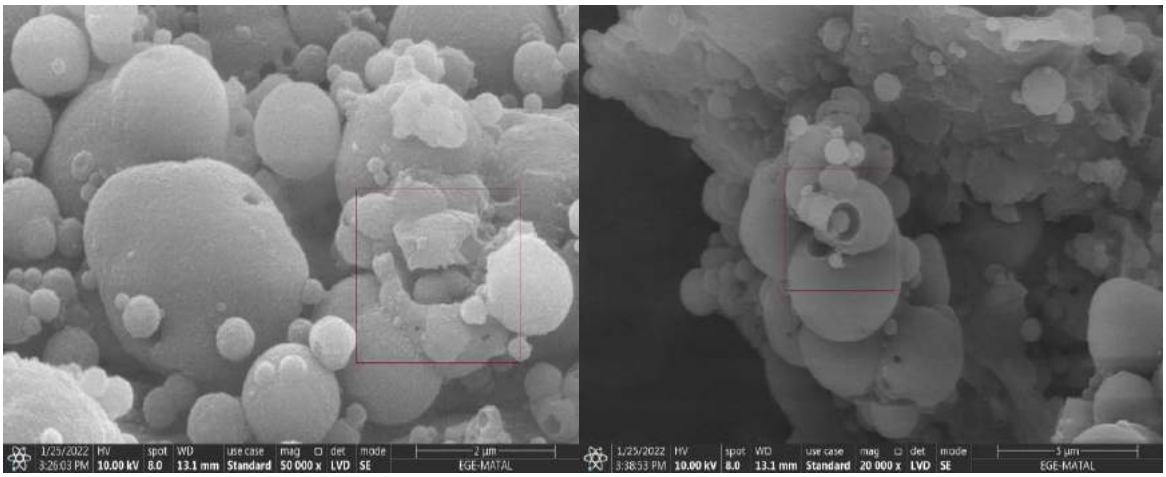

Figure 6. SEM images of multilayer microcapsules after impact force

3.5. Imaging with a Thermal Camera

Fabric temperature of thermal camera images were given in the Table 2 and fabric images of thermal camera were given in Figure 7. When Table 2 and Figure 7 were examined, it was seen that the temperatures of the fabric without microcapsules were the highest at all temperatures. It was observed that the temperature values of both microcapsules were close to each other in the fabrics with microcapsule applied. However, it was determined that the temperature value of the fabric to which the single layer microcapsule was applied showed a lower temperature value than the fabric to which the multilayer microcapsule was applied. It has been estimated that this may be due to the small amount of single layer microcapsules used while producing multilayered microcapsules.

Table 2. Fabric temperature of thermal camera images

	Without Microcapsule	Single Layer	Double Layer
Room Temperature	23.0	23.8	23.9
30 ºC	29.2	28.4	29.0
33 ºC	34.9	32.3	33.8
35 ºC	35.8	34.4	35.6
37 ºC	37.7	35.9	35.5
40 ºC	41.7	39.9	39.4
43 ºC	44.0	42.5	41.9
45 ºC	46.8	43.5	42.6

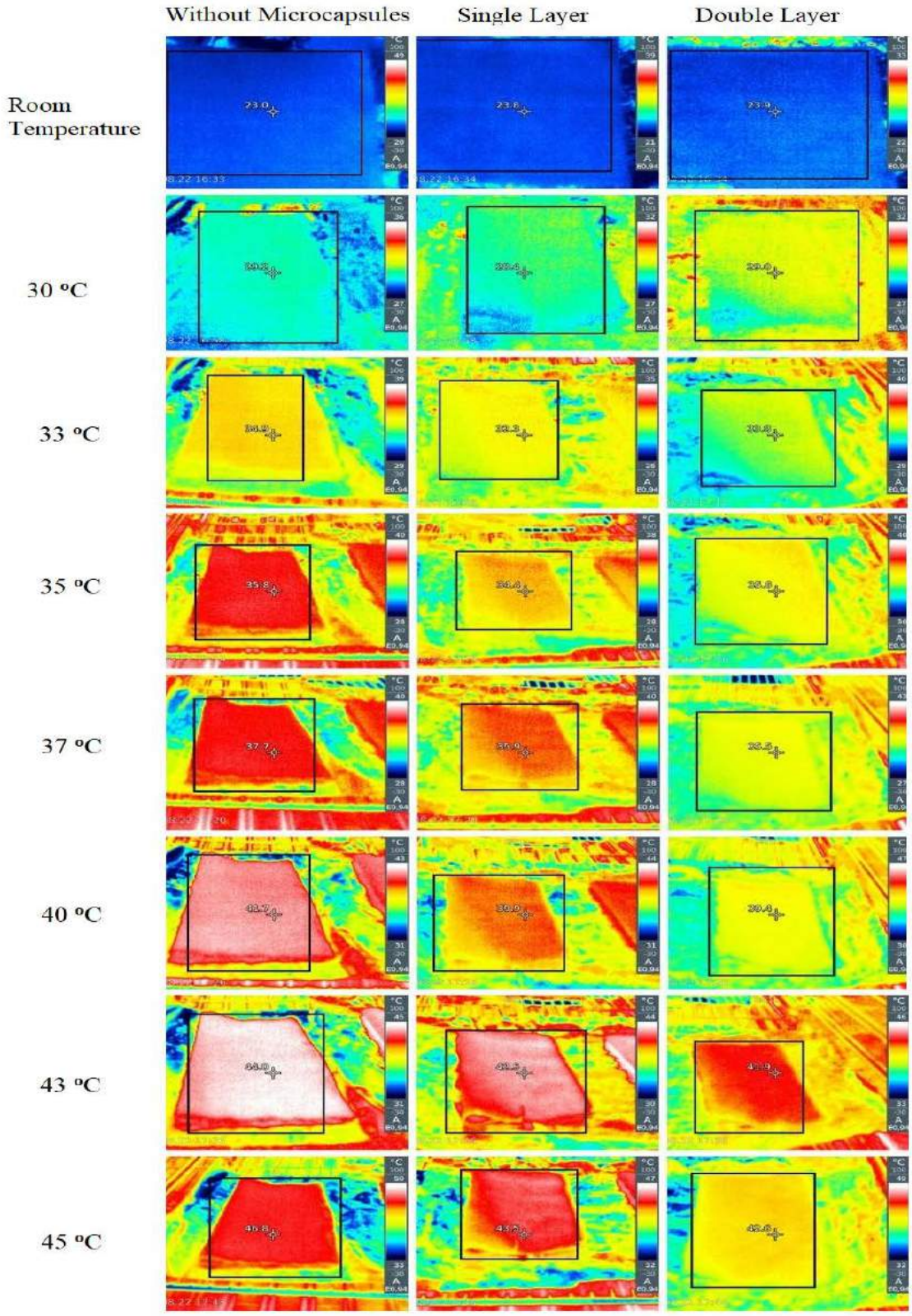

Figure 7. Thermal camera images of fabrics

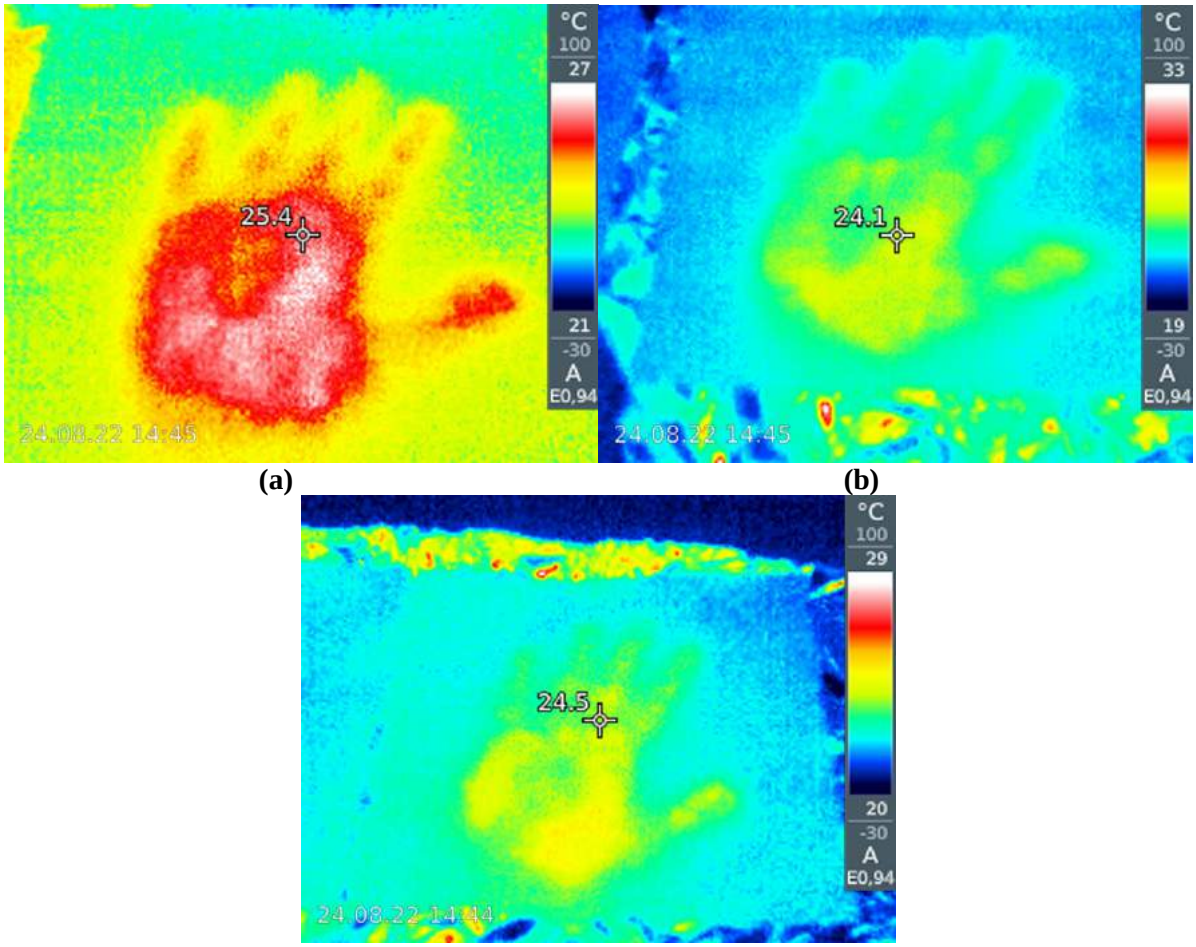

Figure 8. The image of the fabrics was taken with a thermal camera after the hand was pulled over: (a) the fabric without microcapsule, (b) the fabric with single layer micropsules, (c) the fabric with multilayer microcapsules

Also, at room temperature, the hand was pressed on the fabrics for 45 seconds in order to see the reaction of the fabrics to body heat, and after 15 seconds, the image of the fabrics was taken with a thermal camera after the hand was pulled over. When Figure 8 was examined, it was determined that the temperature of the fabric without microcapsule was higher than the fabrics with microcapsule transferred after 15 seconds. It was observed that the temperature values of the fabric with single layer microcapsules and the fabric with the multilayer microcapsules were close to each other.

4. CONCLUSION

In this study, the production of multilayered microcapsules containing two core material (phase change materials and mandarin oil) and their use in the textile industry were investigated. Thus, it was aimed to produce two different active substances in a single process, to obtain them in a single step with less chemical load, cost and energy savings, and to be usable in textiles.

Multilayered microcapsules could be produced according to the particle size and distribution analysis, SEM and FT-IR results obtained. In the thermal camera images taken after the microcapsules were transferred to the fabric, it was seen that both single layer and multilayer microcapsules were successful in regulating the thermal balance. However, according to the obtained DSC results, it was

thought that changes should be made in the formulation to increase the latent heat (enthalpy change-ΔE) of the multilayer microcapsule.

This situation requires detailed studies in later such as improving the formulation and increasing the stored latent heat and also the characterization of the multilayer microcapsules which are transferred to the fabric.

In addition, in future studies, thermal resistance measurements (T-history and alambeta analysis) and washing fastness (resistance to at least 5 washings) of the microcapsule transferred fabric will be performed. The properties added by the second active substance to the microcapsule transferred fabrics will be investigated. Therefore, further investigations might be planned to study extensively in different concentrations and conditions.

REFERENCES

Alay, S. (2010). Isıl Enerji Depolama Özellikli Mikrokapsüller İçeren Akıllı Tekstil Ürünlerinin Geliştirilmesi. *T.C. Süleyman Demirel Üniversitesi Fen Bilimleri Enstitüsü Doktora Tezi*, Isparta.

Bansode, S. S., Banarjee, S. K., Gaikwad, D. D., Jadhav, S. L., Thorat, R. M. (2010). Microencapsulation: a review. *International Journal of Pharmaceutical Sciences Review and Research, 1(2),* 38-43.

Carbajal-Valdez, R., Jiménez-Pérez, J. L., Cruz-Orea, A., Correa-Pacheco, Z. N., Alvarado-Noguez, M. L., Romero-Ibarra, I. C., Mendoza-Alvarez J. G. (2017). Thermal properties of centrifuged oils measured by alternative photothermal techniques. *Thermochimica Acta*, 657, 66–71.

Demirbağ, S. (2014). Kompleks Koaservasyon Metodu İle Isı Depolama Ve Güç Tutuşur Özellikli Mikrokapsül Üretimi Ve Tekstil Uygulamaları. *T.C. Süleyman Demirel Üniversitesi Fen Bilimleri Enstitüsü Yüksek Lisans Tezi*, Isparta.

Enginar, H. & Çayır, M. (2016). Melamin formaldehit reçinesiyle ticari esans mikrokapsülasyonu ve kararlılığının incelenmesi. *Afyon Kocatepe Üniversitesi Fen ve Mühendislik Bilimleri Dergisi, 16(021201),* 212-221.

Esgel, H. (2014). Kordiyerit Esaslı Seramik Malzemeden Yapılmış Termal Enerji Depolama Sisteminin Analizi. *İstanbul Teknik Üniversitesi, Enerji Enstitüsü, Yüksek Lisans Tezi*, İstanbul.

Eyüpoğlu, Ş. & Kut, D. (2016). Mikrokapsülasyon teknolojisi ve tekstil sektöründe kullanımı, *İstanbul Ticaret Üniversitesi Fen Bilimleri Dergisi, 15(29),* 09-28.

Mohaddes, F., Islam, S., Shanks, R., Fergusson, M., Wang, L., Padhye, R. (2014). Modification and evaluation of thermal properties of melamineformaldehyde/n-eicosane microcapsules for thermo-regulation applications. *Applied Thermal Engineering*, 71, 11-15.

Öge, A. (2017). Kapsülasyon Teknolojisi Kullanarak Spor ve Boş Zaman Giysilerinin Fonksiyonelleştirilmesi. *T.C. Dokuz Eylül Üniversitesi Fen Bilimleri Enstitüsü Yüksek Lisans Tezi*, İzmir.

Turan, D. & Yönetken, A. (2016). Enerji depolama sistemlerinin araştırılması ve analizi. *Afyon Kocatepe Üniversitesi Fen ve Mühendislik Bilimleri Dergisi, 16*, 113-121.

Türkoğlu, G. C., Sariisik, A. M., Erkan, G., Kayalar, H., Kontart, O., Öztuna, S. (2017). Determination of Antioxidant Capacity of Capsule Loaded Textile. *Indian Journal of Fibre and Textile Research,* 42, 189-195.

Yataganbaba, A., Ozkahraman, B., Kurtbas, İ. (2017). Worlwide trends on encapsulation of phase change materials: A bibliometric analyses (1990-2015). *Applied Energy, 185*, 720-731.

DEVELOPMENT OF ELECTROTEXTILE SURFACE AND PRODUCT FOR NEWBORN PHOTOTHERAPY TREATMENTS

Ozan KAYACAN[1], Funda ERDOĞAN[2], Nuray DUMAN[2], Bekir BOYACI[3], Tuğçe UYSAL[3]

[1] Dokuz Eylul University, Textile Engineering Department, Izmir, Turkey
[2] Dokuz Eylul University, Faculty of Medicine, Izmir, Turkey
[3] Sun Textile R&D Center, Izmir, Turkey

Corresponding author: ozan.kayacan@deu.edu.tr

Abstract: *Neonatal jaundice is a condition that occurs with yellowing of the skin, with increased levels of bilirubin in the blood in about two-thirds of infants during the first week of life. However, in some cases, it can reach dangerous levels by causing permanent damage to the brain. Phototherapy is the process of exposing the skin to light with a specific wavelength band and it is one of the most commonly used form of jaundice treatment. Today, fluorescent tubes or halogen lamps are used for this kind of treatment. In recent years, light-emitting diodes (LEDs) have been preferred as a new light source. Unfortunately, infants with severe jaundice cases should stay at hospital with a limited interaction with mothers and these situations cause various disadvantages for both babies and mothers. Also traditional photothreaphy devices serve in an unconfortable circumstances because of limited softness. In this study, It is aimed to develop an electrotextile surface produced from 3-D warp knit fabric including blue LED lights with a certain wavelength for phototherapy treatment that is light, easy to install, breathable, washable and also be used as a bed, which can wrap the baby during breastfeeding in the mother's lap, suitable for home and hospital use.*

Keywords: *Phototherapy, neonatal jaundice, electrotextile, medical textiles.*

1. INTRODUCTION

Textile products, which are traditionally used for covering, protection and decoration purposes, are produced with new features that will meet different needs in addition to conventional functions. Technical and smart textiles, which have been developed due to various needs and have different functional properties according to application area, have gained importance in the textile sector in recent years. Smart textiles are the systems formed by integrating various electronic components into textile materials. The medical/health sector is among the important markets for smart and interactive textile products.

Jaundice is one of the most common problems for newborns. About 3 in 5 babies (60 percent) have jaundice. It is a condition that the infant's skin and the white parts of the eyes look yellow. It's caused by the build-up of a substance in the blood called 'bilirubin'. Bilirubin is the end product of red-blood-cell (hemoglobin) breakdown and it must be conjugated in the liver and excreted from the body. Because of the late development of the newborn's liver, especially premature infants suffer from serious health problems as a result of excess bilirubin level in the blood. For instance if the bilirubin level is above critical level in the newborn's blood, the baby need quick treatment to preventing the development of bilirubin encephalopathy (Akobeng, 2005; Agrawal et al., 2001).

There are various methods for newborn jaundice treatment such as exchange transfusion, pharmacological ways and also phototheraphy. Phototherapy is a treatment that allows the bilirubin under the skin to be broken down by a special light that illuminates the baby's body. With the phototherapy method, photoisomers of bilirubin are formed and eliminated from the body without the need for liver conjugation. In this method, LEDs and fiberoptic fibers are also used besides traditional

lightsources such as fluorescent and halogen lamps (Chang et al., 2005; Dani et al., 2001). There are risks such as burns, DNA mutations and retinal damage in traditional methods. Although fiberoptic fibers eliminate these risks, they are also functional disadvantageous due to their low spectrum. Phototherapy devices are available in the market with a light source from above, such as a spot/tunnel, or as systems such as pads/blankets as seen on Figure 1.

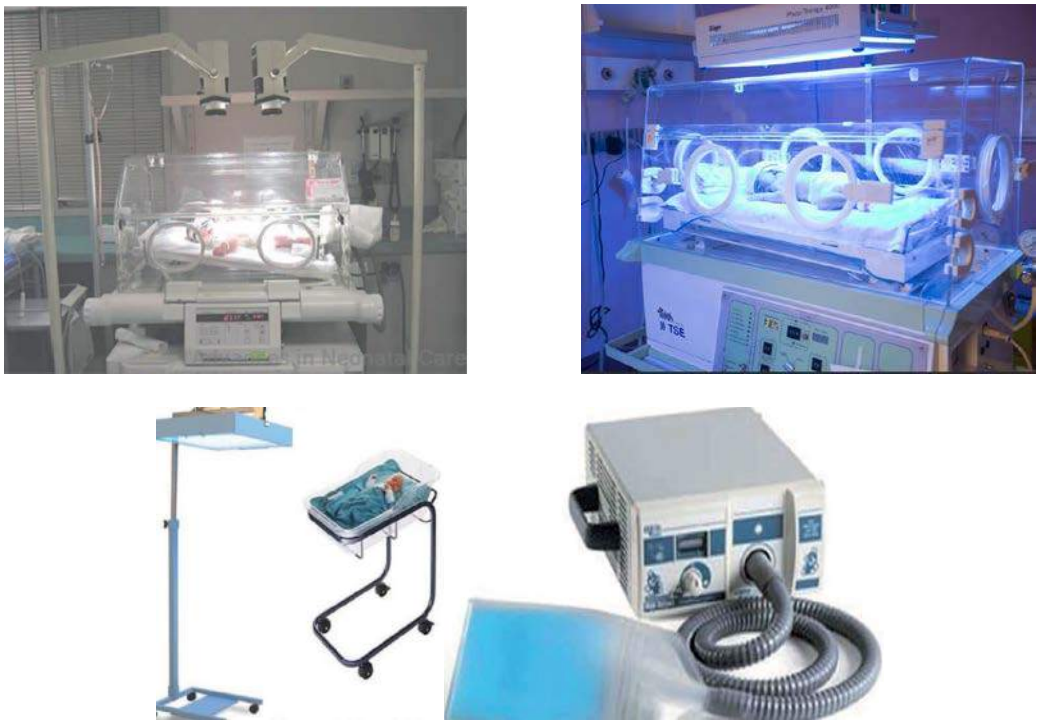

Figure 1. Traditional photothrephy devices with various light sources (Maisels & McDonagh, 2008; Stokowski, 2011)

Unfortunately the traditional devices allow only hospital usage. There are only various prototypes with limited home-usage. On the other hand, It is also very important that some treatment processes can be provided at home, and this situation has become more and more important especially during the pandemic situation in recent years (Noureldein et al., 2021). Also spot/tunnel type devices have large dimensions, pad/blanket type devices negatively affect the baby's sleeping comfort due to the transparent hard plastic surface that transmits the light upwards. In cases where intense phototherapy is required for treatment, the light source is given to the baby from the bottom and the top. Intensive phototherapy is performed with the use of two devices or two-way light sources as seen on Figure 2 (Wang et al., 2021; Çoban et al., 2014; Hansen, 2010; Arnolda et al., 2018).

Figure 2. Intensive phototheraphy devices with two-way lightsource (Stokowski, 2011)

In the early stages of the developments of phototheraphy treatment, various lightsources have been appied. As a result of the recent developments especially in the lighting technologies, LED light sources have become an inovative alternative for the photheraphy applications due to their various adventages. These advantages can be summarized as folllows;

- LED lights are suitable for neonatal jaundice treatment and are long-lasting. The average life of an LED light is 10,000 hours.
- Blue LED light sources have a wavelength of 450-460 nm and can be defined as one of the most effective light sources for phototherapy application.
- It can be positioned close to the baby as it emits little infrared (IR) radiation and does not emit UV radiation.
- Also thanks to its silicone strip forms and easy mounting features the LED strips can be easily folded. For this reason, they have a potential to be adapted to portable products.
- Since the energy requirement of the system is extremely low, it is possible to convert the product into a completely portable format by using external energy sources (battery/portable power supply etc.) in case of need.
- In particular, the non-heat-dissipating feature of the LED light strips enabled these structures to be positioned very close to the skin. Thus, the effectiveness of phototherapy could be increased to much higher levels.

By the help of these advantages, The use of LED lights gives positive results compared to traditional light sources. Besides, LED's dont carry the risks such as burns, DNA mutations and retinal damage like traditional methods owing to above-mentioned characteristics during the treatment.

In this study, a light, easy-to-install, breathable, washable system that can also be used as a bed mattress was developed with the integration of blue LED light into a 3-dimensional fabric. Studies have been carried out on the patterns of the upper and / or lower surfaces of the 3-dimensional warp knitted fabric and the channels in which the LED lights will be integrated. The construction parameters of the fabric such as thickness, arrangement and density of the connecting threads, have been formed according to the most effective light transmittion with the appropriate pressure distribution for the best comfort feeling. In conclusion, a prototype of the phototherapy device was designed.

The experimental studies of the prototype has been performed in Dokuz Eylul University Faculty of Medicine, Department of Pediatrics, Department of Neonatalogy. During the preliminary trials, the

changes of bilirubin amounts were tested before and after the treatments with samples prepared from standard bilirubin solution and the effectiveness of the structure has been observed and discussed.

2. MATERIALS AND METHODS

2.1. Production and Performance Tests of 3-Dimensional Warp Knitted Fabrics

As the main structure for the phototherapy system, 3-dimensional warp knitted (spacer) fabrics were produced in 7 different warp knit fabric structures using 84/36 dtex PES yarns. Various parameters have been considered during the fabric design such as ability to reflect blue light, ability to affect light power and intensity (irradiance power), heat removing characteristics with high air permeability etc.

The physical properties of the 3-D warp knitted fabrics and the relevant standarts for each sample are given in Table 1.

Table 1. The physical properties of the sample 3_D warp knitted (spacer) fabrics

Sample Code		**1**	**2**	**3**	**4**	**5**	**6**	**7**
Linear Density (DIN EN 14971)	**Courses/cm**	12,5	13,5	10	6,5	9,5	9,5	9
	Wales/cm	9	9,5	9	2	3	3	5
Unit weight (g/m2) (DIN EN 12127)		350	391	355	510	528	560	1500
Thickness (mm) (DIN EN ISO 5084)		4	5	7	10	10	10	20
The thickness of the monofilament (mm)		0.1	0.1	0.14	0.24	0.14	0.14	0.2
The thickness of the multifilament (den)		75	75	380	600 &1080	300	300	600
Mesh Density		11,54	13,5	10,25	5,25	10,7	10	9
Full width (cm)		145	165,5	214	155	137	139	165
Usable width (cm)		140	162,5	207	206	127	132	117
Surface structure		One-side open one-side closed	One-side open one-side closed	two-sided open-channel	two-sided open-channel	One-side open one-side closed	One-side open one-side closed	two-sided close-channel

2.2. Integration of Electronic System Into Fabric

3-dimensional warp knitted fabrics with different properties such as thickness, construction, compressibility, air permeability, colour and light diffusion; and polyurethane films with various characteristics such as thickness, transparency, opacity, liquid impermeability, light diffusion, heat and temperature dissipation along the surface, etc. were used together in different layers according to the physical and performance test results, together with the design studies that could optimize the temperature and light intensity. An example of the layered structure is shown in Figure 3.

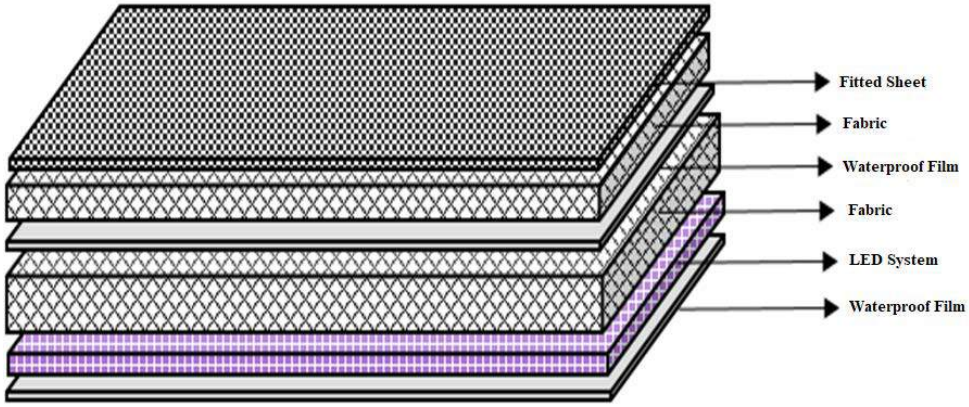

Figure 3. Example of layered structure

Considering the expected performance criteria, blue LED light integration was performed. In the integration studies, the following success criteria were taken into consideration for fabric and blue LEDs.

- Creating an effective treatment area,
- Stable light wavelength during the whole treatment (450-480nm),
- Efficient light intensity (irradiance) during the treatment (>30 μW/cm^2/nm),
- Temperature of the contact surface (≤ 35°C)

The radiance range of the designed flexible LED strip was measured by using a light sphere. The light sphere measurements were measured at 25%, 50%, and 100% brightness levels. The light sphere parameters are given in Table 3 and the result graph is given in Figure 4.

Table 3. Test parameters of the light sphere

Brightness level	Light flux, lm	Light efficiency, lm/W	Wavelength, nm
%25	72,5	11,9	270
%50	147	12,3	270
%100	296,6	12,2	270

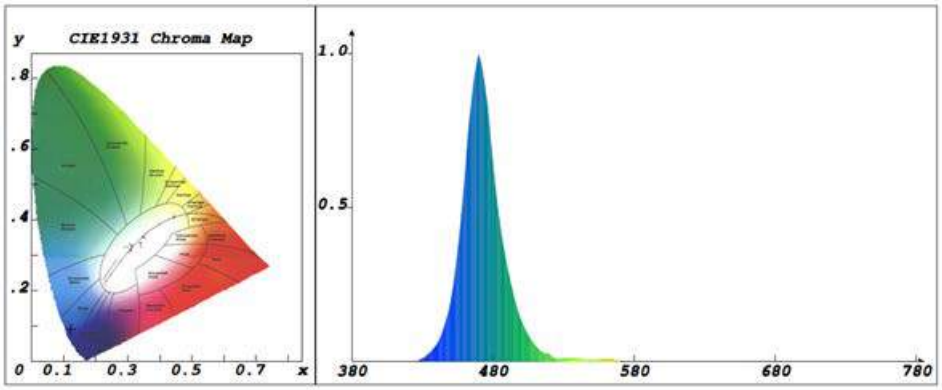

Figure 4. The light sphere test results of the designed LED strips (25% brightness level)

2.3. Measuring Phototherapy Efficacy Using Standard Bilirubin Solution

The efficiency of the blue LED integrated phototherapy system was measured by using the standard bilirubin solution. In order to determine the effectiveness of the prorotype, the system was compared

to a traditional phototherapy device, which has been proven to be effective and is routinely used for newborns in the hospital. In the in-vitro study, standard bilirubin solution was used (B4126-5G Sigma-Aldrich). The experimental trials were carried out in the Department of Neonatalogy, Faculty of Medicine, Dokuz Eylul University.

2.4. Design and Production of Phototherapy Device

The final product designs are based on curability (light efficiency), safety, ease of use and mother-infant comfortable interaction. Besides the protoype design studies, different collections for supplementary materials were also developed and designed for the final product. The safety and performance measurements of the prototype device, verified in terms of engineering design and madical usage, were carried out in accordance with the IEC-60601-1 TYPE Test (Electronic Hardware) standard. All of the results were interpreted according to the reference values. As a result of the experimental studies, it has been observed that the prototype is safe as an electronic equipment, and it has the desired light wavelength and light intensity for phototherapy applications used in newborn jaundice treatment.

3. RESULTS AND DISCUSSION

In order to determine the physical, comfort and performance properties of the prototype, different parameters such as compressibility, air permeability, thermal resistance, water vapor resistance, combustion behaviour were tested according to the relevant standards. The tests for comfort parameters have been performed by using SDL Atlas Sweating Guarded Hotplate device, Mesta 3240A air permeability tester and Zwick Roel Z010 compressibility tester. The test results of the 3-dimensional warp knitted fabric structures are given in Table 4.

Table 4. The test results of the 3-dimensional warp knitted fabric structures

Fabric Code	**1**	**2**	**3**	**4**	**5**	**6**	**7**
Compressibility One Layer, (DIN EN ISO3386-1) %40 (kPa)	-	15.18	23.35	14.74	9.61	14.07	9
Compressibility, Two Layer, 40% (kPa)	8	14.87	15.52	9.72	7.77	9.35	-
Air Permeability ($l/dm^2/min.$)	2084	2167	3812	4018	2536	2671	2189
Thermal Resistance (m^2K/W)	0.064	0.063	0.036	0.049	0.086	0.085	0.201
Water Vapor Resistance (m^2Pa/W)	6	6.2	7.5	7.3	5.7	5.8	3.8
Combustion Behavior	Passed	Passed	Passed	Passed	Passed	Passed	Passed

According to the test results; it was decided to use Fabric 4 with high air permeability as the base pad due to its two-sided open-channel structure. Owing to their high air permeability, high compressibility and high water vapor permeability values, Fabric 2 and Fabric 3 have been considered as the top layer in the product design.

The specially designed LED light source have been placed within the 3-D weft knitted fabric structures. The array of LED strips is shown in Figure 5. In the phototherapy prototype, it is preferred to increase the active area as much as possible, since it is aimed that the baby lies on the system with a direct contact and is directly exposed to the LED light.

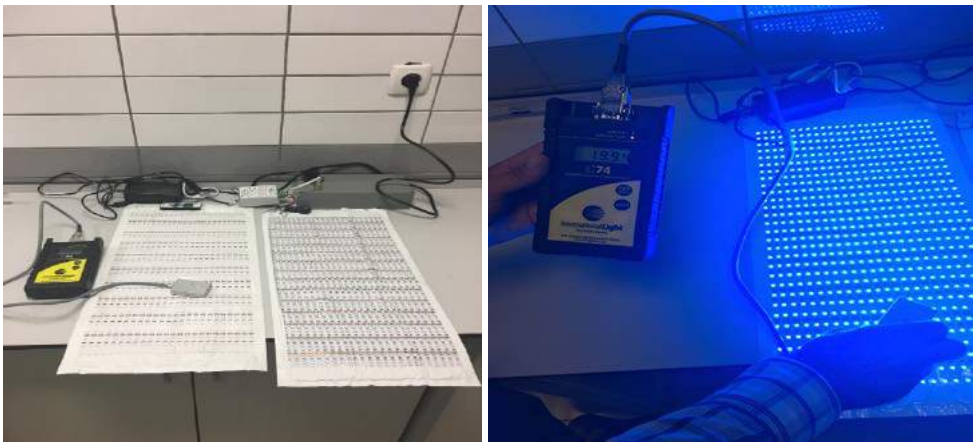

Figure 5. The array of LEDs

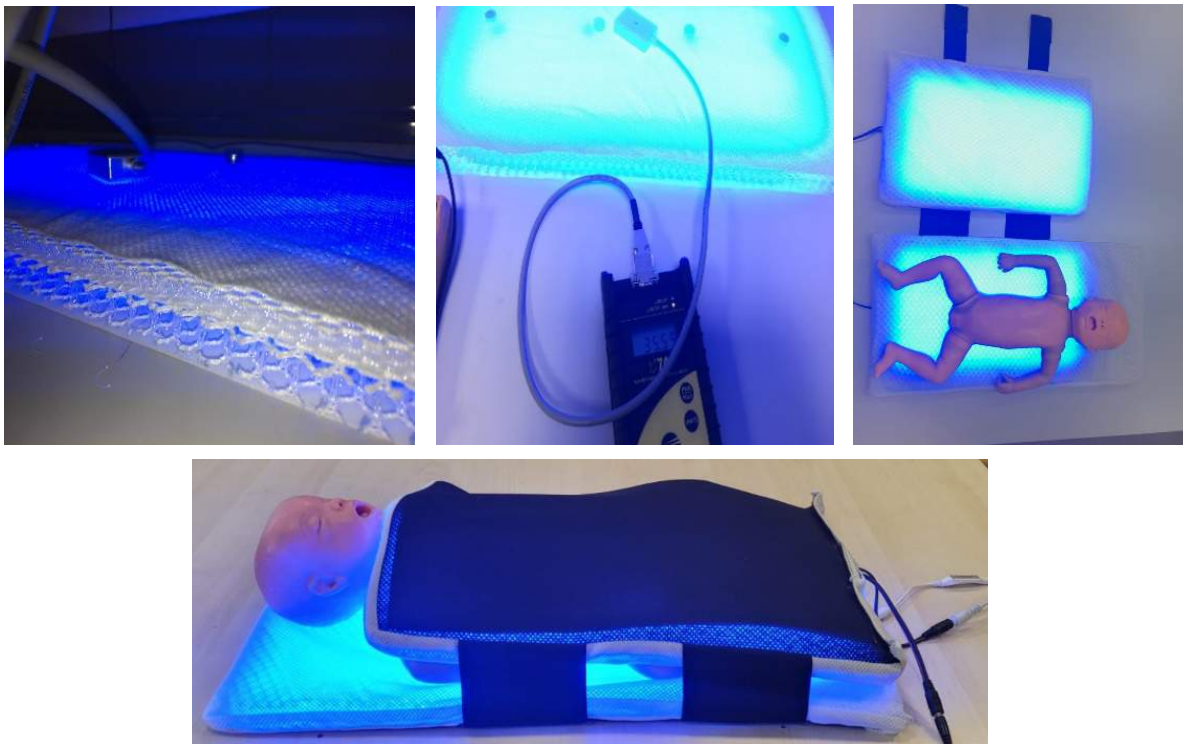

Figure 6. General design of the prototype phototheraphy device

The effect of intensive phototherapy treatment for commercially available LED phototherapy device (CPD) and prototype phototherapy device (PPD) on bilirubin level is shown in Figure 7. When intensive phototherapy was applied in both devices, no statistically significant difference was observed in the rate of decrease in bilirubin ($p>0.05$).

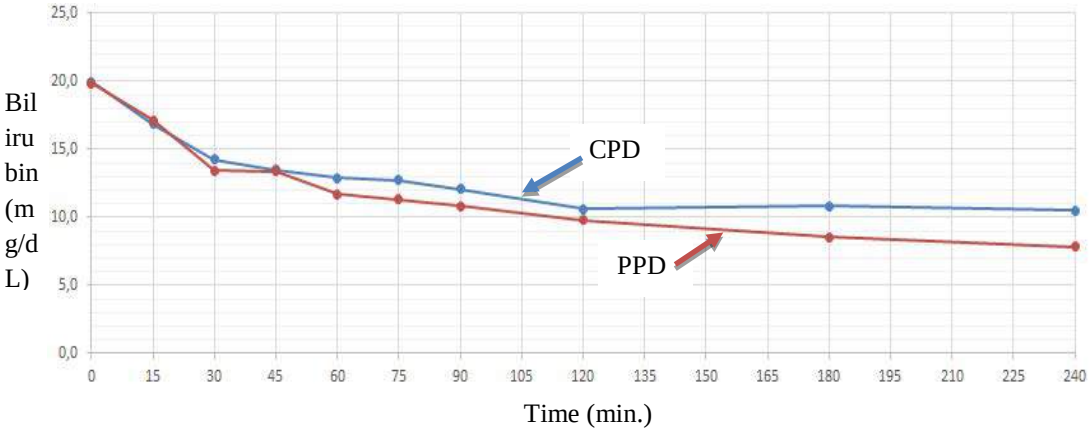

Figure 7. The effect of intensive phototherapy treatment for commercially available phototherapy device (CPD) and prototype phototherapy device (PPD) on bilirubin level

4. CONCLUSION

In this study, blue LED lights with a certain wavelength has been integrated into 3-dimensional warp knitted fabric. The main aim is to develop an electrotextile surface that is light, easy to install and use, breathable, washable and can be used as a baby bed, which can be used during breastfeeding, suitable for home and hospital use with normal and intensive phototherapy applications for newborn jaundice phototherapy.

Thanks to the hollow structure of the 3-dimensional fabric, the light can be easily transmitted to the baby, and the baby's comfort can be provided with its structural feature that provides pressure distribution.

Also by the help of various advantages of silicone LED strip lightsources, the protable devices can be easily applied to phtotheraphy treatments. Also the non-heat-dissipating feature of the LED light strips provides them to be placed very close to the skin. Due low energy requirements portable batteries can be used in-house applications. Thus, the effectiveness of phototherapy could be increased to much higher levels.

The product is also suitable especially for use at home and by this way, it is predicted that it will increase the mother-baby interaction during the phototheraphy treatment by eliminating the necessity of staying in the hospital.

REFERENCES

Agrawal, R., Aggarwal, R., Deorari, A. K., & Paul, V. K. (2001). Jaundice in the newborn. *The Indian Journal of Pediatrics*, *68*(10), 977-980.

Akobeng, A. K. (2005). Neonatal jaundice. *American Family Physician*, *71*(5), 947.

Arnolda, G., Chien, T. D., Hayen, A., Hoi, N. T. X., Maningas, K., Joe, P., ... & Moccia, L. (2018). A comparison of the effectiveness of three LED phototherapy machines, single-and double-sided, for treating neonatal jaundice in a low resource setting. *PloS one*, *13*(10), e0205432.

Chang, Y. S., Hwang, J. H., Kwon, H. N., Choi, C. W., Ko, S. Y., Park, W. S., ... & Lee, M. (2005). In vitro and in vivo efficacy of new blue light emitting diode phototherapy compared to conventional halogen quartz phototherapy for neonatal jaundice. *Journal of Korean medical science*, *20*(1), 61-64.

Çoban, A., Türkmen, M., & Gürsoy, T. (2014). Yenidoğan sarılıklarında yaklaşım, izlem ve tedavi rehberi. *Türk Neonatoloji Derneği*, *1*, 39.

Dani, C., Martelli, E., Reali, M. F., Bertini, G., Panin, G., & Rubaltelli, F. (2001). Fiberoptic and conventional phototherapy effects on the skin of premature infants. *The Journal of pediatrics*, *138*(3), 438-440.

Hansen, T. W. R. (2010, June). Phototherapy for neonatal jaundice—therapeutic effects on more than one level?. In *Seminars in perinatology* (Vol. 34, No. 3, pp. 231-234). WB Saunders.

Maisels J., M.B., B.Ch. and McDonagh A., Ph.D. (2008). Phototherapy for Neonatal Jaundice. *The New England Jounal of Medicine*, 358:920-8.

Noureldein, M., Mupanemunda, G., McDermott, H., Pettit, K., & Mupanemunda, R. (2021). Home phototherapy for neonatal jaundice in the UK: a single-centre retrospective service evaluation and parental survey. *BMJ paediatrics open*, *5*(1).

Stokowski, L. A. (2011). Fundamentals of phototherapy for neonatal jaundice. *Advances in Neonatal Care*, *11*, S10-S21.

Wang, J., Guo, G., Li, A., Cai, W. Q., & Wang, X. (2021). Challenges of phototherapy for neonatal hyperbilirubinemia. *Experimental and therapeutic medicine*, *21*(3), 1-1.

POLYURETHANE COATING PERFORMANCE OF HIGH-TENACITY POLYAMIDE FABRIC

Adem KURT[1], Bekir BOYACI[1], Sinem ÖZTÜRK[1], Sadiye İNCEOĞLU[1]

[1] Sun Textile R&D Center, Izmir, Turkey

Corresponding author: adem.kurt@suntekstil.com.tr

Abstract: *Within the scope of this study, fabric structures that can provide high waterproof performance resistant to external environments have been developed. Raw, prepared for dyeing (PFD), printed, 1-layer polyurethane coated structures of 500 denier polyamide 66 high tenacity, and 1000 denier polyamide 66 high tenacity, plain weave fabric structures, mechanical properties , the amount of added add-on transferred, and hydrostatic water pressure were compared. It is shown how the effects of the coating process on performance characteristics change.*

Keywords: *Coating, knife coating, polyamide, polyurethane, tensile-tear strength*

1. INTRODUCTION

Coating is a process in which one or several layers of material are applied on the surface of some substrate via different processing methods. Textile coating is the process of depositing a resin over a textile substrate, on one or both sides and one or several layers (Shim, 2019). Textile surface materials coated with chemicals have been developed continuously for several last decades. The use of these products is increasing and they are gaining greater importance in the clothing industry. It is preferred especially in protective clothing such as bags, cold climate clothing, ballistic vests, outdoor clothing and tent in the market (Woodruff, 1992). Within the scope of this study, knife coating, which is one of the textile surface coating methods, was preferred. In this method, the coating paste is directly applied to the fabric and spread uniformly by the means of knife. The thickness of the coating is adjusted controlled by gap between the knife and fabric. As a coating polymer polyvinyl acetate, polyacrylate, polyurethane, polyvinyl chloride are mostly preferred. These chemical materials affect the physical and performance properties of the fabric (Fung, 2002). Changes in the properties of carrier fabrics occur with changes such as the type of coating chemical and the number of coating layers.

In this study, it was determined how the performance of high-tenacity polyamide fabrics changed with polyurethane coating using the knife coating method.

2. MATERIALS AND METHODS

2.1. Materials

The materials used in this study are summarized in Table 1. 500 denier (D) and 1000 denier polyamide 66 high tenacity (HT) woven fabrics were tested. Polyurethane (PU) is used as coating material.

Table 1. Fabric types, coating materials and coating layer

Fabric Types	Coating Materials	Coating Layer
500D Polyamide 66 HT	PU	1
1000D Polyamide 66 HT		1

2.2. Coating Process

500D polyamide 66 HT and 1000D polyamide 66 HT fabrics were dried in dryer for 1 minute at 130ºC after the first layer was coated. Then it was fixed in a drying machine at 160°C for 2 minutes. After the coating process, water-repellency finishing was applied to all fabrics.

2.3. Tests

Weight test, tear strength test, tensile strength test and hydrostatic water pressure test were applied to these fabrics. The details of the tests applied are as follows:

Weight Test: Raw, PFD, Printed, 1 layer coating were done according to ISO 12227 standard with 5 repetitions.
Tear Strength Test: It was applied in 5 repetitions according to ISO 13934-2 standard as Raw, PFD, Printed, 1 layer coating.
Tensile Strength Test: It was applied in 5 repetitions according to ISO 13937-1 standard as Raw, PFD, Printed, 1 layer coating.
Hydrostatic Water Pressure: It is made in 5 repetitions according to ISO 811 standard on 2 different fabrics with 1 layer applied.

3. RESULTS AND DISCUSSION

Within the scope of this study, four different fabric types, including raw, prepared for dyeing (PFD), printed, 1 layer coated, were evaluated as weight, add-on, tear strength, breaking strength, water column. For 500D PA 6,6 HT, 1000D PA 6,6 HT Weight, breaking strength and tear strength test results of four different fabrics's values are shown in the Table 2.

Table 2. For 500D, 1000D PA6,6 HT weight, breaking strength and tear strength test results of four different fabrics

Sample		Weight (g/m^2)	Tensile Strength – Weft (N)	Tensile Strength – Warp (N)	Tear Strength – Weft (N)	Tear Strength – Warp (N)
500D PA 6,6 HT	**Raw**	193	1714.56	2998.16	222.80	229.1
	Prepared for Dyeing	199.2	1940.24	3248.23	169.20	179.3
	Printed	206.1	2004.40	3112.46	200.10	241.2
	1 Layer Coating	236.8	1880.10	3040.56	97.98	119.0
1000D PA 6,6 HT	**Raw**	273.3	1802.40	3288.66	526.73	537.48
	Prepared for Dyeing	281.2	2515.18	3569.26	446.91	471.0
	Printed	288.8	2654.15	3410.67	481.00	546.0
	1 Layer Coating	347.0	2445.40	3323.06	376.00	425.0

In Table 2, four different fabric structures were compared in terms of tearing, tensile strength and weight. It was observed that the weight of the PFD structure was higher than the raw weight. When the tear strength is examined, it is seen that it is not parallel with the breaking strength and it is seen that the highest value is obtained in the raw fabric. When analysed in terms of tensile strength, it is seen that PDF structure shows higher tensile strength than raw fabric. It is thought that the coating process reduces the slippage of the fibers over each other. Figure 1 it is showed that, weight of 500D PA 6,6 HT 1000D PA 6,6 HT. The comparison of the weights of different fabric structures with each other is evaluated in figure 1.

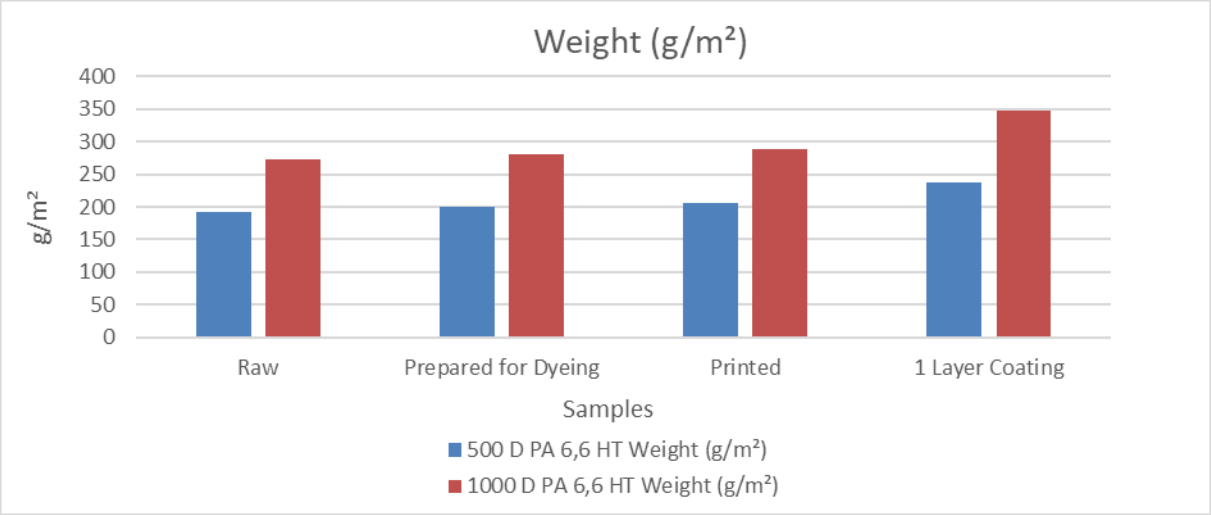

Figure 1. Weight of 500D PA 6,6 HT 1000D PA 6,6 HT

When the weights are examined, it is seen that the weights increases with pfd process, printing process and coating process. It is seen that it increased by 2.93% for 1000D, %3,21 500D after the PFD process compared to the raw fabric.According to raw fabric weight, It is seen that it increases by 5.67% for 1000D, %6,78 500D after the printing process and 26,90% for 1000D, %22,69 500D after the 1 layer coating process. The reason for the increased weight was due to the chemical substance transferred in each process. İt is showed that for 500D PA 6,6 HT, 1000D PA 6,6 HT tensile strenght in warp and weft directions in Figure 2. The comparison of the tensile strenght of different fabric structures with each other is evaluated in Figure 2.

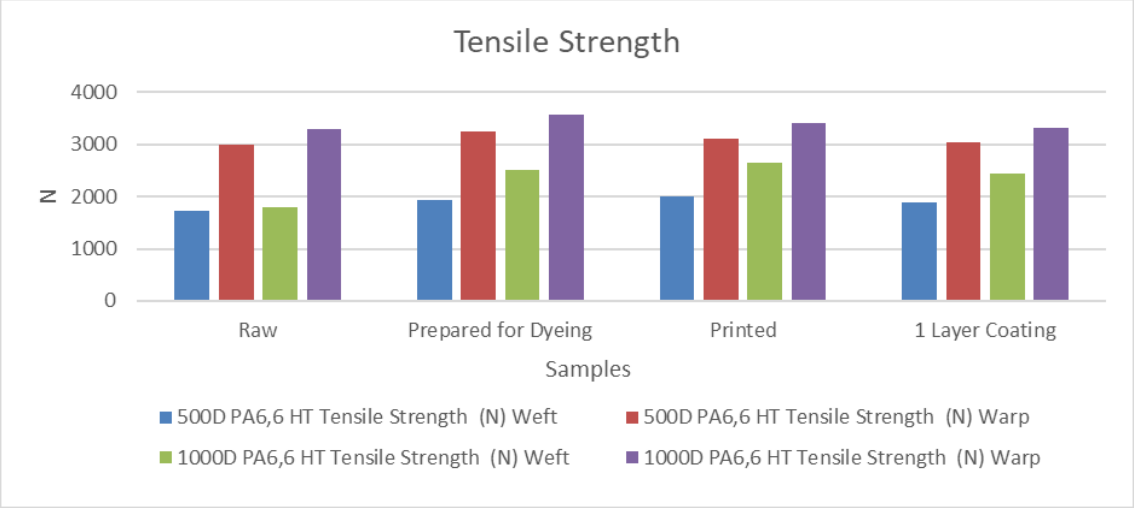

Figure 2. 500D PA 6,6 HT, 1000D PA 6,6 HT tensile strenght in warp and weft directions

It is seen that the PFD process causes an increase of 39,57% for 1000 D and %13,18 for 500D in the breaking values in the weft direction compared to the raw fabric. at the same time It is seen that there is an increase of %8,53 for 1000D, %8,34 for 500D in the warp direction. According to PFD, it is seen that the tensile strength of the printed fabric in the weft direction causes an increase of approximately 5,52 % for 1000D,%3,30 for 500D. It is seen that it causes a decrease of 4.44% for 1000D, %4,17 for 500D in the warp direction. After 1 layer coating, it is seen that it causes a decrease of 7,86% for 1000D, %6,20 500D in the weft direction and 2,5 % for 1000D, %2,31 500D in the warp direction. It is seen that the coating material reduces the fiber flexibility and therefore the breaking and tearing values are reduced. Figure shows 500D PA 6,6 HT, 1000D PA 6,6 HT tear strenght in warp and weft directions. The comparison of the tear strenght of different fabric structures with each other is evaluated in Figure 3.

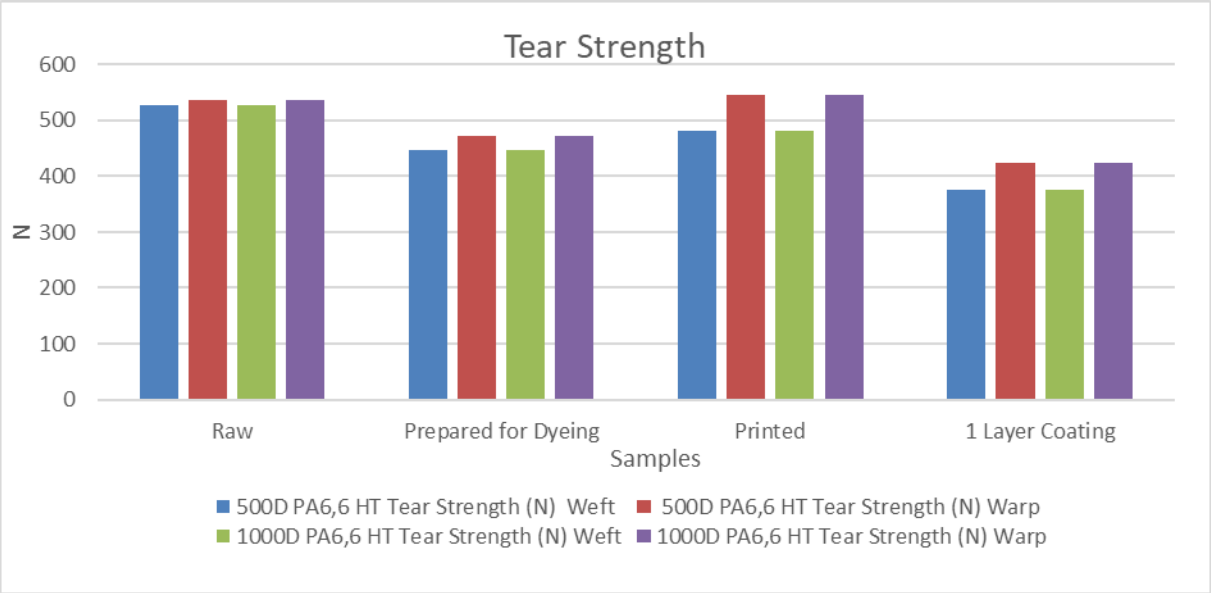

Figure 3. 500D PA 6,6 HT, 1000D PA 6,6 HT tear strenght in warp and weft directions

When the tear strenght are examined, it is seen that the tear strenght of the pfd process, printing process and coating process changed. It is seen that the PFD process shows a decrease of approximately % 15,1 for 1000D and %24,05 for 500D in the tearing values in the weft direction and 12.36% for 1000D, %21,73 500D in the warp direction compared to the raw fabric. According to PFD, it is seen that the tear strength of the printed fabric in the weft direction causes an increase of approximately 7.62% for 1000D, %18,26 500D. It is seen that it causes an increase of 15.92% for 1000D, %34,52 500D in the warp direction. According to printed, After 1 coat of coating, it is seen that it causes a decrease of 21.8 for 1000D, %51,1 500D in the weft direction and 22.16% for 1000D, %50,66 500D in the warp direction. It is seen that the coating material reduces the fiber flexibility and therefore the breaking and tearing values are reduced.

Table 3 shows the add-on and hydrostatic water pressure test results of polyurethane coated fabrics with 1-layer coated fabric.

Table 3. Add-on and hydrostatic water pressure test results of 1-layer coated fabric

Sample	Add-on (g/m^2)	Hydrostatic Water Pressure (mmH_2O)
500 D PA 6,6 HT 1 Layer Coating	43.8	512.6
1000 D PA 6,6 HT 1 Layer Coating	58.2	602.2

43.6g/m^2 add-on was added to 500D PA 6,6 HT fabric and 51 mmH_2O water column was obtained. 58 g/m^2 fabric was added to 1000 D PA 6,6 HT fabric and 622 mmH_20 water column was obtained.

4. CONCLUSION

In this study, the effects of polyurethane coating of polyamide 66 HT fabrics with knife coating method on their performance were investigated. The amount of chemical transferred to the surface by the coating process was calculated and the effects of the coating chemical were evaluated according to the tensile- tear test results. Weights increased after each process step. It is seen that the coating process negatively affects the tear and tensile strength mechanical properties. . If the fabric has been treated with finishing treatments such as synthetic resin or starch, this often increases friction between the yarns and reduces freedom of movement. Thus, it causes a decrease in tear strength (Taylor, 1999). Fabric finishing processes (wet and dry heat treatments) applied to give the fabric the desired properties (Malik and Tanwari, 2009).

REFERENCES

Fung, W. (2002). *Coated and laminated textiles* (Vol. 23). Woodhead Publishing.

Malik, Z. A., & Tanwari, A. (2011). Influence of plain and Twill (3/1) weave designs on the tensile strength of PC blended fabrics. *Mehran University Research Journal of Engineering and Technology*, *30*(1), 23-28.

Shim, E. (2019). Coating and laminating processes and techniques for textiles. In *Smart textile coatings and laminates* (pp. 11-45). Woodhead Publishing.

Taylor, M. A. (1999). *Technology of Textile Properties*, Forbes Publications Ltd., London.

Woodruff, F. A. (1992). Environmentally Friendly Coating and Laminating: New Processes and Techniques. *Journal of Coated Fabrics*, *21*(4), 240-259.

INVESTIGATION OF THE PERFORMANCE PROPERTIES OF MEMBRANE STRUCTURES EXPOSED TO HARSH ENVIRONMENTAL CONDITIONS

Sinem ÖZTÜRK[1], Bekir BOYACI[1], Adem KURT[1], Sadiye İNCEOĞLU[1]
[1]Sun Tekstil Ar-Ge Merkezi, İzmir

Corresponding author: sinem.ozturk@suntekstil.com.tr

Abstract: *This study focuses on the production of laminated fabric layers using different membrane laminates, highlighting their waterproof and breathable properties with optimal performance for outerwear, and the comparison by considering the different membrane. Two different membranes are laminated between the woven outer fabric structure and the Raschel lining fabric. In this context, 100% PES woven fabric was used as the outer layer. Two different membranes were used as the middle layer PES membrane and PTFE/PU membrane. The lining layer is 100% PES Raschel. These two structures are lightweight and designed as waterproof and windproof. The comfort properties of the obtained fabric structures were evaluated before washing and after 20 washings. It was examined in terms of hardness and water column after standing in harsh environments. The results obtained were compared and discussed. In this study, the performances of membranes were investigated only as textile fabrics, not as a clothing system.*

Keywords: *Laminated fabric, membrane, waterproof, breathable, hardness.*

1. INTRODUCTION

The production of textile materials for special-purpose and good thermal comfort clothing is a great challenge nowadays for many manufacturers of fibers, yarns and textile fabrics (woven, knitted, nonwoven). Any kind of human physical activity will create the need for releasing the excessive heat with a view of maintaining a stable body temperature (Huang ,2016). These fabrics are usually used to make windproof garments, typically produced in multi-layered forms to enhance warmth and comfort under windy and cold conditions (Farzandi,2013). Apart from achieving the needed thermal comfort, it is particularly important to prolong the garment life, that is, to produce clothing ensembles (items) the thermal comfort of which will not significantly change during its usage, i.e. maintenance. For effective use of clothing, it is important to predict the period after which certain functional properties will be lost due to maintenance (thermal comfort in this case). Lamination is the process of bringing different surfaces together with various bonding methods with the help of heat and pressure, and then turning them into a single layer. Membrane laminated waterproof, breathable fabrics that can be obtained by lamination methods; it is designed to be used in clothing that provides protection against weather conditions such as rain, wind and heat loss of the body (Wenger, 2019). In addition to all these features, fabrics will be breathable thanks to specially developed micro-porous membranes. The pores of breathable laminated fabrics are 20.000 times smaller than a drop of liquid water, but 700 times larger than a water molecule, so they are small enough not to allow liquid water to pass, but large enough to allow water vapour molecules to pass. Breathable-laminated fabrics either contain micropores or consist of single-layer films containing hydrophilic hydrogen groups in the polymer chains that make up the structure. In some cases, a combination of these two structures is used Ahn, 2011).

2. MATERIALS AND METHODS

2.1. Materials

In this study, membranes of different types, structures and thicknesses that can be used in the

production of softshell jackets suitable for windy-rainy weather were used. One of these membranes is hydrophilic polyester (PES) and the other is bicomponent polytetrafluoroethylene/polyurethane (PTFE/PU). Its properties are briefly given in Table 1. The fabrics used in the lamination process are 100% PES woven fabric and 100% PES raschel knitted fabric. As adhesive was used reactive polyurethane.

Table 1. Properties of the used membranes

Membrane Type / Structure	Thickness (micron)	Weigt (g/m^2)	Colour
PES / Hydrophilic	8	12	White
PTFE-PU / Microporous	20	30	Transparent

2.2. Lamination Process and Performance Tests

Laminated fabrics were obtained by using hot-melt lamination machine. In the first lamination process of the bicomponent membrane, the PTFE face of the membrane is laminated to the inner surface of the fabric surface. In the second lamination process, a raschel knitted fabric was laminated to the PU surface of the bicomponent membrane. In the lamination process with 100% PES membrane is laminated to the inner surface of the fabric. Then the raschel knitted fabric was laminated. Sample description and new codes are shown in Table 2.

After lamination, for curing was waited for 7 days. Then, water repellency chemical was applied to the three layer laminated fabrics.

Table 2. Sample description and new codes

Sample Description	Codes
Before Washing, 100% Pes Woven Fabric + 100% Pes Membrane + 100% Pes Raschel	BW-PES
Before Washing, 100% Pes Woven Fabric + 100% PTFE/PU Membrane + 100% Pes Raschel	BW-Bico
After 20 Washing 100% Pes Woven Fabric + 100% Pes Membrane + 100% Pes Raschel	AW- PES
After 20 Washing, 100% Pes Woven Fabric + 100% PTFE/PU Membrane + 100% Pes Raschel	AW-Bico
Before Washing, Waiting Under Difficult Conditions 100% Pes Woven Fabric + 100% Pes Membrane + 100% Pes Raschel	BW-PES-Cold
Before Washing , Waiting Under Difficult Conditions 100% Pes Woven Fabric + 100% PTFE/PU Membrane + 100% Pes Raschel	BW-Bico-Cold

Weight test, water repellency test, oil repellency test, hydrostatic water proof test and hardness test for the performances of laminated fabrics were performed.

Test Prosedure:

Weight Test: BW-PES, BW-Bico, AW PES, AW-Bico were done according to TS EN 12127 standard with 5 repetitions.

Water Repellency Test: It was applied in 5 repetitions according to ISO 4920 standard as BW-PES, BW-Bico, AW PES, AW-Bico

Oil Repellency Test: It was applied in 5 repetitions according to ISO 14419 standard as BW-PES, BW-Bico, AW PES, AW-Bico

*Hydrostatic Water Pressure Test:*It is made in 5 repetitions according to ISO 811 standard on BW-PES, BW-Bico, AW PES, AW-Bico, BW–PES-Cold, BW-Bico-Cold.

Hardness Testing Test: It was applied in 5 repetitions according to ASTM D4032 standard as BW-PES, BW-Bico, AW PES, AW-Bico, BW–PES-Cold, BW-Bico-Cold.

The performances of laminated fabrics were performed and evaluated based on the following conditions. These conditions are as follows.

- After production,
- After washing at 30ºC 20 times,
- After waiting at -16ºC for 24 hours.

3. RESULTS AND DISCUSSION

Laminated fabrics, membrane performance, was compared for before washing, after 20 washings and after waiting in a cold environment. Laminated fabrics was examined water repellency, oil repellency, water vapor resistance, fabric hardness, hydrostatic pressure test. Test results of before washing and after 20 cycles washing weight, water repellency, oil repellency shown in Table 3.

Table 3. Before washing and after 20 cycles washing weight, water repellency, oil repellency

Sample	Weight (g/m^2)	Water Repellency	Oil Repellency
BW-PES	178.8	ISO 5	1.5
BW-Bico	175.6	ISO 5	6.5
AW- PES	173.6	ISO 3	0
AW-Bico	173.8	ISO 3	0

In Table 3, weight, water repellency and oil repellency were compared before washing and after 20 washings. It is seen that there is no significant change in the weights of BW-PES, BW-Bico, AW-PES, AW-Bico, softshell grades. When water repellency and oil repellency were examined. Water repellency was varied ISO 5 for BW-PES and BW-Bico and after washing process these results were decreased to ISO 3**.** It is thought that the water-repellency polymers on the surface are removed with each washing process. It is seen that the oil repellency value of BW-Bico softshell quality has better oil repellent properties than BW-PES softshell quality in the condition before washing. Face of BW-Bico is an oleophobic PTFE. After 20 washes, it is seen that the oil repellency feature does not remain.

Table 4. Washing before and 20 washing after water vapor resistance test results

Sample Name	Water Vapor Resistance (m^2.Pa/W)
BW-PES	7.5
BW-Bico	6.3
AW- PES	7.34
AW-Bico	5.66

The fact that the BW-Bico sample is lower in water vapor resistance than the BW-PES sample is due to the difference in the membrane used. Microporous membrane was used in sample BW-Bico. In both samples, it is seen that the washing process has a good effect on the water vapour resistance.

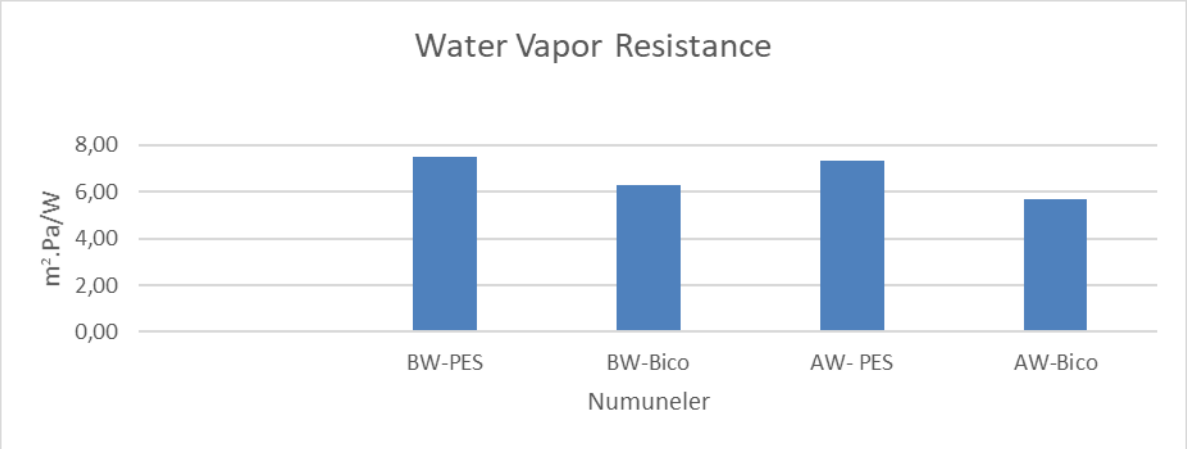

Figure 1: Washing before and 20 washing after water vapor resistance

Before washing water vapor resistance of the 3-layer laminated structure obtained with BW-Bico compared to the 3-layer laminated structure obtained with the BW-PES membrane decreased by approximately %19,4. It is seen from the AW-Pes sample that the water vapor resistance does not change. It is thought to originate from the microporus structure of the bicomponent membrane. After washing, the water vapor resistance of the AW-Bico sample decreases approximately %10,1. It is thought that micropores are damaged after washing.

In Table 5, three different softshell structures are compared in terms of fabric hardness and water column as before washing, after 20 washing and waiting in difficult conditions.

Table 5. Results before washing, after 20 washings and waiting in difficult conditions

Sample Name	**Fabric Hardness (N)**	**Water Column (mmH_2O)**
BW-PES	2.8	>10000
BW-Bico	3.2	>10000
AW- PES	1.9	≧ 8000
AW-Bico	2.0	≧ 8000
BW-PES-Cold	2.5	≧ 8000
BW-Bico-Cold	2.7	≧ 8000

When the values in Table 5 are examined, it is seen that the AW- PES and AW-Bico samples show lower fabric stiffness values than the BW-PES, BW-Bico samples. It is seen that the membrane waterproofing values do not change while the fabric hardness decreases. Membrane performance did not change and fabric hardness decreased, which also provided a good handle. It is observed that the hardness of the fabric increased after waiting under difficult conditions and became embrittled in both membranes used.

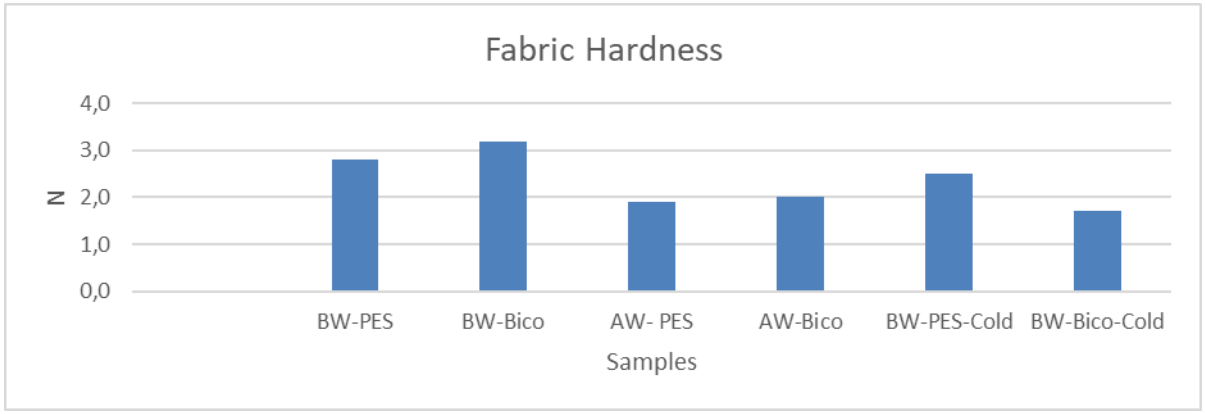

Figure 2: Washing before, 20 washing after and waiting in cold

Before washing process, when the BW-Bico and BW-PES samples are examined, it is seen that the BW-Bico sample is approximately 14.28% softer than the BW-PES sample. After 20 washes, the hardness of both samples decreased. It is observed that the membrane containing PES decreased by approximately 47.36%, while the membrane containing bicomponent decreased by approximately 60%. It was observed that the hardness of BW-Pes-Cold BW-Bico-Cold samples changed after they were stored in a cold environment.

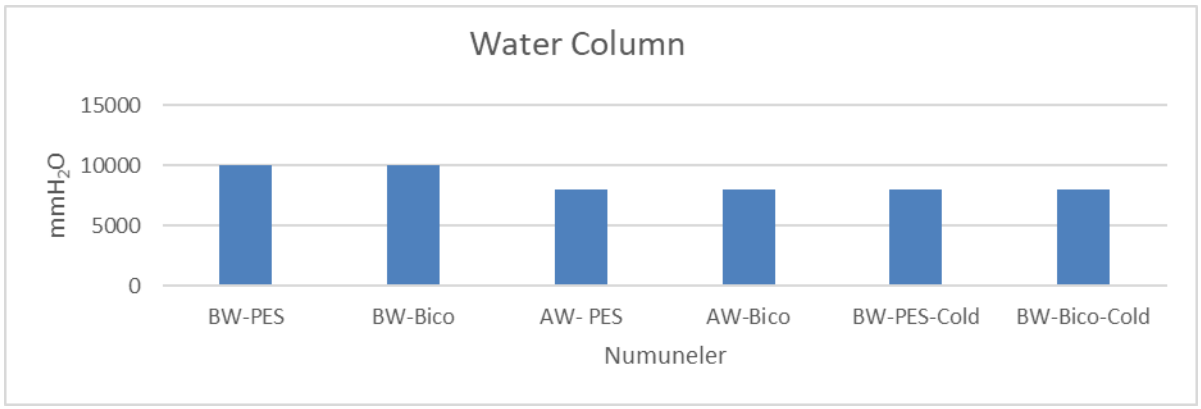

It is observed that there are decreases in the water column after 20 washing processes and waiting under difficult conditions. It is observed that there is a 20% decrease in the water column values both after 20 washes and after waiting in the cold environment.

4. CONCLUSION

Within the scope of this study, the performances of softshell grades obtained with different membranes in long cycle washings and under harsh conditions were evaluated. When the performance values obtained are examined, it is thought that the softshell qualities obtained with both membranes can be used in the apparel industry in terms of comfort, waterproofing and fabric hardness. PTFE surface has oil repellent property due to its own structure, but it loses this property with washing. Considering the results, chemical finishing should be applied to the fabrics for wash-resistant oil-repellent properties. Also, considering the test results given in the tables, the structural properties of the membranes deteriorate in washing and waiting in the cold conditions and the water column values decrease in the tests performed. Washing and waiting in cold were caused a change in the hardness in the 3-layer structure, as it disrupted the membrane structure.

REFERENCES

Wenger, S., Csapo, R., Hasler, M., Caven, B., Wright, T., Bechtold, T., & Nachbauer, W. (2019). The effect of different water vapor permeable jackets on moisture management, subjective perceptions and physiological parameters during submaximal exercise in a cool environment. *Textile Research Journal*, *89*(4), 528-540.

Ullah H. M. K., Lejeune J., Cayla A., Monceaux M., Campagne C. and Devaux E. (2021). A review of noteworthy/major innovations in wearable clothing for thermal and moisture management from material to fabric structure, Textile Research Journal, 1-36, DOI: 10.1177/00405175211027799

Ahn H. W., Park, C. H., & Chung, S. E. (2011). Waterproof and breathable properties of nanoweb applied clothing. *Textile Research Journal*, *81*(14), 1438-1447.

Huang J. (2016) Review of heat and water vapour transfer through multilayer fabrics, Textile Research Journal, 86(3), 325-336.

Farzandi M., Razipour S., Mousazadegan F., Saharkhiz S. (2013). Effects of using interlinings on physical and mechanical properties of wind stoppers, International Journal of Clothing Science and Technology, 25(2) 99 – 108.

POSTER PRESENTATIONS

DEVELOPMENT OF A MULTIFUNCTIONAL WEARABLE TECHNOLOGY WITH BUOYANT

Özgün PALAK[1], Aysu İLDENİZ[1], Duygu YAVUZKASAP AYAKTA[1]

[1]Yünsa Yünlü Sanayi ve Ticaret A.Ş, Ar-Ge Merkezi, Tekirdağ, Türkiye

Corresponding author: opalak@yunsa.com

Abstract: *In recent years, there has been an increased interest in protective clothing and equipment needed with climate changes because of this interest, wearable and protective technical textiles are becoming increasingly important. With the design developed in this context, it is aimed to ensure the life safety of people especially in environmental conditions such as sea, lake and pool, in cases of accident and danger. With the designed system, the life safety of the people are going to be ensured in case of danger and the danger situation will be notified to the people around or to the determined persons with the warning systems.*

Keywords: *Wearable technology, smart textiles, life shirt, wearable sensor*

1.INTRODUCTION

Protective smart clothing is used to protect from bad environmental conditions, unpredictable or unpredictable risks. These garments are designed and developed with the required physical, mechanical and chemical properties. The developments in the field of textile and technology have brought different disciplines together to create designs that protect and facilitate human life.

Technical textiles have never been a single coherent industry sector and market segment. It is developing in many different directions with varying speeds and levels of success. (Mecit, D., et al. 2007).

Smart textiles, which are being used in every field, make our lives easier and provide security in vital situations (Duran, K., et al. 2007). According to the United Nations (UN) World Health Organization's Global Drowning Report, an average of 372,000 people dies each year as a result of drowning. According to statistics, 40 people die from drowning every hour in the world. Drowning can occur not only because of not being able to swim, but also in sudden situations such as accidents and environmental factors (Erdem, K., et al. 2021). Especially in times of accident and danger, the use of smart devices will become more common in the near future. Existing practices are not comprehensive and do not provide an integrated solution for all possible risks. The design system that is the subject of the study will ensure that the person is noticed in dangerous situations and at the same time stays on the surface of the water.

2. MATERIALS AND METHODS

A system has been designed to provide information to the people around and predetermined people in situations that may be dangerous in ambient conditions such as the sea. In this design, in potentially dangerous situations, the user will be able to stay on the water surface thanks to the kapok fiber, which is less dense than the water. In addition, thanks to various sensors and dyestuffs that change colour according to environmental conditions, rescue efforts will be accelerated and the safety of the person will be ensured. A product that can be adjusted according to the user's demand and that can be disabled in non-hazardous situations will be designed (Figure1).

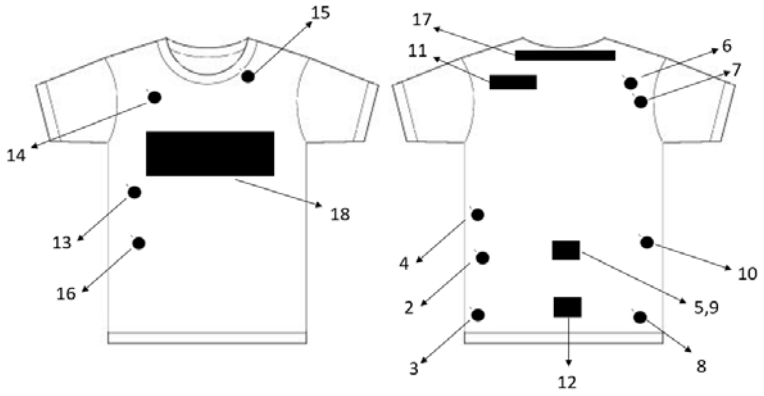

Figure 1. The designed product

The technical details designed in Figure 1 are given in Table 1.

Table 1. The Technical Details

No	Item	No	Item
1.	Product	10.	Oxygen Sensor
2.	Accelerometer	11.	Solar panel
3.	Pressure Sensor	12.	Battery
4.	Temperature Sensor	13.	Power button
5.	Microprocessor	14.	Air inflation kit
6.	The Light Device	15.	Kapok
7.	Sound device	16.	Alarm whistle cap
8.	Air pump	17.	Emergency Button
9.	GPS/GSM Module	18.	Color changing material

Pressure sensors and temperature sensors are going to detect contact with water in the study. The microprocessor evaluates the received information. It activates stimulating devices such as light and sound that enable the user to be noticed. It will inflate the product to keep the user on the water surface. The microprocessor also detects the user's vital values such as temperature and oxygen. It will send the user's vital values and GPS location as an emergency message to the designated contacts. Flexible solar panels and rechargeable batteries will be used to provide energy for the microprocessor, sensors and circuit elements.

3.RESULTS AND DISCUSSION

Thanks to the systems and sensors to be developed, information systems can be established. Thanks to the developed system, it is planned to reduce the rate of drowning due to accidents and environmental factors. In addition, it is thought that the product can be used easily in military or health fields.

4. CONCLUSION

With the designed integrated wearable technology, the life safety of the users is ensured in case of accident and danger in environmental conditions such as sea, lake and pool. It is ensured that precautions and actions are taken in vital situations. The work carried out in the project continues as an equity project. At the end of the project, a product that can be used for babies, children, non-swimmers and adults who cannot swim due to sudden accident or injury. This product is a project that can turn into a commercial product.

REFERENCES

Mecit, D., Ilgaz, S., Duran, D., Başal, G., Gülümser, T. & Tarakçıoğlu, I. (2007). Technical Textiles and Applications (part 2) . Textile and Apparel, 17 (3), 154-161.Retrieved from https://dergipark.org.tr/tr/pub/tekstilvekonfeksiyon/issue/23627/251645

Duran, K., Bahtiyari, M. İ. & Atav, R. (2007). PROTECTIVE NONWOVEN TECHNICAL TEXTILES. Textile and Apparel,17(3),174-177.Retrieved from https://dergipark.org.tr/tr/pub/tekstilvekonfeksiyon/issue/23627/251643

Ma, B, Zheng, C., Sun, R., (2003), 'Physical Properties of Surface Oxidized Wool' Textile Research Journal, Vol. 73 (12): 1100-1102.

Turgut, A., Işın, A. & Akdağ, E. (2018). Yüzme Havuzlarındaki Suda Boğulma Vakalarının İncelenmesi. İstanbul Üniversitesi Spor Bilimleri Dergisi, 8 (1), 69-76. Retrieved from https://dergipark.org.tr/tr/pub/iuspor/issue/36948/401910

DEVELOPMENT OF FUNCTIONAL FINISHING PROCESSES IN DENIM GARMENTS TO REDUCE WATER USAGE DURING HOME CARE

İsmail İVEDİ, Zafer SÜMER, Ahmet KOCATAŞ

Roteks Tekstil İhr. San. Ve Tic. A.Ş., İzmir, Türkiye

Corresponding author: ismailivedi@roteks.com.tr

Abstract: *Increased consumption, population growth, climate change, and water scarcity will cause significant problems for many countries of the world in the coming years. In order to minimize the risk of water scarcity, it is of great importance that countries, companies, and even all individuals pay attention to these issues and turn to processes and products that create fewer water footprints throughout their life cycle.*

In this study, it was aimed to reduce the contamination rate of denim products thereby washing them less by the consumer. Denim garments developed in this direction have gained the feature of stain repellent features. In order to reduce the amount of water and chemicals used during production, the finishing process was applied according to the spraying method. Fluorine-free, hydrocarbon-based 3D polymer dispersion chemical was used for oil and water repellent applications. Amine-modified polydimethylsiloxane and silicone-based softeners were used as softeners. Oil and water repellence tests (AATCC 118-2012: Oil Repellancy: Hydrocarbon Resistance Test) were applied to the developed products, both after the application and after 5 home launderings. The effect of the softener type used on the finishing process was examined. Tear strength, elasticity, and recovery analyses were interpreted comparatively. It was seen that %12 difference was observed between conventional denim pants and stain-resistance finishing applied samples according to air permeability analysis results. Reducing the amount of water and chemicals used during the production of the product, a homogeneous application at low liquor ratio of 1:2 was achieved. When the tear strength analysis results are examined, the tear strength of the finished samples increased by 16% in the weft direction and 68% in the warp direction compared to the control sample. Elasticity, on the other hand, decreased by 23%.

Keywords: *Sustainability, water scarcity, denim, oil repellent*

1. INTRODUCTION

The concepts of sustainability, product life cycle and ecological production have become more and more important considering the dangers that may affect the entire ecosystem, such as global warming. Therefore, companies and consumers become more conscious day by day. According to a report published by the world bank, the textile and fashion industry is the second most polluting industry in the world and is responsible for 20% of the water consumed on our planet (Kant, 2012).

The development of textiles with new finishes is an effective way to modify their behaviors by improving specific features through surface functionalization and the combination of new materials and technologies (Scacchetti et al., 2017). Denim garments have been deeply people's favourites due to their easy and simple style. It's constructed in a twill weave which included the indigo-dyed warp and white weft yarns. Along with the evolution of denim clothing, the self-characterized washing technique, for its production impose, has an antique appearance and comfortable texture, which becomes the essential element leading to fashion (Li et al., 2020).

With the increase in greenhouse gas emissions and the risk of lack of water, many countries, companies, and organizations around the world have started to implement innovative initiatives and technologies in order to re-evaluate their activities and produce their products both using less water

and causing low carbon emissions (Pekin et al., 2006). Table 1 shows the amount of water consumed during the product life cycle of one denim pair of trousers (Periyasamy et al., 2017).

Table 1. Cradle to the grave water consumption of denim garment

Production Stages	Water Consumption Amount By Phase (Liters)	Water Consumption Percentage By Phase
Fiber Production	2565	68%
Consumer Care	860	23%
Fabric Production	236	6%
Sundries & Packaging	77	2%
Cutting & Sewing & Finishing	34	1%

As it can be seen from the Table, after the fiber production stage, the highest water consumption is in the consumer care stage with a rate of 23%. Therefore, stain-repellent finishing has been applied to denim garments in order to reduce the amount of water consumed by the consumer. Fluorine-free, hydrocarbon-based 3D polymer dispersion chemical was used for oil and water repellent applications. Amine-modified polydimethylsiloxane and silicone-based softeners were used as softeners. Oil and water repellency tests (AATCC 118-2012: Oil Repellency: Hydrocarbon Resistance Test) were applied to the developed products, both after the application and after 5 home launderings. The effect of the softener type used on the finishing process was examined. Tear strength, elasticity, and recovery analyses were interpreted comparatively. In addition, an air permeability test was applied to examine the effect of the coating applied with the finishing process on the comfort properties of denim clothing.

2. MATERIALS AND METHODS

Indigo-dyed denim fabric was purchased from Kipaş Tekstil, Turkey. Composition of the fabric includes %75 pre-consumer cotton, %20 post-consumer cotton, %3 elastomultiester and %2 recycled elastane. The fabric has a 3/1 twill weave structure, and the weight of the fabric is 12 oz/yd^2. Fluorine-free, hydrocarbon-based 3D polymer dispersion chemical was supplied from Tanatex, Netherland. The ethoxylated carboxylic acid compound was also supplied from Tanatex, Netherland. It was used to increase absorbency and create an antistatic effect. Drum-type washing machines (Tolkar's 3700 model, Turkey) were used for pre-washing and finishing processes. A spray system (Method Makine, Turkey) combined with a tumbler machine was used for the stain resistance finishing process. The solution is sprayed on the products with 0.1-4 mm narrow nozzles of the spraying system with 3-4 bar pressure coming from the compressor in a tumbler machine. Table 2 shows the experimental plan.

Table 2. Experimental plan of the finishing process

Sample Code	Pre-washing	Oil repellent (%)	Antistatic (%)	Softener (%)	Liquor Ratio	Spraying machine settings	Drying
R27	10 g/l NaOH, 10 min, 60°C, 2 g/ml Pumice stone, 30 min, 40°C 50 ml/l NaClO, 13 min, 50°C	-	-	-	-	-	-
R28		10	5	2.5 silicone	1:2	50 g/min 3-4 bar	120°C, 10 min + 70°C, 30 min tumbler drying
R29		10	5	2.5 alkanolamine ester derivatives	1:2	50 g/min 3-4 bar	
R30		10	-	2.5 alkanolamine ester derivatives	1:2	50 g/min 3-4 bar	

After the finishing process is applied, the following tests were carried out on the products.

- Air permeability analysis according to EN ISO 9237, ASTM D 737 standards
- Elasticity and recovery analysis according to ASTM D3107-07 standard
- Tear strength analysis according to ISO 13937-2:2000 standard
- Oil Repellency: Hydrocarbon resistance test according to AATCC 118-2012 standard*

*Since it was aimed to preserve the functional properties of the products up to 5 home launderings, the oil repellency test was carried out after 5 home launderings.

3. RESULTS AND DISCUSSION

The air permeability analysis results of the finished samples are given in Table 3.

Table 3. Air permeability analysis result of the samples

Sample Code	**R30**	**R27**
Air permability values (mm/s)	17.0	21.5
	18.6	20.8
	18.1	22.1
	18.8	20.2
	18.6	21.6
	18.9	20.4
	17.9	22.8
	17.1	22.3
	20.5	19.1
	21.8	21.8
Mean	**18.7**	**21.3**
Standard deviation	1.47	1.17
Coefficient of variation (%)	7.8	5.53

There was a %12 difference observed between conventional denim pants and stain-resistance finishing applied samples according to air permeability analysis results. Table 4 shows the physical analysis results of the finished garments.

Table 4. Physical analysis results of the trials

Sample Code	**Tear strength (N) (warp)**	**Tear strength (N) (weft)**	**Elasticity (%)**	**Recovery (%)**
R27	9.98	19.15	41.98	8
R28	18.38	22.29	54.91	9
R29	14.98	22.61	54.23	6
R30	16.95	21.76	46.04	8

When the physical analysis results are examined, it can be seen that the control sample has lower tear strength and elasticity values than the finished trials. It was attributed that the finishing process in the polymer structure applied increases the strength of the fabric by clinging between the fibers. At the same time, the softener used had a positive effect on the elasticity feature. When the softeners were compared in each other, it was seen that there was no significant contribution to the physical properties of the product. The antistatic chemical also did not have a significant effect on the physical properties of the product.

In the oil repellency analysis, 5 domestic-washed samples were contaminated with tea, coffee, wine, ketchup, milk, and cherry juice. The results were evaluated out of 5 points. Table 5 shows the oil repellency analysis results of the samples.

Table 5. Oil repellency: Hydrocarbon resistance test analysis results

Sample Code	**Stain Type**					
	Tea	**Coffee**	**Wine**	**Ketchup**	**Milk**	**Cherry juice**
R27	2.5	2.5	3	4.5	4.5	4
R28	3	3.5	3.5	5	5	4
R29	3	3	3	5	5	3.5
R30	3	3	3	5	5	4

Stain images of samples are shown in Figure 1, 2, 3 and 4.

Figure 1. R27 (control sample) stain image

Figure 2. R28 stain image

Figure 3. R29 stain image

Figure 4. R30 stain image

When the results were examined, the control sample was the one with the lowest stain-repellent property as expected. The other trials are compared within themselves, it was seen that R28 has the highest stain repellent efficiency. This result is attributed to the fact that the silicon-derived softener used in the finishing process of R28 creates a thin layer and lubricity on the fabric surface, which reduces the surface tension of the fabric and increases its stain-repellent property.

4. CONCLUSION

When the amount of water used in the product life cycle of denim garments is examined, the second stage in which the most water consumption occurs is during the care of the user. In this study, denim products having stain-resistance properties were developed to reduce the water footprint in the total product life cycle. Fluorine-free stain-repellent finishing was applied to denim products. Thus, it was aimed for the user to reduce the frequency of washing the product at homecare. The finishing process was applied to the products by spraying method instead of conventional impregnation or exhaustion methods. Thus, reducing the amount of water and chemicals used during the production of the product, a homogeneous application at a low liquor ratio of 1:2 was achieved.

An air permeability test was carried out to examine the effect of the applied finishing process on the comfort properties of the product. When the results were evaluated, there was no significant difference observed with conventional denim pants according to air permeability analysis results.

It was observed that the applied finishing process was increased the tear strength and elasticity properties of the product, however, did not have a significant effect on the recovery property.
It has been observed that silicone-derived softeners give better results in terms of stain repellency and elasticity.

As a result of the study, it has been observed that the developed samples have stain-repellent properties event after 5 home launderings.

REFERENCES

Kant, R. (Eds.). (2012). Textile Dyeing Industry an Environmental Hazard, In: Natural Science, 4, 1.
Pekin, M., Soruşbay, C. (Eds.). (2006). Greenhouse Gas Emissions Produced by Transportation Sector, In: Thesis (M.Sc.), İstanbul Technical University, Institute of Science and Technology.

Li, S., Fang, X., Zhou, X., Bie, B., Xu, J., & Yi, C. (2020). Optimization of Chlorine Bleaching Parameters for Indigo Denim Textile Based on the Model of Response Surface Model and Genetic Algorithm. *Journal of Physics: Conference Series*, Vol. 1621, No. 1, p. 012026. IOP Publishing.

Scacchetti, F. A. P., Pinto, E., & Soares, G. (2017). A multifunctional cotton fabric using TiO2 and PCMs: introducing thermal comfort and self-cleaning properties. *Materials Science and Engineering*, Vol. 254, No. 12, p. 122011. IOP Publishing

Periyasamy, A. P., & Militky, J. (2017). Denim and consumers' phase of life cycle. *Sustainability in denim*, pp. 257-282. Woodhead Publishing.

WATER DECONTAMINATION USING CONDUCTIVE KNITTED FABRIC

Muhammet UĞAN[1*], Ahmet KOLUMAN[2], Sultan ARAS ELİBÜYÜK[3], Mustafa ÇÖREKCİOĞLU[4]

[1*,2]Pamukkale University, Faculty of Technology, Department of Biomedical Engineering
[3,4]Ozanteks Tekstil San. ve Tic. Inc. R&D Center.

Corresponding author: muhammetugan@outlook.com

Abstract: *Every day, our water resources around the world are decreasing and we never realize it. In this period when our water resources are facing depletion, people use it extravagantly, as if they have unlimited resources. Sustainable water use is the efficient use of water in a way that is compatible with the environment without wasting even a single drop of water. Water resources that cannot be purified from biological pollution at a sufficient level affect 2.4 million people every year. These water sources spread typhoid, cholera and other diseases. The main threat that is invisible and has an acute effect on water resources is biological pollution. There are many methods used against biological threats in the potable water supply chain, and physical filtration processes are applied. In our study, decontamination was carried out with the application of electricity from different silver-containing knitted structures in cooperation with the university-industry. For this purpose, a controlled electric current was created on the knitted structures by validating the (in-house method) developed in our laboratory. The efficiency of the filtration created for this purpose was examined.*

Keywords: *Filtration textiles, filtration mechanisms, liquid filtration, technical textile*

1. INTRODUCTION

Although three quarters of the earth's surface is covered with water, the amount of fresh water suitable for human use is quite limited. The total amount of fresh water on Earth is approximately 35 million km^3 (2.5% of the total water on Earth), of which only 0.3% consists of fresh water resources suitable for ecosystem and human use. The remaining fresh water is mostly trapped in glaciers and underground reserves at the poles and high mountains (Muluk, et al. 2014). The rational and sustainable use of water resources can be achieved by the coordination of spatial and intersectoral planning and decision-making processes. One of the important issues in the management of water resources; protection of water resources and the other is the sustainable use of water resources (Kırtorun and Karaer, 2018).

With the efficient use of water in industry, savings are encouraged in many interrelated sectors. The way to ensure the sustainability of water in production is through many different efficiency practices such as reducing the use of mains water, increasing the rate of reused or recycled water, investing in gray water recycling technologies, using rainwater collection equipment and smart water meters (Çevreciyiz, 2016). In general, domestic water obtained from treated collection or wastewater should be hygienic and microbiologically safe, colorless and completely free of solid waste (Karahan, 2011).

In the Dictionary of Filtration Terms prepared by Wakeman (1985), the filter structure is defined as 'permeable material on or in which solid particles are stored and used for filtration'. Sutherland and Purchas (2002) stated that this definition is not broad enough and defined the filter as 'the structures that are permeable to one or more components of a mixture, solution or suspension, and impermeable to other components, under the specified filtration conditions' (Arslan and Kaplan, 2017). Filtration is generally a separation process and the purpose of this process is to increase the purity of the filtered material. The filtration process can be realized by different mechanism methods (Hutten, 2007). In this study, filtration work was carried out by creating knitted structures with special threads containing silver.

This filtration mechanism is used to remove particles from liquids and is also effective if the particle is smaller than its size at any point in the pore. It occurs with the effect of one of the factors of filtration,

inertia, stopping, diffusion or electrostatic attraction rather than simple stopping mechanisms where the particle size should be larger than the pore size (Arslan and Kaplan, 2017). Antimicrobial filter structures contain chemicals that prevent the growth and reproduction of microorganisms such as fungi, bacteria and yeast. At the same time, these structures can be used to prevent the migration of biological pests into the filtered or filtered product (Hutten, 2007).
Bacteria multiply very quickly thanks to the appropriate temperature ranges and humidity on the textile surfaces. While uncontrolled bacterial growth harms the environment and human health, it causes loss of comfort and formation of bad odor. In addition, negative effects can be observed in terms of discoloration, performance losses and stain formations that may occur on the fabric. Textile products with antibacterial properties help to reduce and eliminate the negative effects caused by bacteria (Mucha et al. 2006). The textile structure to be used in the filtration system has been gained with silver-containing threads, which have antibacterial properties in their natural chemistry.Since the conductive fabrics with silver thread content have high washing resistance, the antibacterial properties of these products will be a reason for preference for users.

The aim we want to achieve with the concept with the filtration system to be made within the scope of the study is to design an innovative, easy-to-use, high-efficiency water filtration system against the water scarcity that the whole world is facing. For this purpose, the contribution of knitted fabrics containing different proportions of silver fibers to water hygiene was evaluated, and in addition, different voltages and electrical decontamination (electrodecontamination) possibilities with DutyCycle were tried. This study includes the trials of decontamination of knitted fabric alone and by passing electricity.

2. MATERIALS AND METHODS

2.1. Materials

Elastane threads containing silver-containing special threads are used in the production of conductive and antibacterial seamless products. Ultrapure water contaminated with Escherichia coli (ATCC 25922) was used for water passage. It was produced with a 3D printer by grounding the fabric tensioning apparatus and the funnel so that the seamless samples remain stable during the water passage and can be connected to the seamless products of the electrode-contamination circuit. In the electrical decontamination process, 50V DC regulated power supply was used for voltage control and Arduino Mega was used for signal control.

2.2. Methods

While the samples were created from silver yarns, with 30% silver content tightly knit and 30% silver content sparsely knit, 100% polyamide samples were also formed and subjected to the test. Seamless products with two different structures were knitted with a Santoni M-8 seamless knitting machine. In the study, it was decided to use ISO 20645-method and Agar diffusion method for the antimicrobial properties of silver-containing knitted fabric. For this purpose, textile samples cut in certain sizes will be contacted with different microorganisms and the inhibition zones formed on the contact surface and around the textile at the end of incubation were measured (Anon., 2004).

According to the antimicrobial effect, knitted fabrics with the highest effect were determined to be combined with electronic circuit. Single or multiple regression models to be used in the project, factor analyses and other statistical tests and analysis studies required according to the quality of the data to be obtained will also be used in the interpretation of the experimental results.

The parts in figure 1 are designed to keep the fabric taut while the contaminated liquid passes through the knitted fabric and to collect the liquid passing through the fabric directly into the balloon.

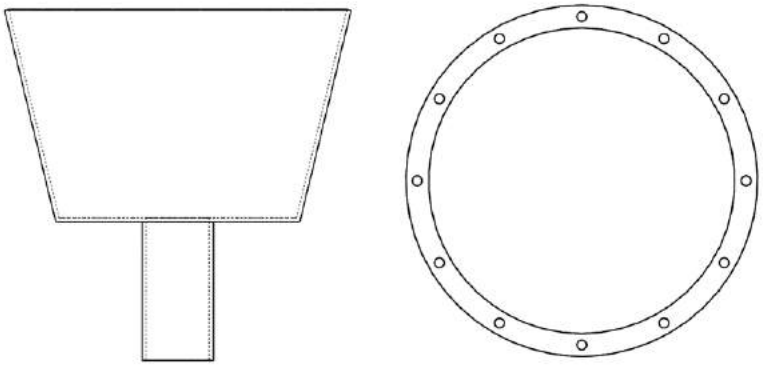

Figure 1. Design of contaminated fluid passage through knitted fabric.

Voltages of 25V and 50V amplitudes were applied to knitted fabrics at 10 KHz frequency with 25%, 50% and 100% DutyCycle (Figure 2). The distance between the cables providing the transmission of electrical signals to the filter surface was kept constant at 5 cm in each sample. The products to be used in the experiment were cut in appropriate sizes and sewn to the tensioning apparatus with equal tension. The obtained filters were sterilized by keeping them in autoclave conditions at 121°C for 15 minutes. .In order to test the antimicrobial properties of the fabrics and to evaluate them independently of the effectiveness of electrode decontamination, the passage of contaminated water is provided from each fabric without applying tension. Ultrapure water contaminated with 10^8 E.coli was used during the experiments (Figure 3). The volume of contaminated water that the fabrics would be exposed to during each experiment was kept constant at 50mL.

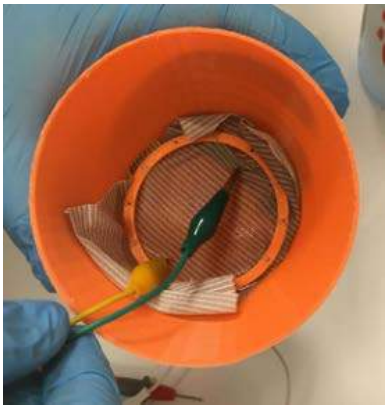

Figure 2. Tension Applied to Knitted Fabrics

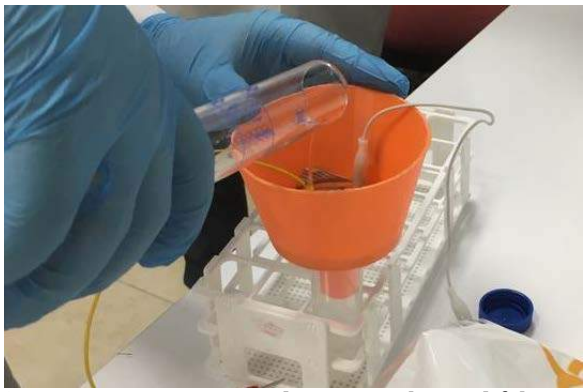

Figure 3. Pure water application to knitted fabrics

2.3. Experiment design

The controlled variables in the whole experiment are the silver density in the fabrics, the tension applied to the fabrics, the DutyCycle and the number of reuses of the fabrics. The distance between the electrodes to which voltage is applied during the experiment will be 5 cm. The experiments to be carried out in this context are shown in Figure 4.

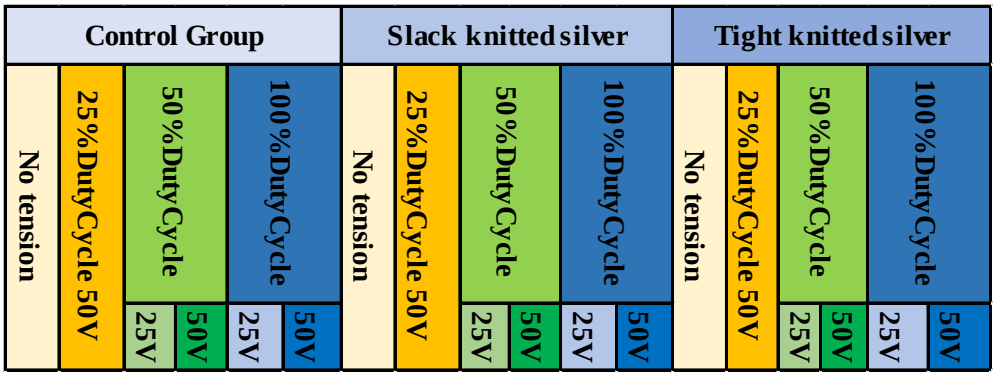

Figure 4. Experimental design to be used in the study.

3. RESULTS AND DISCUSSION

Antibacterial properties of conductive seamless products containing silver were measured. Then, the sample, which accumulated in the 50 ml falcon as a result of the passage of contaminated water through the fabrics, was taken to the nutrient medium and the growth that occurred after a 24-hour incubation period at 37°C was evaluated. In the first experiments, the zone diameters of the fabric pieces and sample liquid, which were kept in incubation at 37 °C, according to the bacteria were examined. All kinds of zone formation observed as a result of incubation showed that the product was antibacterial (figure 5), and it was observed that the yield obtained from the decontamination process increased with the applied voltages.

Figure 5. Zone formation observed above 1mm of incubation

As a result of the study, the data obtained from the media were evaluated in the light of biostatistics methods. As a result of these evaluations, the data satisfying the $p<0.05$ condition are given in Table 1.

Table 1. Efficiency from decontamination with applied voltages

	Actionless Control	**Often Silver**	**Sparse Silver**	**No Silver**
50V DC	8,00E+00	5,64E+00	5,40E+00	6,40E+00
25V DC	8,00E+00	5,53E+00	5,32E+00	6,66E+00
50V %50	8,00E+00	5,40E+00	6,01E+00	6,18E+00
25V %50	8,00E+00	5,58E+00	5,20E+00	6,43E+00
50V %25	8,00E+00	5,78E+00	5,90E+00	6,40E+00
No Voltage	8,00E+00	5,52E+00	5,38E+00	6,43E+00
	Mean	5,60E+00	5,69E+00	6,44E+00
Standard Deviation	1,09E-01	2,88E-01	1,31E-01	
T-Test	2,67838E-13	0,399903186	8,2125E-05	
p<0,05 Significant p	2,67838E-15	0,003999032	8,2125E-07	

When the data in Table 1 are examined, it has been observed that there is no significant difference between the fabric with intense silver content and the fabric with lower silver content. It is observed that the results of the experiment have a positive effect.

In line with the data obtained from the experiments, it is seen that the reproduction in the samples applied with 50V voltage is much less than in the samples applied with 25V voltage. In addition, it is observed that the samples applied 50% DutyCycle 50V voltage are the samples with the maximum efficiency, followed by the samples that directly applied 50V voltage.

In the light of these data, it is more appropriate to prefer the fabric containing rare silver in order to keep the price performance value of the fabric to be used in the design of an electrode decontamination system for water to be created in the light of these data, it is more appropriate to choose the fabric containing sparse silver, keeping the voltage to be applied at the maximum amplitude provides a greater advantage in the log drop, and the applied voltage is reduced by 50% duty cycle. It has been observed that the impact of the pulsed application will be much higher.

4. CONCLUSION

In this study, the contribution of knitted fabrics containing silver fibers in different proportions, which are known to have conductive and antibacterial effects, to water hygiene was evaluated, and in addition, the possibilities of electrical decontamination (electrodecontamination) with different current and voltage to be applied were evaluated. Pure water prepared with Escherichia coli was applied to the fabrics and electrical current was applied to the fabrics with different voltages and signals during the application. After the application, samples were taken from the liquid passing through the fabrics and from the fabrics, and the zone formations were checked. It was observed that the experiment was successful in the first attempts made. No zone formation was observed in the silver seamless samples that were incubated after the filtering process. When the zones formed in the filtered liquids are examined, it has been observed that the applied voltage and signals increase the decontamination efficiency compared to the direct filtration process, the fabrics containing silver are more efficient than the fabrics without silver in terms of electrode decontamination efficiency, but the silver density does not provide a significant benefit in this regard. In further studies, it is aimed to develop a decontamination system and to conduct trials in wastewater.

ACKLOWKEDGEMENT

This study was developed by industry-university cooperation within the scope of TÜBİTAK-2209-B Industry-Oriented Undergraduate Research Projects Support Program and was supported by the Ozanteks Tekstil R&D Center's equity project numbered 21U02. In addition, it supports the development of sustainable products within the scope of TÜBİTAK 2244 Industry Doctorate Program Project with the number 119C070 with the filtration system created from the textile structures made in the study.

REFERENCES

Anonim, (2004). International Standardization Organization, Textile Fabrics, Determination of antimicrobial activity, Agar diffusion test

Arslan, S., Kaplan, S., (2010). Filtrasyon Tekstilleri: Kullanılan Hammaddeler, Üretim Yöntemleri Ve Kullanım Alanları, The Journal of Textiles and Engineer, Cilt 17 - Sayı 79, Sayfa 24

Çevreciyiz (2016). Sürdürülebilir Kalkınma, http://www.cevreciyiz.com/makale-detay/1035/su-verimliligi-uygulamalariyla-sanayide-suyun-ayak-izi-azaliyor erisim tarihi:27.04.2022.

Hutten , I.M., (2007), Handbook of Nonwoven Filter Media, Burlington, USA.

Karahan, A. (2011). Gri suyun değerlendirilmesi, X. Ulusal Tesisat Mühendisliği Kongresi, 14-18 Nisan, TMMOB, İzmir, 44-46.

Kırtorun, E., Karaer, F., (2018). Su Yönetimi ve Suyun Sürdürülebilirliği, Sürdürülebilir Mühendislik Uygulamaları ve Teknolojik Gelişmeler Dergisi, 1(2): 151-159

Mucha, H., Höfe, D., Swerev, M., 2006, Antimikrobiyel Terbiye ve Türleri, Tekstil Maraton, Ocak – Subat 1/2006, s 64-69.

Muluk, Ç., Kurt, B., Turak, A., Türker, A., Çalışkan, M., Balkız, Ö., Gümrükçü, S., Sarıgül, G., Zeydanlı, U. (2014). Türkiye'de suyun durumu ve su yönetiminde yeni yaklaşımlar: çevresel perspektif, Sürdürülebilir Kalkınma Derneği, FAO, Doğa Koruma Merkezi, Yaşama Dair Vakıf, Türkiye.

ILLUMINATED SMART TEXTILE

Teoman KARADAĞ[1], Mehmet ALTUĞ[2], Onur KARLIK[3]

[1] İnönü University, Department of Electrical and Electronic Engineering, Malatya, Türkiye
[2] İnönü University, Department of Machinery and Metal Technologies, Malatya, Türkiye
[3] Çalık DENİM, Department of Research and Development, Malatya, Türkiye

Corresponding author: teoman.karadag@inonu.edu.tr

Abstract: *In the presented study, optical fiber threads are used on the textile material. Said optical fiber is multiple on the textile material and is associated with a light source. The end of each optical fiber creates a pattern on the textile material. The light source is illuminated by giving light on these patterns. In addition, it is possible to create a meaningful light animation by giving light in different colors. For this purpose, it is to create a fabric that can emit meaningful light depending on temperature, humidity, movement, emotion change, pulse, Saturation (SPO2 oxygen level in the blood), electromagnetic field change, gas, radiation. In order to realize all the above-mentioned objectives and which will emerge from the detailed description of the study, the present study is a fabric capable of emitting light to the environment by means of at least one light source and at least one fiber optic.*
Keywords: *Smart textiles, fibre textiles, illuminated textiles, technical textiles.*
Patent Number: *2021/013048*

1. INTRODUCTION

As the most common material today, textile gains an important functionality with the addition of electronic components. Smaller, more technologically effective electronic components have greatly influenced the world of wearable textiles. In this context, important studies that combine polymer technology and textile technology have also been put forward. Polymers are insulators or semiconductors in their pure form. Polymers can be a suitable choice for wearable technologies due to their flexibility, mechanical stiffness, and structure compatible with stretchable electronic devices (Elschner et al. 2010; Kaltenbrunner et al. 2013; Yuhao Liu, Pharr, and Salvatore 2017). In the light of the developed technologies, it is possible to obtain conductive polymer coated yarns and fibers. Conductive polymer coated textiles can be used in a wide range of applications from defense to aviation (Cetiner et al. 2010; Mule et al. 2019; G. Wang, Hou, and Wang 2020). (Koncar 2019) stated that conductive polymers can be used to form conductive fibers through spinning techniques. He stated that the coating of fibers with electrically conductive materials and the use of fibers with conductive polymers are an important approach (Koncar 2019). (Takamatsu et al. 2012) fabricated woven, die-coated yarns to make a pressure sensitive textile and conductive rows using a perfluoropolymer spacer (Takamatsu et al. 2012). Traditional weaving patterns are used to produce textile materials with conductive materials. Combination of different types of conductive yarns and conventional polymeric yarns, both are used together in the loom. Conductive threads can be positioned as weft or warp in these woven structures to form electrical (Ismar et al. 2020; Swallow and Thompson 2006). Active materials that are important for smart textiles are electroactive polymers, which have the advantage of being light, soft and flexible. Electroactive polymers can also be easily processed with inorganic materials. Conducting polymers have been mostly explored as active materials for flexible electrochromic devices due to their broad color spectrum, good coloring efficiency, low operating voltage and fast switching capabilities. However, the planar shape and airtight nature limit its applications in microelectronics and wearable electronics (Weng et al. 2016).

In addition, conductive fibers were used in combination with textiles. (Bedeloglu, Sunter, and Bozkurt 2011) produced conductive yarns by wrapping metal wires around cotton fibers and made smart fabric applications (Bedeloglu, Sunter, and Bozkurt 2011). (Kim, Kwon, and Na 2019; Ma et al. 2014) obtained important results in terms of stretchability and flexibility in fabric and yarn by using conductive fibers in their studies (Kim, Kwon, and Na 2019; Ma et al. 2014). (Šalej, Fajfar, and Rijavec 2011) developed medical and smart textiles by using Nickel-Titanium-based shape memory alloys (Šalej, Fajfar, and Rijavec 2011). Conventional weaving patterns are used to manufacture textiles with electrically conductive materials. A combination of different types of conductive yarns and conventional polymeric yarns are used together during weaving. Conductive threads are positioned in the form of weft or warp in these woven structures to form electrical circuits (Bedeloglu, Sunter, and Bozkurt 2011; Ismar et al. 2020; Kim, Kwon, and Na 2019; Ma et al. 2014; Šalej, Fajfar, and Rijavec 2011; Stoppa and Chiolerio 2014; Swallow and Thompson 2006; Weng et al. 2016). In this context, it has been tried to create knitted circuits for antennas, electromagnetic shielding and USB applications related to the production of fabric-based circuits by weaving conductive yarns (Dhawan et al. 2004; Gimpel et al. 2004; Hertleer et al. 2008). Double-layer woven fabric structures are special types of woven fabrics. In a double-layer woven construction, the upper warp thread layer is combined with a lower weft thread layer to create a durable and connected fabric structure. In this structure, the conductive yarn can be buried through these layers (as a middle layer) and hence by hidden insertion of the conductive yarns, which prevents possible short circuits from this layered structure (S. K. Bahadir et al. 2011; S. K. Bahadir, Koncar, and Kalaoglu 2012; Ismar et al. 2020). It has also been in businesses that produce textiles using metal threads and fibers. Thremshield LLC metallized woven nylon fabrics, Baltex heatable textiles and electromagnetic shielding materials (Technical Textiles & Knitted Fabrics - Baltex n.d.), Chr. Dalsgaard, with the development of micro-sensors, tried to integrate panels such as keyboard and screen into fabrics with the help of a copper thread coated with a silver layer and coated with polyester (Ohmatex 2013). In another study, (M. C. Bahadir and Bahadir 2015) analyzed the signal performance by creating an electrical circuit in the woven structure using silver-plated polyamide (PA), stainless steel and insulated copper threads (Hughes-Riley, Dias, and Cork 2018).

Sensors are also widely used in electronic textiles. The use of sensors in electronic textiles started with Wearable mainboard, fabric tension sensors, etc., and later became widespread with wireless communication in patient monitoring system and military equipment (Hughes-Riley, Dias, and Cork 2018). Conductive textiles that change their electrical properties as a result of environmental influence can be used as sensors. Textiles that react to deformations, such as pressure sensors and breathing sensors. On the other hand, there is the possibility of making biopotential sensors with smart textiles (Stoppa and Chiolerio 2014). Among the wearable sensors, tension/motion and touch/pressure sensors have received the most attention (Heo et al. 2018). (Cho et al. 2011) The first motion-measuring textile-based sensor was used to predict and measure changes in electrical resistances accompanying changes in angle at the elbow joint. A braided advanced piezoresistive textile showed more accurate resistance changes as well as better durability (Cho et al. 2011). A new graphene woven fabric (GWF) / polydimethylsiloxane (PDMS) composite as a highly flexible, sensitive tension sensor capable of detecting weak human movements with an extremely high piezoresistive indicator factor at a tension of 3% and excellent durability. has used. The wireless wearable musical instrument prototype made of composite sensor demonstrated the transformation of human movements into music of different instruments and sounds (X. Liu et al. 2017). (Abdul et al. 2017) developed a method to durablely coat reduced graphene oxide (rGO) on complex fibers of Nylon fabric. He investigated the durability of this coating with the help of pressure sensors (Abdul et al. 2017). (R.Paradiso, Caldani, and M.Pacelli

2014) stated in their study that multi-layered woven and knitted structures will offer a variety of different fabric pattern designs that can lead to different sensing performances. He demonstrated that the conductive yarn as an electrode could be placed between the insulating layers of the multilayer fabric structure in a sandwich form (R.Paradiso, Caldani, and M.Pacelli 2014). (Masuda et al. 2010) and (T., H., and A. 2014) stated in their studies that sandwich-like structures containing conductive yarns cause voids in the structure by helping the yarns to be arranged in an inclined position. When pressure is applied to these structures, the gap between the layers decreases and the pressure sensing circuit mechanism takes place (Masuda et al. 2010; T., H., and A. 2014). (Hoffmann, Eilebrecht, and Leonhardt 2011) used a similar principle for a system to measure respiratory rate; where two conductive fabrics are placed on either side of a 3D spacer textile (Hoffmann, Eilebrecht, and Leonhardt 2011). (Holleczek et al. 2010) created a sensor using an electrode and a resin release material and integrated the sensor into socks (Holleczek et al. 2010). (Mannsfeld et al. 2010) developed a highly flexible and inexpensive capacitive pressure sensor using a microstructured thin film as the dielectric layer of capacitors (Mannsfeld et al. 2010). (Gu, Gorgutsa, and Skorobogatiy 2011) created a conductive capacitive fiber from copper wire embedded in a 0.12 mm diameter fiber (Gu, Gorgutsa, and Skorobogatiy 2011). Self-powering fibers/fabrics that respond to tension or pressure can also be designed based on mechanisms other than the piezoelectric effect. The fiber-shaped sensing device produced electrical signals upon stretching of the substrate as the double-stranded fibers approached each other. This kind of stretchable fiber sensor can be easily woven into commercial textiles to monitor body movements with high stability and durability. Other self-powered fiber/cloth sensors based on triboelectric mechanism have also been investigated and have shown good sensing properties (Ha et al. 2015) (Z. L. Wang 2014). In some other studies, textile-based moisture sensors could be prepared by a simple dip coating method of polymers on commercial fabrics with high strength, flexibility and high surface area (Low et al. 2015). The most efficient way to manufacture chemical fabric sensors on a large scale is to coat the sensing material onto the fabric. However, chemical sensors made from pure conductive polymers have a relatively slow response time with an irreversible deterioration in their conductivity. Also, an ideal chemical sensor should be sensitive to a particular chemical. However, existing chemical sensors can be sensitive to many chemicals, and the response to one chemical is easily affected by the presence of other chemicals.

Carbon Nanotubes (CNTs) are frequently used to produce electronic textiles. CNTs have electrical conductivity, superior thermal stability (4000 K), high tensile strength (63 GPa) and low density (1.3-1.4 g/cm3) (Khair, Islam, and Shahariar 2019; Purohit et al. 2014). Deposition of CNTs on textile substrates is mostly accomplished by dip coating, flexographic printing, ink-jet printing, and scraper blade technology due to their simplicity (Bøggild 2018)(Shahariar 2017). In addition, CNT coated textiles have flame retardancy, UV absorption and water repellency (Yuyang Liu et al. 2008). (Shim et al. 2008) stated that the technology could be used for biosensing, with carbon nanotube cotton threads being used to detect albumin, an important protein in the blood (Shim et al. 2008). (Jost, Dion, and Gogotsi 2014) focused on coated, fiber, woven as well as knitted supercapacitors and batteries (Jost, Dion, and Gogotsi 2014). (Uddin et al. 2013) obtained energy efficiency by coating CNTs in their study (Uddin et al. 2013). (Hu et al. 2010) fabricated high-conductivity textiles by a simple "dip and dry" process using single-walled carbon nanotube (SWNT) ink to produce a stretchable conductive textile. In this way, such conductive textiles kept the same stretchability of regular fabric. Moreover, the porous nature of textiles facilitates accessibility from any electrolyte, and such porous and stretchable conductors find wide application in the field of e-textiles (Hu et al. 2010). (Quintero et al. 2015)

Energy storage is an important step in electronic textiles. In this field, flexible supercapacitor, electric double-layer capacitor and battery, piezo-resistor, solar cell, fuel cell are widely used devices to store energy produced from energy collector. (Jost et al. 2011) investigated the electrochemical behavior of porous carbon materials impregnated on woven cotton and polyester fabrics using the printing technique (screen printing). The porous nature of such fabrics has allowed for supercapacitor applications that require porous films for ion transfer between electrodes.

Luminescent threads have started to be used for illumination purposes in electronic textiles in (T Dias and Monaragala 2010; Tilak Dias and Monaragala 2012) and some other studies (T Dias and Monaragala 2010; Tilak Dias and Monaragala 2012; HO. 2018). In addition, (Pas 2012) and some other studies stated that commercially illuminated textiles are produced with the use of LED technology (2017) n.d.; Cutecircuit n.d.; Pas 2012).

Some important studies about smart textiles are the production of textiles that can obtain energy. (Bedeloglu et al. 2009) produced solar cells (photovoltaic) by adding additional materials to polypropylene substrates in textile products (Bedeloglu et al. 2009). (Zhang et al. 2014) developed a fully solid, lightweight, flexible and wearable polymer solar cell (PSC) textile with photovoltaic performance (Zhang et al. 2014). (Lee et al. 2014) have done a comprehensive study on Organic photovoltaic cells (OPV) for the next generation flexible power supply due to its unique features such as flexibility, lightness, easy workability, cost-effectiveness and environmental friendliness (Lee et al. 2014). (Sahito et al. 2015) focused on reducing the cost of dye-sensitized solar cells available in textiles and making them flexible by using versatile materials that could make this energy conversion technique more economical and increase its applications (Sahito et al. 2015).

2. MATERIALS AND METHODS

Picanol Optimax-I was used as a weaving loom in the study. Picanol Optimax-I, Easy insertion of any weft yarn. From weft thread detection to the unique quickstep weft server and various weft cutting systems, the entire system has been designed to handle the maximum variety of weft threads in the smoothest possible way. In the study, weaving was done at 350 rpm. Neither 30 nor dyed cotton yarn was used as the warp yarn, and 0.25 mm fiber optic yarn was used as the weft yarn. The size of the warp thread used is Ne 30. Cotton Thread System (Ne): It is used for numbering cotton threads. It is the number of 840 yards in 1 pound of yarn. In other English systems, this length varies. For example; The accepted length in English flax, hemp is 300 Yards, while in Worsted it is 560 yards. The fiber optic rope used in the study is given in figure 1a.

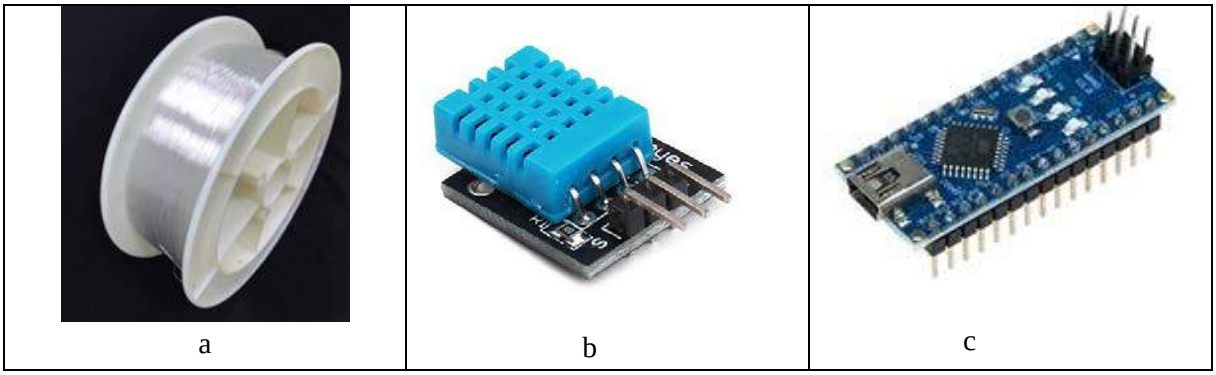

a b c

Figure 1. Materials rope, sensor and processor

The size of the processor here is 50mmx50mm. If the system is desired to be reduced, it can be fit into millimetric dimensions with a card to be prepared only in processor sizes.

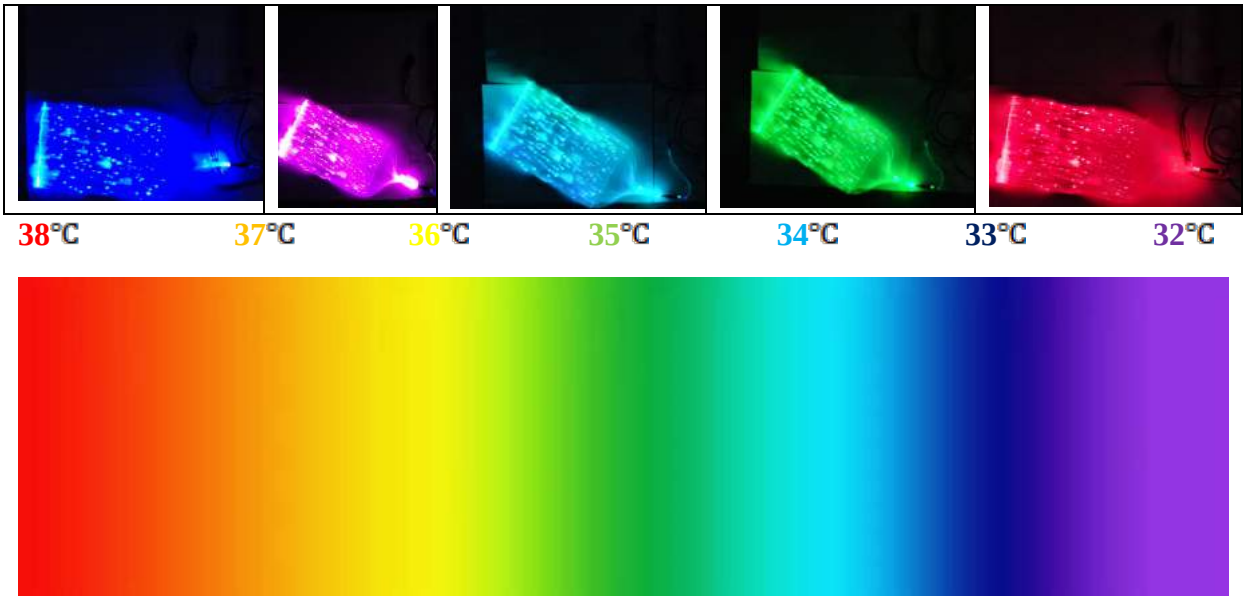

Figure 2. Illuminated smart textile and colour scale

As a result of the weaving process, fabrics of different sizes were produced. In this study, x-y size fabric is used. DTH 11 was used as the sensor used for the study to be meaningful. This sensor board has been chosen for its easy use with Arduino. When the system is desired to be downsized, "FTNT55XH103FA1A050" Flexible film temperature sensors can be used for wearable products, so the sensor size can be reduced to 100µm. DTH 11 temperature and humidity sensor is shown in Figure 1b. The unit can measure temperature between 0 and 50°C with an error margin of 2°C, and can measure humidity between 20-90% RH with a 5% RH margin of error. Arduino nano was used as the processor is shown Figure 1c. Arduino Nano; It is an Atmega328 based microcontroller board. It has 14 digital input/output pins (6 of which can be used as PWM outputs), 8 analog inputs, 16Mhz crystal, usb socket, ICSP connector and reset button. There is everything necessary for the operation of the microcontroller on the board. It can be easily connected to a computer via a USB cable, powered by an adapter or a battery. Illuminated smart textile and colour scale shown in Figure 2.

4. CONCLUSION

As a result, the fiber braided illuminated fabric produced, the different colors of the light were made meaningful by the software. The study was based on body temperature. If 36°C is considered as normal body temperature, the color change with the increase in body temperature is observed as a change towards red color as seen in the color scale above, and the decrease in body temperature is observed as a color change towards purple color. All intermediate color values can also be obtained with a sensor with a higher temperature tolerance. Thus, the fiber braided illuminated fabric, which is made meaningful, will find many different uses. If we give an example from medical, military and daily life. In medical applications, especially in patients who require follow-up, instead of regularly going to the bedside of the patient and measuring his temperature, it can be easily monitored remotely in this way. As can be seen in the study, it can be ensured that the fabric in that color tone flashes for the highest and lowest temperature values to be determined. In this study, fiber yarns were fed with a visible light source. If it is illuminated by being fed at a wavelength that the eye cannot perceive as a light source and this is made visible with glasses that will make that wavelength visible, it can be used

for military purposes for critical missions. Today, with the Covid-19 pandemic, fever measurements are made at the entrances to closed places (Shopping Centers , Airport, Public Spaces, etc.). In order to facilitate the follow-up of these temperature measurements. Fiber braided illuminated tapes with LM35 temperature sensor and a micro circuit can be produced at low cost and can be a widely used solution.

REFERENCES

Bahadir, M Cagatay, and Senem Kursun Bahadir. 2015. "Selection of Appropriate E-Textile Structure Manufacturing Process Prior to Sensor Integration Using AHP." *The International Journal of Advanced Manufacturing Technology* 76(9): 1719–30. https://doi.org/10.1007/s00170-014-6399-x.

Bahadir, Senem Kursun et al. 2011. "A Study on the Beam Pattern of Ultrasonic Sensor Integrated to Textile Structure." *International Journal of Clothing Science and Technology* 23(4): 232–41. http://www.deepdyve.com/lp/emerald-publishing/a-study-on-the-beam-pattern-of-ultrasonic-sensor-integrated-to-textile-fZrMwJ9Y37.

Bahadir, Senem Kursun, Vladan Koncar, and Fatma Kalaoglu. 2012. "Wearable Obstacle Detection System Fully Integrated to Textile Structures for Visually Impaired People." *Sensors and Actuators, A: Physical* 179: 297–311.

Bedeloglu, Ayse, Ali Demir, Yalcin Bozkurt, and Niyazi Serdar Sariciftci. 2009. "A Flexible Textile Structure Based on Polymeric Photovoltaics Using Transparent Cathode." *Synthetic Metals* 159(19–20): 2043–48.

Bedeloglu, Ayse, Nilsen Sunter, and Yalcin Bozkurt. 2011. "Manufacturing and Properties of Yarns Containing Metal Wires." *undefined* 26(11): 1378–82.

Bøggild, Peter. 2018. "The War on Fake Graphene." *undefined* 562(7728): 502–3.

Cetiner, Suat et al. 2010. "Polymerization of Pyrrole Derivatives on Polyacrylonitrile Matrix, FTIR-ATR and Dielectric Spectroscopic Characterization of Composite Thin Films." *Synthetic Metals* 160(11–12): 1189–96. https://cris.vtt.fi/en/publications/polymerization-of-pyrrole-derivatives-on-polyacrylonitrile-matrix.

Cho, Gilsoo et al. 2011. "Performance Evaluation of Textile-Based Electrodes and Motion Sensors for Smart Clothing." *undefined* 11(12): 3183–93.

Cutecircuit. "Cutecircuit. Available Online: Http://Cutecircuit.Com/ (Accessed on 22 August 2017)." http://cutecircuit.com/.

Dhawan, Anuj, Abdelfattah M Seyam, Tushar K Ghosh, and John F Muth. 2004. "Woven Fabric-Based Electrical Circuits: Part I: Evaluating Interconnect Methods." *Textile Research Journal* 74(10): 913–19. https://doi.org/10.1177/004051750407401011.

Dias, T, and R M Monaragala. 2010. "Electro-Luminant Fabric Structures US20100003496A1."

Dias, Tilak, and Ravi Monaragala. 2012. "Development and Analysis of Novel Electroluminescent Yarns and Fabrics for Localized Automotive Interior Illumination." *Textile Research Journal* 82(11): 1164–76. https://journals.sagepub.com/doi/full/10.1177/0040517511420763.

Elschner, A et al. 2010. "PEDOT: Principles and Applications of an Intrinsically Conductive Polymer." *undefined*.

Gimpel, S et al. 2004. "Index Volume 33, 2004." *undefined* 33(4): 281.

Gu, Jian Feng, Stephan Gorgutsa, and Maksim Skorobogatiy. 2011. "A Fully Woven Touchpad Sensor Based on Soft Capacitor Fibers." *undefined*.

Ha, Minjeong, Jonghwa Park, Youngoh Lee, and Hyunhyub Ko. 2015. "Triboelectric Generators and Sensors for Self-Powered Wearable Electronics." *ACS Nano* 9(4): 3421–27. https://pubs.acs.org/doi/full/10.1021/acsnano.5b01478.

Heo, Jae Sang, Jimi Eom, Yong Hoon Kim, and Sung Kyu Park. 2018. "Recent Progress of Textile-Based Wearable Electronics: A Comprehensive Review of Materials, Devices, and Applications." *undefined* 14(3).

Hertleer, Carla, Anneleen Tronquo, Hendrik Rogier, and Lieva Van Langenhove. 2008. "The Use of Textile Materials to Design Wearable Microstrip Patch Antennas." *undefined* 78(8): 651–58.

HO., D O U K. 2018. "Self-Lighting Textile Using Optical Fiber."

Hoffmann, T, B Eilebrecht, and S Leonhardt. 2011. "Respiratory Monitoring System on the Basis of

Capacitive Textile Force Sensors." *undefined* 11(5): 1112–19.
Holleczek, Thomas, Alex Rüegg, Holger Harms, and Gerhard Tröster. 2010. "Textile Pressure Sensors for Sports Applications." *undefined*: 732–37.
Hu, Liangbing et al. 2010. "Stretchable, Porous, and Conductive Energy Textiles." *undefined* 10(2): 708–14.
Hughes-Riley, Theodore, Tilak Dias, and Colin Cork. 2018. "A Historical Review of the Development of Electronic Textiles." *Fibers 2018, Vol. 6, Page 34* 6(2): 34. https://www.mdpi.com/2079-6439/6/2/34/htm.
Ismar, Ezgi et al. 2020. "Futuristic Clothes: Electronic Textiles and Wearable Technologies." *Global Challenges* 4(7): 1900092. https://onlinelibrary.wiley.com/doi/full/10.1002/gch2.201900092.
Jost, Kristy et al. 2011. "Carbon Coated Textiles for Flexible Energy Storage." *Energy & Environmental Science* 4(12): 5060–67. https://pubs.rsc.org/en/content/articlehtml/2011/ee/c1ee02421c.
Jost, Kristy, Genevieve Dion, and Yury Gogotsi. 2014. "Textile Energy Storage in Perspective." *undefined* 2(28): 10776–87.
Kaltenbrunner, Martin et al. 2013. "An Ultra-Lightweight Design for Imperceptible Plastic Electronics." *Nature* 499(7459): 458–63.
Khair, Nipa, Rashedul Islam, and Hasan Shahariar. 2019. "Carbon-Based Electronic Textiles: Materials, Fabrication Processes and Applications." *undefined* 54(14): 10079–101.
Kim, Seung Woo, Sung Nam Kwon, and Seok In Na. 2019. "Stretchable and Electrically Conductive Polyurethane- Silver/Graphene Composite Fibers Prepared by Wet-Spinning Process." *undefined* 167: 573–81.
Koncar, Vladan. 2019. "Smart Textiles for Monitoring and Measurement Applications." *Smart Textiles for In Situ Monitoring of Composites*: 1–151.
Lee, Seungwoo, Younghoon Lee, Jongjin Park, and Dukhyun Choi. 2014. "Stitchable Organic Photovoltaic Cells with Textile Electrodes." *Nano Energy* 9: 88–93. https://www.sciencedirect.com/science/article/pii/S2211285514001232.
Liu, Xu et al. 2017. "A Highly Sensitive Graphene Woven Fabric Strain Sensor for Wearable Wireless Musical Instruments." *Materials Horizons* 4(3): 477–86. https://pubs.rsc.org/en/content/articlehtml/2017/mh/c7mh00104e.
Liu, Yuhao, Matt Pharr, and Giovanni Antonio Salvatore. 2017. "Lab-on-Skin: A Review of Flexible and Stretchable Electronics for Wearable Health Monitoring." www.acsnano.org.
Liu, Yuyang, Xiaowen Wang, Kaihong Qi, and J H Xin. 2008. "Functionalization of Cotton with Carbon Nanotubes." *undefined* 18(29): 3454–60.
Low, Karen et al. 2015. "Composition-Dependent Sensing Mechanism of Electrospun Conductive Polymer Composite Nanofibers." *Sensors and Actuators, B: Chemical* 207(Part A): 235–42.
Ma, Rujun et al. 2014. "Knitted Fabrics Made from Highly Conductive Stretchable Fibers." *undefined* 14(4): 1944–51.
Mannsfeld, Stefan C B et al. 2010. "Highly Sensitive Flexible Pressure Sensors with Microstructured Rubber Dielectric Layers." *undefined* 9(10): 859–64.
Masuda, A et al. 2010. "J. Text. Eng." *J. Text. Eng.* 181: 56.
Mule, Anki Reddy et al. 2019. "Wearable Single-Electrode-Mode Triboelectric Nanogenerator via Conductive Polymer-Coated Textiles for Self-Power Electronics." *ACS Sustainable Chemistry and Engineering* 7(19): 16450–58. https://khu.elsevierpure.com/en/publications/wearable-single-electrode-mode-triboelectric-nanogenerator-via-co.
Ohmatex. 2013. "Smart Textile Technology." *http://www.ohmatex.dk*.
Pas, L Van De. 2012. "Bring Spaces Alive." In In Proceedings of the Smart Fabrics Conference.
Purohit, Rajesh et al. 2014. "Carbon Nanotubes and Their Growth Methods." *undefined* 6: 716–28.
Quintero, A Vásquez et al. 2015. "Capacitive Strain Sensors Inkjet-Printed on PET Fibers for Integration in Industrial Textile." *Procedia Engineering* 120: 279–82.
R.Paradiso, L Caldani, and M.Pacelli. 2014. Academic Press *In Wearable Sensors (Eds: E. Sazonov, M. R. Neuman)*.
Sahito, Iftikhar Ali et al. 2015. "Graphene Coated Cotton Fabric as Textile Structured Counter Electrode for DSSC." *Electrochimica Acta* 173: 164–71.

https://www.sciencedirect.com/science/article/pii/S0013468615011470.
Šalej, A, P Fajfar, and T Rijavec. 2011. “Application of Nickel-Titanium Alloys (NiTiNOL) in Smart Textiles and Clothes.”
Shahariar, H. 2017. “Process Engineering & Materials Characterization for Printing Flexible and Durable Passive Electronic Devices on Nonwoven.” *undefined*.
Shim, Bong Sup et al. 2008. “Smart Electronic Yarns and Wearable Fabrics for Human Biomonitoring Made by Carbon Nanotube Coating with Polyelectrolytes.” *undefined* 8(12): 4151–57.
Stoppa, Matteo, and Alessandro Chiolerio. 2014. “Wearable Electronics and Smart Textiles: A Critical Review.” *undefined* 14(7): 11957–92. www.mdpi.com/journal/sensors.
Swallow, Stan S, and Asha Peta Thompson. 2006. “25 – Applications for Woven Electrical Fabrics.”
T., Kuroda, Takahashi H., and Masuda A. 2014. *In Wearable Sensors (Eds: Sazonov E., Neuman M. R.)*.
Takamatsu, Seiichi et al. 2012. “Fabric Pressure Sensor Array Fabricated with Die-Coating and Weaving Techniques.” *Sensors and Actuators A: Physical* 184: 57–63.
“Technical Textiles & Knitted Fabrics - Baltex.” https://www.baltex.co.uk/home/.
Uddin, M J, B Davies, T J Dickens, and O I Okoli. 2013. “Self-Aligned Carbon Nanotubes Yarns (CNY) with Efficient Optoelectronic Interface for Microyarn Shaped 3D Photovoltaic Cells.” *undefined* 115: 166–71.
Wang, Gang, Chengyi Hou, and Hongzhi Wang. 2020. “Flexible and Wearable Electronics for Smart Clothing.” *Flexible and Wearable Electronics for Smart Clothing*: 1–346. https://onlinelibrary.wiley.com/doi/book/10.1002/9783527818556.
Wang, Zhong Lin. 2014. “Triboelectric Nanogenerators as New Energy Technology and Self-Powered Sensors – Principles{,} Problems and Perspectives.” *Faraday Discuss.* 176(0): 447–58. http://dx.doi.org/10.1039/C4FD00159A.
Weng, Wei et al. 2016. “Smart Electronic Textiles.” *Angewandte Chemie (International ed. in English)* 55(21): 6140–69. https://pubmed.ncbi.nlm.nih.gov/27005410/.
Zhang, Zhitao et al. 2014. “A Lightweight Polymer Solar Cell Textile That Functions When Illuminated from Either Side.” *Angewandte Chemie International Edition* 53(43): 11571–74. https://onlinelibrary.wiley.com/doi/full/10.1002/anie.201407688.

EMBROIDERY THREAD DESIGN WITH BIOCERAMIC ADDED MATERIAL FOR INCREASED BALANCE

Naime SERTAÇ ÇAVUŞOĞLU[1], Melek KUNT HACIOĞLU[1],

[1] Durak Tekstil A.Ş, Durak Tekstil Tasarım Merkezi, Bursa, Türkiye

Corresponding author: mhacioglu@durak.com.tr

Abstract: *In this study; It is aimed to design embroidery thread, a smart medical textile product in high quality continues fiber polyester structure, using bioceramic additive materials with biological functionality to be used in all areas of sports, nature and daily life, where physical balance and athletic performance are especially important. In this direction, a process that applies bioceramic added materials to textile material with a special finishing process has been designed and a functional product has been developed.*

In the end user of the product obtained from the study; It is expected to prevent energy loss of the body, store body temperature, improve balance, increase athletic performance and quality of life by absorbing FIR (Far Infrared Radiation) radiation emitted from the user and reflecting it back to the body. It is thought that the designed product will make an innovative contribution to smart textiles.

Keywords: *Medical textiles, bioceramic, physical balance, far infrared ray, polyester yarn*

1. INTRODUCTION

Today, the developments in technology which are increasing without slowing down, have affected the textile sector as well as in every sector and it has become inevitable to make innovative transformations in this field. Now, in addition to the protective properties of textile materials, it also offers smart solutions to many sectors such as medical, automotive, agriculture and health with its technological product portfolios.

The benefits of infrared rays to human health have been demonstrated by various studies. The human body also has the feature of emitting infrared rays and textile products have been developed by taking advantage of this feature. In addition, the heat absorbed by the skin passes through the blood circulation and medium so that the heat energy reaches the body tissues, promotes human blood circulation and metabolism and has the functions of eliminating fatigue, restoring physical strength and relieving pain. Figure 1 is a schematic diagram of the human body affected by far-infrared fibers(Didi and Yanmei 2021).

Far infrared radiation (FIR) is called rays with wavelengths between 5.6-1000 microns and cannot be seen with the human eye. Any material above absolute zero emits IR (infrared). At room temperature, these materials emit radiation in the far infrared region of the appreciable spectrum, usually at concentrations in the 8-25 μm range (Dyer, 2011).

Bioceramic powders are one of the materials that can emit far infrared radiation. In particular, they can emit rays in the 8-14 μm wavelength range over 0.9 epsilon (Leung, 2015). Some bioceramic powders that can be added to the textile structure to gain far-infrared feature are as follows: Magnesium oxide (MgO), zirconium dioxide (ZrO2), aluminum oxide (Al2O3), iron III oxide (Fe2O3), silicon dioxide (SiO2), germanium, titanium dioxide (TiO2). In addition to these compounds, minerals such as jade, apatite, pearl powder, tourmaline found in nature can also be added to textile structures in powder form. These materials are believed to retain body heat. Bioceramic materials re-radiate FIR deep into the joints, thereby increasing the blood flow of the tissues (Dyer, 2011;Wang et al., 2011; Biocera, Accessed 07.01.2017; Lin et al., 2015; Cobb, Retrieved 27.12.2016).

It has been demonstrated in many studies that infrared rays (FIR) are beneficial to human health. Among these benefits, you can charge yourself while you sleep, increase the oxygen level with the acceleration of blood flow, faster removal of toxic wastes from the body, increase in balance and athletic performance. It is thought that the potential of these products will continue to increase in the future.

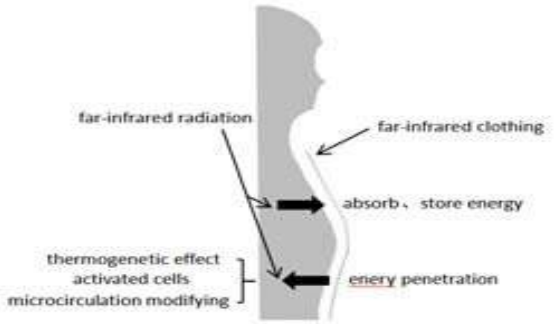

Figure 1. Schematic diagram of the far-infrared fiber acting on the human body (Didi and Yanmei 2021)

2. MATERIALS AND METHODS

2.1. Designing of Bioceramic Added Textile Material

For material design, polyester embroidery thread was chosen as the most suitable material for chemical uptake trials in various embroidery thread groups. In the study area, the most suitable yarn winding machines operating according to different principles were selected for the application of bioceramic added chemical to polyester embroidery thread. The working principle of the selected machine is realized by the contact of the chemical with the yarn by the rotational movement of the wheel. The most important parameter to be determined here is the tension setting of the yarn. As a result of the trials, the appropriate setting was selected in the range of 10-40 rpm. In practice, when pretreatment and bioceramic additives are added to 1 kg of yarn, it has been observed that the weight change is between 5% and 15%. Many attempts have been made for optimum fixing conditions. Accordingly, the product was dry-fixed at 120-180°C for 10-45 minutes. In the second stage, the fixed product was subjected to finishing processes with standard content in order to prevent problems such as heating caused by friction in the end user's embroidery machine and then peeling and breaking due to heating.

With the product containing bioceramic material obtained after the process, a surface must be created in order to observe the effectiveness. The created surface was kept in the closest position to the balance center system of the user and applied to the participants with certain balance tests.

2.2. Inhouse Test Method

In order for the balance thread to be effective, a surface must be created. The closer the designed product is positioned to the cerebellum which is our balance center in our body, the more effective it is. We have developed an in-house method to test whether the created surface is effective. Here are our test steps:

1. Participant stands on one leg.
2. He spreads his arms to both sides.

3. With arms outstretched and standing on one leg, a force is applied to the participant's arm from the side of the airborne leg.
4. It is seen that no matter how hard he tries to resist the applied force, he falls, shakes and cannot stay in balance.
5. The same steps are repeated so that the designed yarn surface touches the participant's neck.
6. When force is applied to the participant in the same way, it is observed that he does not shake and stays in balance.

3. RESULTS AND DISCUSSION

We put the developed bioceramic additive stabilizing embroidery thread material to the test. We observed 85% measurable success in experiments with about 200 participants. Some participants reacted with surprise to the results, expressing how effective the product was, while very few participants thought it was a placebo effect. As a result, most participants observed a significant increase in their physical balance. In addition to the increase in balance, it is effective in absorbing the energy emitted by the body based on the effects of bioceramic materials on the human body and then reflecting it back to the body as FIR radiation. FIR technology is effective in dilating blood vessels, increasing blood flow, removing toxic wastes from the body faster and maintaining body temperature. It is also possible to increase the quality of sleep with the acceleration of blood flow. In addition, it is predicted that the products on which this application is made are highly resistant to washing in the end user. Considering the potential in the technical textiles sector, it is a very strong study that such innovative products will guide the market both in the technical textiles market and in the medical textile applications, and to initiate new and innovative studies.

4. CONCLUSION

Far-infrared textiles cause radiation to be released in the human body and by reflecting this radiation back to the body and thus giving it back to the body, the human body has a warming effect and resonance effect, the skin temperature rises, thus protecting the heat, expanding the superficial tissues and capillaries and accelerating blood circulation. Thus, it can effectively alleviate lactic acid accumulation and sports fatigue. Currently, experts and scientists in many fields are examining sports fatigue from various perspectives and researching ways to alleviate sports fatigue and increase physical balance at the same time. We hope to contribute to the literature in the field of smart medical textiles, as well as providing a functional and innovative solution to our product, which was designed with our study.

ACKNOWLEDGMENT

We would like to thank Durak Tekstil and our managers for providing us with all kinds of resources and supporting our work in this study.

REFERENCES

DYER J. (2011): Infrared functional textiles. 184-197. [Editors: Pan N., Sun G. Functional textiles for improved performance, protection and health. Woodhead Publishing Ltd.]

Dyer, 2011;Wang et al., 2011; Biocera, Accessed 07.01.2017; Lin et al., 2015; Cobb, Retrieved 27.12.2016

Lv Didi and Li Yanmei 2021 *J. Phys.: Conf. Ser.* 1790 012023

INVESTIGATION OF BIOBASED OR BIODEGRADABLE BLEND YARN PRODUCTION AND USAGE PERFORMANCES

Gökhan TANDOĞAN[1], Kıymet Kübra DENGE[1], Ali İBRİKCİİ[1], Tolga FİDAN[1]

[1]Kipaş Textile Bussines Inc. R&D Center, Kahramanmaraş, Türkiye

Corresponding author:gtandogan@kipas.com.tr

Abstract: *In this study, to popularize the use of biodegradable materials with a sustainability approach; The blending possibilities of biodegradable polyester varieties and bio-based polyester varieties with other non-biodegradable fibers that are standard in the market or that have sustainability features were evaluated, and product types with biodegradable properties at certain rates were developed. The performance and biodegradability tests of different fiber structures were investigated by applying the same finishing processes to the developed woven fabric structures. At the same time, it is aimed to eliminate the deficiencies in the literature in this field by developing environmentally friendly woven fabric products that meet industrial standards from biodegradable fibers.*

Keywords: *Biodegradable, Sustainable, ecological fabrics, environmental cycle*

1. INTRODUCTION

Fibers, which are the most basic textile materials, have been used in the textile industry for thousands of years in the production of clothes, fabrics, and surfaces. While natural fibers obtained from plants and animals such as cotton, linen, wool, and silk were used at first, man-made fiber production started in the 19th century (Dündar, 2008). Various fibers produced today have a wide range of uses. In addition to its traditional uses such as clothing and home textiles, fibers are also used in the production of industrial tape, filters, automobile tires, aviation, building materials, medical supplies, and even active implantable medical devices (Okur, 2006).

As is known, natural or regenerated polymer-based textile materials; When they are buried in the soil, are degraded by the microorganisms in the soil. This is called biodegradability or biodegradability (biodegradation). Biodegradability has recently been used as a standard measure for textile products to be environmentally friendly. (Park vd., 2004). The biodegradation of textile materials is affected by factors such as crystalline ratio, orientation and degree of polymerization, and hydrophilicity/hydrophobicity. In addition, the condition of the soil in which the textile materials are buried and the type of microorganisms in the soil also affect.

The same is true for a wide variety of plastic materials, not just textiles. More than 300 million tons of petroleum-based synthetic plastics produced each year are used as packaging materials. These packaging materials are disposed of in underground storage areas as solid waste. The structure of the organisms in the soil and all environmental effects are important for the biodegradation of the wastes released to nature. It is important for the environment that it is converted into simpler compounds and mineralized with the help of organic chemicals in the biosphere, that is, its biodegradation (Ergin, 2020).

As an alternative to synthetic polymers generally obtained from petroleum derivatives. Plastics obtained from polymers produced from renewable animal and vegetable sources such as corn, pea, vegetable oil, or microbial are called Biodegradable Plastics because they are more easily dissolved in na-

ture and are harmless. The greenhouse gas emission rate of products produced from biodegradable plastic packaging materials, which causes global warming, is 4 times less. For this reason, the use of soil-soluble plastic packaging materials is increasing in the American and European Union countries. Biodegradable plastics decompose in the soil in a short period of 1-6 months and mix with nature (Anonym, 2018).

Biopolymers are a new generation of intelligent textile materials based on petroleum, agricultural or animal resources, providing a convenient solution for the economy. Researchers have established several standard test methods for evaluating the composting ability and biodegradability of polymers using mixed methods. Life cycle analysis is one of the methods simulating the development of biopolymers. Green fibers have a shorter life cycle than oil-based ones. Many researchers have investigated the effects of blend ratios on the degradation process of biopolymers. Biodegradable polymers are smart polymers that are currently used in many fields such as tissue culture, biomedical, agriculture, food, and smart textiles. The properties and degradation rate of the blended polymers determine the degradability of the main mix. (Ergin, 2020). Biodegradable materials play an important role in the development of green nanotechnology as smart and smart materials, one of these examples is nano-sized polysaccharides. An important feature of intelligent biopolymers is their potential adaptation to their environment in response to stimuli that affect them. These properties make them suitable materials for the textile industry. (Younes, 2017). Polylactic acid (PLA) is an environmentally friendly aliphatic polyester that can be obtained from 100% renewable sources. PLA was first produced by Carothers in 1932 by heating lactic acid in a vacuum environment with a low molecular weight (Avinc, Owens, Bone, Wilding, Phillips, and Farrington 2011). PLA in the textile industry; jackets, sportswear, wedding dresses, and nonwoven products; in the automotive sector, ceiling and floor coverings and in-car plastic are used in the evenings, in the construction industry laminates and wall coverings, in the field of electricity and 16 electronics, it is used in cable coatings and various device parts (Hamamci and at al 2018).

The most important feature of polylactic acid is that it is a biodegradable polymer produced from starch-rich plant sources such as corn, sugar cane and wheat. In addition to these features, PLA's environmental friendliness and biocompatibility; It provides potential use in plastic applications, especially in the textile sector, in the field of packaging, agricultural products, and disposable products (Üner and Koçak, 2012).

2. MATERIALS AND METHODS

2.1. Raw Materials

The properties of the fibers used in the study are given in Table 1.

Table 1. Fibers used in the study

Fiber Code	Raw Material	Fineness (denier)	Length
1	Cotton US	1,1	30 mm
2	Viscose	1,4	38 mm
3	Polyester	1,6	38 mm
4	30%Plant –Based Polyester-70%Resine polymer	1,2	38 mm
5	Biodegradable Polyester	0,9	38 mm
6	Biodegradable Polyester	1,2	32 mm
7	Recycled Polyester	1,4	38 mm

2.2. Methods

Biodegradable and bio-based fibers have been produced in different compositions in 28/2 Ne, 20/1 and 30/1 Ne, and fabrics in the form of woven fabrics with similar weights and weaves have been produced. The compositions of the fabrics produced are given in Table 2. A and B fabrics are produced in weft and warp elastane bi stretch constructions, while C, D and E fabrics are produced in weft elastane weft stretch constructions due to their structure.

Table 2. Construction information of the fabrics produced

Article	Code	Composition	Warp Ne	Weft Ne	Fabric weight
A	NA 622084	64% Biodegrable Polyester(5)-31%Viscose-5%Elastane	28/2	28/2	290
B	Reference 1	64% Repreve Polyester(7)-31%Viscose-5% Elastane	28/2	28/2	290
C	NA 931174	67%Cotton -30%Bio based polyester (4)-3% Elastane	30/1	20/1	250
D	NA 941313	67%Cotton-30% Biodegrable Polyester(6)-3%elastane	30/1	20/1	250
E	Reference 2	67%Cotton-30% Polyester(3)-3% Elastane	30/1	20/1	250

The process and finishing processes applied to woven fabrics produced from bio-based and biodegradable fibers with different properties are as in Table 3.

Table 3. Finishing processes applied to the fabrics produced

Article	Code	Process	Chemical finishing
A	622084	Washing-Drying- Fixing-Singeing-Jet Dyeing-Drying-Fixing with chemical	15 ml/lt Polyethylene 0,5 ml/lt Acetic acid
B	Reference 1	Washing-Drying- Fixing-Singeing-Jet Dyeing-Drying-Fixing with chemical	15 ml/lt Polyethylene 0,5 ml/lt Acetic acid
C	931174	Singeing+Cold bleaching-Washing-Mercerized-Drying-Jet Dyeing-Drying-Finishing-Sanforized	15 ml/lt Polyethylene 0,5 ml/lt Acetic acid
D	941313	Singeing+Cold bleaching-Washing-Mercerized-Drying-Jet Dyeing-Drying-Finishing-Sanforized	15 ml/lt Polyethylene 0,5 ml/lt Acetic acid
E	Reference 2	Singeing+Cold bleaching-Washing-Mercerized-Drying-Jet Dyeing-Drying-Finishing-Sanforized	15 ml/lt Polyethylene 0,5 ml/lt Acetic acid

3. RESULTS AND DISCUSSION

In this study, 2/1 Z structure woven fabrics produced from 4, 5 and 6 fibers were produced based on two different reference fabrics in terms of using alternative properties to polyester fiber that can be added to standard cotton fiber.

The same finishing process was applied to the fabrics produced within the scope of the study, taking into account the biodegradability tests. The performance tests of the fabrics produced are given in Table 4. B and E fabrics were taken as reference from the developed fabrics. According to the construction structure, A fabric was evaluated with B fabric as a reference, and C and D fabric were evaluated with E fabric as a reference.

Table 4. Fabric performance test results

Article	Code	Width	Weight	Tensile Strength		Tear Strength	
				Warp	Weft	Warp	Weft
A	622084	131	295	140	71	9936	6690
B	Reference 1	130	298	144	68	8912	7023
C	931174	141	244	107	37	2877	1403
D	941313	140	250	109	56	1921	1557
E	Reference 2	140	256	128	71	2877	1688

In comparisons in terms of breaking and tear strength; While there was no significant difference in the A fabric compared to the B fabric, the values of the C and D fabrics in the weft and warp direction decreased by 15% compared to the E fabric.

Table 5. Biodegradability test results of fabrics

Article	Reference	Composition	Results
A	622084	64% Biodegrable Polyester(**5**)-31%Viscose-5%Elastane	11.20%
B	Reference 1	64% Repreve Polyester(**7**)-31%Viscose-5% Elastane	12.10%
C	931174	67%Cotton -30%Bio based polyester (**4**)-3% Elastane	16.40%
D	941313	67%Cotton-30% Biodegrable Polyester(**6**)-3%elastane	26.20%
E	Reference 2	67%Cotton-30% Polyester(**3**)-3% Elastane	18%

Biodegradable tests were tested in Edenresearch Laboratories with the 91-day subsoil decay method according to the ASTM D5511 method.

In the biodegradability test, the weight losses between the A and B samples were measured at close values with small tolerances, assuming the effect of fiber losses during the removal of the samples from the soil or in the washing and drying processes slightly affects the weight loss.
However, according to the E fabric reference, the biodegradability test in the C and D fabric There was a difference of up to 30% in the measurements.

4. CONCLUSION

Since polyester, which dominates the textile fiber market, is produced from petroleum derivatives and does not decompose after use, harming the nature for centuries, the search for alternative materials, namely new fibers, continues. Among these fibers, polyester-based fibers such as 6, 5 and 4, whose trade names are hidden and used in the project, stand out among other fibers, thanks to their biodegradable/biocompostable properties by being produced from renewable resources.

In this study, among the fibers no. 4, 5 and 6 examined as an alternative to standard polyester fiber, the D fabric produced by using fiber no. 6 in terms of biodegradability achieved the highest biodegradation in the same period when evaluated in terms of biodegradability.

When fabric A, produced using fiber no. 5 from other trials, was compared to Reference 1, there was no difference in terms of biodegradability, while a 5% decrease was observed in the strength values in the weft direction.

The C fabric produced using fiber no. 4, on the other hand, was lower than the standard polyester in terms of biodegradability when compared to Reference 2. This situation shows that although fiber no. 4 is produced on a bio-based basis, its biodegradable feature is weak.

ACKNOWLEDGMENT

We would like to thank fiberpartner company and Edenresearch laboratories for their contributions in fiber supply processes and measurement of biodegradability tests within the scope of the project, as well as Kipastextiles R&D Center.

REFERENCES

Anonim(2018) Mısır, Bezelye ve Bitkisel Yağdan Plastik Üretimi: PLA Nedir?. https://www.copunesahipcik.org/misir-bezelyeden-bitkisel-yagdan-plastik-uretimi-planedir/ (erişim tarihi,20.02.2020.

Avinc, O., Owens, H., Bone, J., Wilding, M., Phillips, D., Farrington, D. A (2011) Colorimetric Quantification of Softened Polylactic Acid and Polyester Filament Knitted Fabrics to 'Waterspotting'. *Fibers Polym.* Vol 10, 893–903.

Dündar E. (2008). Çeşitli Selülozik Elyaflardan Üretilen Örme Kumaşların Performanslarının Karşılaştırılması. *İTÜ, Fen Bilimleri Enstitüsü, Yüksek Lisans Tezi,* İstanbul.

Ergin C. (2020). Biyobozunur Lif İçeren Dış Giyimlik Dokuma Kumaş Özelliklerinin İncelenmesi. NKU, Fen Bilimleri Enstitüsü, Yüksek Lisans Tezi, Tekirdağ.

Hamamcı B, Çiftci M, Aktaş T. (2018). Yeşil Kompozitlerde Biyopolimerlerin Kullanımının Önemi. *Kafkas Üniversitesi, Karadeniz Fen Bilimleri Dergisi* No.8: 12-24s.Trabzon.

Okur N. (2006). Bambu Lifi ve İplik Özelliklerinin Diğer Lif ve İplikleri Performans Özellikleri ile Karşılaştırılmalı olarak İncelenmesi. *İTÜ, Fen Bilimleri Enstitüsü, Yüksek Lisans Tezi,* İstanbul.

Park, H.C., Kang, K.Y., Im, S.S., 2004. Biodegradability of Cellulose Fabrics. *Journal of Applied Polymer Science*, Vol. 94, s.248–253.

Üner İ. Koçak E D. (2012). Poli (Laktik Asit)'in Kullanım Alanları ve Nano Lif Üretimdeki Uygulamaları. *İstanbul Ticaret Üniversitesi Fen Bilimleri Dergisi*. No.11: 79-88s.İstanbul.

Younes B. (2017) Classification, Characterization, And The Production Processes of Biopolymers Used İn The Textiles İndustry, *The Journal of The Textile Institute*, Vol.108:5, 674-682sp, Damascus, Syria.

INVESTIGATION OF THE PERFORMANCE OF ESTERS IN DIFFERENT STRUCTURES IN TEXTILE APPLICATIONS

Zeynep Nihan KIR, Ayşe MARTIN, Deniz ÇELIK

EKSOY CHEMISTRY, Adana, Türkiye

Corresponding author: denizc@eksoy.com

Abstract: *Esters play an important role as a softener in textile chemistry. Softness is one of the most frequently requested properties in textile chemistry. The aim of this study is to examine the performance of 3 different esters as a softener in textile chemistry. After applying stearic acid, coco acid and oleic acid esters on the fabric, color change, whiteness, antistatic properties, slipperiness and hydrophilicity were investigated and their performances were compared. As a result, the oleic acid ester showed the best performance.*

Keywords: *Textile applications, fabric softener, performance test,esters*

1. INTRODUCTION

While 65% of the use of auxiliary substances in textile finishing occur in finishing processes, a large part of this, corresponding to about 30%, is made up of softeners (Çoban S., 1999).
Our skin is very sensitive to touch; more important than aesthetic appeal, wearers will only feel comfortable if garments offer the required soft feel. Hence, manufacturers of apparel are always careful to see that the softening finishes applied to garments are durable, without sacrificing the functional properties. A simple example of this is terry towels: the basic aim of towel material is to exhibit a very high level of absorbency, but it cannot be at the cost of softness. No one is going to prefer a very absorbent towel that is harsh to the touch; nor is anyone going to be satisfied with very soft towels with negligible absorbency, which is its expected primary property (M.D. Teli, n.d).

The softness is lost due to the removal of natural substances such as oil, wax, pectin, which are in the structure of natural fibers, which provide softness to the fiber during finishing processes such as pre-treatment, dyeing and printing. The purpose of softening agents is to regain the lost soft touch of the fabric and even to improve the initial flexibility and softness (A.T Ozgüney, K. Ozkaya, 2008). Ester softeners are the one molecule which is used as a fabric softener to provide smoothness, softness to the textile widely (Z. Miao, J. Yang, L. Wang, et al.,2008).

Mechanisms of softening; The softeners consist of two distinct parts: hydrophobic and hydrophilic. The hydrophobic part is water hating and does not mix with water. The hydrophilic part is water loving, resulting in compounds dispersing in water. When the surfactant is floated on the surface of the liquid, it lowers the surface tension and ionizes to create positive ions containing the hydrophobic groups. The hydrophobic part has a positive electrical charge, while the hydrophilic part is negatively charged (S. Mishra, V.K. T.Yagı, 2006).

Different types of fibres carry differing electric charges, causing variations in exhaustion and the orientation of the softener molecules and giving a differentiated softening performance. Almost all fibres give rise to negative zeta potential in the water; the extent of this depends on the relative hydrophilicity/hydrophobicity of the fibre, the presence of ionizable functional groups, etc.(B.Wahle and J. Falkowski, 2002). Cationic softeners orient themselves with their positively charged ends

toward the partially negatively charged fiber (zeta potential), creating a new surface of hydrophobic carbon chains that provide the characteristic excellent softening and lubricity seen with cationic softeners. Anionic softeners, on the other hand, orient themselves with their negatively charged ends repelled away from the negatively charged fiber surface. This leads to higher hydrophilicity, but less softening than with cationic softeners. The orientation of non-ionic softeners depends on the nature of the fiber surface, with the hydrophilic portion of the softener being attracted to hydrophilic surfaces and the hydrophobic portion being attracted to hydrophobic surfaces (M. I. Kiron, 2013).

The aim of this study is to examine the performance of 3 different esters as a softener in textile chemistry. After applying stearic acid, coco acid and oleic acid esters on the fabric, color change, whiteness, antistatic properties, slipperiness and hydrophilicity were investigated and their performances were compared.

In this study, stearic acid, coco acid, oleic acid were used for ester synthesis. Stearic acid, also called Octadecanoic Acid, one of the most common long-chain fatty acids, found in combined form in natural animal and vegetable fats. Commercial “stearic acid” is a mixture of approximately equal amounts of stearic and palmitic acids and small amounts of oleic acid. It is employed in the manufacture of candles, cosmetics, shaving soaps, lubricants, and pharmaceuticals (K.Rogers, n.d).

Coconut Fatty Acid is used in soaps, bath products, and household and industrial cleaning products as a surfactant, cleansing agent, emulsifier and a foam booster. Its high Lauric content makes an excellent lathering and conditioning bath soap. Coconut Fatty Acid and its esters are also used in the manufacture of intermediates for the textile industry, lubricants and metal working fluids.

Oleic acid as its sodium salt is a major component of soap as an emulsifying agent. It is also used as an emollient. Small amounts of oleic acid are used as an excipient in pharmaceuticals, and it is used as an emulsifying or solubilizing agent in aerosol products (Carrasco, F. 2009).

Table 1. Physical and chemical properties of the fatty acids used

	Stearic Acid	**Coco Acid**	**Oleic Acid**
CAS Registry No	57-11-4	61788-47-4	112-80-1
Chemical Formula	$CH_3(CH_2)_{16}COOH$	$C_{19}H_{21}NO_5$	$C_{18}H_{34}O_2$
Molecular Weight (g/mol)	284.48	343.37	282.47
Density (g/cm^3)	0.845	0,89	0.9
Melting Point (°C)	68-70	22-26	16.3
Boiling Point (°C)	370	160	286.11
Structure formula	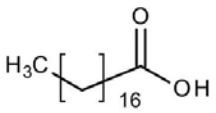	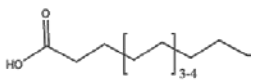	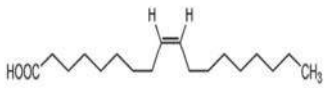

2.MATERIALS AND METHODS

2.1.Materials

The chemicals such as stearic acid, coco acid, oleic acid and acetic acid was purchased from Merck. Forlab brand padding machine was used for softener application. James Heal Titan 4 was used for smoothness measurement. Datacolor 850 spectrophotometer was used for color measurements. Mahlo brand antistatic device was used for antistatic measure.

2.2.Methods

The fabric was padded using 1-dip 1 nip in an ester aqueous solution finishing bath with 80–85% wet pickup. Then the padded fabric was dried at 105 °C for 180 s. Softness was reviewed by 5 panelists. A score between 1 and 5 is given. (1 lowest, 5 highest). The hydrophility was investigated by wicking high method. The fabrics are cut to a lenght of 10 cm and a width of 2 cm. Drawn with 1 cm intervals from the weft direction.It is dipped into the dye solution from the bottom part and left for 2 minutes.In this way, it is determinated how much liquid is absorbed by the fabric. Static electrification of the fabrics was measured with an antistatic device. The slipperiness of the fabrics was measured with the Titan 4 device. The color change of the dyed cotton fabric and the whiteness of the cotton fabric ready for dyeing were measured with the Datacolor 850 color spectrophotometer device.

3.RESULTS AND DISCUSSIONS

The softness has been evaluated by the panel feel test where the softness has been qualitatively assessed and rating has been given in terms of one to five, with rating 5 being the best and rating 1 showing the poor softness. As shown in Tables 2 the softness has increased as the amount of usage of the softener on the fabric increasing from 50 to 100 g/L in case of padding. The best results were obtain from the oleic acid ester and the stearic acid ester.

Table 2. Evaluation of softness on application of esters on cotton fabrics finished by padding method of application.

	Softness Rating (1-5 points)	
	50 g/L	**100 g/L**
Oleic Acid Ester	4	5
Stearic Acid Ester	4	5
Coco Acid Ester	3	4

Color difference values are the only method used for the quantitative evaluation of color quality. There are some tolerance values for color difference values in the textile industry. There is no international standard for these values (M. Kıroglu, R. Fettahov, M. Kaplan, 2017). ΔE value less than 1 is an acceptable value. As seen in Table 3, oleic acid ester gave the lowest color change value. After applying esters to white cotton fabric, it is checked whether there is any yellowing an its color. Whiteness value measured with Datacolor 850 spectrophotometer.Whiteness values of L* range from 0-100. This value 0 for black and 100 for white (Y.Yeşil,2006). As seen in Table 3, oleic acid gave the best whiteness value.

Table 3. Evaluation of color change and whiteness on application of esters on dark green dyed cotton fabrics finished by padding method of application.

	Whiteness (L*)		Color Change (ΔE)	
	50 g/L	**100 g/L**	**50 g/L**	**100 g/L**
Oleic Acid Ester	95.0	95,6	0.61	0.75
Stearic Acid Ester	94,86	94,1	0.80	0.81
Coco Acid Ester	93,79	93,67	0.92	1.0

Static electricity prevents smooth operation, especially when working with synthetic fibers. In addition, there are sometimes problems when working with protein-based fibers. Static electricity not only prevents smooth operation, but also causes fabric or threads to attract dust and thus become dirty quickly. It is not possible to produce smooth yarn due to the winding of the fiber cluster on cylinders and taking unintentional shapes during yarn production with fibers that are not antistatically finished (Anonim, 2013). For this reason, it is desirable to have a high antistatic value. As seen in Table 4, while oleic acid gave the highest antistatic value, stearic acid gave a value close to it.

Table 4. Evaluation of antistatic value on application of esters on polyester fabrics finished by padding method of application.

		Antistatic Value	
	Blank	**50 g/L**	**100 g/L**
Untreated fabric	23		
Oleic Acid Ester		45	68
Stearic Acid Ester		48	59
Coco Acid Ester		45	53

Table 5 gives the static and kinetic friction coefficient values applied by the T28 jaw to the fabric. The softness of the fabric increases as the kinetic friction coefficient between the fabric and the disc in motion and the static friction coefficient between the stationary disc and the fabric decrease (Z.N.Kır, A.Martin, N.Benli, 2022). Therefore, oleic acid and stearic acid showed the best soft handling.

Table 5. Evaluation of friction coefficient values on application of esters on cotton fabrics finished by padding method of application.

	Static Force (N)	**Kinetic Force (N)**	**Static COF (Us)**	**Kinetic COF (UK)**
Untreated Fabric	1.097	0.846	0.501	0.432
Oleic Acid Ester	0.655	0.432	0.234	0.155
Stearic Acid Ester	0.678	0.475	0.245	0.167
Coco Acid Ester	0.835	0.514	0.314	0.263

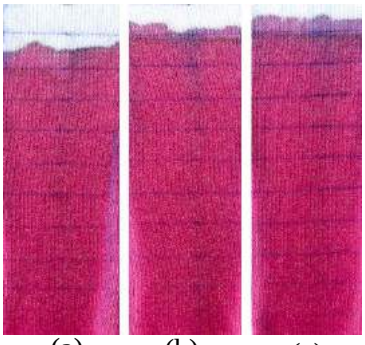

(a) (b) (c)

Fig. 1: Wicking high test results (a) coco acid ester, (b) oleic acid ester, (c) stearic acid ester

Its hydrophility checked by wiking high test method. As a result of the wiking high test method performed after the application of 3 esters to the fabric, it was seen that they had good hydrophilicity. (Fig. 1)

4. CONCLUSION

Many studies are carried out in order to improve many properties of textile products, from water absorbing to smoothness, from softness to dirt-repellent. One of the most important qualities sought in textile products is softening. Esters are one of the important chemicals used for softening in textile technology.

In this study, esters with 3 different structures such as coco acid, stearic acid and oleic acid esters synthesized in the laboratory were examined by textile application. After applying stearic acid, coco acid and oleic acid esters on the fabric, color change, whiteness, antistatic properties, slipperiness and hydrophility were investigated and their performances were compared. The softness has increased as the amount of usage of the softener on the fabric increasing from 50 to 100 g/L in case of padding. Best result taken from the oleic acid ester and stearic acid ester. Oleic acid ester gave the lowest color change value and the best whiteness value. Oleic acid gave the highest antistatic value, stearic acid gave a value close to it. Oleic acid and stearic acid showed the best soft handling. When the results were examined, it was seen that the best performance was obtained in oleic acid, and it performed close to it in stearic acid.

REFERENCES

Çoban S.,(1999). Genel Tekstil Terbiyesi ve Bitim İşlemleri, *Tekstil ve Konfeksiyon Araştırma Uygulama Merkezi Yayınları* 135-146.

M.D. Teli, (n.d). Softening finishes for textiles and clothing, *Institute of Chemical Technology* (ICT),Mumbai, India.

A.T Ozgüney, K. Ozkaya, (2008). Effects of the Softeners on the Colour Change Which Occours During the Curing of Cotton Fabric in Screen Printing Conditions, *Tekstil ve Konfeksiyon* 2,121-129.

Z. Miao, J. Yang, L. Wang, et al.,(2008). Synthesis of biodegradable lauric acid ester quaternary ammonium salt cationic surfactant and its utilization as calico softener, *Mater. Lett. Elsevier* 2450-2452.

S. Mishra, V.K. T.Yagı, (2006). Biodegredable Ester-Amide Fabric Softeners,*Journal of Oleo Science* 6, 267-275.

B.Wahle and J. Falkowski,(2002). Softeners in textile processing, Prog. Color, 32(1):118 – 124.

M. I. Kiron,(2013). Softening Finishes in Textile Mechanism of the Softening Effect on Fabric,*Textile learner*.

K.Rogers, (n.d). Stearic acid, Britannica. https://www.britannica.com/science/stearic-acid

Carrasco, F. (2009).Ingredientes Cosméticos,Diccionario de Ingredientes (4th ed.). p. 428.

M. Kıroglu, R. Fettahov, M. Kaplan, (2017). Reaktif Boyama İşleminden Sonra İşletme ve Laboratuvar Yıkama Uygulamalarının Renk Değişimine Etkisinin İncelenmesi, *Journal of Bartin University Engineering and Technological Sciences* Vol. 5 Issue 1, 35-39.

Y.Yeşil, (2006). Melanj Elyaf Karışımlarında Renk Değerlerinin Yeni Bir Algoritma Geliştirilerek Tahmin Edilmesi, *Çukurova Üniversitesi* Proje, Proje No: MMF.D20.

Anonim, (2013). Antistatik Apre, *Milli Eğitim Bakanlığı, Tekstil Teknolojisi*, Ankara.

Z.N.Kır, A.Martin, N.Benli,(2022). Farklı Yapıdaki Katyonik Yumuşatıcı Malzemelerinin Kumaşta Uzama Değerine Etkisinin İncelenmesi, *Tekstil&Teknik* Mayıs 2022.

INVESTIGATION OF THE MECHANICAL PROPERTIES OF NON-WOVEN FABRICS PRODUCED BY USING RECYCLED GRANULAR RAW MATERIAL FROM WASTE PET BOTTLES

Halil Can ATEŞ[1], Volkan BALCI[1], Halil BÖLER[1], İbrahim Onur ÇEVIK[1]

[1]Mogul Tekstil San ve Tic A.Ş. Gaziantep, Turkey, Tel.: +90 342 337 14 99, Fax: +90 342 337 1413

Corresponding author: halil.ates@mogulsb.com

Abstract: *With the increasing population growth, the rapid depletion of natural resources has led to an increase in raw material and energy costs. This situation reveals the importance of using new and sustainable resources in all sectors. In this sense, with the development of technology, the number of studies and applications related to recycling is increasing. Recycling PET bottle waste, which is one of the best examples of recycled products, for use in different sectors reduces the amount of waste, while contributing to the protection of natural resources and energy savings. Within this context, and with this study, nonwoven fabric was obtained from PET granule raw materials which was obtained by recycling from waste PET bottles, and the mechanical properties of these fabrics were investigated.*

Keywords: *Recycle, Nonwoven, PET*

1. INTRODUCTION

In recent years, recycling has been an attractive issue for researchers considering sustainability of the wastes arising from different engineering applications. In this scope, r-PET fibers which are mechanically and chemically recycled from PET bottles can be reused in non-woven production technology in profitable amounts.

Textile wastes can be classified as producer (Pre-consumer) waste and final (Post) consumer waste. In this project, it is aimed to examine the mechanical properties and processability of nonwoven fabrics obtained by the extrusion method of granulated raw materials from PET bottles, which are the final consumer waste. Using 3 different production technologies, the non-woven fabric was obtained;

- Mono Pet spunbond technology(Mopet®)
- Bicompenent Pet spunbond technology(Buffalo®)
- Microfilament (Spunbond/spunlace hybrid) technology(Madaline®)

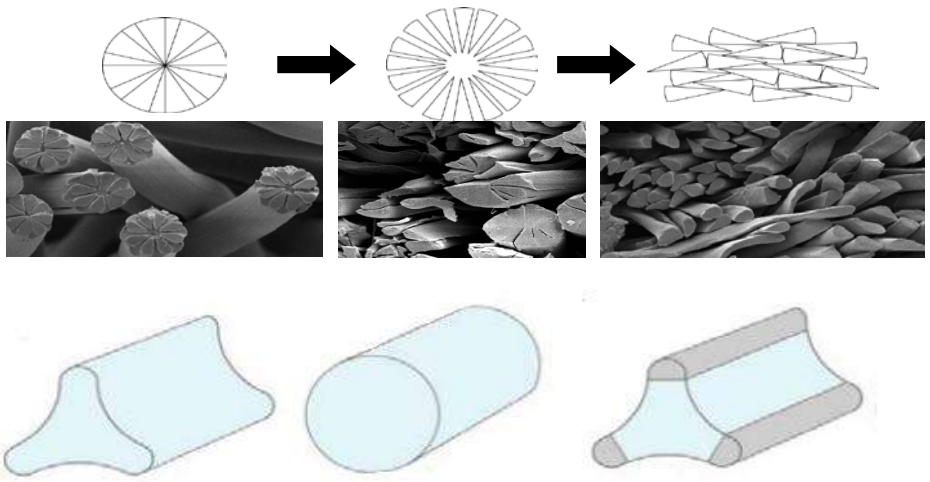

Figure 2. Monopet and bicompenet cross section

2. MATERIALS AND METHODS

In this study, for the production of microfilament nonwovens (Madaline®); 70% PET (virgin) 30%PA6 (virgin) and 70% recycle PET (Repreve®) 30%PA6 (virgin),for the production of Bicompenent Pet spunbond nonwoven fabric (Buffalo®); 85% PET(virgin), 15% coPET (virgin) and 85% Recycle PET (Repreve®) and 15% coPET (virgin), for the production Mono Pet spunbond nonwoven fabric(Mopet®); 100% PET (virgin) and 100% Recycle PET (Repreve®) granular raw materials were used. In Bicompenent and Mono Pet spunbond productions, trilobal and round cross-sections were produced.

3. RESULTS AND DISCUSSION

MD (Machine direction) and CD (Cross direction) tensile strength values were examined in tests performed according to NWSP 110.4.R0.15 standard. In Figure 3, the tensile strength test results of virgin and recycle madaline microfilament nonwoven fabrics in different weights in md and dc directions are expressed. As seen in the graph, no significant change is observed between the results.

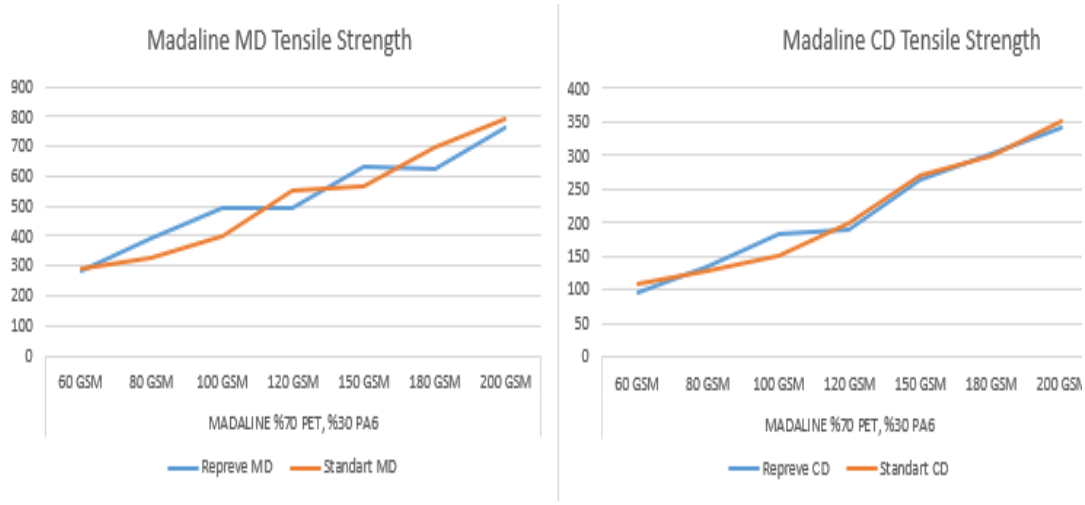

Figure 3. MD/CD Tensile Strength Madaline microfilament

In Figure 4, the tensile strength test results of virgin and recycle bicompenent nonwoven fabrics in different weights in md and dc directions are expressed. As seen in the graph, no significant change is observed between the results.

In Figure 5, the tensile strength test results of virgin and recycle mono pet nonwoven fabrics in different weights in MD and DC directions are expressed. As with microfilament and bicomponent fabric, no significant difference is observed between the results.

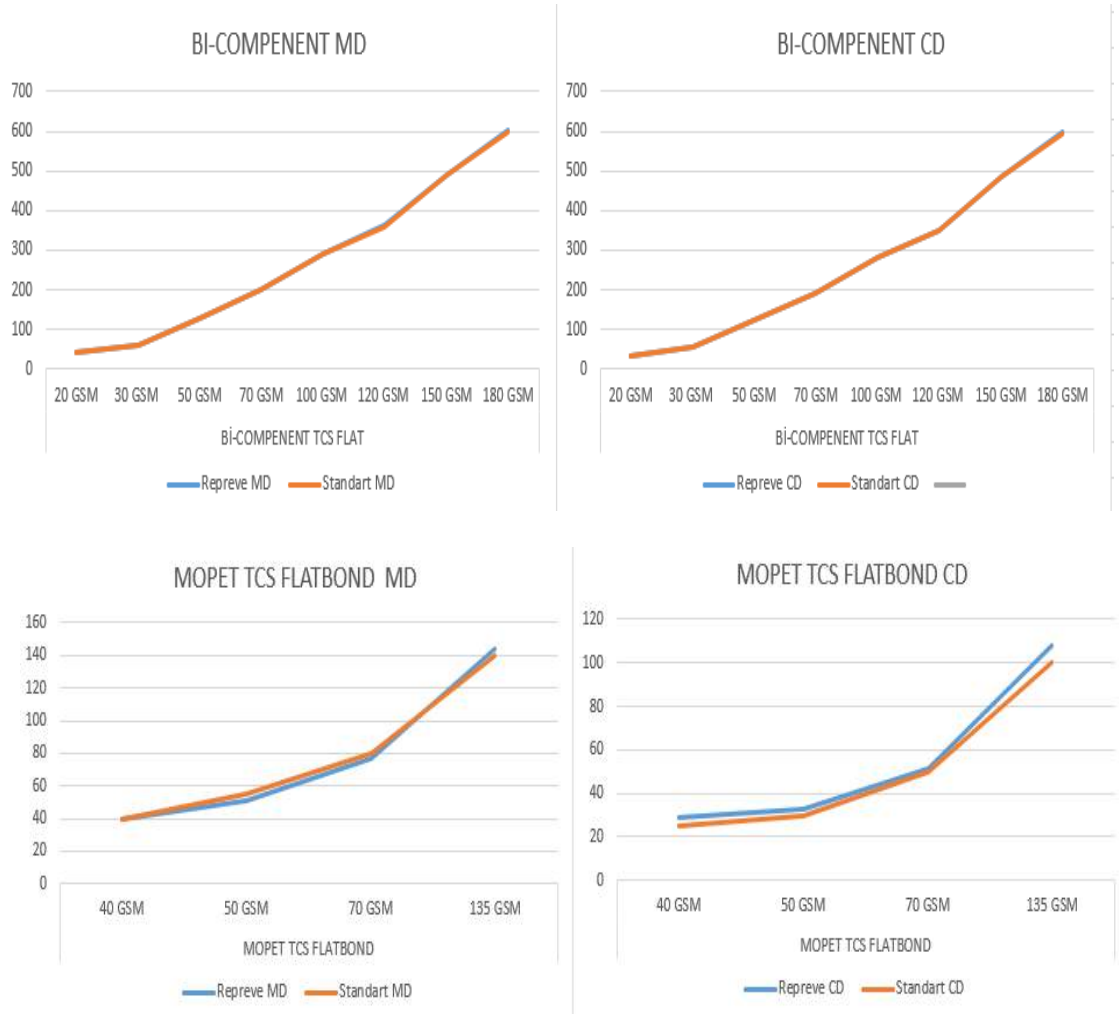

Figure 5. MD/CD Tensile Strength Monopet Spunbond

4. CONCLUSION

As seen in the test results in the chart above; No significant difference was observed when the mechanical properties of virgin and recycle fabrics produced with microfilament technology were compared. No significant difference was observed when the mechanical properties of virgin and recycle fabrics produced with Mono Pet spunbond technology and Bicompenent Pet spunbond technology were compared. However, fabrics produced with a round cross-section could not be processed. It is thought that this problem is caused by the filament diameters of fabrics with round cross-sections being lower than the filament diameters with trilobal cross-sections.

REFERENCES

Sharma R, Goel A (2017) Development of Nonwoven Fabric from Recycled Fibers. *J Textile Sci Eng* 6: 289

Abdurrahman Telli, Nilgün Özdil, Osman Babaarslan (2012): PET Şişe Atıklarının Tekstil Endüstrisinde Değerlendirilmesi ve Sürdürülebilirliğe Katkısı, *Tekstil ve Mühendis*, 19: 86, 49-55.

S Üstün Çetin and A E Tayyar ‘’Physical properties of recycled PET non-woven fabrics for buildings’’ *2017 IOP Conf. Ser.: Mater. Sci. Eng.* 254 192016,

EAntolinc, D.; Filipi˘c, K.E. Recycling of Nonwoven Polyethylene Terephthalate Textile into Thermal and Acoustic Insulation for More Sustainable Buildings. *Polymers 2021*, 13, 3090

DEVELOPMENT OF HYBRID YARN FOR CUT-RESISTANT SURFACES WITH PARAARAMID FIBERS

İrem Tuğçe ÇELİK[1]

[1]Uğurlular Textile, Research and Development Center, Denizli, Turkey

Corresponding author: irem.celik@ugurlular.com.tr

Abstract: *Many glove manufacturers developing new products for cut protection have turned to high-performance fibers such as para-aramids instead of traditional textile fibers. The higher strength-to-weight ratios of these polymers are their biggest advantage over conventional steel metals and alloys, and they also allow efficient operation as many of them are flexible. Para-aramid gloves offer exceptional cut resistance and can significantly reduce the risk of hand and finger injuries in glass and metalworking operations. In this study, a cut-resistant hard-core hybrid para-aramid yarn has been developed to be used in the production of protective textile products, which are produced from the fiber and polymer mixtures used in protective textile materials against mechanical impact, in order to protect from cut injuries, which are the most common occupational accidents. The obtained 8 Ne yarn was woven with a 30*13 density plain cloth and sent to lab for cut resistance test and the average cutting length was found to be 43.48 mm.*

Keywords: *Protective textiles materials, textiles resistant to mechanical impact, composite materials, high performance yarns.*

1. INTRODUCTION

According to the International Labor Organization (ILO) figures, approximately 2 million 200 thousand people die yearly from occupational accidents. Approximately 30% of these occupational accidents are cuts or lacerations and approximately 70% of these injuries are to the hands or fingers, which has led to the development of protective gloves. Various protective gloves were initially developed, such as wire-knitted steel gloves, leather gloves, and gloves made of some alloys from traditional textile fibres. Still, most of them were thick and stiff, preventing them from working effectively and providing little protection. In some cases, it has been observed that thick gloves increase the risk of injury (Ertekin, 2017; Ertekin & Kirtay, 2016).

The protective textiles market, which has an essential and indispensable place in technical textiles with its wide product range, is a market open to new products, suppliers and innovations, and it has become remarkable for companies day by day. While protective surfaces were used only to protect the past, today it is expected to respond to comfort and fashion requirements in addition to this feature (Ertekin, 2014; Alpyıldız et al. 2011). The safety of people can basically be ensured in two ways; first, processes, materials and products are safe; the second is to ensure that the person is protected with appropriate protective equipment in cases where it cannot be prevented from approaching the source of damage for any reason. In the literature, various studies examine the mechanical risks and heat and flame resistance properties of protective gloves. Protective gloves against mechanical threats are designed to protect against cuts, tears, abrasions and punctures in addition to their grip properties to hold objects in a dry or wet environment (Özen, 2016). From this, protective materials can be an important solution in cases where environments, processes and products cannot be made safe. In this study, it is targeted to develop a hard-core hybrid para-aramid yarn that is resistant to cutting from fiber and polymer blends used in protective textile materials against mechanical impact.

2. MATERIALS AND METHODS

2.1. Yarn manufacture

Literature and market research has been done and textile polymers to be used in production have been determined. In the production of the desired yarn, 95% para aramid, 3% meta aramid and 2% antistatic yarn were used. The fiber length we use in the production of paraaramid-added composite yarn is 51 mm. The average fiber length we use in our spinning mill is in the range of 30-40 mm. Optimization studies have been carried out so that 51 mm fiber can work in our current facility. At 60% humidity, 30 °C temperature conditions, antistatic spray and fiber additives were obtained with 45-62 Draw frame gauze. The wick is executed with a 1mm clip. In the ring machine, execution was provided with 45-80 gauges, 4 mm clips, 83 shore sleeves and 5 kg gun pressure. Hardcore yarn was obtained with steel filament by giving 0.98 drafts in the ring.

2.2. Yarn properties

The quality values of the yarn we obtained are as follows (Table 1).

Table 1. Quality values of the obtained composite yarn

	Ne	Twist	Elongation %	Strength %	Strength CV
	8,14	700 T/m	7,94	32,88	10,24

2.3. Fabric manufacture

With the 8Ne yarn we obtained, 30*13 plain cloth was woven.

Figure 1. Prototype image of yarn and fabric produced

2.4. Cut resistance

It was evaluated in the Technical Textiles Research and Development Center İzmir (TEKSMER) according to ISO 13997 test standard by weaving a 30*13 plain cloth with 8 Ne yarn produced.

After the aramid-based fabric sample to be tested was delivered to the laboratory, 3 samples were prepared with the dimensions of 5x15 cm at the right angle (45 ±10)° of the knife cuts to the sample machine. Conditioning of the samples was carried out at 20±2°C and 65±4% relative humidity for 24 hours in accordance with the TS EN ISO 139 "Textile - Standard Environments for Conditioning and Testing" Standard.

3 pieces of 5x15 cm aramid-based fabric samples were conditioned in the laboratory with a 20 mm blade stroke in the SATRA-STM610 Model Shear Tester (C1015). The shear force measurements required to split the sample were made. In accordance with the TS ISO 3801 Standard, the unit area mass (gram weight) of the test sample in g/m² was measured after the conditioning process. The mass per unit area of the test sample is 336.71 g/m². In the processes carried out in accordance with the TS EN ISO 13997 Standard, serial measurement tests were carried out to apply a series of forces perpendicular to the sample surface of the blade movement of 3 mm to 50 mm in length. The force (N) used and the measured cutting stroke length (mm) values were recorded.

3. RESULTS AND DISCUSSION

The cut resistance of the sample material is expressed as the shear force required to be applied to a standard sharp blade to split the material with a 20 mm blade stroke. In cotton, this value is on average: 5.9 N. It is aimed that this measurement shear force value is greater than 20 N. Cutting stroke length (L) in millimeters was measured at 5.0 N using a Neoprene calibration material with a thickness of 1.57±0.05 mm and a hardness of 50±5 Shore A.

C=K/L

C: correction factor,

L: cutting stroke length in millimeters at 5.0 N on neoprene,

K = 20

Knife sharpness correction factor (C): 0.428

All measured cutting stroke length values were multiplied by the blade sharpness correction factor (C) to calculate the 'Adjusted Cutting Stroke Lengths (mm)' (Table 2).

Table 2. Applied Force, Cutting Length and Adjusted Cutting Length

Force	Cutting Lenght	Adjucted Cutting Stroke Lenght (mm)
20	59	25,25
21	39	16,69
22	16,6	7,10
24	5,9	2,53

'Adjusted Cutting Stroke Length (mm) etc. the applied Force (N)' graph is obtained (Figure 2). From the graph obtained in Figure 2, the force required to cut the sample at 20 mm shear stroke was determined. With the determined force, 5+5 more measurements were made and the average cutting stroke length obtained from the measurements was calculated. These processes were carried out at 20±2°C temperature and 65±4% RH humidity conditions.

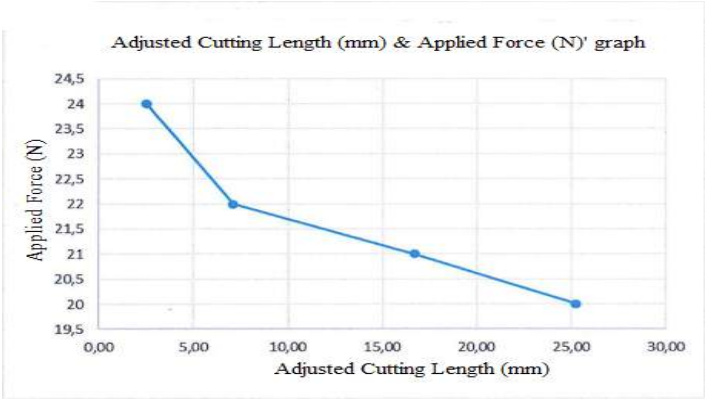

Figure 2. Adjusted Cutting Stroke Length (mm) vs. Applied Force (N)' graph

In order to create the graphic shown in Figure 2; a linear curve could not be obtained in the graph created with the data obtained from the 15 measurements that should be taken according to the standard. Therefore, there are only 4 measurements in the graph shown in Figure 2.

The force required to cut the sample at 20 mm cutting stroke is approximately 20.5 N.
5 measurements were made by applying a force of 20.5 N.

Table 3. Cutting stroke lengths measured by applying 20.5 N force (mm) - First 5 Measurements

Test no	Applied Force (N)	Cutting Stroke Length (mm)
1	20,5	39,4
2	20,5	32,6
3	20,5	47,1
4	20,5	50,7
5	20,5	34,4

Average Cutting Length: 40.84 mm → average cutting stroke length is not between 18.0 mm and 22.0 mm.
5 more measurements were made by applying a force of 20.5 N.

Table 4. Cutting stroke lengths measured by applying 20.5 N force (mm) - Second 5 Measurements

Test no	Applied Force (N)	Cutting Stroke Length (mm)
1	20,5	34,5
2	20,5	47,4
3	20,5	56,2
4	20,5	48,6
5	20,5	43,9

Average Cutting Length: 43.48 mm was found.
According to the test results, the fabric obtained from the yarn we produce has the desired properties and can be used in the products to be produced for use in works where there is a risk of cuts.

4. CONCLUSION

In this study, it is aimed to develop a hard-core hybrid para-aramid yarn that is resistant to cutting from fiber and polymer blends used in protective textile materials against mechanical impact. At the end of the study, a product has been developed that will not affect the efficient operation and provide full protection, since fiber with a high strength to weight ratio and flexible structure such as para-

aramid is used. The developed yarn will be used in the production of protective textile products; Injuries in the form of cuts, mostly due to work accidents, can be prevented.

ACKNOWLEDGMENT

We would like to thank Technical Textiles Research and Development Center İzmir (TEKSMER) for helping us get our test results.

REFERENCES

Ertekin, M., (2017). Effect of Coating on the Performance Properties of Protective Gloves, *Tekstil ve Mühendis*, 24: 107, 172-180.

Ertekin, M. and Kirtay, HE., (2016). Cut resistance of hybrid para-aramid fabrics for protective gloves, *The Journal of The Textile Institute*, 107:10, 1276-1283.

Ertekin, G. Mekanik Darbeye Dayanikli Tekstil Ürünlerinin Performans Ve Konfor Özellikleri Üzerine Bir Araştirma. Doktora Tezi, Ege Üniversitesi, 2014.

Alpyıldız, T., Rochery, M., Kurbak, A., Flambard, X., (2011). Stab and Cut Resistance of Knitted Structures: A Comparative Study, *Textile Research Journal*, 81(2), 205– 2

Özen, O. Yerli Üretim İş Eldivenlerinin Ürün Güvenliğinin Değerlendirilmesi, İş Sağlığı ve Güvenliği Uzmanlık Tezi, Ankara Çalışma ve Sosyal Güvenlik Bakanlığı İş Sağlığı ve Güvenliği Genel Müdürlüğü, 2016.